

UTILIZING MULTIDISCIPLINARY METHODS TO UNDERSTAND TRACE
ELEMENT ACCUMULATION IN NORTHERN GULF OF MEXICO
ODONTOCETES

by

Meaghan A. McCormack, B.S., M.S.

A dissertation submitted to the Graduate Council of
Texas State University in partial fulfillment
of the requirements for the degree of
Doctor of Philosophy
with a Major in Aquatic Resources and Integrative Biology
August 2021

Committee Members:

Jessica Dutton, Chair

Weston Nowlin

Aaron Roberts

Todd Swannack

Floyd Weckerly

COPYRIGHT

by

Meaghan A. McCormack

2021

FAIR USE AND AUTHOR'S PERMISSION STATEMENT

Fair Use

This work is protected by the Copyright Laws of the United States (Public Law 94-553, section 107). Consistent with fair use as defined in the Copyright Laws, brief quotations from this material are allowed with proper acknowledgement. Use of this material for financial gain without the author's express written permission is not allowed.

Duplication Permission

As the copyright holder of this work I, Meaghan A. McCormack, refuse permission to copy in excess of the "Fair Use" exemption without my written permission.

ACKNOWLEDGEMENTS

I would like to thank my advisor Dr. Jessica Dutton for her continued guidance and support throughout my doctoral program. I would also like to thank my committee members, Dr. Weston Nowlin, Dr. Aaron Roberts, Dr. Todd Swannack, and Dr. Butch Weckerly; each committee member's knowledge and feedback improved the quality of my dissertation. I extend a special thanks to all the current and past undergraduate and graduate students in Dr. Dutton's lab, especially those who helped with sample processing including Stacey Britton, Kristyn Armitage, Taylor Gold Quiros, and Amylee Van. I also thank Jenny Litz, Gina Rappuci, and Lauren Noble from the National Oceanic and Atmospheric Administration (NOAA) National Marine Fisheries (NMFS), and Heidi Whitehead and Dr. Sarah Piwetz from the Texas Marine Mammal Stranding Network for providing the samples for my dissertation, as well as the various marine mammal stranding networks and their volunteers. In addition, I wish to thank Wayne E. McFee, Brian P. Jackson, and Francesca Battaglia, who contributed to the formal analyses. I would also like to thank the Analysis Research Service Center (ARSC) at Texas State University, especially Jonathan Anderson and Brian Samuels for training and use of the SEM-EDS. This dissertation was funded by Texas State University start-up funds (Jessica Dutton) and the Doctoral Research Support Fellowship (Meaghan McCormack). I am grateful for my family and friends who have supported me throughout my academic career. Finally, I wish to thank the Clearwater Marine Aquarium, especially a dolphin

named Sunset Sam, the first stranded dolphin in Florida to survive in a rehabilitation center, for inspiring me to pursue a career in marine mammal science.

TABLE OF CONTENTS

	Page
ACKNOWLEDGEMENTS	iv
LIST OF TABLES	ix
LIST OF FIGURES	xi
ABSTRACT	xvi
 CHAPTER	
I. MARINE MAMMAL ECOTOXICOLOGY: CONTAMINANTS AND RESEARCH APPROACHES	1
Introduction to Marine Mammal Ecotoxicology	1
Case Study 1: POPs, Herpes Virus, and Cancer in California Sea (<i>Zalophus californianus</i>).....	9
Case Study 2: Bottlenose Dolphins as Sentinel Species for Hg Exposure in Humans	10
Case Study 3: Persistent Organic Pollutants and Hg Concentrations differ among Sympatric Dolphin Species	11
Case Study 4: Trace Elements in Pinniped Teeth suggest Historic Variation in Exposure to Pollutants	12
Principles of Trace Element Toxicology	14
Trace Element Accumulation in Odontocetes	17
Gulf of Mexico (GoM) Habitats and Odontocetes	21
The Northern Gulf of Mexico Cetacean Unusual Mortality Event and Deepwater Horizon Oil Spill	24
Dissertation Objectives	24
 II. MERCURY CONCENTRATIONS IN BLUBBER AND SKIN FROM STRANDED BOTTLENOSE DOLPHINS (<i>TURSIOPS TRUNCATUS</i>) ALONG THE FLORIDA AND LOUISIANA COASTS (GULF OF MEXICO, USA) IN RELATION TO BIOLOGICAL VARIABLES	 39
Abstract	39
Introduction.....	40
Methods.....	44

Results	51
Discussion	56
III. EFFECT OF TROPHIC POSITION ON MERCURY CONCENTRATIONS IN BOTTLENOSE DOLPHINS (<i>TURSIOPS TRUNCATUS</i>) FROM THE NORTHERN GULF OF MEXICO	77
Abstract	77
Introduction	78
Methods	83
Results	91
Discussion	95
Conclusions	105
IV. RELATIONSHIP BETWEEN MERCURY AND SELENIUM CONCENTRATIONS IN TISSUES FROM STRANDED ODONTOCETES IN THE NORTHERN GULF OF MEXICO	117
Abstract	117
Introduction	118
Methods	123
Results	128
Discussion	134
Conclusions	147
V. EFFECTS OF FORMALIN FIXATION ON TRACE ELEMENT CONCENTRATIONS IN BOTTLENOSE DOLPHIN (<i>TURSIOPS TRUNCATUS</i>) TISSUES	166
Abstract	166
Introduction	167
Methods	169
Results	176
Discussion	181
Conclusions	188
VI. EXPLORING THE USE OF SEM-EDS ANALYSIS TO MEASURE THE DISTRUBTION OF MAJOR, MINOR, AND TRACE ELEMENTS IN BOTTLENOSE DOLPHIN (<i>TURSIOPS TRUNCATUS</i>) TEETH	209
Abstract	209

Introduction	210
Methods	214
Results	219
Discussion	221
VII. CONCLUSIONS	237
APPENDIX SECTION	244
REFERENCES	310

LIST OF TABLES

Table	Page
1.1. Essential and non-essential elements, anthropogenic sources, and their biological roles (Liu et al., 2008)	28
2..1. Biological data from stranded dolphins collected between 2011-2016 from the Florida and Louisiana coasts.....	66
2.2. Best fit generalized linear model (GLM) and parameter estimates selected based on the lowest Akaike Information Criteria (AICc)	67
2.3. Comparison of THg concentrations (mean \pm SD) in bottlenose dolphin blubber and skin between the present study and previously published studies in $\mu\text{g/g}$ dry wt	69
3.1. $\delta^{15}\text{N}$ values (mean \pm 1 standard deviation or standard error*) for primary consumer used to predict bottlenose dolphin trophic position according to node assignments based on Hohn et al. (2017).....	107
3.2. Stable isotope ratios [mean, standard deviation (SD), minimum (Min), maximum (Max), and range] for bottlenose dolphins according to node assignment	108
3.3. Results of AICc model selection for skin THg and $\delta^{15}\text{N}$ in relation to explanatory variables	109
4.1. Sex, number of individuals sampled (n), and body length [mean \pm standard deviation; range in parentheses], for odontocete species stranded along the coast of Florida and Louisiana.....	149
4.2. Dry and wet weight THg and Se concentrations, and Se:Hg molar ratios (mean \pm standard deviation; range in parentheses) in each tissue and species	150
4.3. Final models fitted to THg and Se concentrations in bottlenose dolphin blubber, kidney, liver, lung, and skin	156
5.1. Number of samples above the detection limit for formalin-fixed and frozen <i>Tursiops truncatus</i> tissues in the long-term study	189
5.2. Trace element concentrations [mean \pm standard deviation; $\mu\text{g/g}$ dry wt] in frozen and	

formalin-fixed <i>Tursiops truncatus</i> tissues following long-term (3-7 years) preservation.....	191
5.3. P-values from the paired t-tests or Wilcoxon signed rank tests (†) comparing the effects of preservation method (formalin fixation, freezing) on <i>Tursiops truncatus</i> tissue trace element concentrations following long-term (3-7 years) preservation and the mean bias between preservation methods	195
5.4. Absolute percent differences [mean ± standard deviation] in trace element concentrations between frozen and formalin-fixed <i>Tursiops truncatus</i> tissues following long-term preservation (3-7 years).....	197
5.5. Trace element concentrations [mean ± standard deviation; µg/g dry wt] in frozen and formalin-fixed <i>Tursiops truncatus</i> tissues following short-term (6 weeks) preservation.....	199
5.6. P-values from the paired t-tests or Wilcoxon signed rank tests (†) comparing the effects of preservation method (formalin fixation, freezing) on <i>Tursiops truncatus</i> tissue trace element concentrations following short-term (6 weeks) preservation and the mean bias between preservation methods	201
5.7. Absolute percent differences [mean ± standard deviation] in trace element concentrations between frozen and formalin-fixed <i>Tursiops truncatus</i> tissues following short-term preservation (6 weeks)	202
6.1. Stranding year, straight-line body length, sex, and estimated age of bottlenose dolphins used in the study.....	228
6.2 Weight percentage (wt %) of major, minor, and trace elements across the enamel and pre-natal dentin (PND) for all dolphins combined (mean ± standard deviation; range of wt % in parenthesis)	229
6.3 Weight percentage (wt %) of major, minor, and trace elements at seven points across the approximate location of growth layers groups (GLG's) moving from point 1 (edge of tooth) towards the pulp cavity for all combined (mean ± standard deviation; range of wt % in parenthesis)	230

LIST OF FIGURES

Figure	Page
1.1. Graphical representation of bioaccumulation and biomagnification	30
1.2. Atmospheric, marine, and terrestrial sources of contaminants in marine systems ...	31
1.3. Dose-response curves for essential (A) and non-essential trace elements (B)	32
1.4. Flowchart depicting factors that influence the effect of a contaminant on individuals and populations beginning with the source	33
1.5. Levels of biological organization and focuses of toxicology studies	34
1.6. Conceptual diagram outlining the ecological and physical processes that influence methylmercury (MeHg) concentrations in wildlife	35
1.7. Map showing the Gulf of Mexico bathymetric contours and oceanic currents	36
1.8. Map showing the Gulf of Mexico Level 1 Marine Ecosystems	37
1.9. Map showing the watershed that contribute to the freshwater to the Gulf of Mexico	38
2.1. Bottlenose dolphin (<i>Tursiops truncatus</i>) stranding locations in Florida (FL; n = 63) and Louisiana (LA; n = 121)	71
2.2. THg concentration (mean + SD) in blubber and skin of Florida (FL) and Louisiana (LA) bottlenose dolphins	72
2.3. Relationship between body length and age in Florida (FL) and Louisiana (LA) bottlenose dolphins with growth curves fitted using the Gompertz model	73
2.4. Relationship between THg concentrations in blubber and skin of bottlenose dolphins from Florida (FL) and Louisiana (LA) in relation to body length (left column) and age (right column)	74
2.5. Relationship between Log ₁₀ THg concentrations in blubber and skin and Log ₁₀ body length (left column) and Log ₁₀ age (right column).....	75

2.6. Florida (FL) and Louisiana (LA) bottlenose dolphin $\delta^{13}\text{C}$, $\delta^{15}\text{N}$, and $\delta^{34}\text{S}$ values in relation to body length (left column) and age (right column)	76
3.1. Locations where the majority of stranded dolphin in Hohn et al. (2017) were assigned to each habitat (A) and bottlenose dolphin (<i>Tursiops truncatus</i>) stranding locations in the present study according to predicted node assignment following the recursive partition analysis of Hohn et al. (2017) (B)	110
3.2. Box and whisker plots showing the stable isotope ratios for stranded bottlenose dolphins (<i>Tursiops truncatus</i>) according to predicted node assignment (number in parentheses) following the partition analysis by Hohn et al. (2017)	111
3.3. Effect plots for the predictors of bottlenose dolphin (<i>Tursiops truncatus</i>) skin $\delta^{15}\text{N}$ values	112
3.4. Box and whisker plots showing total Hg concentration ($\mu\text{g/g}$ dry wt) in stranded bottlenose dolphin (<i>Tursiops truncatus</i>) skin according to the predicted node assignment (number in parentheses) following the recursive partition analysis by Hohn et al. (2017)	113
3.5. Effect plots for the predictors of bottlenose dolphin (<i>Tursiops truncatus</i>) skin Log_{10} THg concentration ($\mu\text{g/g}$ dry wt)	114
3.6. Estimated trophic position distribution of bottlenose dolphins (<i>Tursiops truncatus</i>) according to node assignment using a mean \pm standard deviation trophic enrichment factor (TEF) for $\delta^{15}\text{N}$ of $2.14 \pm 0.53\text{‰}$ (A) and of $3.4 \pm 1\text{‰}$ (B)	115
3.7. Relationship between $\delta^{15}\text{N}$ and Log_{10} THg concentration ($\mu\text{g/g}$ dry wt) (A), trophic position and Log_{10} THg concentrations ($\mu\text{g/g}$ dry wt) using a mean TEF for $\delta^{15}\text{N}$ of 3.4‰ and 2.14‰ , respectively (B and C), and $\delta^{15}\text{N}$ and Log_{10} THg concentration ($\mu\text{g/g}$ dry wt) showing trophic position estimated using TEF for $\delta^{15}\text{N}$ of 3.4‰ and of 2.14‰ , respectively (D and E) in skin from bottlenose dolphins (<i>Tursiops truncatus</i>).....	116
4.1. Stranding locations of odontocetes sampled in this study	158
4.2. Relationship between Se:Hg molar ratio and THg concentration ($\mu\text{g/g}$ dry wt) in the blubber, kidney, liver, lung, and skin of odontocetes	159

4.3. Relationship between THg concentration ($\mu\text{g/g}$ dry wt) and body length (cm) in the blubber, kidney, liver, lung, and skin of stranded bottlenose dolphins	160
4.4. Scatterplots and linear regression lines showing the relationship between Log_{10} THg concentrations ($\mu\text{g/g}$ dry wt), body length (cm), and stranding location, when applicable, in the blubber, kidney, liver, lung, and skin of stranded bottlenose dolphins.....	161
4.5. Relationship between Se concentration ($\mu\text{g/g}$ dry wt) and body length (cm) in the blubber, kidney, liver, lung, and skin of stranded bottlenose dolphins	162
4.6. Scatterplots and linear regression lines showing the relationship between Log_{10} Se concentrations ($\mu\text{g/g}$ dry wt), body length (cm), and stranding location, when applicable, in the blubber, kidney, liver, lung, and skin of stranded bottlenose dolphins	163
4.7. Relationship between Log_{10} THg concentration ($\mu\text{mol/g}$ dry wt) and Log_{10} Se concentration ($\mu\text{mol/g}$ dry wt) in tissues from stranded bottlenose dolphins	164
4.8 Relationship between the Se:Hg molar ratio and body length (cm) in the blubber, brain, kidney, liver, lung, and skin of stranded bottlenose dolphins	165
5.1. Bland-Altman plots comparing arsenic (As) concentrations ($\mu\text{g/g}$ dry wt) in formalin-fixed and frozen <i>Tursiops truncatus</i> tissues following long-term preservation and p values from the paired t-tests	204
5.2. Bland-Altman plots comparing mercury (Hg) concentrations ($\mu\text{g/g}$ dry wt) in formalin-fixed and frozen <i>Tursiops truncatus</i> tissues following long-term preservation and p values from the paired t-tests or Wilcoxon signed-rank tests	205
5.3 Bland-Altman plots comparing arsenic (As) concentrations ($\mu\text{g/g}$ dry wt) in formalin-fixed and frozen <i>Tursiops truncatus</i> tissues following short-term preservation and p values from the paired t-tests or Wilcoxon signed-rank tests	206

5.4 Bland-Altman plots comparing cadmium (Cd) concentrations ($\mu\text{g/g}$ dry wt) in formalin-fixed and frozen <i>Tursiops truncatus</i> tissues following short-term preservation and p values from the paired t-tests (left panel) and linear regressions between Cd concentrations ($\mu\text{g/g}$ dry wt) in formalin-fixed and frozen <i>T. truncatus</i> tissues (right panel)	207
5.5. Bland-Altman plots comparing mercury (Hg) concentrations ($\mu\text{g/g}$ dry wt) in formalin-fixed and frozen <i>Tursiops truncatus</i> tissues following short-term preservation and p values from paired t-tests or Wilcoxon signed-rank tests (\dagger) (left panel) and linear regressions between Hg concentrations ($\mu\text{g/g}$ dry wt) in formalin-fixed and frozen <i>T. truncatus</i> tissues (right panel)	208
6.1. Cross-sectioned image of the top half of tooth of GA1603 (the split in the tooth was likely a result of being frozen in long-term storage) (A), backscattered electron image showing the enamel and pre-natal dentin (PND), along with a rectangle that indicates the approximate area of SEM-EDS analysis (B), and a zoomed in image of the area of the EDS analysis showing the locations for point analysis (point 1 = outer enamel, point 2 = mid-enamel, point 3 = inner enamel, point 4 = pre-natal dentin near the enamel dentin junction, and point 5 = inner pre-natal dentin) (C)	231
6.2 Cross-sectioned image of the top half of tooth of GA1603 (the split in the tooth was likely a result of being frozen in long-term storage) along with a rectangle that shows general location for elemental analysis (A), and a backscattered electron image showing the general area of point analyses (points 1 - 7) used to explore the distribution of elements across the approximate location of the growth layer groups (GLG's), with newest layers deposited closet to the pulp cavity (B)	232
6. 3 Selective point analyses for elements in the enamel and pre-natal dentin (PND) expressed as weight percentage (wt %): outer enamel (point 1), mid-enamel (point 2), inner enamel (point 3), PND near enamel dentin junction (EDJ) (point 4), inner PND (point 5). Results of the repeated-measures linear effects ANOVA and Tukey's post-hoc test are shown in each panel	233
6.4. Backscattered electron image of analysis area of sample GA 260 showing the enamel and pre-natal dentin (PND) (panel A) and elemental maps for Al (panel B), C (panel C), Ca (panel D), Cl (panel E), Mg (panel F), Na (panel G), O (panel H), and P (panel I).....	234

6.5. Selective point analyses for elements approximating where growth layers groups (GLG's) are present. Elements presented as a weight percentage (wt %), moving from the tooth edge (point 1) towards the tooth center (point 7), with points closest to the tooth edge being the oldest deposited dentin layers and points closest to the tooth center being the newest deposited dentin layers	235
6.6. Backscattered electron image of analysis area of sample GA 1755 showing the dentin and pulp cavity (panel A) and elemental maps for Al (panel B), C (panel D), Na (panel E), O (panel F), and P (panel G).....	236

ABSTRACT

Due to their long lifespan and top trophic position, odontocetes (toothed whales) can accumulate high concentrations of trace elements [e.g., cadmium (Cd), mercury (Hg)] in their tissues. In addition, for many species, their coastal distribution makes them appropriate sentinels for ecosystem and human health. Acquiring odontocete tissues for ecotoxicology studies is a challenge due to logistical and legal constraints. Although data is opportunistic, collecting tissues from deceased stranded individuals is a viable alternative to sampling free-ranging populations. In this dissertation, I focused on trace element accumulation in odontocetes, primarily bottlenose dolphins (*Tursiops truncatus*), that stranded along the northern Gulf of Mexico (nGOM) coast. Many samples were from dolphins that stranded during the nGOM Cetacean Unusual Mortality Event (2010-2014), which provided access to an unusually large number of individuals (> 250). The primary objectives were to 1) measure the concentration of total Hg (THg) in blubber and skin from bottlenose dolphins that stranded along the Florida (FL) panhandle and Louisiana (LA) coasts and explore the relationship between total Hg (THg) concentration and sex, body length, age, stranding location, diet/relative trophic position, ($\delta^{13}\text{C}$ and $\delta^{15}\text{N}$, respectively), and foraging habitat ($\delta^{34}\text{S}$); 2) assign bottlenose dolphins to predicted habits east and west of the Mississippi River Delta (MRD) using $\delta^{13}\text{C}$ and $\delta^{34}\text{S}$ values, and determine whether variation in THg concentrations could be explained by differences in trophic positions among dolphins; 3) explore the tissue-specific accumulation of Hg and selenium (Se) and the potential protective role of Se against Hg toxicity by

measuring the concentrations of THg and Se in multiple tissues from 11 species of odontocetes that stranded along the FL panhandle and Louisiana coast and calculating the Se:Hg molar ratios; 4) determine the effects of long-term and short-term formalin fixation on the concentration of 14 trace elements in bottlenose dolphin tissues; and 5) utilize a scanning electron microscope (SEM) equipped with energy dispersive X-ray spectroscopy (EDS) to determine the distribution of major (e.g., Ca, P), minor (e.g., Cl, Mg, Na), and trace elements (e.g., Cd, Hg, Pb, Zn) in teeth from 12 bottlenose dolphins.

To address objective 1, I measured THg concentrations in bottlenose dolphin skin and blubber using a direct mercury analyzer and stable isotope ratios were measured in dolphin skin. In both tissues, there was a positive relationship between THg concentration and body length/age ($p < 0.001$). Dolphins that stranded in FL had greater THg concentrations than those that stranded in LA ($p < 0.001$). Next, to address objective 2, I assigned dolphins to predicted habitats using $\delta^{13}\text{C}$ and $\delta^{34}\text{S}$ values and estimated trophic positions using $\delta^{15}\text{N}$ values from stranded dolphin skin and primary consumers taken from the literature following a Bayesian framework. I found that dolphins assigned to estuarine habitats east of the MRD, particularly those associated with habitats along the FL panhandle, had greater THg concentrations and higher estimated trophic positions, suggesting that differences in trophic positions among bottlenose dolphins contribute to variation in Hg concentrations. To address objective 3, I measured the THg and Se concentrations across several tissues and species using inductively coupled plasma mass spectrometry (ICP-MS). The concentration of THg was greatest in the liver and lowest in

the blubber, lung, or skin. Se:Hg molar ratios decreased with increasing THg concentration tissues following an exponential decay relationship. On average, in bottlenose dolphins, Se:Hg molar ratios were approximately 1:1 in the liver and $> 1:1$ in the other tissues, suggesting that Se likely protects against Hg toxicity. In objective 4, trace elements were measured in several bottlenose tissues using ICP-MS. Following both short-term (6 weeks) and long-term preservation (3-7 years), there were significant differences in tissue trace element concentrations between preservation methods. Evidence of both leaching of trace elements from tissues and contamination of tissues with trace elements, presumably from formalin, was observed; however, the results suggest that it may be possible to account for the effects of formalin fixation for some trace elements. Finally, to address objective 5, I used SEM-EDS to explore the distribution of major, minor, and trace elements within dolphin teeth. There was variation in the weight percentage (wt %) of major and minor elements between the enamel and pre-natal dentin. Except of Al, which may be a result of backscatter from the SEM stub, trace elements were not detected. However, trace elements may be present but at wt % values below the detection limit.

Overall, this dissertation contributes to knowledge of several trace elements in odontocete tissues. In particular, this work contributes to the understanding of Hg and Se accumulation in inshore bottlenose dolphins from the nGoM. Further, I address methodological questions related to tissue preservation and the use of SEM-EDS to

measure major, minor, and trace elements in dolphin teeth which will benefit future studies.

I. MARINE MAMMAL ECOTOXICOLOGY: CONTAMINANTS AND RESEARCH APPROACHES

Introduction to Marine Mammal Ecotoxicology

Due to both their longevity and position at the top of the food web, marine mammals, particularly odontocetes or toothed whales, can accumulate contaminants, such as trace elements [e.g., cadmium (Cd), mercury (Hg); Gui et al., 2017; Cáceres-Saez et al., 2018; Martínez-López et al., 2019; Monteiro et al., 2020], pesticides [e.g., dichloro-diphenyl-trichloroethane (DDT); Romero et al., 2018; Tsygankov et al., 2018; Pedro et al., 2020; Trukhin et al., 2020] and other persistent organic pollutants (POPs) [e.g., polychlorinated biphenyls (PCBs), polybrominated diphenyl ethers (PBDEs), and per- and polyfluoroalkyl substances (PFAS); Lynch et al., 2019; Alava et al., 2020; Taylor et al., 2020; Villanger et al., 2020] to high concentrations in their tissues. In general, contaminants are defined as “any physical, chemical, biological, or radiological substance or matter that has an adverse effect on air, water, soil, or living organisms” (D’Surney and Smith, 2005). However, throughout this dissertation, contaminants will refer to those of chemical origin including, legacy contaminants (e.g., DDT, PBCs), trace elements (e.g., Hg), and contaminants of emerging concern, such as PFAS, pharmaceuticals, phthalates, current-use pesticides (e.g., chlorpyrifos, diazinon) and their metabolites (Bossart et al., 2011; Sauvé et al., 2014). While most POPs are not naturally present in the environment and are a consequence of anthropogenic activities, trace elements occur naturally. However,

environmental trace element concentrations can also become elevated because of human activities (Liu et al., 2008; El-Shahawi et al., 2010). For example, Lamborg et al. (2014) estimated that anthropogenic activities (e.g., fossil fuel combustion and artisanal gold mining, pulp, paper, and paperboard mills, municipal waste combustion; U.S. EPA, 2011) have tripled the amount of Hg present in surface ocean waters compared to pre-anthropogenic conditions.

Marine mammals are exposed to contaminants primarily through the diet (Gray, 2002; Nigro et al., 2002; Das et al., 2003; Hong et al., 2012). Once ingested, contaminants can be metabolized or excreted. When dietary exposure rates exceed excretion rates, contaminants bioaccumulate within an organism over time (Gray, 2002; Hammerschmidt and Fitzgerald, 2006; Chen et al., 2009). Additionally, some contaminants, such as Hg and PCBs, biomagnify, increasing in concentration with increases in trophic position (Figure 1.1) (Gary, 2002; Burreau et al., 2006; Hammerschmidt and Fitzgerald, 2006; Chen et al., 2009; Hong et al., 2013; Remili et al., 2021). Consequently, contaminants reach the highest concentrations in long-lived marine carnivores, particularly odontocetes. Exposure to high concentrations of contaminants may result in adverse individual and population-level health effects (Ylitalo et al., 2005; Schaefer et al., 2011; Gallagin et al., 2019; Kershaw et al., 2019).

Often the primary objectives of marine mammal toxicological studies are either to measure the tissue distribution of contaminants (e.g., Cardellicchio et al., 2000; Capelli et al., 2008; Isobe et al., 2009; Rojo-Nieto et al., 2017; Sun et al., 2020), to establish spatial-temporal trends in contaminant concentrations (e.g., Aubail et al., 2010; Gui et al., 2017; Borrell et al., 2014; Lynch et al., 2019; Villanger et al., 2020; De María et al., 2021), or

to determine the relationship between contaminant exposure and adverse health effects on individuals and populations (Yitalo et al., 2005; Schaefer et al., 2011; Titcomb et al., 2017; Cáceres-Saez et al., 2018; Gallagin et al., 2019; López-Berenguer et al., 2020; Levin et al., 2020). In addition to the health of organisms themselves, because marine mammals often inhabit coastal habitats and consume similar fish to human populations, they are appropriate sentinels to monitor ecosystem health and identify potential hazards to human health (Bossart, 2011; Reif et al., 2015). Furthermore, because the diet is the primary route of entry for contaminants, tissue contaminant concentrations in odontocetes, along with other ecological tracers (e.g., stable isotopes ratios), have been used to understand marine mammal ecology and population structure (Dirtu et al., 2016; Balmer et al., 2019; Barragán-Barrera et al., 2019; Damseaux et al., 2021; Remili et al., 2021). Finally, because teeth are hard tissues that can be easily preserved, teeth have been used to assess historical changes in environmental contaminant exposure (Outridge et al., 2002; Ozersky et al., 2017; Poste et al., 2018; Clark et al., 2021; De María et al., 2021).

However, opportunities to measure the concentrations of contaminants in marine mammal tissues are limited and assessing the effects of contaminants on individual and population health is challenging, given the complexity of measuring and interpreting tissue contaminant concentrations (Weijjs et al., 2016; Simmonds et al., 2018; Sanganyado et al., 2020). Contaminant exposure is among several stressors (e.g., climate change, habitat degradation, fishery interactions, noise pollution, pathogens) that may negatively impact marine mammal

populations. Consequently, determining cause-and-effect relationships between contaminant exposure and adverse effects becomes increasingly complex given the number of potential confounding variables (Das et al., 2003; Marcogliese and Pietrock, 2011; Simmonds et al., 2018; Page-Karjian et al., 2020). Free-ranging marine mammals are exposed to a mixture of contaminants that may have additive, synergistic, or antagonistic effects (De Guise, 1998; Eaton and Gilbert, 2008; García-Barrera et al., 2012; Gajdosechova et al., 2016; Desforges et al., 2017). In the marine environment, contaminants come from both natural and anthropogenic sources and can originate from atmospheric deposition, marine (e.g., oil and gas facilities, aquaculture, dredging; Tornero and Hanke, 2016) or terrestrial systems (e.g., industrial effluents, surface runoff) (Figure 1.2; Macko, 2018; Sanganyado et al., 2019). Marine contaminants can be further categorized as point and non-point pollutants. Point source pollutants are those for which sources can easily be identified (e.g., sewage outflow pipe), whereas non-point source pollutants (e.g., those transported through storm runoff) originate from more diffuse sources that cannot be identified (Connell et al., 2009).

Marine mammals consist of a taxonomically diverse group of organisms, including species from three orders (Carnivora, Cetacea, and Sirenia) that rely on marine ecosystems for survival. As such, marine mammals have specialized adaptations for aquatic existence. Some species are fully aquatic [e.g., species of the order Cetacea including those of the suborders Mysticeti (baleen whales) and Odontoceti (toothed whales) and species of the order Sirenia (e.g., manatees and dugongs)]. Other marine mammals are semi-aquatic, spending a portion of their time at sea to forage but returning to land to rest and breed [e.g., polar bears (*Ursus maritimus*) and species of the suborder

Pinnipedia including phocids (earless seals), otariids (eared seals), and Odobenidae (*walrus*)] (Martin and Reeves, 2002). Marine mammal populations often span large geographic areas. Further, in some cases, species are deep diving inhabiting primarily offshore environments, which makes them even more challenging to study [e.g., Cuvier's beaked whales (*Ziphius cavirostris*)] (Würsig et al., 2017).

In the U.S., all marine mammals are protected under the Marine Mammal Protection Act (MMPA) of 1972, which makes it illegal to import marine mammals or marine mammal parts into the U.S. without a permit. It also prohibits the "take" of marine mammals without a permit; according to the MMPA, a "take" may include the act of or attempt "to harass, hunt, capture, or kill any marine mammal" (16 U.S.C. 1362). In some cases, exemptions to the MMPA are permitted for scientific research and public display. For toxicological studies, sampling techniques include both live and post-mortem sampling. The methodologies utilized are dependent on the life history, size, and legal protection status of the animals (Godard-Codding et al., 2018; Sanganyado et al., 2020).

Live sampling procedures for marine mammals are limited to non-lethal methodologies. Today these methods generally refer to samples collected from animals in the field and not from animals in managed care facilities, although there are some exceptions. Methods include capture-release health assessments [described for bottlenose dolphins (*Tursiops truncatus*) in Barratclough et al. 2019], which involve physically capturing animals, and less invasive procedures that do not require capture and restraint (e.g., skin and blubber biopsies). Of the

two approaches, the capture-release methodologies can provide more including tissues for biopsies, urine, blood and blow samples, and morphometric measurements. However, capture-release assessments are logistically challenging, limited in scope, and stressful to animals (Barratclough et al., 2019). In contrast, skin and blubber biopsies do not require the physical constraint of animals. In this procedure, while onboard a vessel, researchers deploy a small dart into the animal using an air gun or crossbow to take a skin and blubber sample (Godard-Codding et al., 2018). In rare cases, non-lethal, minimally invasive, *in vivo* studies may be conducted on marine mammals in managed care facilities under controlled conditions (e.g., Nigro et al., 2002; Hong et al., 2012).

Before the MMPA, there were several controlled dietary studies on pinnipeds, where animals were administered a known dose of Hg, and the effects were observed; in some studies, exposures resulted in fatalities (e.g., Tillander et al. 1972; Ramprashad and Ronald, 1977; Reijnders, 1986). Today, the few toxicological studies on marine mammals in managed care are different. In general, research focuses on collecting baseline information to understand contaminant body burdens (e.g., Takeuchi et al., 2016), understanding the relationship between dietary uptake rates and tissue contaminant concentrations (Nigro et al., 2002; Hong et al., 2013), and exploring the relationship between contaminant concentrations and individual health (Reddy et al., 2001; Sorensen et al., 2008). In all cases, contaminants are not added to the diet, and sampling methodologies are limited to non-invasive techniques (e.g., blubber biopsy, blood sampling). The research on bottlenose dolphins held at the U.S. Navy Department of Defense facility in San Diego, California, is unique and highlights the importance of these studies. Over the years, blubber, blood, and milk samples from the dolphins have

been analyzed has to understand the maternal transfer of organic contaminants (e.g., DDT and PCBs] and the impacts of contaminants on reproduction (Reddy et al., 2001). Sorensen et al. (2008) also used dolphins at the U.S. navy facility to explore the relationship between 20 trace elements and liver enzyme function, using alanine aminotransferase (ALT) and gamma-glutamyl transferase (GGT) as indicators of liver function.

An alternative to sampling live free-ranging populations is to collect tissue samples from deceased stranded animals or, in some cases, animals caught as bycatch (Peltier et al., 2012, 2014; Lemos et al., 2013; Monteiro et al., 2016, 2020; Cáceres-Saez et al., 2018). A stranded marine mammal may refer to an animal that was: 1) found dead either on the beach or floating in the water, 2) found alive on the beach but could not return to the water or natural habitat without assistance, or 3) found alive on the beach and required immediate medical attention (Geraci and Lounsbury, 2005). Stranded animals found alive are either returned to the water, euthanized, or taken to a rehabilitation center (Geraci and Lounsbury, 2005). For toxicological studies, methods related to sampling stranded animals are referring to deceased animals. Several countries, including the U.S., have protocols that outline the procedures for tissue collection from stranded marine mammals (Becker et al. 1994; Ballarin et al. 2005; Geraci and Lounsbury, 2005). Sampling stranded animals provide access to the internal organs (e.g., brain, liver, kidney, spleen), which can accumulate high concentrations of contaminants (Meador et al., 1999; Cardellicchio et al., 2000; Roditi-Elasar et al., 2003; Capelli et al., 2008; Noren and Mocklin, 2011; Méndez-Fernandez et al.,

2016; Cáceres-Saez et al., 2018; Martínez-López et al., 2019). However, data from stranded animals are opportunistic; the origin of the stranded animals is often unknown, and sample decomposition may influence contaminant concentrations (Peltier et al., 2012, 2014; Martínez-López et al., 2019). Stranded animals may also be stressed and in poor body condition which can influence contaminant burdens. Regardless of whether samples were collected from live animals or stranded animals, sample sizes are limited.

Additionally, there are also *in vitro* techniques and modeling approaches that do not require the use of live animals. For *in vitro* studies, cells (e.g., skin fibroblast cells, blood leucocytes) collected from stranded individuals are exposed to varying concentrations of contaminants, and the molecular response recorded (De Guise, 1998; Nakata et al., 2002; Desforges et al., 2017; Sanganyado et al., 2020; Huang et al., 2020; Levin et al., 2020). Although useful, in-vitro studies have also been criticized because they do not replicate real-world conditions. Many studies focus on a single contaminant and cell, excluding the interaction between contaminants and organs (Weijs and Zaccaroni, 2016). Some toxicokinetic models attempt to address these concerns (Hickie et al., 1999, 2007, 2013; Hall et al., 2006; Ewald et al., 2019). For example, Ewald et al. (2019) developed a toxicokinetic model to explore the distribution of Hg among organs and between life stages in ringed seals (*Phoca hispida*). Individual-based models to predict population-level effects of contaminants have also been developed. For example, Hall et al. (2006) developed an individual-based model to predict PCB accumulation in bottlenose dolphins, the effect of PCBs on reproduction, and the long-term effects of PCBs on depressing population growth. However, how well the model can replicate real-world scenarios is dependent on our understanding of the processes which influence

contaminant exposure and bioaccumulation. For marine mammal studies, species-specific parameter estimates (e.g., ingestion rates, elimination rates, partition coefficients, biotransformation rates) are limited. As a result, studies often rely either on parameter estimates from species studied in managed care facilities (e.g., bottlenose dolphin) or on parameter estimates taken from literature for terrestrial mammals (Wejis et al., 2014; Ewald et al., 2019).

The focus of my dissertation is on trace element accumulation in stranded odontocetes from the Gulf of Mexico (GoM). However, to introduce the sampling procedures and methodologies and highlight the diversity and challenges in marine mammal toxicology, I will first present four case studies that include other marine mammal taxonomic groups, contaminants, and geographic locations.

Case Study 1: POPs, Herpes Virus, and Cancer in California Sea Lions (*Zalophus californianus*)

In wild California sea lions, the prevalence of cancer is amongst the highest observed in wild mammal populations worldwide. Over the past 40 years, between 18-23% of California sea lions that were stranded and examined post-mortem along the west coast of North American had uncontrolled cell growth, termed neoplasia, with the most common cancer being urogenital carcinoma (Gulland et al., 1996; Deming et al., 2018; Gulland et al., 2020). Studies have identified that organochlorine concentrations and the otariine herpesvirus-1 virus may explain cancer prevalence (King et al., 2002; Yitala et al., 2005; Buckles et al., 2006). Other research has suggested there may also be a genetic component

that influences the probability of cancer development (Browning et al., 2014). More recently, research has utilized a case-control design, with samples from 394 individuals over 20 years, to explore the relative importance of the previously identified factors (genetics, contaminants, and herpes virus) in explaining carcinoma prevalence. The study reported that in sea lions infected with OtHv-1, the odds were 43.57 times higher of developing cancer. In addition, for every approximate tripling of contaminant concentration in the blubber, the odds of developing cancer were 1.48 times higher (Gulland et al., 2020). This study demonstrates the importance of long-term data collection from stranded animals. In summary, this data highlights the complexity of determining cause and effect relationships between contaminant exposure and adverse effects in marine mammals and the importance of multidisciplinary collaboration.

Case Study 2: Bottlenose Dolphins as Sentinel Species for Hg Exposure in Humans

As part of the Bottlenose Dolphin Health and Risk Assessment (HERA), blood samples from live bottlenose dolphins in the Indian River Lagoon, Florida (FL), a 250 km estuary on the east coast of FL, and in Charleston Harbor, South Carolina, were analyzed to understand the relationship between blood and skin total mercury (THg) concentrations and health-related parameters (Schaefer et al. 2011). The results indicated that dolphins from the Indian River Lagoon, FL had greater blood (0.67 $\mu\text{g/l}$ wet wt) and skin (7.24 $\mu\text{g/g}$ dry wt) THg concentrations compared to dolphins sampled in Charleston Harbor, SC. [blood (0.15 $\mu\text{g/l}$ wet wt) and skin (1.68 $\mu\text{g/g}$ dry wt)]. In addition, blood THg concentrations were negatively associated with the number of lymphocytes and eosinophils, and positively associated with blood urea nitrogen and gamma-glutamyl

transferase, suggesting that exposure to Hg may suppress the immune system and negatively impact liver and renal function. The study prompted researchers to explore the Hg exposure of humans. More than 2.5 million residents live in the counties that border the Indian River Lagoon, and Schaefer et al. (2014) hypothesized that residents who regularly consumed local seafood could potentially expose themselves to harmful levels of Hg. In the study, the authors compared residents' seafood consumption patterns with their hair Hg concentration. The study found that those consuming seafood one or more times a day were 3.71 times more likely to have a total hair mercury concentration over the U.S EPA reference dose of 1.0 $\mu\text{g/g}$ than those who consumed seafood less frequently. Further, residents who obtained most of their seafood from recreational sources had the highest Hg concentrations. Together, these studies demonstrate the use of biomarkers to assess the effects of contaminants on marine mammals and how marine mammals are sentinels for human health, proving an early warning of the presence of high concentrations of contaminants.

Case Study 3: Persistent Organic Pollutants and Hg Concentrations differ among Sympatric Dolphin Species

Understanding dietary sources are vital to explaining contaminant burdens in marine mammals; in the past, diet analyses were limited to direct observation or the examination of stomach contents, which was difficult for cryptic and protected species (Silva, 1999; Blanco et al., 2001; Tollit et al., 2010). Today studies increasingly measure contaminant concentrations along with stable isotope

ratios [e.g., carbon ($\delta^{13}\text{C}$), nitrogen ($\delta^{15}\text{N}$), and sulfur ($\delta^{34}\text{S}$) stable isotopes], to better comprehend the influence of foraging habitat, dietary sources, and trophic position on tissue contaminant concentrations (Newsome et al., 2010; Wilson et al., 2012; Liu et al., 2015; Dirtu et al., 2016; Barragán-Barrera et al., 2019; Damseaux; et al., 2021; De María et al., 2021). For example, Dirtu et al. (2016) contrasted the concentration of PCBs and Hg in the blubber of two free-ranging sympatric dolphin species [spinner dolphins (*Stenella longirostris*) with Indo-Pacific bottlenose dolphins (*Tursiops aduncus*)] from the south-western Indian Ocean. The authors also measured the $\delta^{13}\text{C}$ and $\delta^{15}\text{N}$ values in the dolphin skin and the muscle of several teleost fish. Their results found considerable variation in the concentrations of PCBs and Hg, with bottlenose dolphins having consistently higher concentrations than spinner dolphins. Despite the spatial and temporal overlap of the species using the multi-tracer approach, researchers were able to determine that in addition to higher contaminant burdens, bottlenose dolphins also had elevated $\delta^{15}\text{N}$ values compared to spinner dolphins. The results suggest that they may be foraging on different prey items, perhaps at higher trophic positions.

Case Study 4: Trace Elements in Pinniped Teeth suggest Historic Variation in Exposure to Pollutants

Hard tissues (e.g., teeth, bone) are easily preserved; therefore, they have been used to assess temporal variation in environmental contaminant concentrations. For example, De María et al. (2021) explored the temporal changes in trace element concentrations [e.g., copper (Cu), Cd, lead (Pb)] in two sympatric pinniped species, [South American sea lion (*Otaria flavescens*; formerly *Otaria byronia*) and the South

American fur seal (*Arctocephalus australis*)], along the Uruguayan coastline between 1941 and 2010. Compared to the South American fur seal, the South American sea lion, which has a more coastal distribution and forages primarily on benthic organisms, had greater concentrations of Pb and C. In contrast, the South American fur seal, which has a more offshore distribution and forages primarily on pelagic species, had greater concentrations of Cd. In both species, across the entire time series, samples from the 1970s and 1980s had the greatest concentration of Cr, which the authors suspect is due to overlap with the tannery industry development in Uruguay.

The abovementioned studies highlight the diversity of methodological approaches in marine mammal toxicology and applications. The challenges associated with understanding the toxicokinetics of the contaminants, coupled with the logistical and legal difficulties associated with studying marine mammals, emphasize the importance of cross-disciplinary studies, more innovative collection technologies, and new methodologies.

The abovementioned studies highlight the diversity of methodological approaches in marine mammal toxicology and applications. The challenges associated with understanding the toxicokinetics of the contaminants, coupled with the logistical and legal difficulties associated with studying marine mammals, emphasize the importance of cross-disciplinary studies, innovative collection technologies, and new methodologies.

Principles of Trace Element Toxicology

Trace elements are "elements that occur in natural and perturbed environments in small amounts and that, when present in sufficient bioavailable concentrations, are toxic to living organisms" (Adriano, 2001). Measured in parts per million (ppm), trace elements are categorized as essential or non-essential, depending on their role in biological systems, and can originate from both natural and anthropogenic sources (Markert and Friese, 2000; Swaine, 2000; Adriano, 2001; Lui et al., 2008; Richir and Gobert, 2016; Hameed et al., 2020). Essential trace elements [e.g., cobalt (Co), copper (Cu), iron (Fe), magnesium (Mg), Manganese (Mn) selenium (Se), zinc (Zn)] are necessary for normal biological function. In contrast, non-essential trace elements [e.g., aluminum (Al), arsenic (As), Cd, Hg, Pb, tin (Sn)] serve no biological function (Adriano, 2001; Soto-Jiménez, 2011; Pancaldi et al., 2021). While trace elements are present in natural systems, anthropogenic activities have increased the environmental concentrations of several trace elements (Lui et al., 2008; Connell et al., 2009; Zhu et al., 2020). Natural sources of trace elements include weathering of rocks, volcanic emissions, forest fires, and undersea smokers (Swaine, 2000). Anthropogenic sources include coal combustion, liquid fuel combustion, non-ferrous smelting, pesticide and fertilizer production, mining and metal smelting, ferrous smelting, pig iron and steel production, vehicle traffic, non-metallic mineral manufacturing, municipal waste incineration (Pacyna and Pacyna, 2001; Connell et al., 2009; Zhu et al., 2020). An overview of the trace elements investigated in this dissertation, including their anthropogenic origins and biological role, when applicable, is provided in Table 1.1.

Dose-response curves depict the relationship between the exposure to contaminants and the observed effects in organisms. Figure 1.3 shows contrasting dose-response curves for essential and non-essential elements. For non-essential elements, low and high concentrations may result in deficiencies and toxicities, respectively. In the intermediate range, concentrations are high enough to maintain normal metabolic function but not high enough to cause toxicity. For non-essential elements, there is a range of concentrations that do not cause toxicity but, once concentrations exceed a threshold concentration, toxicity is observed (Eaton and Gilbert, 2008). The relationship between the dose and response has led to the maxim "The dose makes the poison"(Eaton and Gilbert, 2008).

The amount of a trace element that enters the bloodstream depends on the bioavailability and absorption rates (Leham-McKeen, 2008). Bioavailability is defined "as the amount of chemical that is taken up from the environment and is available to cause a biological response" (NRC 2003). Elemental speciation and environmental conditions influence bioavailability. Absorption is defined as "the process by which toxicants cross body membranes and enter the bloodstream" (Lehman-McKeen, 2008). The ability of a trace element to cross the cell membrane is related to its water solubility, size, and lipid solubility. Aqueous pores transport small hydrophilic molecules across the membrane, whereas small hydrophobic molecules cross the lipids portion of the membrane itself; in both cases, diffusion rates correspond to the size of the molecule. Larger contaminants take longer to cross the membrane. Finally, lipid solubility influences diffusion

rates, with more lipid-soluble contaminants diffusing faster than less lipid-soluble contaminants (Lehman-McKeen, 2008).

Once absorbed, trace elements are distributed throughout the body through the bloodstream. Preferential accumulation may occur in specific tissues, reflecting tissue-specific binding affinities or processes related to storage and excretion (Lehman-McKeen, 2008). For example, because of the strong binding affinity between methylmercury (MeHg) and sulfhydryl groups, MeHg accumulates in tissues that are rich in sulfhydryl groups (e.g., muscle) (Bloom, 1992). The liver, kidney, and spleen also accumulate trace elements to high concentrations, which is related to the role of these organs in the storage and detoxification of contaminants (Gregus, 2008). Contaminants are eliminated from the body through excretory pathways including, urinary and fecal excretion (Gregus, 2008; Lehman-McKeen, 2008). The ability of the body to excrete a contaminant depends on its chemical properties (Lehman-McKeen, 2008). If absorption rates exceed excretion rates, trace elements bioaccumulate within an organism over time. The biological half-life is a measure of how long it takes for one-half of a contaminant to be eliminated from the body. As a result, those trace elements with long biological half-lives (e.g., Hg, Cd; Itano and Kawai, 1986; Stoeppler, 1991) are more likely to bioaccumulate, potentially reaching concentrations that cause adverse effects.

In organisms, tissue trace element concentrations are influenced by element-specific variables related to environmental concentrations, bioavailability, exposure rates, internal circulation, and elimination rates. Exposure to elevated concentrations of contaminants may result in lethal and sublethal individual-level effects, which may eventually lead to population and cascade to create ecosystem-level effects (Figure 1.4).

Characterizing the numerous adverse effects of contaminant exposure can be complex. In ecotoxicology, studies may focus on the influence of environmental contaminants across a broad range of biological and ecological systems, ranging from the effects of contaminants on cells or cellular components to population and ecosystem-level impacts (Figure 1.5) (Di Giulio and Newman, 2008).

Trace Element Accumulation in Odontocetes

Since the 1960s, researchers have studied tissue trace element concentrations in marine mammals (Helminen et al., 1968; Henriksson et al., 1969, reviewed by O'Shea & Tanabe, 2003). While early studies drew attention to the pervasive nature of environmental contaminants, there was little to no focus on the potential effects these contaminants may have on marine mammal health or their role as sentinel species. As analytical methods progressed, making it easier to measure tissue trace element concentrations, and multi-disciplinary approaches were embraced, researchers began to ask more refined questions. Specifically, studies began to ask how individual contaminants affected an individual organism and how differences in growth and diet influenced tissue concentrations.

Odontocetes can be exposed to trace elements through diet, the ingestion of seawater, uptake from the atmosphere during inhalation, absorption through the skin, and maternal transfer both during gestation and lactation, but, like other mammals, diet is the primary exposure pathway (Storelli & Marcotrigiano, 2000; Frodello et al., 2002; Gray et al., 2002; Das et al., 2003). Tissue trace element concentrations within and among odontocete species are highly variable,

reflecting the ecological and physiological processes that influence trace element accumulation (Figure 1.6; Chételat et al., 2020). In general, concentrations of essential trace elements are less variable than non-essential trace elements, although there are some exceptions; for example, the coaccumulation of Hg and Se (Capelli et al., 2008; Cáceres-Saez et al., 2018; Kershaw et al., 2019; Martínez-López et al., 2019).

Several ecological processes influence dietary exposure to trace elements. First, the concentrations of trace elements in the environment and environmental conditions that affect bioavailability will influence tissue element concentrations. For example, given the appropriate environmental conditions, inorganic Hg (Hg^{2+}) can be converted to MeHg (CH_3Hg^+), which has a greater bioavailability than Hg^{2+} (Mason et al., 1996; Hammerschmidt and Fitzgerald, 2006; Fitzgerald et al., 2007). Therefore, tissue Hg concentrations are influenced not only by the environmental concentrations but also by factors that affect the element speciation and bioavailability. Consequently, exposure to trace elements is highly site-specific and is dependent on the concentration of trace elements in the prey and the rate of food consumption. Within and among odontocete species, differences in foraging habitats and diets will also influence tissue trace element concentration (Kehrig et al., 2016; Titcomb et al., 2017; Barragán-Barrera et al., 2019). Individuals or species that forage on higher trophic level prey are likely to have higher concentrations of contaminants that biomagnify (e.g., Hg) (Endo et al., 2010; Cáceres-Saez et al., 2020; Durante et al., 2020). Specialized diets may also impact trace element concentrations. For example, species that forage primarily on cephalopods often have greater tissue concentrations of Cd than species that consume mostly fish (Liu et al., 2015).

Following ingestions, physiological factors also influence tissue trace element concentrations. Before trace elements enter the bloodstream and are distributed throughout the body, they first must be absorbed across the gastrointestinal tract (Kershaw et al., 2019). After absorption, trace elements display tissue-specific accumulation patterns depending on the blood flow to the respective tissues and the binding affinity of the trace element with different tissues (Frodello et al., 2000; Lehman-McKeen, 2008; Cáceres-Saez et al., 2019; Lischka et al., 2021). Concentrations in tissues may also be related to the role of the tissue in maintaining homeostasis; for example, the liver and kidney often accumulate high concentrations of non-essential trace elements and are important sites of storage, detoxification, and excretion of harmful contaminants (Capelli et al., 2008; Cáceres-Saez et al., 2018; Cáceres-Saez et al., 2019; Lischka et al., 2021). In odontocetes, trace elements are eliminated primarily through feces and urine. In some cases, trace elements may also be eliminated through keratinized tissues (e.g., Hg loss through molting of skin in beluga whales) (Nigro et al., 2002; Das et al., 2003; Wagemann et al., 2005; Chételat et al., 2020). In addition, for females, maternal transfer during gestation and lactation serves as an additional excretory pathway (Frodello et al., 2002; Das et al., 2003; Chételat et al., 2020; Page-Karjian et al., 2020). When exposure rates outpace elimination rates, trace elements bioaccumulate. Odontocetes have been shown to accumulate several non-essential trace elements (e.g., Hg, Cd, Pb), which negatively impact health (Capelli et al., 2008; Monteiro et al., 2020).

For example, in odontocetes, exposure to elevated Hg can cause deleterious neurological (Bellante et al., 2017; López-Berenguer et al., 2020) and immunological effects (Schaefer et al., 2011). Mercury can negatively affect liver and kidney function in odontocetes (Rawson et al., 1993; Schaefer et al., 2011). Cadmium is another non-essential element that has been shown to bioaccumulate in odontocete tissues, especially the kidney, which can cause renal damage (Gallien et al., 2001; Chen et al., 2017; Monteiro et al., 2020). However, despite high concentrations of heavy metals, odontocetes show few signs of metal toxicity compared to their terrestrial counterparts. One method of metal detoxification is through the binding of metals to metallothioneins (MTs) (Das et al., 2003; Esposito et al., 2020; Hauser-Davis et al., 2020). In addition, for Hg, odontocetes have an additional method of detoxification, which includes the sequestering of Hg in toxically inert mercury selenide (HgSe) compounds (Lailson-Brito et al., 2012; Gajdosechova et al., 2016; Cáceres-Saez et al., 2018). If present in molar excess (i.e., Se:Hg molar ratio > 1:1), it is suggested that Se may reduce Hg toxicity (Ruelas-Inzunza and Páez-Osuna, 2005; Branco et al., 2007; Kaneko and Ralston, 2007; Ralston, 2008; Peterson et al., 2009; Ralston and Raymond, 2010; Bellante et al., 2017; Cáceres-Saez et al., 2018; Azad et al., 2019; McCormack et al., 2020a).

Both Hg and Cd are non-essential trace element which can cause deleterious health effects in odontocetes at low concentrations; however, essential trace elements, if present in excess, can also cause negative health effects. Iron (Fe) is an essential element required for the oxygen-carrying enzymes hemoglobin and myoglobin (Sydeman, 1998). To compensate for long dives, marine mammals have high concentrations of myoglobin, which help deliver oxygen to muscles. As a result, blood Fe concentrations in marine

mammals can be as high as 1000 $\mu\text{g/g}$ wet weight (Sydeman,1998). However, in mammals, elevated concentrations of Fe can be determinantal to health, leading to the formation of hydroxyl radicals that decrease respiratory enzyme function (Hershko, 2007).

Other factors related to bioenergetics are also important considerations when interpreting tissue trace element concentrations. For example, in young odontocetes, body mass is added rapidly, which can reduce the concentration of contaminants (e.g., Hg) in tissues.; this process is called growth dilution. As juveniles age and growth rates slow, bioaccumulation is no longer offset by growth (Andre et al., 1991; Monteiro et al., 2016). Consequently, elements can bioaccumulate with age. Dietary sources also change as an odontocete is weaned and matures, which may influence trace element concentrations. Although sex is often an important explanatory variable in predicting tissue concentrations of persistent organic pollutants, differences between sexes are less likely to be observed for trace element concentrations (Das et al., 2003).

Gulf of Mexico (GoM) Habitats and Odontocetes

The GoM—the 9th largest body of water worldwide— is on average 4 km deep and spans 1.6 million km^2 . Approximately 32% of the area of the GoM is broad continental shelf <200 meters in depth; the remaining 41% and 24% of the area comprised of continental slope (>200 m and < 3,000 m in depth) and abyssal plain (>3,000 m in depth), respectively (Harris et al., 2012; Ward and Tunnell, 2017). The shoreline spans approximately 5,696 km and is bordered by the United

States, Mexico, and Cuba (Tunnel, 2009; Ward and Tunnell, 2017). The dominant oceanic current in the GoM is the Loop Current, which transports warm waters from the Caribbean Sea to the GoM through the Straits of Yucatan; the Loop Current moves northward toward the center of the GoM before moving southeast and exiting the GoM through the Florida Straits (Ward and Tunnell, 2017) (Figure 1.7). There are five, level one marine ecoregions in the GoM: the northern GoM, southern GoM, South Florida/Bahamian Atlantic, Caribbean Sea, and Greater Antilles (Figure 1.8).

All ecoregions act as receiving basins; overall, five countries (Canada, Cuba, Guatemala, Mexico, and the United States) contribute to the watershed drainage that enters the GoM (Figure 1.9; Ward and Tunnell, 2017). In the northern GoM, the Mississippi River, draining approximately 66% of the continental United States, is the prominent watershed feature. The coastal waters of the northern GoM support productive salt marshes, oyster reefs, and seagrass beds; however, eutrophication leads to habitat degradation and contributes to large expanses of hypoxic conditions (Ward and Tunnell, 2017). Although concentrations vary spatially, the presence of contaminants (e.g., trace elements, POPs) in sediment and resident organisms is ubiquitous throughout the coastal regions (Apeti et al., 2012; Kennicutt, 2017a). While concentrations of several trace elements (e.g., Cu, Cd, Pb, Hg, Ni) and pesticides (e.g., DDT, PCBs) have decreased due to increased environmental protections like the Clean Water Act of 1972, legacy pollutants persist in the environment (Sañudo-Wilhelmy and Gill, 1999; Santschi et al., 2001; Scholz et al., 2012). Further, pollution from non-point sources is challenging to manage and requires multinational cooperation to combat. Finally, the region is highly susceptible to oil spills from tankers and oil and gas platforms (Kennicutt, 2017b).

Twenty-nine confirmed species of marine mammals inhabit the GoM including, 27 species of the order Cetacea (21 species are of suborder Odontoceti and seven species are of the suborder Mysticeti) and one species manatee of the order Sirenia (Würsig, 2017). Although they have been documented, except for the Bryde's whale (*Balaenoptera brydei*), there are few records of mysticetes in the GoM. Of the odontocetes, there are 14 species from the family Delphinidae (dolphins), three species from the family Physeteridae (sperm whales), and four species from the family Ziphiidae (beaked whales) (Würsig, 2017). Only two species occur in waters <200 m. Bottlenose dolphins inhabit inshore (within the confines of bays, sounds, and estuaries), coastal (outside bays, sounds, and estuaries but within the 20m depth contour), continental shelf habitats (between 20m and 200m depth contours), and oceanic habitats (>200m depth). In contrast, Atlantic spotted dolphins (*Stenella frontalis*) occur primarily in continental shelf habitats. The remaining odontocete species occur in deeper offshore environments, either in waters above the continental slope or deep-oceanic habitats (Würsig, 2017).

Potential threats to marine mammals of the GoM include habitat degradation (e.g., eutrophication, harmful algal blooms), contaminants, ingestion of physical debris (e.g., plastics, derelict fishing gear), prey depletion, noise pollution, fisheries interactions (e.g., bycatch), vessel collisions, climate change, oil spills, and disturbances from humans (Würsig, 2017).

The Northern Gulf of Mexico Cetacean Unusual Mortality Event and Deepwater Horizon Oil Spill

The samples utilized in four of five data chapters in this dissertation were collected from odontocetes that stranded during and in the two years following the northern GoM Cetacean Unusual Mortality Event (UME) (2010-2014). A UME is defined by the Marine MMPA as a “stranding of marine mammals that is unexpected, resulting in a significant amount of die-off that demands an immediate response” (16 U.S.C. 1421h). While the northern GoM Cetacean UME included all stranded whales and dolphins, 87% of reported strandings were bottlenose dolphins (Litz et al., 2014). Of the remaining cetaceans, 8% could not be identified, and 5% were from species of the following genera: Balaenoptera, Feresa, Gloicephala, Grampus, Kogia, Mesoplodon, Peponocephala, Physeter, Stenella, and Steno. This UME was a unique event due to a variety of factors: first, it was the longest in duration (48 months) and resulted in the greatest number of cetacean mortalities (estimated 1,141) in the region (Litz et al., 2014), and second, two months following the declaration of the UME, the Deep-Water Horizon Oil Spill occurred, further perpetuating environmental stressors (Lane et al., 2015).

Dissertation Objectives

My dissertation focused on the use of stranded odontocetes, primarily bottlenose dolphins, from the northern GoM, to understand factors related to trace element accumulation in odontocetes. Chapter 2 explored the differences in skin and blubber Hg concentrations between bottlenose dolphins that stranded along the FL panhandle and LA coasts during and in the two years following the northern GoM Cetacean UME (2010-

2014). I investigated the influence of body length, age, sex, and stranding location on THg concentration in blubber and skin. Carbon ($\delta^{13}\text{C}$), nitrogen ($\delta^{15}\text{N}$), and sulfur ($\delta^{34}\text{S}$) stable isotope ratios in dolphin skin were also measured to determine if differences in dietary carbon source, relative trophic position, and foraging habitat could help explain variation in THg concentrations. Finally, I compared the use of body length and age as predictors of THg concentration using general linear models (GLMs). Body length is often used as a proxy for age since estimating age requires the analyses of annual growth layers in teeth. However, dolphins can continue to age after asymptotic length; therefore, I predicted that age would be a stronger predictor of tissue THg concentration than body length.

Chapter 3 is an expansion of the work presented in Chapter 2. Since Chapter 2 did not assign dolphins to local populations or source stocks, I was not able to explicitly address the influence of spatial and trophic variation on Hg concentrations in the skin of the stranded dolphins. In Chapter 3, I build on the work of Chapter 2 by (i) predicting the habitat (e.g., estuarine, barrier island, coastal) of stranded dolphins from FL and LA; (ii) estimating the mean trophic position of dolphins in each habitat, and (iii) determining the influence of trophic position on Hg levels. To accomplish these objects, first, I assigned dolphins to habitats according to the habitats based on their skin $\delta^{13}\text{C}$ and $\delta^{34}\text{S}$ following the splitting criterion reported in Hohn et al. (2017). Next, I estimated the trophic positions for stranded dolphins associated with each habitat by incorporating $\delta^{15}\text{N}$ values from dolphin prey and the stranded dolphins using a Bayesian approach. Finally, I compared the trophic positions and Hg concentrations between dolphins

of the different habitats to determine if trophic position influenced Hg concentrations.

Chapter 4 expanded beyond bottlenose dolphins, exploring the tissue-specific accumulation of Hg and Se and the potential protective role of Se against Hg toxicity in 11 tissues [blubber (dermis and subcutis), brain, kidney, liver, lung, muscle, placenta, skin (epidermis), spleen, umbilical cord, uterus] from 11 species of odontocetes [Atlantic spotted dolphin (*Stenella frontalis*), Blainville's beaked whale (*Mesoplodon densirostris*), bottlenose dolphin, dwarf sperm whale (*Kogia sima*), melon-headed whale (*Peponocephala electra*), pantropical spotted dolphin (*Stenella attenuata*), pygmy killer whale (*Feresa attenuata*), pygmy sperm whale (*Kogia breviceps*), Risso's dolphin (*Grampus griseus*), rough-toothed dolphin (*Steno bredanensis*), short-finned pilot whale (*Globicephala macrorhynchus*)] that stranded along the FL panhandle.

Chapter 5 investigated the effects of formalin preservation on trace element concentrations in bottlenose dolphin tissues. Formalin fixation is a common preservation technique, used particularly in marine mammal fields for histopathology; however, it is unclear if formalin fixed tissues can be used for trace element analyses or if formalin fixation changes trace element concentrations either by leaching contaminants from tissues or introducing elements to tissues. Having by chance obtain tissue sample pairs from bottlenose dolphins that had been preserved in formalin and frozen, I performed a long-term study to determine if trace element concentrations in tissues (blubber [dermis and subcutis], brain, kidney, liver, lung, and skin [epidermis]) that had been subsampled from the same individual dolphin, with one subsample frozen and the other subsample preserved in formalin for between 3 and 7 years varied. I measured the concentration of nine essential trace elements [cobalt (Co), chromium (Cr), Cu, Fe, Mn, nickel (Ni), Se,

vanadium (V), and Zn] and five nonessential elements (As, Cd, Hg, Pb, Sn). The long-term study was followed up by a short-term study that compared the effects of formalin on bottlenose dolphin liver, kidney, and lung trace element concentrations in a controlled study that lasted six weeks.

Compared to the previous data chapters that focus on determining trace element concentrations in soft tissues, Chapter 6 focused on trace element accumulation in teeth. Like the rings of a tree, dolphin teeth grow incrementally throughout their lives, with growth layers being deposited annually (Hohn et al., 1989). During tooth formation, trace elements incorporated into the tooth structure from dietary and environmental sources remain largely unaltered (Aubail et al., 2010). Tissue trace element concentrations may vary throughout an individual life due to biological factors and energy requirements, and growth layers of teeth provide a way to assess how trace elements change within an individual over time (Ando et al., 2005). In Chapter 6, I used a scanning electron microscope (SEM) equipped with Energy Disruptive Spectroscopy (EDS) to explore the distribution of major, minor, and trace elements within teeth from twelve bottlenose dolphins that stranded along the northern Texas coast in Galveston County between 1987 and 2014. The primary objectives were to assess if the presence and distribution of elements differed between tooth tissues (e.g., enamel vs. dentin) and if elements varied across the growth layers.

Table 1.1. Essential and non-essential elements, anthropogenic sources, and their biological roles (Liu et al., 2008)

Trace Elements	Anthropogenic Sources	Biological function (if applicable)
Essential elements		
Copper (Cu)	Mining and welding activities; antifouling paints; chromated copper arsenate wood preservatives	Component of metalloenzymes
Cobalt (Co)	Byproduct of copper and nickel mining	Cobalamin in an essential component of vitamin B12
Trivalent Chromium (Cr III)	Ferrochrome production; fertilizers; paper production; chrome plating	Glucose, protein, and fat metabolism
Iron (Fe)	Fossil fuel combustion	Component of hemoglobin, myoglobin, and heme enzymes
Magnesium (Mg)	NA	Cofactor for enzymes particularly related to the glycolytic cycle
Manganese (Mn)	Manganese based organometallic pesticides	Cofactor for enzymes particularly related to the glycolytic cycle
Nickel (Ni)	Crude oil; electroplating industry; fossil fuel combustion	Unknown
Selenium (Se)	Fossil fuel combustion	Selenoproteins; and component of glutathione peroxidase
Vanadium (V)	Crude oil; fossil fuel combustion	Cofactor for enzymatic reactions
Zinc (Zn)	Electroplating and smelting processes	Protein synthesis; enzymatic reactions
Non-essential elements		
Arsenic (As)	Pesticide manufacturing; burning of coal; copper arsenate wood preservatives	no known biological function
Cadmium (Cd)	Zinc and lead smelting; industrial emissions; fertilizers	
Hexavalent Chromium (Cr VI)	Ferrochrome production	
Lead (Pb)	Leaded gasoline; lead based paints; sheathing	
Mercury (Hg)	Coal fired power plants; artisanal gold mining; municipal waste	

Tin (Sn)	May be inorganic or organic tin; fungicide; slimicide (e.g., Tributyltin)	
----------	---	--

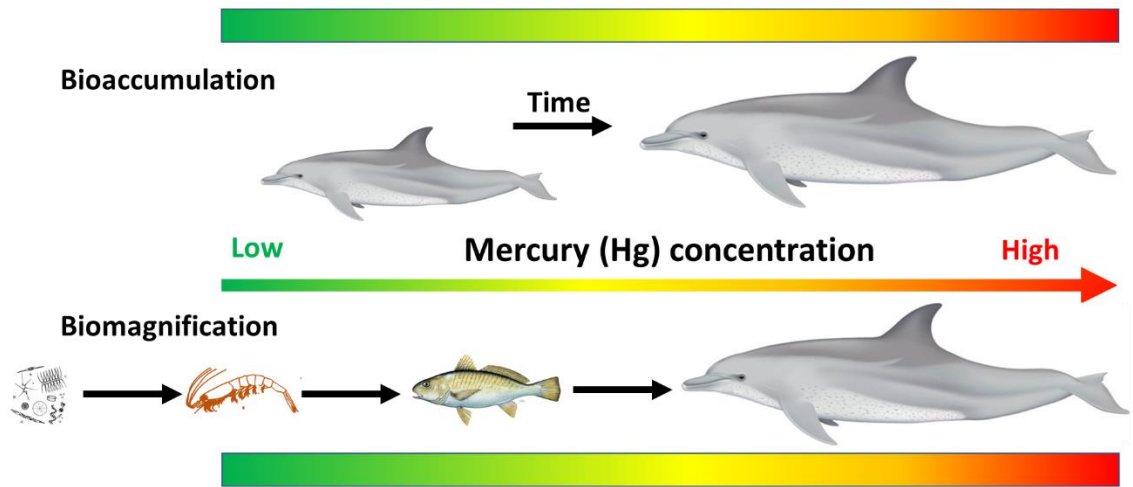


Figure 1.1. Graphical representation of bioaccumulation and biomagnification.

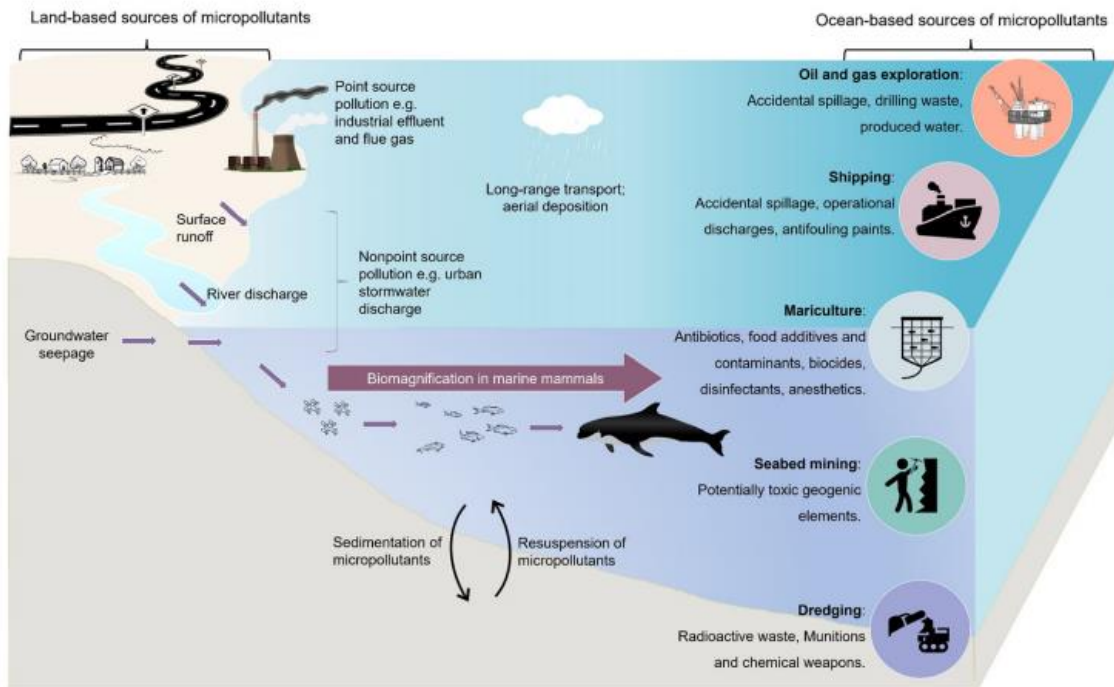


Figure 1.2. Atmospheric, marine, and terrestrial sources of contaminants in marine systems. Reproduced from Sanganyado, E., Bi, R., Teta, C., Buruaem Moreira, L., Yu, X., Yajing, S., Dalu, R., Rashid Rajput, ILiu, W. 2020. Toward an integrated framework for assessing micropollutants in marine mammals: Challenges, progress, and opportunities. *Crit. Rev. Environ. Sci. Technol.* 1-48. <https://doi.org/10.1080/10643389.2020.1806663>.

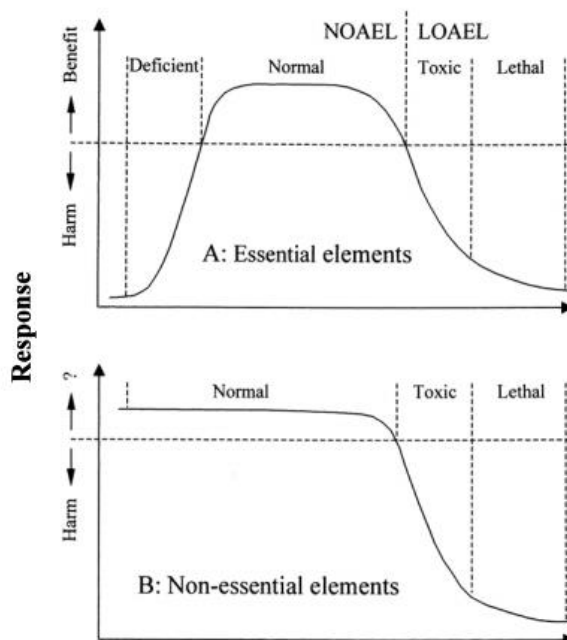


Figure 1.3. Dose-response curves for essential (A) and non-essential trace elements (B). NOAEL represents the first concentration to have no observable negative effect and LOAEL represents the lowest concentrations that negative effects begin to be observed. Republished with permission of Springer, from Trace Elements in Terrestrial Environments: Biogeochemistry, Bioavailability, and Risks of Metals, Domy C. Adriano, 2nd edition, 2002; permission conveyed through Copyright Clearance Center, Inc.

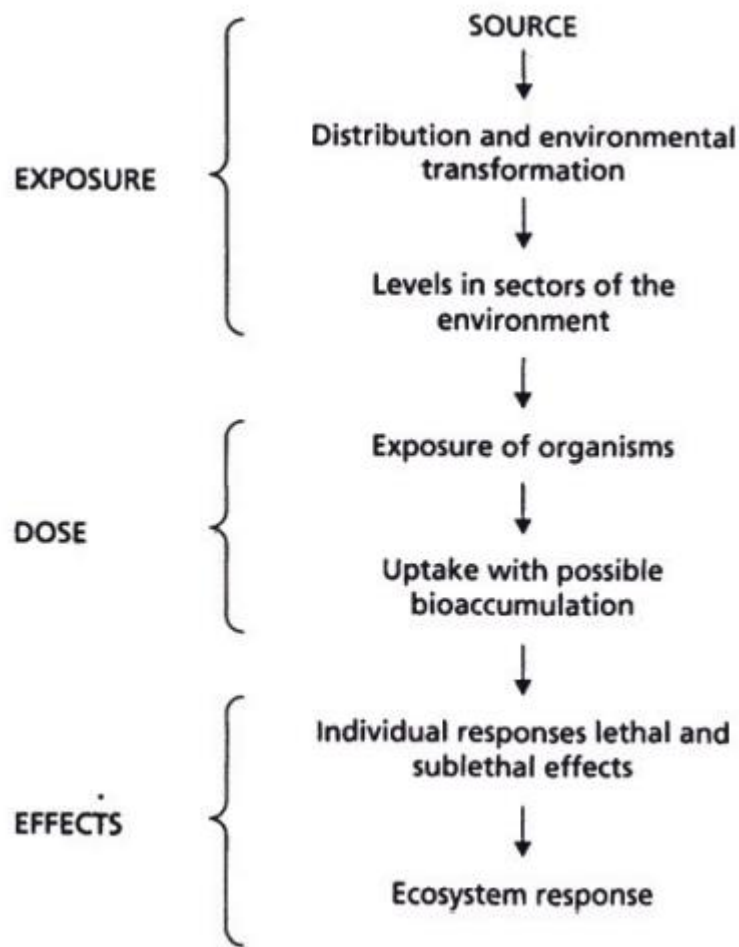


Figure 1.4. Flowchart depicting factors that influence the effect of a contaminant on individuals and populations beginning with the source. Republished with permission of John Wiley & Sons – Books, from Introduction to Ecotoxicology, Des W, Connell, Paul Lam, Bruce Richardson, Rudolf Wu, 1st edition, 2009; permission conveyed through Copyright Clearance Center, Inc.

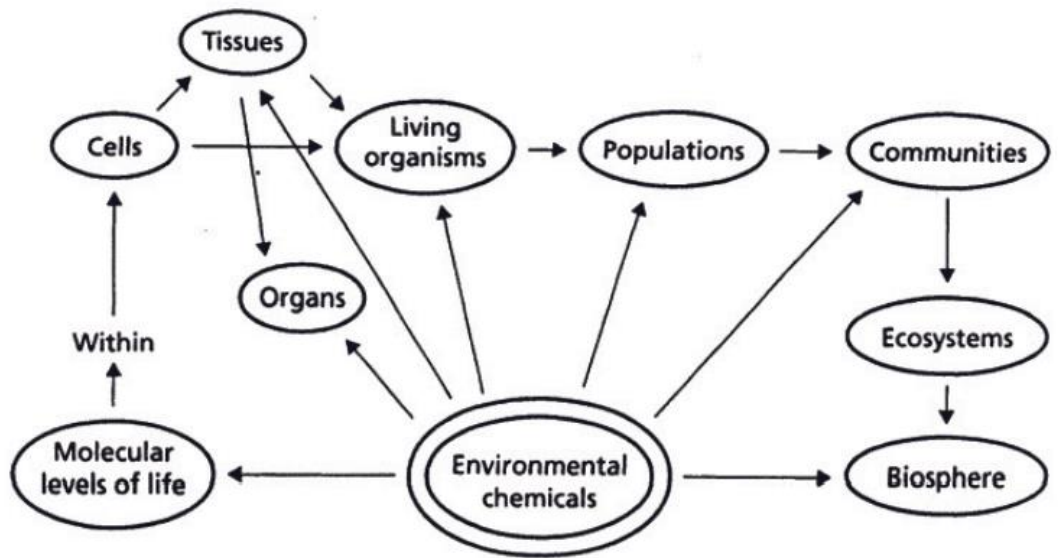


Figure 1.5. Levels of biological organization and focuses of toxicology studies. Republished with permission of John Wiley & Sons – Books, from Introduction to Ecotoxicology, Des W, Connell, Paul Lam, Bruce Richardson, Rudolf Wu, 1st edition, 2009; permission conveyed through Copyright Clearance Center, Inc.

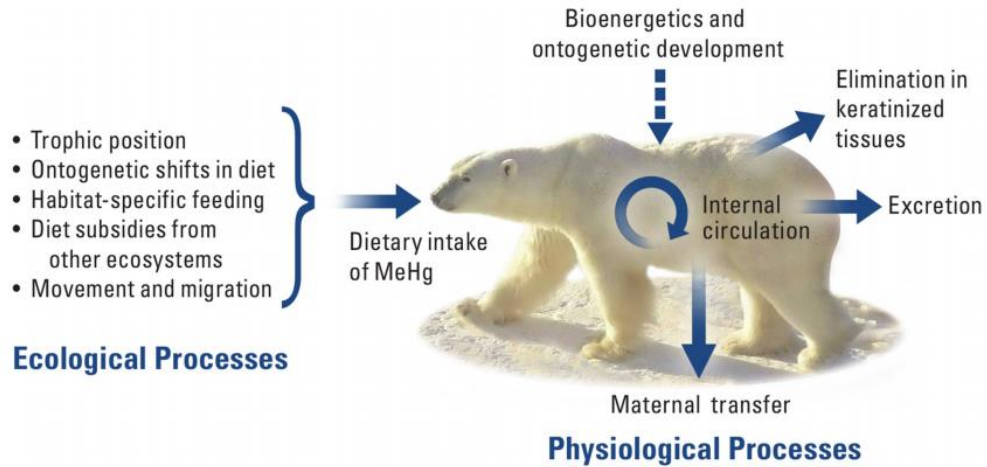


Figure 1.6. Conceptual diagram outlining the ecological and physical processes that influence methylmercury (MeHg) concentrations in wildlife reproduced Reprinted from Science of the Total Environment, 711, Chételat, J., Ackerman, J.T., Eagles-Smith, C.A., Hebert, C.E., Methylmercury exposure in wildlife: a review of physiological processes affecting contaminant concentrations and their interpretation, 135117, Copyright (2020), with permission from Elsevier.

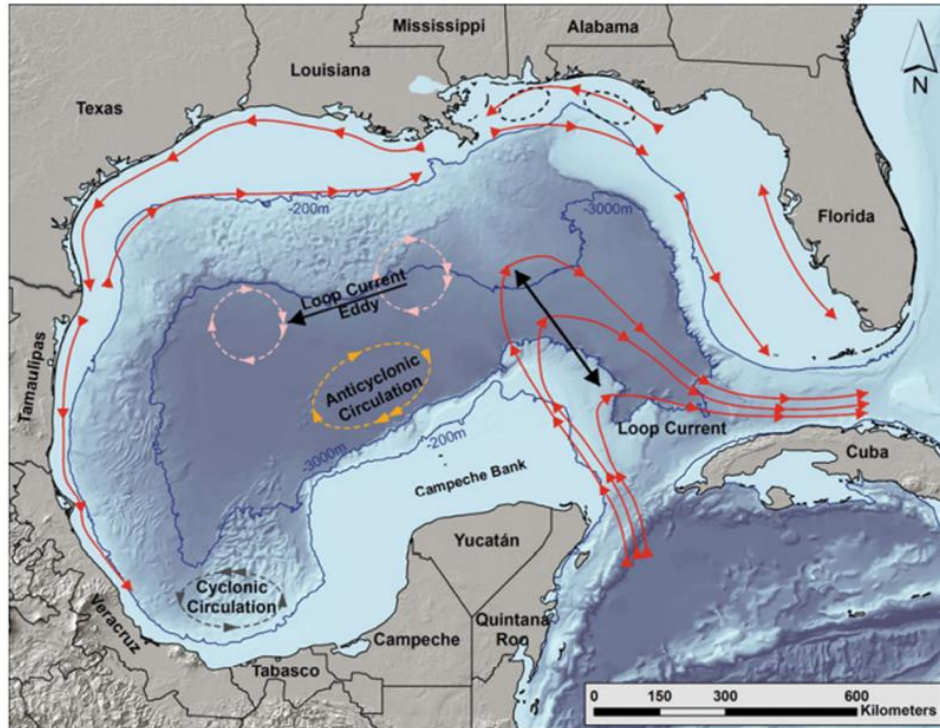


Figure 1.7. Map showing the Gulf of Mexico bathymetric contours and oceanic currents reproduced from Mendelssohn I.A., Byrnes M.R., Kneib R.T., Vittor B.A. (2017) Coastal Habitats of the Gulf of Mexico. In: Ward C. (eds) Habitats and Biota of the Gulf of Mexico: Before the Deepwater Horizon Oil Spill. Springer, New York, NY. Licensed CC BY-NC 2.5. https://doi.org/10.1007/978-1-4939-3447-8_6.

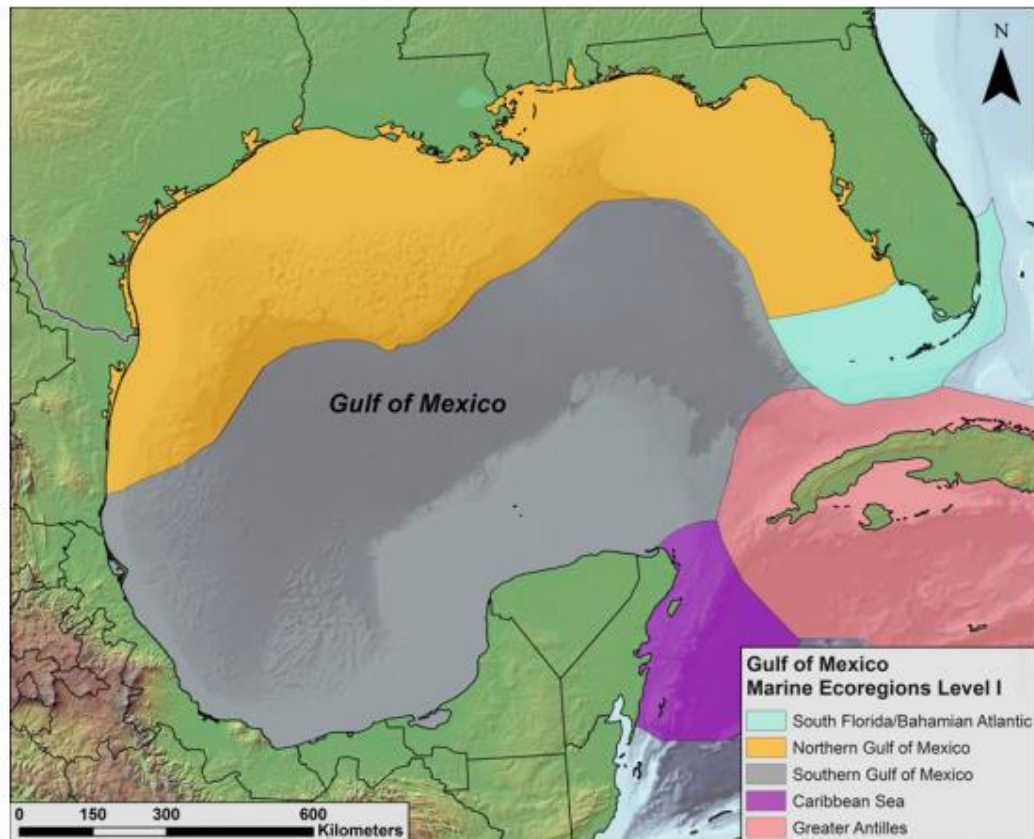


Figure 1.8. Map showing the Gulf of Mexico Level 1 Marine Ecosystems reproduced from Ward, C.H., Tunnell, J.W. Jr. 2017. Habitats and biota of the Gulf of Mexico an overview. In Ward, H.E. (Ed). Habitats and Biota of the Gulf of Mexico: Before the Deepwater Horizon Oil Spill. Volume 1: Water Quality, Sediments, Sediment Contaminants, Oil and Gas Seeps, Coastal Habitats, Offshore Plankton and Benthos, and Shellfish. Springer. New York, NY. pp 1-54. Licensed CC BY-NC 2.5. https://doi.org/10.1007/978-1-4939-3447-8_1.

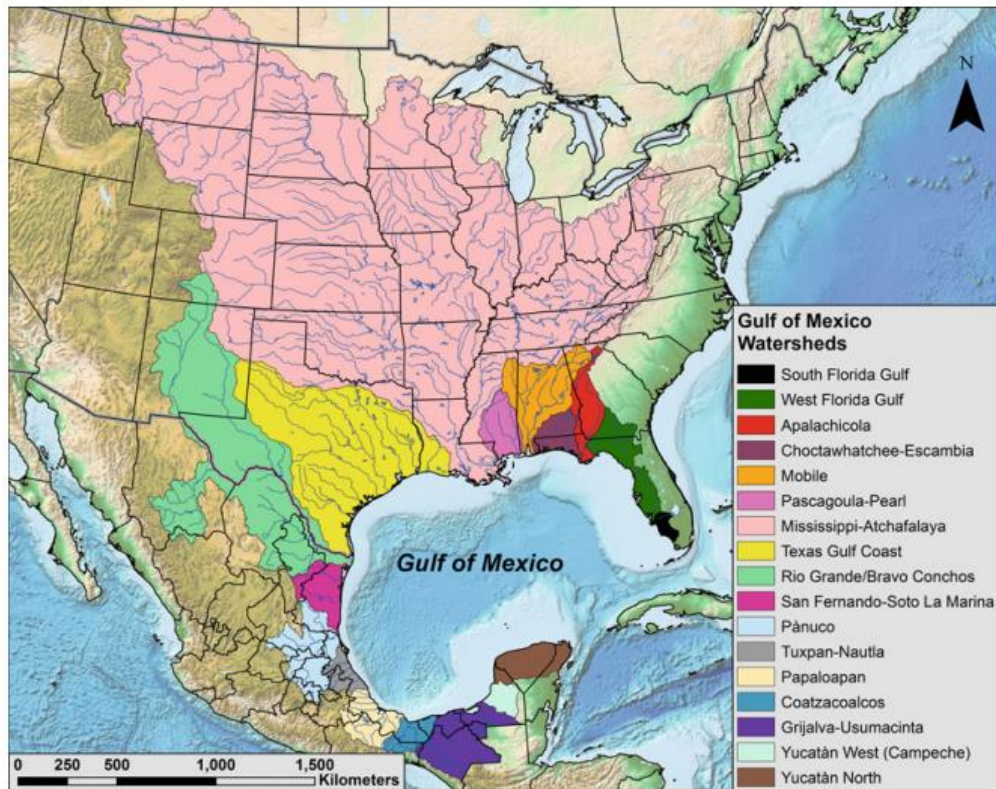


Figure 1.9. Map showing the watershed that contribute to the freshwater to the Gulf of Mexico reproduced from Mendelsohn I.A., Byrnes M.R., Kneib R.T., Vittor B.A. (2017) Coastal Habitats of the Gulf of Mexico. In: Ward C. (eds) Habitats and Biota of the Gulf of Mexico: Before the Deepwater Horizon Oil Spill. Springer, New York, NY. Licensed CC BY-NC 2.5. https://doi.org/10.1007/978-1-4939-3447-8_6.

**II. MERCURY CONCENTRATIONS IN BLUBBER AND SKIN FROM
STRANDED BOTTLENOSE DOLPHINS (*TURSIOPS TRUNCATUS*)
ALONG THE FLORIDA AND LOUISIANA COASTS (GULF OF
MEXICO, USA) IN RELATION TO BIOLOGICAL VARIABLES**

Citation: McCormack, M. A., Battaglia, F., McFee, W. E., & Dutton, J. (2020). Mercury concentrations in blubber and skin from stranded bottlenose dolphins (*Tursiops truncatus*) along the Florida and Louisiana coasts (Gulf of Mexico, USA) in relation to biological variables. *Environmental Research*, 180, 108886.

Abstract

Due to their long life-span and top trophic position, odontocetes can accumulate high concentrations of mercury (Hg) in their tissues. This study measured the concentration of total Hg (THg) in the blubber and skin of bottlenose dolphins (*Tursiops truncatus*) that stranded along the Florida (FL) panhandle and Louisiana (LA) coasts and investigated the relationship between total Hg (THg) concentration and sex, body length, age, stranding location, diet/trophic position ($\delta^{13}\text{C}$ and $\delta^{15}\text{N}$, respectively), and foraging habitat ($\delta^{34}\text{S}$). Additionally, we compared models using body length and age as explanatory variables to determine which was a better predictor of THg concentration. In both tissues, sex was not an influential predictor of THg concentration and there was a positive relationship between body length/age and THg concentration ($P < 0.001$). Florida dolphins had greater mean blubber and skin THg concentrations compared to LA dolphins ($P < 0.001$). There was a modest improvement in model fit when age was used

in place of body length. $\delta^{13}\text{C}$, $\delta^{15}\text{N}$, and $\delta^{34}\text{S}$ differed between stranding locations and together with age were significant predictors of THg concentrations ($R^2 = 0.52$, $P < 0.001$). Florida dolphins were $\delta^{13}\text{C}$ enriched compared to LA dolphins ($P < 0.001$) and THg concentrations were positively correlated with $\delta^{13}\text{C}$ ($R^2 = 0.22$, $P < 0.001$). Our results demonstrate spatial variability in THg concentrations from stranded bottlenose dolphins from the northern Gulf of Mexico; however, future research is required to understand how fine-scale population structuring of dolphins within FL and LA impacts THg concentrations, particularly among inshore (bay, sound, and estuary) stocks and between inshore and offshore stocks, as variations in biotic and abiotic conditions can influence both stable isotope ratios and THg concentrations.

Introduction

Mercury (Hg) is a pollutant of great concern for both human and ecosystem health due to its toxicity and persistence in the environment (Selin, 2009). In marine systems, sulfate-reducing bacteria convert inorganic Hg (Hg^{2+}) to methylmercury (CH_3Hg^+ ; MeHg) which enters the food web via phytoplankton, bioaccumulates in organisms, and biomagnifies up marine food webs (Hammerschmidt and Fitzgerald, 2006; Fitzgerald et al., 2007). Due to their long-life span and top trophic position, odontocetes can accumulate high concentrations of Hg in their tissues (Das et al., 2003; Stavros et al., 2007; Hong et al., 2013; Monteiro et al., 2016). Mercury, particularly MeHg, can cause adverse neurological, behavioral, and reproductive effects in wildlife (Scheuhammer et al., 2007). Given that dolphins are long-lived species, which have few offspring, populations would be slow to recover from the toxic effects of a pollutant such

as Hg; therefore, it is important to monitor Hg levels in dolphins to determine potential threats to individual and population health.

In the Gulf of Mexico, certain fish species [e.g., golden tilefish (*Lopholatilus chamaeleonticeps*), king mackerel (*Scomberomorus cavalla*), and Spanish mackerel (*S. maculatus*)] as well as bottlenose dolphins (*Tursiops truncatus*) have greater Hg concentrations compared to conspecifics from the Atlantic Ocean (Hall et al., 1978; Stein et al., 2003; Adams and McMichael, 2007). While atmospheric wet Hg deposition rates along the Gulf of Mexico coast are amongst the highest in the U.S., the Atlantic Ocean—which delivers Hg via the Loop Current—is estimated to be the predominant source of Hg to the Gulf of Mexico as a whole (National Atmospheric Deposition Program, 2007; Selin and Jacob, 2008; Harris et al., 2012). However, within the Gulf of Mexico, Hg is not evenly distributed, and some regions are more influenced by riverine (e.g., Mississippi River) and atmospheric Hg sources (Harris et al., 2012). Spatial differences in Hg concentrations within the Gulf of Mexico have been observed in resident fish [e.g., red drum (*Sciaenops ocellatus*); red snapper (*Lutjanus campechanus*)] and oysters [e.g., American oyster (*Crassostrea virginica*)]; these spatial differences in lower trophic level consumers may be biomagnified through the food web and, in turn, reflected in the tissues of top predators such as bottlenose dolphins (Adams and Onorato, 2005; Apeti et al., 2012; Sluis et al., 2013).

Bottlenose dolphins are one of the most abundant cetacean species in the Gulf of Mexico and are categorized as inshore (e.g., bay, sound, and estuarine), coastal (up to 20-m isobath), continental shelf (20 – 200 m depth), and oceanic (> 200 m depth) stocks (Vollmer and Rosel, 2013; Waring et al., 2015). For management purposes, in the

northern Gulf of Mexico, the National Oceanic and Atmospheric Administration (NOAA)/National Marine Fisheries Service (NMFS) has designated 31 distinct bay, sound, and estuary and 3 coastal bottlenose dolphin stocks (eastern, northern, and western) (Vollmer and Rosel, 2013; Waring et al., 2015). Bay, sound, and estuary stocks were designated in 1995, in response to studies from the 1970s and 1980s which documented year-round residency of individual dolphins in Sarasota Bay, Florida, and bays in Texas; since these early studies residence patterns have been confirmed throughout the northern Gulf of Mexico in the majority of locations for which photo-identification and/or tagging studies have been conducted (Shane, 1977; Gruber 1981; Irving et al., 1981; Wells and Scott, 1990; Hubbard et al., 2004; Irwin and Würsig, 2004; Balmer et al., 2008; Bassos-Hull et al., 2013; Waring et al. 2015; Wells et al., 2017). Previous studies have shown that body length, age, sex, diet, and habitat can influence Hg concentrations in dolphins; such findings merit further investigation in the northern Gulf of Mexico because inshore populations of bottlenose dolphins often show strong habitat associations and are highly susceptible to Unusual Mortality Events (Meador et al., 1999; Stavros et al., 2007; Hong et al., 2012; Litz et al., 2014; Monteiro et al., 2016; Damseaux et al., 2017).

Dolphins are primarily exposed to Hg through their diet, incorporating Hg, mostly in the form of MeHg, from the muscle tissue of their prey (Hong et al., 2012). To understand differences in Hg concentrations among dolphin populations, it is important to identify differences in dietary sources and foraging habitats. Traditionally, dietary studies for dolphins were limited to direct observation or analysis of stomach contents (Silva, 1999; Blanco et al., 2001; Tollit et al., 2010). More recently, carbon ($\delta^{13}\text{C}$), nitrogen

($\delta^{15}\text{N}$), and sulfur ($\delta^{34}\text{S}$) stable isotope ratios in dolphin tissues have been used to obtain estimates of an individual's dietary carbon source, trophic position, and foraging habitat, respectively (Loseto et al., 2008; Newsome et al., 2010; Tollit et al., 2010). Therefore, stable isotope ratios may help explain variation in Hg concentrations among dolphin populations. Dolphin skin is commonly utilized in stable isotope studies, reflecting the diet, trophic position, and foraging habitat of an individual over a period of approximately 6 to 8 weeks, and Hg concentrations in dolphin skin have been successfully utilized to differentiate between populations (Browning et al., 2014; Dirtu et al., 2016; Damseaux et al., 2017; Hohn et al., 2017). While there have been several studies that report Hg concentrations in bottlenose dolphins from the Gulf of Mexico, particularly from the Florida (FL) peninsula as well as the Texas coast, there are no studies on Hg concentrations in dolphins from inshore populations along the FL panhandle and only one study which reported Hg concentrations in a single dolphin from Louisiana (LA) (Kuehl and Haebler, 1995; Meador et al., 1999; Stein et al., 2003; Bryan et al., 2007; Woshner et al., 2008; Damseaux et al., 2017). In addition, in the northern Gulf of Mexico, there are no studies that analyze Hg in combination with stable isotope ratios in bottlenose dolphins from the northern and western coastal stocks and corresponding bay, sound, and estuary stocks.

The objective of this study was to compare total Hg (THg) concentrations between stranded bottlenose dolphins along the FL panhandle and LA coasts. In the present study, the epidermis, hereafter referred to as skin, was removed from the blubber (dermis and subcutis) (Cozzi et al., 2017). We investigated the influence of body length, age, sex, and stranding location on THg concentration in blubber and skin. In addition,

we measured the $\delta^{13}\text{C}$, $\delta^{15}\text{N}$, and $\delta^{34}\text{S}$ stable isotope ratios in dolphin skin to determine if differences in dietary carbon source, trophic position, and foraging habitat could help explain variation in THg concentrations. Finally, general linear models (GLMs) were used to determine whether body length or age was a better predictor of THg concentration.

Methods

Sample collection

In total, tissue samples from 184 bottlenose dolphins which stranded along the FL panhandle (n=63) and LA (n=121) coasts between 2011 and 2016 (Figure 2.1) were collected by local stranding networks authorized by NOAA. Because the source stock of the stranded individuals was unknown, samples were separated by stranding location (e.g., FL, LA); however, based on carcass drift models developed specifically for the northern Gulf of Mexico, we expect the stranded animals originated primarily from nearby inshore and coastal stocks (DWH MMIQT, 2015). Collecting samples from large numbers of dolphins is rare and was only possible due to the Northern Gulf of Mexico Cetacean Unusual Mortality Event (2010-2014) (Litz et al., 2014). However, for many individuals, both tissues were not available for the present study [blubber: FL (n=48), LA (n=112); skin: FL (n=36), LA (n=93)]. Twenty-four individuals from FL and 84 individuals from LA had both blubber and skin samples. At the time of sampling, body length, sex, and condition code were recorded. A summary of the biological data collected from the stranded dolphins can be found in Table 2.1. Condition codes ranged from 2-4 (code 2 = fresh, code 3 = moderate decomposition, code 4 = advanced

decomposition; Smithsonian Institution Coding System; Geraci and Lounsbury, 2005). In FL, 43%, 31%, and 26% of blubber samples came from code 2, 3, and 4, individuals, respectively. In LA, 4%, 9% and 87% of blubber samples came from code 2, 3, and 4, individuals, respectively. In FL, 19%, 19%, and 62% of skin samples came from code 2, 3, and 4, individuals, respectively. In LA, 4%, 7%, and 89% of skin samples came from code 2, 3, and 4 individuals, respectively. While samples from code 2 or code 3 individuals are preferable for Hg and stable isotope analysis, other studies have successfully utilized samples from code 3 and code 4 individuals (Payo-Payo et al., 2013; Hohn et al., 2017; Martínez-López et al. 2019). Samples were stored at -20° C at a NOAA facility and shipped to Texas State University where they were held at -20° C until THg analysis. Teeth were also collected at the time of necropsy and preserved for age determination. All samples in this study were obtained under a NOAA parts authorization letter pursuant to 50 CFR 216.22.

Age determination

Teeth were collected from the left lower mandible (generally teeth positioned at numbers 13-16 in the row), stored in 10% neutral-buffered formalin for up to 48 h, rinsed in tap water, and archived in 70% ethyl alcohol. Teeth were then prepared for sectioning using standard procedures (Myrick et al., 1983; Hohn et al., 1989). A 1-2 mm thick section (slab) was taken from each tooth of dolphins > 140 cm body length. For dolphins with a body length of < 140 cm, a slab was not taken, but rather the tooth was decalcified whole and then thin sectioned. The slabs were cut using a diamond wafer blade mounted on a Buehler Isomet low speed saw (Emerson Industrial Automation, Lake Bluff, IL), rinsed in tap water for approximately 6 h, and then decalcified in RDO (rapid

decalcifying agent of acids; Apex Engineering Products Corporation, Aurora, IL) for 6-12 h based on the thickness of the slab. The slabs were then rinsed overnight and thin-sectioned on a Leica SM2000R sledge microtome (Leica, Inc., Nussloch, Germany) attached to a Physitemp freezing stage (Physitemp, Inc., Clifton, NJ). Thin sections were stained in Mayer's hematoxylin, blued for 30 s in a weak ammonia solution, dried on a slide, and mounted in 100% glycerin.

Sections were read three times using a Nikon SMZ1500 stereomicroscope (Nikon Instruments, Inc., Lewisville, TX). At least one week elapsed between readings to reduce bias. Teeth were aged based on Hohn et al. (1989); if two of the three readings were the same, that was used as the age estimate, whereas if differences between readings were < 2 growth layer groups (GLG's), a fourth reading was made. Differences > 2 GLG's required another tooth to be sectioned and the process repeated. Age estimates < 1 GLG were calculated from measurements using SPOT Imaging software (Diagnostic Instruments, Inc., Sterling Heights, MI), while others > 1 GLG were rounded to 0.50 GLG. Most teeth > 5 GLG's were estimated to the last GLG.

THg analysis

Samples were thawed, the skin (epidermis) was separated from the blubber (dermis and subcutis) using a ceramic knife, and the wet weight (wet wt) of each tissue was recorded. During sample processing, samples were visually inspected, and those that were severely decomposed—to the point at which the boundary between the epidermis and blubber was not clear—were excluded from the study. Samples were then freeze-dried (Labconco FreezeZone 2.5; Labconco, Kansas City, MO) for 48 h at -54°C and the dry weight (dry wt) was recorded. The % water content (mean \pm 1 SD) was $41 \pm 14\%$

(range: 11-80%) and $47 \pm 14\%$ (range: 14-84%) for blubber and skin, respectively. Using a clean stainless-steel scalpel, both skin and blubber samples were cut into approximately 4x4 mm pieces.

The THg concentration in blubber (10-15 mg) and skin (10-20 mg) was determined using a Direct Mercury Analyzer (DMA-80; Milestone Inc., Shelton, CT) using thermal decomposition, gold amalgamation, and atomic absorption spectrometry as described in EPA method 7473 (U.S. EPA, 2007). The DMA was calibrated using certified reference materials [CRM; MESS-4 marine sediment, 0.08 $\mu\text{g/g}$ THg; TORT-3 lobster hepatopancreas, 0.292 $\mu\text{g/g}$ THg; and PACS-3 marine sediment, 2.98 $\mu\text{g/g}$ THg; National Research Council Canada (NRCC)] as needed. Quality control included blanks ($n = 70$) and CRMs ($n = 71$) [DORM 4 (fish protein, NRCC, 0.412 $\mu\text{g/g}$ THg) or ERM-CE464 (tuna fish, European Reference Material, 5.24 $\mu\text{g/g}$ THg)] with every 10 samples analyzed. The blanks had a THg concentration $< 0.0000 \mu\text{g/g}$ and the recovery values for the CRM/SRM were $96.8 \pm 3.8\%$ for DORM-4 ($n = 41$) and $98.7 \pm 2.1\%$ ERM-CE464 ($n = 30$). In addition, duplicates of blubber ($n = 26$) and triplicates of skin ($n = 133$) samples were analyzed. The mean \pm SD of the relative percent difference for blubber duplicates was $16 \pm 14\%$ (range = 0.18 – 0.55%); differences in oil content in blubber samples among individual dolphins may account for the wide range in relative percent differences. Triplicates of skin samples were analyzed because of the heterogeneous condition of the samples and all triplicate samples had $< 10\%$ relative difference.

Stable isotope analysis

Freeze-dried skin samples from FL ($n = 34$) and LA ($n = 90$) dolphins were lipid extracted using methanol and chloroform following the method described in Post et al.

(2007) and cut into approximately 1x1 mm pieces. Between 0.5-1.0 mg and 2.5-3.5 mg of each sample was weighed and packaged into tin capsules for dual $\delta^{13}\text{C}/\delta^{15}\text{N}$ and $\delta^{34}\text{S}$ analysis, respectively. Stable isotope ratios were determined using an elemental analyzer [$\delta^{13}\text{C}/\delta^{15}\text{N}$ (PDZ Europa ANCA-GSL); $\delta^{34}\text{S}$ (Elementar vario ISOTOPE cube)] interfaced to a continuous-flow isotope ratio mass spectrometer [$\delta^{13}\text{C}/\delta^{15}\text{N}$ (PDZ Europa 20-20; Sercon Ltd., Cheshire, UK); $\delta^{34}\text{S}$ (SerCon 20-22 IRMS; Sercon Ltd., Cheshire, UK)] at the UC Davis Stable Isotope facility (Davis, CA). Results were expressed in δ -notation using the following equation:

$$\delta_{\text{Sample}}(\text{‰}) = [(R_{\text{Sample}}/R_{\text{Standard}}) - 1] \times 1000$$

where R is the molar ratio of heavy to light isotopes ($\text{C}^{13}/\text{C}^{12}$, $\text{N}^{15}/\text{N}^{14}$, or $\text{S}^{34}/\text{S}^{32}$). The standards used were Vienna Pee Dee Belemnite, atmospheric nitrogen, and Vienna-Canyon Diablo Troilite for $\delta^{13}\text{C}$, $\delta^{15}\text{N}$, and $\delta^{34}\text{S}$, respectively. To determine the analytical accuracy of $\delta^{13}\text{C}$ and $\delta^{15}\text{N}$, replicate samples of bovine liver (nominal $\delta^{13}\text{C} = -21.7\text{‰}$, measured $\delta^{13}\text{C} = -21.7\text{‰} \pm 0.08$; nominal $\delta^{15}\text{N} = +7.72\text{‰}$, measured $\delta^{15}\text{N} = +7.63\text{‰} \pm 0.07$; n = 4), glutamic acid (nominal $\delta^{13}\text{C} = -16.7\text{‰}$, measured $\delta^{13}\text{C} = -16.6\text{‰} \pm 0.12$; nominal $\delta^{15}\text{N} = -6.8\text{‰}$, measured $\delta^{15}\text{N} = -6.77\text{‰} \pm 0.06$; n = 11), enriched alanine (nominal $\delta^{13}\text{C} = +43.0\text{‰}$, measured $\delta^{13}\text{C} = +43.0\text{‰} \pm 0.13$; nominal $\delta^{15}\text{N} = +41.1\text{‰}$, measured $\delta^{15}\text{N} = +41.1\text{‰} \pm 0.06$; n = 8), and nylon-6 (nominal $\delta^{13}\text{C} = -27.8\text{‰}$, measured $\delta^{13}\text{C} = -27.8\text{‰} \pm 0.04$; nominal $\delta^{15}\text{N} = -10.5\text{‰}$, measured $\delta^{15}\text{N} = -10.5\text{‰} \pm 0.06$; n = 46) were analyzed. To determine the analytical accuracy of $\delta^{34}\text{S}$, replicate samples of cysteine (nominal $\delta^{34}\text{S} = +34.2\text{‰}$; measured $\delta^{34}\text{S} = +34.2\text{‰} \pm 0.28$; n = 25), hair (nominal $\delta^{34}\text{S} = +2.7\text{‰}$; measured $\delta^{34}\text{S} = +2.8\text{‰} \pm 0.32$; n = 63), Mahi-Mahi muscle (nominal $\delta^{34}\text{S} = +19.5\text{‰}$; measured $\delta^{34}\text{S} = +19.5\text{‰} \pm 0.25$; n = 71), whale

baleen (nominal $\delta^{34}\text{S} = + 17.5\text{‰}$; measured $\delta^{34}\text{S} = + 17.7\text{‰} \pm 0.43$; $n = 69$), and taurine (nominal $\delta^{34}\text{S} = - 2.5\text{‰}$; measured $\delta^{34}\text{S} = - 2.5\text{‰} \pm 0.20$; $n = 30$) were analyzed.

Duplicates ($n = 18$) were run for every 20 samples and the relative % difference among duplicate samples was 5% for $\delta^{13}\text{C}$, 3% for $\delta^{15}\text{N}$, and 3% for $\delta^{34}\text{S}$.

Statistical analysis

All data were explored for outliers and collinearity following Zuur et al. (2010). For both stranding locations, a one-way ANOVA was performed to determine if mean THg concentrations differed between blubber and skin tissues. One-way ANOVAs were also used to compare THg concentrations between stranding locations for both tissues. To compare THg concentrations between dolphins which stranded in FL and LA, for both blubber and skin tissues, multiple linear regressions were used to determine the effect of body length (continuous), age (continuous), sex (categorical, reference: female), condition code (integer), stranding location (categorical, reference: FL), and stranding year (categorical, reference: 2011) on THg concentration. Body length and age were not included in the same model due to the correlation between these two covariates. To assess potential differences in dietary carbon source, trophic position, and foraging habitat between dolphins which stranded in FL and LA, multiple linear regressions were used to determine the effect of body length, age, sex, condition code, stranding location, stranding year, and stranding month (categorical, reference: January) on $\delta^{13}\text{C}$, $\delta^{15}\text{N}$, and $\delta^{34}\text{S}$ in skin tissues. Multiple linear regressions were also used to describe the combined influence of body length or age, stable isotope ratios, condition code, and stranding year on skin THg concentrations. Month was included as a predictor in stable isotope models because, the isotopic values in dolphin skin reflects prey consumption from the previous

6 to 8 weeks (Browning et al., 2014); however, month was excluded from models in which THg was the response variable because, Hg, particularly MeHg, which has an estimated biological half-life of 1000 days in striped dolphins (*Stenella coeruleoalba*), is retained in the body over time (Itano and Kawai, 1981; Nigro et al., 2002).

Because the response variables (THg, $\delta^{13}\text{C}$, $\delta^{15}\text{N}$, or $\delta^{34}\text{S}$) could be influenced by several predictors, an Akaike Information Criterion (AIC) model selection was used to determine which combination of explanatory variables best explained the variation in the response variable. To account for small sample sizes, AIC_c was estimated. For each set of models, after all combinations of explanatory variables were considered, an optimal model was chosen based on the lowest AIC_c value (Akaike, 1973; Symonds and Moussalli, 2011). However, because the penalty for one additional parameter is +2 AIC units it is possible to obtain a competing model within 2 AIC units of the top model that differs in only one parameter. In some cases, the additional parameter is uninformative and does not explain enough variation to justify inclusion in the model (Arnold, 2010). Following Arnold (2010), all models were reported in the supplementary data (Table S2.1-S2.12), but uninformative parameters ($P > 0.157$) were removed from the final model reported in the text. A Gaussian distribution was applied as all response variables (THg, $\delta^{13}\text{C}$, $\delta^{15}\text{N}$, and $\delta^{34}\text{S}$) were continuous variables. Models were validated by checking the assumptions of normality and homoscedasticity through the visual inspection of residual plots. If models failed to meet the assumptions data were Log10 transformed. Final models were compared using R^2 values to determine whether body length or age best explained the variation in Hg concentrations. A Gompertz growth

curve was fit to age and body length data for each stranding location to determine asymptotic growth using the following equation:

$$\text{Body length} = \text{Asym} * \exp(-b2 * b3^x)$$

where asym = asymptote, b2 = the x axis displacement, b3 = growth rate, and x = age (R Core Team, 2018; R packages: nlme and nlshelper). Finally, to account for potential ontogenetic effects which could influence the interpretation of isotopic results, a two-factor ANOVA was used to determine the effect of life stage and stranding location on stable isotope ratios. Life stage was categorized based on body length (calves \leq 183 cm; juveniles/adults $>$ 183 cm) and age (calves \leq 3.5 years; juvenile/adults $>$ 3.5 years) and analysis was performed using both categorization methods (Wells et al., 1987; Knoff et al., 2008). A single separation between calves and juveniles/adults was chosen to identify potential isotopic differences between nursing calves and dolphins which were independently foraging. Data analysis was performed in R v.3.4.0 (R Core Team, 2018) and the level of significance was set at $\alpha = 0.05$ for all analyses except for model parameter selection as described above.

Results

Blubber and skin THg concentrations

Mean blubber THg concentrations were significantly less than mean skin THg concentrations in both FL (ANOVA; $P < 0.001$) and LA (ANOVA; $P = 0.005$) (Figure 2.2). In FL dolphins, the mean \pm SD blubber THg concentration was 2.36 ± 2.71 $\mu\text{g/g}$ dry wt (range: 0.0378 – 13.9 $\mu\text{g/g}$ dry wt) or 1.25 ± 1.21 $\mu\text{g/g}$ wet wt (range: 0.0295 – 5.69 $\mu\text{g/g}$ wet wt) and the mean \pm SD skin THg concentration was 4.36 ± 3.55 $\mu\text{g/g}$ dry wt

(range: 0.562 – 14.7 $\mu\text{g/g}$ dry wt) or 2.25 ± 2.41 $\mu\text{g/g}$ wet wt (range: 0.225 – 12.3 $\mu\text{g/g}$ wet wt). In LA dolphins, the mean \pm SD blubber THg concentration was 1.33 ± 2.78 $\mu\text{g/g}$ dry wt (range: 0.0163 – 24.9 $\mu\text{g/g}$ dry wt) or 0.679 ± 1.18 $\mu\text{g/g}$ wet wt (range: 0.0125 – 8.96 $\mu\text{g/g}$ wet wt) and the mean \pm SD skin THg concentration was 1.94 ± 3.51 $\mu\text{g/g}$ dry wt (range: 0.0531 – 25.2 $\mu\text{g/g}$ dry wt) or 1.06 ± 1.81 $\mu\text{g/g}$ wet wt (range: 0.0305 – 9.98 $\mu\text{g/g}$ wet wt). There were significant differences in mean THg concentrations between FL and LA dolphins for both blubber (ANOVA; $P < 0.001$) and skin (ANOVA; $P < 0.001$).

Blubber and skin THg concentrations in relation to explanatory variables

Overall, bottlenose dolphins in this study had a mean (\pm SD) body length of 212 cm \pm 53 (range: 74 – 285 cm). Dolphins that stranded in FL and LA had a mean (\pm SD) body length of 207 cm \pm 54 (range: 90 – 278 cm) and 218 cm \pm 54 (range 74 – 285 cm), respectively. Age was determined for 141 dolphins for which teeth were available. Dolphins ranged from < 2 months to 35 years old with the mean (\pm SD) being 14.7 ± 10.0 years. A Gompertz growth curve provided a good fit to the data for both FL and LA dolphins (Figure 2.3). In both locations, there was a rapid increase in growth through age 5 followed by a slowing of growth until an asymptotic body length was reached (243 cm and 252 cm for combined male and female FL and LA dolphins, respectively).

For blubber, when using body length as a proxy for age, the optimal model based on the lowest AIC_c value included body length, stranding location, and condition code as significant predictors of THg concentration. For skin, when using body length as a proxy for age, the optimal model based on the lowest AIC_c value included body length, stranding location, and stranding year as significant predictors of THg concentration. Sex was not an influential predictor of THg for either tissue (Table 2.2). In both tissues, THg

concentrations increased with body length, but there was greater variation in THg concentrations among larger (> 225 cm) individuals compared to smaller individuals (≤ 225 cm) (Figure 2.4). When body length was used as a covariate, FL dolphins had greater THg concentrations compared to LA dolphins. In the blubber model, condition code had a positive influence on THg concentration; however, the addition of condition code to the model did not improve the overall model fit. Condition code was not influential in the skin model, but our analysis was limited because, most skin samples were from code 4 samples. In the skin model, stranding year was also an influential predictor of THg, but the influence of stranding year was likely driven by differences in the proportions of calves and juveniles/adults among sampling years (Table 2.2). For skin, THg concentrations were lower in 2011 compared to other samplings years; however, in 2011 a greater proportion of calves (40%) were sampled whereas in all other years between 75-100% of sampled individuals were juveniles/adults which have greater THg concentrations compared to calves.

Similarly, when using age as a predictor, in both blubber and skin, THg concentrations significantly increased with age and FL dolphins had greater THg concentrations compared to LA dolphins. For both tissues, sex was not a significant predictor of THg concentrations. Condition code positively influenced skin Hg concentrations; however, the addition of condition code as a parameter did not improve overall model fit. Stranding year was not determined to be an influential predictor in age models (Table 2.2). Since the influence of stranding year appeared to be driven by sample collection and was not significant in age models, stranding year was excluded in the multiple linear regressions shown in Figure 2.5. Condition code was also excluded from

Figure 2.5 as it did not improve the model fit. For both blubber and skin models, there was slight improvement in model fit when age was used as a predictor of THg concentration instead of body length. Overall, skin models explained more of the variation in THg concentrations than blubber models (Table 2.2; Figure 2.5).

Stable isotope ratios in relation to explanatory variables

Optimal models based on the lowest AIC_c values revealed that stranding year and month were not influential predictors of $\delta^{13}\text{C}$, $\delta^{15}\text{N}$, or $\delta^{34}\text{S}$. Sex was only influential in the $\delta^{13}\text{C}$ and body length model. Body length and age were significant predictors of $\delta^{13}\text{C}$ and $\delta^{15}\text{N}$, but not of $\delta^{34}\text{S}$. $\delta^{13}\text{C}$ was positively influenced by body length/age while $\delta^{15}\text{N}$ was negatively influenced by body length/age. Stranding location was a significant predictor of $\delta^{13}\text{C}$, $\delta^{15}\text{N}$, and $\delta^{34}\text{S}$. Condition code positively influenced $\delta^{13}\text{C}$ and $\delta^{15}\text{N}$, but not $\delta^{34}\text{S}$ (Table 2.2). In FL, code 4 individuals were on average 0.50‰ and 0.71‰ more enriched in $\delta^{15}\text{N}$ and $\delta^{13}\text{C}$, respectively, compared to code 2 individuals. In LA, code 4 individuals were on average 1.5‰ and 0.75‰ more enriched in $\delta^{15}\text{N}$ and $\delta^{13}\text{C}$ respectively, compared to code 2 individuals. Overall, FL dolphins were $\delta^{13}\text{C}$ enriched ($-15.5\text{‰} \pm 1.60$), $\delta^{15}\text{N}$ deplete ($+14.6\text{‰} \pm 1.21$), and $\delta^{34}\text{S}$ deplete ($+11.5\text{‰} \pm 3.04$) relative to LA dolphins ($\delta^{13}\text{C} = -17.2\text{‰} \pm 1.58$; $\delta^{15}\text{N} = +16.5\text{‰} \pm 1.05$; $\delta^{34}\text{S} = +13.3\text{‰} \pm 1.65$).

To explore potential ontogenetic effects a two-way ANOVA was performed to determine the effect of life stage and stranding location on stable isotope ratios. Condition code was not included as most samples were code 4 and it did not improve model fit in previous analyses. Boxplots for isotopic data using body length and age to categorize life stage are shown in Figure 2.6. For $\delta^{13}\text{C}$, there was no difference between

using body length and age. In both analyses, life stage and location were significant predictors of $\delta^{13}\text{C}$ (ANOVA; $P < 0.01$). Florida dolphins were $\delta^{13}\text{C}$ enriched compared to LA dolphins and calves were $\delta^{13}\text{C}$ deplete relative to juveniles/adults in both stranding locations. For $\delta^{15}\text{N}$, when using body length to categorize life stage, there was a significant interaction term which prohibited the statistical interpretation of the main effects (ANOVA; $P < 0.05$). It appeared, based on the boxplots, that life stage influenced $\delta^{15}\text{N}$ in FL, but not in LA. However, when age was used to categorize dolphins, the interaction term was not significant and only location significantly influenced $\delta^{15}\text{N}$, with LA dolphins being $\delta^{15}\text{N}$ enriched compared to FL dolphins. Similarly, for $\delta^{34}\text{S}$ analysis, when body length was used to categorized life stage there was a significant interaction term (ANOVA; $P < 0.05$) and life stage appeared to be influential in FL, but not in LA. However, when age was used to categorize life stage only stranding location was a significant predictor of $\delta^{34}\text{S}$ with FL dolphins being $\delta^{34}\text{S}$ deplete relative to LA dolphins.

Skin THg concentrations in relation to stable isotope ratios

$\delta^{13}\text{C}$, $\delta^{15}\text{N}$, $\delta^{34}\text{S}$, stranding year, condition code, and body length/age were found to be significant predictors of skin THg concentrations. $\delta^{13}\text{C}$, $\delta^{34}\text{S}$, and body length/age positively influenced THg concentrations while $\delta^{15}\text{N}$ negatively influenced THg concentrations (Table 2.2). Stranding year was only significant in the body length model and was likely driven by sampling bias as previously discussed. When using body length as a predictor, condition code was also a significant predictor, but it did not improve model fit (Table 2.2). Looking at the isotopes individually, when accounting for body length, condition code, and stranding year, there was no relationship between $\delta^{15}\text{N}$ and THg concentrations ($P = 0.27$) and $\delta^{34}\text{S}$ and THg concentrations ($P = 0.34$); however,

there was a significant positive relationship between $\delta^{13}\text{C}$ and THg ($P < 0.001$) (data not shown). In a simple linear regression, $\delta^{13}\text{C}$ explained 22% of the variation in THg ($R^2 = 0.22$; $P < 0.001$ (data not shown)).

Discussion

Within a species, THg concentrations can vary widely and several biological (e.g., tissue type, body length/age, sex) and ecological (e.g., foraging behavior, environmental THg concentrations) factors have been invoked to explain this variability (Meador et al. 1999; Hong et al., 2012; Monteiro et al., 2016; Dirtu et al., 2016; Damseaux et al., 2017). Independently, THg concentrations and stable isotope ratios have been used to distinguish between populations of bottlenose dolphins in the Gulf of Mexico (Barros et al., 2010; Wilson et al., 2012, 2013; Rossman et al., 2015, 2016; Hohn et al., 2017; Damseaux et al., 2017); however, the present study is unique in that it utilized both THg and stable isotope analysis to better understand Hg accumulation in northern Gulf of Mexico bottlenose dolphins.

Mercury tissue distribution and comparison to other studies

Consistent with previously reported distribution patterns, in both FL and LA dolphins, mean THg concentrations were greater in the skin compared to the blubber (Carvalho et al., 2002; Aubail et al., 2013; Dirtu et al., 2016). Methylmercury, the predominant form of Hg found in marine organisms, demonstrates preferential binding to tissues rich in sulfhydryl groups, particularly muscle tissue (Bloom, 1992). Although MeHg is lipid soluble, it has a moderate octanol-water distribution coefficient ($\log K_{ow} = 1.7-2.5$) compared to other lipophilic contaminants such as polychlorinated biphenyls

(PCBs) ($\log K_{ow} = 6-7.5$) (Halbach, 1985; Major et al., 1991; Metcalf and Metcalf, 1997). Therefore, because MeHg has a low octanol-water distribution coefficient and is preferentially distributed in muscle tissues, blubber THg concentrations are generally less than other tissues (e.g., kidney, liver, muscle, and skin) (Cardellicchio et al., 2002; Carvalho et al., 2002; Aubail et al., 2013). In contrast, dolphin skin (epidermis) has been shown to accumulate THg over time and between 70-100% of the THg found in bottlenose dolphin skin is in the form of MeHg (Yang et al., 2002; Stavros et al., 2007, 2011; Woshner et al., 2008; Aubail et al., 2013; Borrell et al., 2015).

Blubber and skin THg concentrations were compared to THg concentrations in bottlenose dolphins reported in the literature (Table 2.3). There were no studies which reported blubber THg concentrations in bottlenose dolphins from the Gulf of Mexico or the nearby Atlantic Ocean. In the present study, mean skin THg concentrations for FL bottlenose dolphins ($4.36 \pm 3.55 \mu\text{g/g dry wt}$) were comparable to the mean skin THg concentration found in bottlenose dolphins from Sarasota Bay, FL ($4.02 \pm 2.61 \mu\text{g/g dry wt}$), but greater than the mean skin concentrations reported in bottlenose dolphins off the South Carolina (SC) coast ($1.7 \pm 0.92 \mu\text{g/g dry wt}$) (Bryan et al., 2007; Stavros et al., 2007, 2011). In contrast, the mean skin THg concentration found in LA dolphins in the present study ($1.94 \pm 3.56 \mu\text{g/g dry wt}$), was less than the mean concentration reported in Sarasota Bay, FL, but comparable to concentrations reported in dolphins off the SC coast (Bryan et al., 2007; Stavros et al., 2007; 2011). Annual wet Hg deposition across the northern Gulf of Mexico is greater than the wet deposition in SC, which may explain the greater THg concentration found in FL dolphins (Selin and Jacob, 2008); however, wet

deposition patterns do not explain why THg concentrations in dolphins from LA and SC are similar.

Both FL and LA bottlenose dolphins in the present study had mean skin THg concentrations which were less than those reported in bottlenose dolphins from the Florida Coastal Everglades (11.1 ± 7.71 $\mu\text{g/g}$ dry wt) and Indian River Lagoon (IRL), FL (7.0 ± 5.9 $\mu\text{g/g}$ dry wt) (Stavros et al., 2007, 2011; Damseaux et al., 2017). Intermediate mean skin THg concentrations were reported for dolphins from the lower FL Keys (2.94 ± 2.08 $\mu\text{g/g}$ dry wt) (Damseaux et al., 2017). Skin Hg concentrations reported by Damseaux et al. (2017) from bottlenose dolphins from the Florida Coastal Everglades are the highest in the literature for the Gulf of Mexico region; mangrove forests in this region are rich in organic content, which can support anaerobic bacteria which in turn may facilitate the conversion of Hg^{2+} to MeHg that can be incorporated into the food web (Bergamaschi et al., 2012). The IRL—a shallow estuary on the east coast of FL—has low flushing rates which may result in the accumulation of Hg (Smith, 1993).

Compared to blubber THg concentrations reported worldwide, both FL (2.36 ± 2.71 $\mu\text{g/g}$ dry wt) and LA (1.33 ± 2.78 $\mu\text{g/g}$ dry wt) bottlenose dolphins in the present study had mean blubber THg concentrations that were greater than those reported in the Northeast Atlantic Ocean (0.8 ± 0.7 $\mu\text{g/g}$ dry wt; 1.28 ± 0.04 $\mu\text{g/g}$ dry wt), but less than those reported in the Mediterranean Sea (2.54 ± 5.42 $\mu\text{g/g}$ dry wt) and Canary Islands (83.4 ± 35.5 $\mu\text{g/g}$ dry wt) (Carvalho et al., 2002; Roditi-Elasar et al., 2003; Aubail et al., 2013; García-Alvarez et al., 2015). It has been suggested that dolphins in the Mediterranean have elevated concentrations of THg compared to those in the Atlantic due to natural cinnabar deposits (Bacci, 1989, Andre et al., 1991; Cardellicchio et al.,

2002; Pompe-Gotal et al., 2009). The authors did not explain the exceptionally high THg values reported in blubber tissues from Canary Islands. In contrast, both FL and LA dolphins in the present study had mean skin THg concentrations which were less than the Northeast Atlantic Ocean ($5.7 \pm 2.9 \mu\text{g/g}$ dry wt; $11.6 \pm 4.5 \mu\text{g/g}$ dry wt); however, similar to blubber, both FL and LA dolphins in the present study had mean skin THg concentrations that were less than those reported in the Mediterranean Sea ($7.92 \pm 5.66 \mu\text{g/g}$ dry wt) (Carvahlo et al., 2002; Roditi-Elasar et al., 2003; Aubail et al., 2013). A limitation of this study is that the source stock of the stranded dolphins was unknown, and THg concentrations may vary among inshore (bay, sound, and estuarine) stocks within FL and LA and between inshore and nearby coastal stocks. It would be beneficial in future studies to differentiate between source stocks either isotopically, genetically, or through photo-identification to determine if THg concentrations vary among source stocks. Furthermore, our THg concentrations were determined in stranded animals which may not be representative of healthy free-ranging populations.

Mercury concentrations in relation to body length, age, sex, and condition code

The present study found no difference in THg concentration between sexes, consistent with the findings of previous studies (Woshner et al., 2008; Aubail et al., 2013; García-Alvarez et al., 2015; Monteiro et al., 2016). This is most likely because although Hg can be maternally transferred via gestation and lactation, the amount of Hg deposited is small compared to Hg derived from dietary sources (Storelli and Marcotrigiano, 2000; Frodello et al., 2002; Hong et al., 2012). In some cases, condition code positively influenced THg concentrations. This may be a result of lipid loss due to poor body condition and/or decomposition of the sample. The concentration of THg has been shown

to decrease with lipid content. Since Hg does not preferentially bind to lipids, greater lipid concentrations can dilute THg concentrations (Lavoie et al., 2014). Body condition of the stranded animals utilized in the present study was not available, but previous studies have reported that bottlenose dolphins inhabiting Barataria Bay, LA in 2011, within the spatial and temporal extent of this study, were in poor body condition (Schwacke et al., 2014).

The present study also found significant positive relationships between THg concentration and body length/age in both the blubber and skin, supporting the findings of previous studies (Yang et al., 2002; Stavros et al., 2007, 2011; Woshner et al., 2008; Aubail et al., 2013). The increase in THg concentration with increasing body length/age likely reflects bioaccumulation as a result of continuous dietary exposure and the low excretion rate of Hg, particularly MeHg, from the body (Itano and Kawai, 1981; Nigro et al., 2002); however, it may also be a result of larger dolphins eating larger and/or higher trophic level prey which inherently have higher THg concentrations [e.g., pinfish (*Lagodon rhomboides*) vs. spotted seatrout (*Cynoscion nebulosus*)] (Berens McCabe et al., 2010; Miller et al., 2011). The wide variation in THg concentrations among dolphins > 225 cm is likely because after reaching asymptotic body length, individuals may exhibit variability in prey selection or feeding locations which could lead to variation in THg concentrations. In addition, as asymptotic body length is approached, growth rates slow and Hg accumulation is no longer offset by growth dilution (Andre et al., 1991). Rapid growth followed by a period of slowed growth until an asymptotic body length is reached is consistent with the literature (Read et al., 1993; Stolen et al., 2002; McFee et al., 2012). This suggests that age may be a more accurate predictor of THg compared to body

length, which was supported by the increase in model fit when using age as a predictor in place of body length. However, the increase in model fit was not substantial and body length can be a good proxy for age when age is not available, especially for smaller individuals before asymptotic body length is reached (approximately 250 cm).

Variation in THg concentrations between FL and LA dolphins

On average, when body length or age was used as a covariate, dolphins from FL had greater THg concentrations compared to dolphins from LA. Similar spatial patterns of THg concentrations were found in American oyster tissues from the northern Gulf of Mexico; Apeti et al. (2012) measured the THg concentrations in oyster tissues from the northern Gulf of Mexico and found that oysters from certain regions of FL (Apalachee Bay, Florida Bay, Tampa Bay, the Florida Everglades, and Pensacola Bay) had the greatest THg concentrations, whereas oysters in Louisiana, Alabama, and Mississippi had the lowest THg concentrations. The greatest median THg concentrations were reported in Apalachee Bay, FL which is included in the spatial extent of the present study.

Lower THg concentrations in dolphins from LA may be a result of indirect influences from the Mississippi River. The Mississippi River which drains 41% of the contiguous United States delivers large amounts of sediments and nutrients to the central northern Gulf of Mexico (Presley et al., 1998; Apeti et al., 2012). Large amounts of sediments could dilute atmospherically deposited Hg with material that is lower in Hg concentration and large influxes of nutrients support higher phytoplankton productivity which can reduce THg concentrations in fish; it is plausible that lower concentrations in fish may be reflected in dolphins (Presley et al., 1998; Chen and Folt, 2005; Apeti et al., 2012). In addition, seasonally occurring hypoxic zones spanning from the Mississippi

delta west through upper coastal Texas, can cause hydrogen sulfide in the sediment to be released which inhibits Hg methylation (Benoit et al., 1999; Rabalais et al., 2001; Fitzgerald et al., 2007, Sluis et al., 2013). In contrast, in the FL panhandle there are no major rivers delivering sediments and nutrients to dilute atmospheric Hg inputs; this may explain why dolphins inhabiting FL have greater THg concentrations compared to those in LA.

Stable isotope ratios and relationship with THg concentration

The isotopic values reported in the present study were within the ranges reported by other studies in the northern Gulf of Mexico for bottlenose dolphin skin (Wilson et al., 2012; Wilson et al., 2013; Hohn et al., 2017). However, as was the case with the THg analysis, categorizing dolphins by stranding location (FL vs. LA) as a proxy for source stock is inherently flawed as this categorization failed to account for differences in stable isotope ratios among stocks within FL and LA.

In marine systems, differences in $\delta^{13}\text{C}$ between benthic (i.e., high $\delta^{13}\text{C}$) and pelagic (i.e., low $\delta^{13}\text{C}$) producers can be reflected in higher trophic levels, providing an indirect way to assess the foraging habitat of a predator (Barros et al., 2010). Florida bottlenose dolphins were enriched in $\delta^{13}\text{C}$ compared to LA bottlenose dolphins which may indicate that FL dolphins utilize a mixture of seagrass habitats as well as pelagic based food webs whereas LA dolphins are less likely to utilize seagrass habitats (Barros et al., 2010; Rossman et al., 2015). These findings are consistent with seagrasses distribution patterns in the northern Gulf of Mexico. Seagrasses are moderately present in western FL panhandle but are less common in LA (Love et al., 2013). Additionally, LA dolphins may be receiving depleted dissolved organic carbon (DOC) from the Mississippi

River (Chanton and Lewis, 1991). There was a decrease in $\delta^{13}\text{C}$ with increasing body length/age suggesting that there may be changes in foraging behavior between age classes (Rossman et al., 2015). There was a positive relationship between $\delta^{13}\text{C}$ and THg which may be driven by differences in $\delta^{13}\text{C}$ between stranding locations suggesting that FL dolphins are feeding on prey with higher THg concentrations compared to LA dolphins. However, sampling of dolphin prey in both locations would be necessary to evaluate this hypothesis. Sex was influential in the body length model, which suggests that males and females may exhibit different feeding preferences, but similar results were not seen in the age model. Finally, we found that condition code positively influenced $\delta^{13}\text{C}$. This is consistent with Burrows et al. (2014) which reported that $\delta^{13}\text{C}$ values in decomposed killer whale (*Orcinus orca*) skin were 1.0‰ more enriched than non-decomposed skin.

$\delta^{15}\text{N}$ is used as a measure of trophic position with more enriched $\delta^{15}\text{N}$ being associated with higher trophic positions, but differences in the organic matter sources within an ecosystem can confound the interpretation of trophic position (Wilson et al., 2009; Newsome et al., 2010; Wilson et al., 2012). If organic matter sources differ in $\delta^{15}\text{N}$ by more than 4‰, a consumers' nitrogen values are reflective of both isotopic fractionation and a mixture of organic matter sources (Wilson et al., 2009). Bottlenose dolphins from FL were $\delta^{15}\text{N}$ deplete ($+ 14.61\text{‰} \pm 1.22$) compared to LA dolphins ($+ 16.45\text{‰} \pm 1.05$); however, they differed less than the 3‰ which is approximately the difference between trophic levels (Peterson and Fry, 1987). Enriched $\delta^{15}\text{N}$ in LA may also be a result of high levels of nutrient runoff (e.g., wastewater, fertilizers) from the Mississippi River (Valiela et al., 1997). Multiple linear regression analysis revealed there was a decrease in $\delta^{15}\text{N}$ with increasing body length/age which is consistent with calves

transitioning from nursing to independently foraging (Knoff et al., 2008). However, we did not see similar trends in the ANOVA analysis when determining the influence of life stage and location on $\delta^{15}\text{N}$. We categorized calves as being either ≤ 183 cm or ≤ 3.5 years old, but calves may nurse for longer periods and experience transition periods in which they are both nursing and foraging which could have influenced our results (Mann et al., 2000). Contrary to what was expected, we did not find a positive relationship between $\delta^{15}\text{N}$ and THg concentration, possibly due to differences in $\delta^{15}\text{N}$ signatures between stranding locations and the wide variety of prey consumed by bottlenose dolphins. Further research would be needed to sample the food webs of both FL and LA dolphins to better understand the relationship between $\delta^{15}\text{N}$ and THg. Contrary to Hohn et al., 2017, we found that $\delta^{15}\text{N}$ values increased with increasing condition code. Enrichment of $\delta^{15}\text{N}$ following decomposition has also been reported in killer whale skin (Burrows et al., 2014). Finally, our samples were from stranded animals, potentially adding a confounding factor to our results as $\delta^{15}\text{N}$ values may be higher than expected in healthy free-ranging populations due to nutritional stress and resultant catabolism of tissues (Payo-Payo et al., 2013; Hohn et al., 2017).

In nearshore marine sediments, sulfate reduction results in ^{34}S -deplete sulfides, between the range of 0 to -20‰ ; these $\delta^{34}\text{S}$ products are then taken up by benthic producers and the $\delta^{34}\text{S}$ deplete signature reflected in higher trophic levels (Chanton et al., 1987; Chasar et al., 2005). In contrast, seawater sulfate has a $\delta^{34}\text{S}$ value of $+21\text{‰}$ (Peterson et al., 1985). As a result, consumers' $\delta^{34}\text{S}$ is reflective of the relative importance of benthic and water column production (Barros et al., 2010). Both FL and LA dolphins in the present study had $\delta^{34}\text{S}$ values consistent with nearshore habitats.

Florida bottlenose dolphins were $\delta^{34}\text{S}$ deplete compared to LA dolphins which may reflect differences between estuary and barrier island stocks. Hohn et al. (2017) utilized carbon, nitrogen, and sulfur stable isotope ratios to assign stranded dolphins from the northern Gulf of Mexico to source stocks. According to their results, most FL dolphins from the present study would be assigned to estuary stocks whereas most of the LA dolphins would be assigned to barrier island stocks. There was no relationship between $\delta^{34}\text{S}$ and body length suggesting there were no differences among age classes in foraging habitat. There was also no relationship between $\delta^{34}\text{S}$ and THg concentration suggesting that there were no differences in Hg accumulation between inshore and offshore foraging habitats; however, this interpretation is limited because most individuals from the present study appear to be from estuarine and barrier island stocks. Differences in stable isotope ratios and THg concentrations between FL and LA dolphins suggests that differences in dietary sources and foraging habitat influence THg concentrations in northern Gulf of Mexico bottlenose dolphins. However, further research is required to understand how fine-scale population structuring of dolphins from the northern Gulf of Mexico impacts THg concentrations both among inshore (bays, sounds, and estuaries) stocks and between inshore and offshore stocks.

Table 2.1. Biological data from stranded dolphins collected between 2011-2016 from the Florida and Louisiana coasts. Life stage was categorized by body length, as age was not available for every individual, with calves being ≤ 183 cm and juveniles/adults being > 183 cm following Knoff et al. (2008).

Stranding Location	Sex	Life Stage	n	
Florida	Female	Calf	6	
		Juvenile/Adult	26	
	Male	Calf	6	
		Juvenile/Adult	22	
	Unknown	Calf	2	
		Juvenile/Adult	1	
	Total			63
	Louisiana	Female	Calf	3
			Juvenile/Adult	27
Male		Calf	13	
		Juvenile/Adult	54	
Unknown		Calf	4	
		Juvenile/Adult	20	
Total			121	

Table 2.2. Best fit generalized linear model (GLM) and parameter estimates selected based on the lowest Akaike Information Criteria (AIC_c). *Indicates variables were Log10 transformed.

Final Model	R ²	p value
(1) THg in relation to sex, body length, and stranding location		
Blubber Hg* = - 6.3 + 2.7(Body Length*) + - 0.5(Stranding Location: LA) + 0.13(Code)	0.43	<0.001
Skin Hg* = - 4.7 + 2.2(Body Length*) + - 0.6(Stranding Location: LA) + 0.39(Year: 2016) + 0.25(Year: 2015) + 0.27(Year: 2014) + 0.17(Year: 2013)	0.56	<0.001
(2) THg in relation to sex, age, and stranding location		
Blubber Hg* = - 0.39 + 0.58(Age*) + - 0.34(Stranding Location: LA)	0.47	<0.001
Skin Hg* = -0.28 + 0.58 (Age*) + - 0.61(Stranding Location: LA) + 0.09(Code)	0.64	<0.001
(3) Stable isotope ratios in relation to sex, body length, and stranding location		
δ ¹³ C Skin = - 25.9 + 3.9(Body Length*) + - 2.0(Stranding Location: LA) + 0.47(Code) + - 0.49(Sex:male)	0.27	<0.001
δ ¹⁵ N Skin = 18.7 + - 2.2(Body Length*) + 1.7(Stranding Location: LA) + 0.29(Code)	0.42	<0.001
δ ³⁴ S Skin = 11.5 + 1.7(Stranding Location: LA)	0.11	<0.001
(4) Stable isotope ratios in relation to sex, age, and stranding location		
δ ¹³ C Skin = - 17.9 + 0.90(Age*) + - 1.8(Stranding Location: LA) + 0.46(Code)	0.23	<0.001

$\delta^{15}\text{N Skin} = 13.8 + - 0.34(\text{Age}^*) + 1.9(\text{Stranding Location: LA}) + 0.29(\text{Code})$	0.45	<0.001
---	------	--------

$\delta^{34}\text{S Skin} = 11.5 + 1.7(\text{Stranding Location: LA})$	0.11	<0.001
--	------	--------

(5) THg in relation to stable isotope ratios

$\text{Skin Hg}^* = -1.7 + 1.8(\text{Body Length}^*) + 0.11(\delta^{13}\text{C}) + - 0.06(\delta^{15}\text{N}) + 0.03(\delta^{34}\text{S}) + 0.47(\text{Year: 2016}) + 0.24(\text{Year:2015}) + 0.34(\text{Year: 2014}) + 0.22(\text{Year: 2013}) + - 0.11 (\text{Code})$	0.53	<0.001
---	------	--------

$\text{Skin Hg}^* = 2.3 + 0.47(\text{Age}^*) + 0.10(\delta^{13}\text{C}) + - 0.10(\delta^{15}\text{N}) + 0.05(\delta^{34}\text{S})$	0.52	<0.001
---	------	--------

Table 2.3. Comparison of THg concentrations (mean \pm SD) in bottlenose dolphin blubber and skin between the present study and previously published studies in $\mu\text{g/g}$ dry wt. *values were converted from wet wt using a moisture content of 41% and 47% for blubber and skin, respectively as determined in the present study.

Tissue	THg ($\mu\text{g/g}$ dry wt)	n	Location	Reference
Blubber	83.4 \pm 35.5	29	Canary Islands	García-Alvarez et al., 2015
	2.36 \pm 2.71	48	Florida – panhandle	This study
	1.33 \pm 2.78	11	Louisiana	This study
	2.54 \pm 5.42*	14	Mediterranean Sea – Israel	Roditi-Elasar et al., 2003
	1.28 \pm 0.04	2	Northeast Atlantic Ocean – Portugal	Carvalho et al., 2002
	0.8 \pm 0.7	16	Northeast Atlantic Ocean – Portugal and France	Aubail et al., 2013
Skin	11.1 \pm 7.71	22	Florida – Coastal Everglades	Damseaux et al., 2017
	4.36 \pm 3.55	36	Florida – panhandle	This study
	7.0 \pm 5.9	75	Florida – Indian River Lagoon	Stavros et al., 2007
	8.57 \pm 7.04	15	Florida – Indian River Lagoon	Stavros et al., 2011
	2.94 \pm 2.08	9	Florida – Lower FL Keys	Damseaux et al., 2017
	4.02 \pm 2.61*	40	Florida – Sarasota Bay	Bryan et al., 2007
	1.94 \pm 3.51	93	Louisiana	This study
	7.92 \pm 5.66*	13	Mediterranean Sea – Israel	Roditi-Elasar et al., 2003

11.6 ± 4.5	2	Northeast Atlantic Ocean – Portugal	Carvalho et al., 2002
5.7 ± 2.9	16	Northeast Atlantic Ocean – Portugal and France	Aubail et al., 2013
1.7 ± 0.92	74	South Carolina – Charleston	Stavros et al., 2007
1.8 ± 1.8	12	South Carolina	Stavros et al., 2011

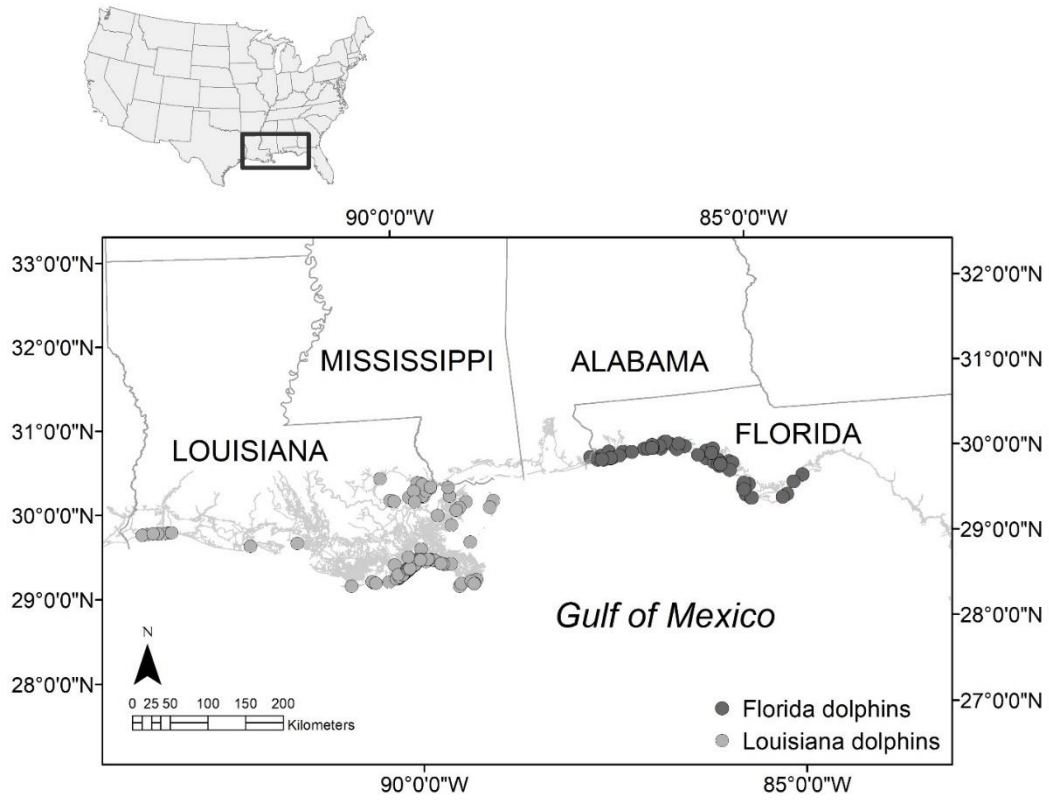


Figure 2.1. Bottlenose dolphin (*Tursiops truncatus*) stranding locations in Florida (FL; n = 63) and Louisiana (LA; n = 121).

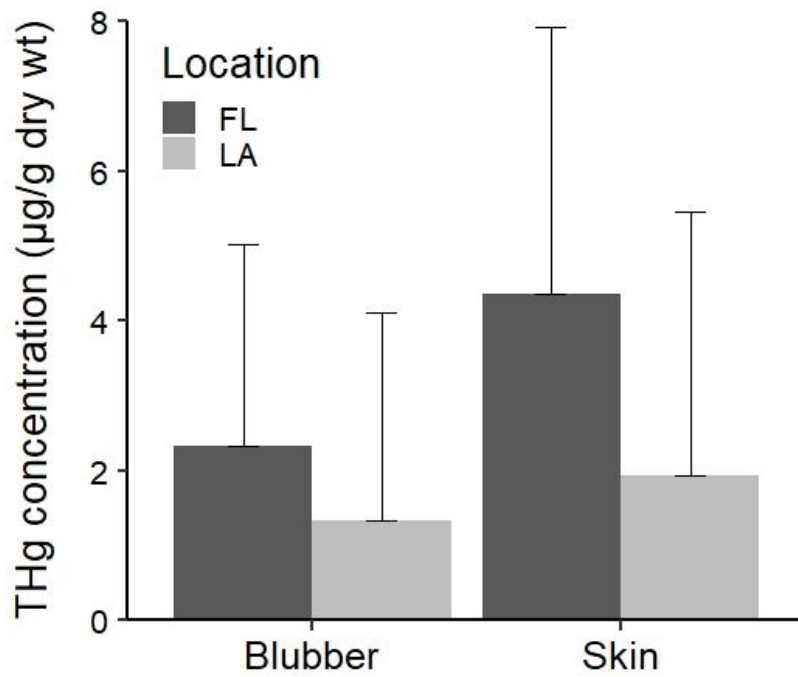


Figure 2.2. THg concentration (mean + SD) in blubber and skin of Florida (FL) and Louisiana (LA) bottlenose dolphins.

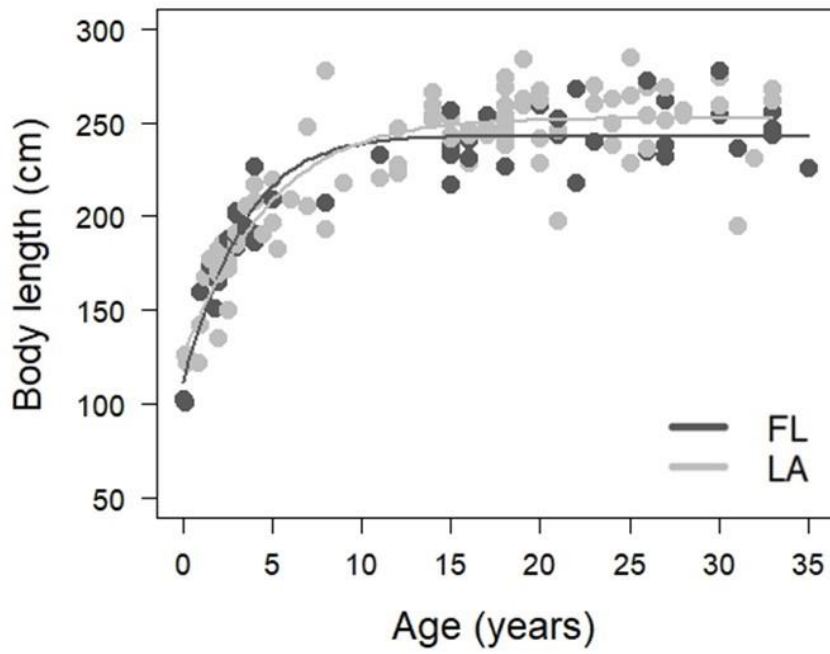


Figure 2.3. Relationship between body length and age in Florida (FL) and Louisiana (LA) bottlenose dolphins with growth curves fitted using the Gompertz model.

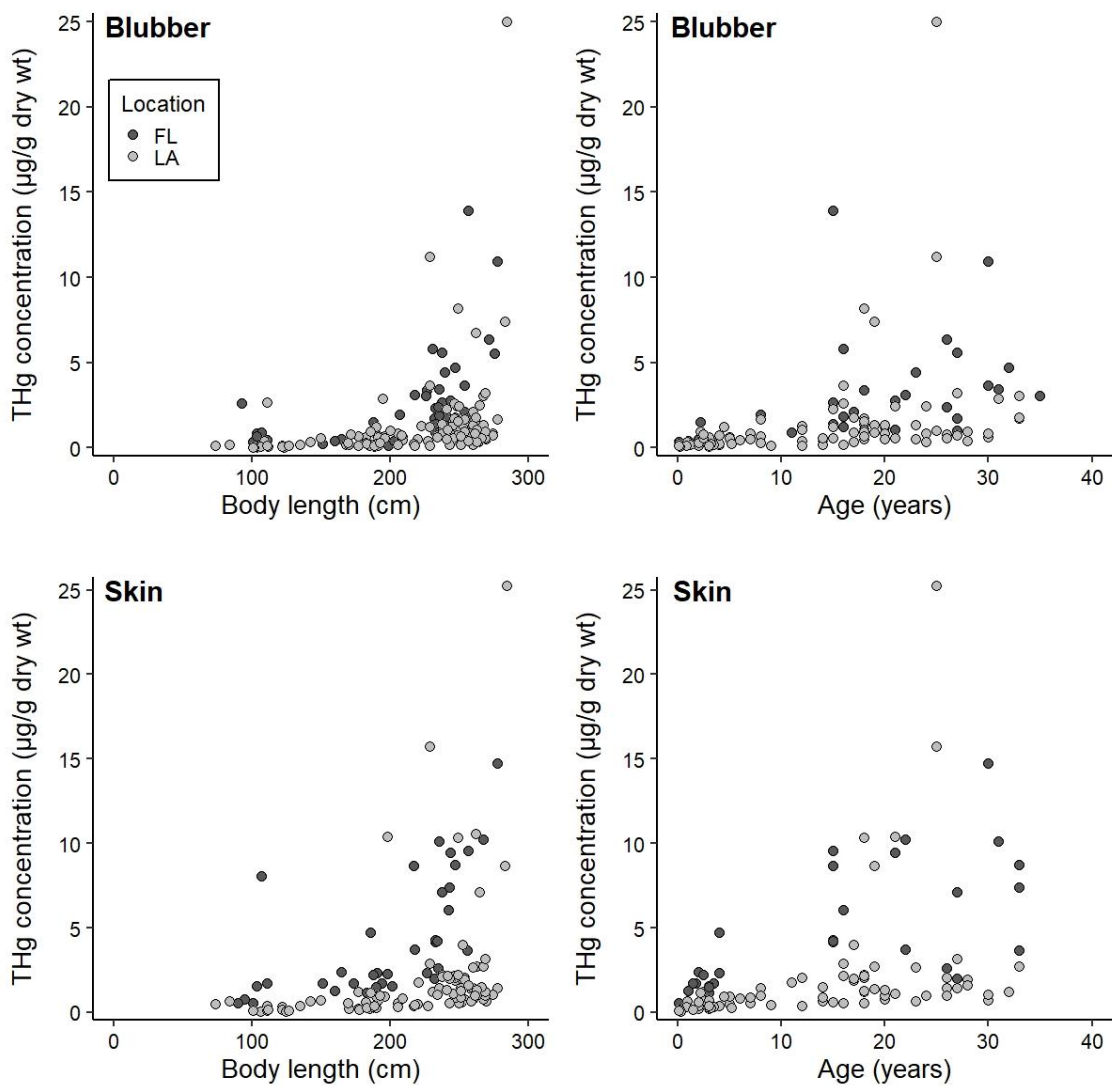


Figure 2.4. Relationship between THg concentrations in blubber and skin of bottlenose dolphins from Florida (FL) and Louisiana (LA) in relation to body length (left column) and age (right column).

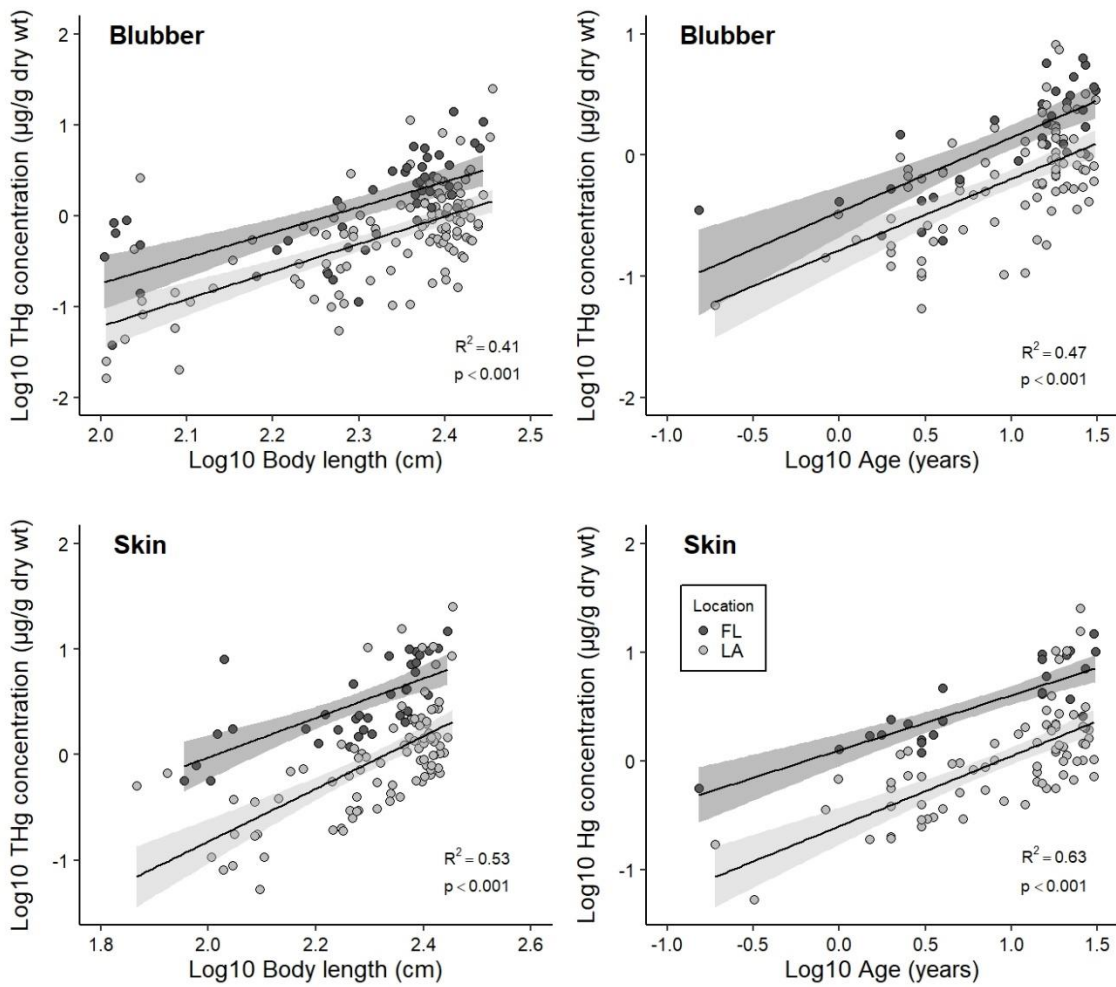


Figure 2.5. Relationship between Log₁₀ THg concentrations in blubber and skin and Log₁₀ body length (left column) and Log₁₀ age (right column). Regression lines (Log₁₀ Hg = β_0 + Stranding Location + Log₁₀ Body length/Age) and 95% CI are shown.

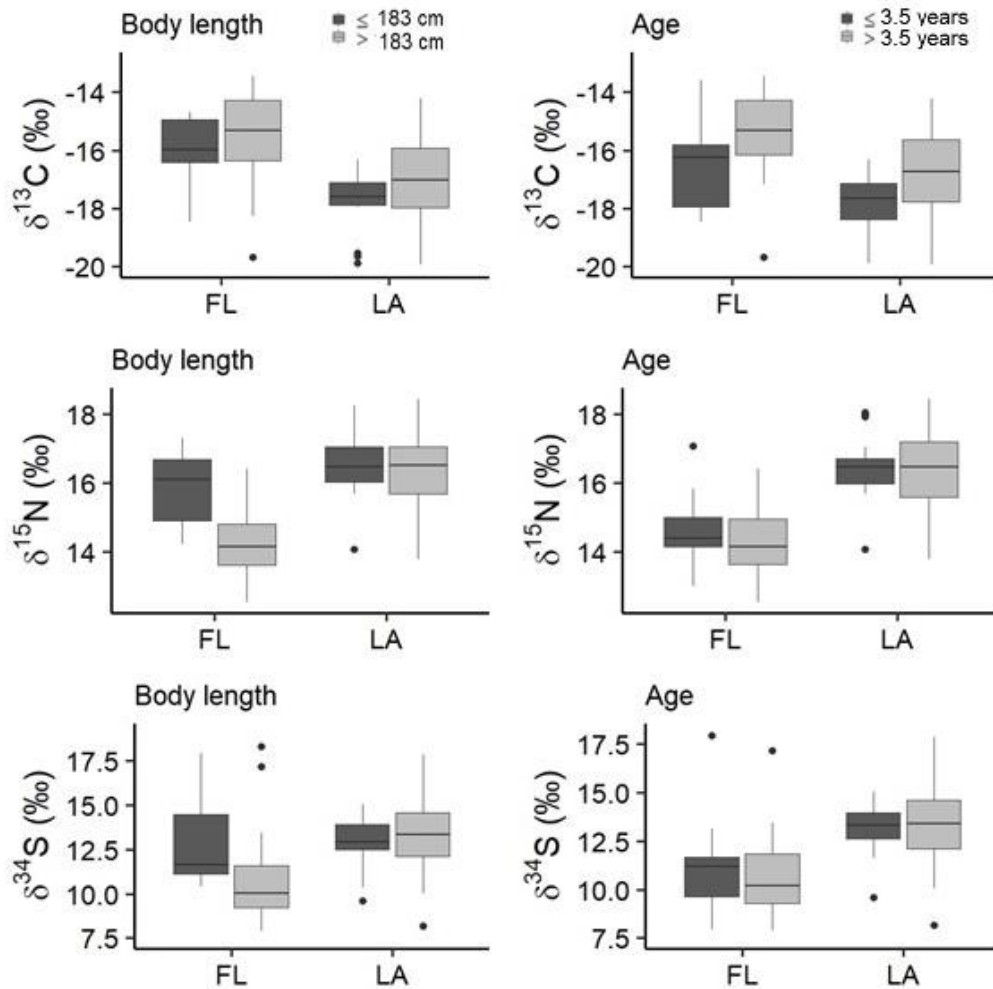


Figure 2.6. Florida (FL) and Louisiana (LA) bottlenose dolphin $\delta^{13}\text{C}$, $\delta^{15}\text{N}$, and $\delta^{34}\text{S}$ values in relation to body length (left column) and age (right column). Dark gray boxes represent calves (≤ 183 cm or ≤ 3.5 years) and light gray boxes represent juveniles/adults (>183 cm or >3.5 years). Whiskers show the minimum and maximum values, excluding outliers which are shown as black dots.

III. EFFECT OF TROPHIC POSITION ON MERCURY CONCENTRATIONS IN BOTTLENOSE DOLPHINS (*TURSIOPS TRUNCATUS*) FROM THE NORTHERN GULF OF MEXICO

Abstract

Marine species from the Gulf of Mexico often have higher mercury (Hg) concentrations than conspecifics in the Atlantic Ocean. Spatial differences in Hg sources, environmental conditions, and microbial communities influence both Hg methylation rates and the bioavailability of Hg to organisms at the base of the food web. Mercury bioaccumulates within organisms and biomagnifies in marine food webs, and therefore reaches the greatest concentrations in long-lived marine carnivores, such as dolphins. In this study, we explored whether differences in trophic position and foraging habitat among bottlenose dolphins (*Tursiops truncatus*) from the northern Gulf of Mexico (nGoM) contributed to their observed variation in total Hg (THg) concentrations. Using the $\delta^{13}\text{C}$ and $\delta^{34}\text{S}$ values in dolphin skin, we assigned deceased stranded dolphins from Florida (FL; $n = 29$) and Louisiana (LA; $n = 72$) to predicted habitats (estuarine, barrier island, and coastal) east and west of the Mississippi River Delta (MRD). We estimated the mean trophic position of dolphins from each habitat using $\delta^{15}\text{N}$ values from stranded dolphin skin and primary consumers taken from the literature following a Bayesian framework. Finally, we compared trophic positions and THg concentrations among dolphins from each habitat, accounting for sex and body length. Estimated marginal mean THg concentrations ($\mu\text{g/g}$ dry weight) were greatest in dolphins assigned to the coastal habitat and estuarine habitats east of the MRD, particularly those associated with the FL

panhandle (range: 2.59 – 4.81), and lowest in dolphins assigned to estuarine and barrier island habitats west of the MRD (range: 0.675 – 0.993). On average, dolphins from habitats with greater THg concentrations also had higher estimated trophic positions, with the exception of coastal habitat dolphins. Our results suggest that differences in trophic positions among dolphins, Hg sources, and environmental conditions between foraging habitats likely contribute to spatial variability in Hg observed among nGoM bottlenose dolphins.

Introduction

Elevated mercury (Hg) concentrations in marine fishes from the Gulf of Mexico (GoM) have led to concerns regarding the health of marine life and human populations exposed to Hg through seafood consumption (Adams and McMichael, 2007; Selin and Jacob, 2008; Karouna-Renier et al., 2011; Adams and Sonne, 2013; Evans et al., 2015). Mercury is a toxic non-essential trace element that originates from both natural (e.g., volcanic eruptions) and anthropogenic (e.g., coal-burning power plants, artisanal gold mining) sources (Selin, 2009; Pirrone et al., 2010). Heavy metals, including Hg, are environmental pollutants of particular concern because of their persistence and bioaccumulative properties (Ali et al., 2019). A substantial portion of the Hg entering coastal waters is in the form of inorganic Hg (Hg^{2+}); however, given appropriate environmental conditions, sulfate-reducing bacteria in the sediment convert Hg^{2+} to methylmercury (CH_3Hg^+ ; MeHg) (Fitzgerald et al., 2007; Selin, 2009; Pirrone et al., 2010). Both MeHg and Hg^{2+} are bioconcentrated in phytoplankton from seawater and transferred up the food web (Mason et al., 1996; Lee and Fisher, 2016). Compared to

Hg²⁺, MeHg has a greater trophic transfer efficiency; consequently, MeHg is more likely to be biomagnified in marine food webs and is the predominant Hg species in fish (Mason et al., 1996; Hammerschmidt and Fitzgerald, 2006). When uptake of Hg exceeds the loss rate from the body, Hg gradually bioaccumulates within an organism, increasing in concentration over time (Hammerschmidt and Fitzgerald, 2006; Adams and McMichael, 2007). Marine fish are exposed to Hg both in water during respiration and through food; however, for odontocetes, diet is the primary route of uptake (Hong et al., 2012; Bradley et al., 2017; Ali et al., 2018).

Sources of Hg to the GoM include atmospheric (wet and dry deposition), terrestrial (e.g., rivers including the Mississippi and Atchafalaya), and Atlantic Ocean inputs (primarily the Loop Current (Harris et al., 2012a). However, within the broader global Hg cycle, the majority of terrestrial and oceanic Hg inputs originate from atmospheric deposition (Fitzgerald et al., 2007; Harris et al., 2012a). Point sources of Hg contamination to the GoM may also include industrial sources (e.g., coal-fired power plants), hydrothermal vents, and oil and gas exploration (Neff, 2002; Lamborg et al., 2006; U.S. EPA, 2011; Harris et al., 2012a,b; Mason et al., 2012; Sherman et al., 2012; Kennicutt, 2017). The relative importance of these sources varies spatially; linking Hg concentrations in marine life to Hg sources is further complicated as varying physical, chemical, and biological conditions can influence Hg bioavailability, which in turn impacts Hg biomagnification in food webs (Fitzgerald et al., 2007; Harris et al., 2012a,b; Perrot et al., 2019). In the northern Gulf of Mexico (nGoM), consistent spatial variation in Hg concentrations has been observed among a variety of resident species including oysters [e.g., eastern oyster (*Crassostrea virginica*)], fish [e.g., spotted seatrout

(*Cynoscion nebulosus*) and golden tilefish (*Lopholatilus chamaeleonticeps*)], and seabirds [e.g., brown pelicans (*Pelecanus occidentalis carolinensis*)] (Ache et al., 2000; Apeti et al., 2012; Harris et al., 2012a; Evans et al., 2015; Perrot et al., 2019; Ndu et al., 2020).

For migratory species which assimilate Hg from different foraging habitats, geographic differences in Hg concentrations between locations may average out and not be apparent; furthermore, for species inhabiting offshore environments, mixing reduces gradients in Hg concentrations (Cai et al., 2007; Evans et al., 2015). Although bottlenose dolphins (*Tursiops truncatus*) can travel long distances, especially those of the offshore ecotype (e.g., > 4000 km; Wells et al., 1999; Vollmer and Rosel, 2013), in some cases, dolphins have relatively small home ranges (e.g., < 100 km²; Wells et al., 2017).

Throughout the nGoM, photo-identification and telemetry studies have confirmed the presence of long-term resident communities of bottlenose dolphins; these communities, termed bay, sound, and estuary stocks (BSE), occur within enclosed, semi-enclosed, or contiguous bodies of water adjacent to coastal waters (Shane, 1977; Gruber, 1981; Hubard et al., 2004; Irwin and Würsig, 2004; Balmer et al., 2008; Tyson et al., 2011; Bassos-Hull et al., 2013; Shippee, 2014; Wells et al., 2017; Hayes et al., 2019). The National Marine Fisheries Service (NMFS), an office of the National Oceanic and Atmospheric Administration (NOAA), has delineated boundaries for 31 BSE stocks, which for management purposes meet the definition of demographically independent populations (Hayes et al., 2019).

In the nGoM, although large proportions of BSE stocks exhibit high levels of site fidelity and can be categorized as year-round residents, there is some behavioral variability both within and among BSE stocks (Würsig, 2017). The presence of seasonal

migrants either from nearby BSE stocks or adjacent coastal stocks (outside BSE stock boundaries and up to the 20m isobath), as well as transient dolphins (i.e., those that are seen once and are rarely seen again), suggest some BSE stocks are not entirely closed populations (Balmer et al., 2008; Tyson et al., 2011; Shippee, 2014; Balmer et al., 2019; Toms, 2019). For example, in Barataria Bay, Louisiana (LA), satellite telemetry data following the Deepwater Horizon Oil Spill documented long-term (multi-year), year-round residency of bottlenose dolphins. 93% of dolphins were observed in Barataria Bay for more than one year (Wells et al., 2017). In contrast, results from photo-identification studies in the FL panhandle suggest greater variation in residency patterns. Tyson et al. (2011) identified two year-round populations of bottlenose dolphins between St. Vincent Sound and Alligator Harbor. In St. Vincent Sound/Apalachicola Bay, which coincides with the spatial extent of the present study, Tyson (2011) estimated that transients made up 28% of the population. In St. Joseph Bay, in addition to year-round residents, Balmer et al. (2008) documented a substantial influx of seasonal migrants in the spring and autumn, which the authors suspect come from the northern coastal stock (Balmer et al., 2008). In contrast, in nearby St. Andrew Bay, Balmer et al. (2019) found only 7% of dolphins were observed in both St. Andrew Bay and the adjacent waters of the northern coastal stock, suggesting limited connectivity between the stocks.

In previous studies, McCormack et al. (2020a,b) compared the total Hg (THg) concentrations in blubber, kidney, liver, lung, and skin between bottlenose dolphins that stranded along the FL panhandle and LA coast. After accounting for sex, body length, stranding year, and degree of sample decomposition, THg concentrations in all tissues were greater in dolphins that stranded in FL compared to those that stranded in LA.

However, these previous studies did not identify the source stock of the stranded animals (i.e., the spatial origin of the stranded dolphin) and thus could not associate differences in dolphin THg concentrations to their spatial origin. Sampling deceased stranded animals is a viable alternative to collecting tissues from free-ranging populations, which is cost-prohibitive, legally and logistically challenging, and limited to non-lethal and minimally invasive techniques (e.g., skin biopsies). However, the data collected from stranded cetaceans is opportunistic, and information such as the source stock of the individual is often unknown; for instance, dolphins may have stranded in an area outside of their normal habitat range (Peltier et al., 2012, 2014; Hohn et al., 2017).

Stable isotope ratios, particularly carbon ($\delta^{13}\text{C}$) and nitrogen ($\delta^{15}\text{N}$), are widely used as ecological tracers, reflecting dietary sources and relative trophic position, respectively (Newsome et al., 2010; Loizaga de Castro et al., 2016). The inclusion of sulfur ($\delta^{34}\text{S}$) stable isotope ratios increases the ability to differentiate between foraging habitats among groups of bottlenose dolphins (Barros et al., 2010; Rossman et al., 2016; Hohn et al., 2017). Hohn et al. (2017) used $\delta^{13}\text{C}$ and $\delta^{34}\text{S}$ values in skin from free-ranging bottlenose dolphins from known habitats off the coast of Alabama (AL), Mississippi (MS), and LA to assign stranded dolphins to habitats. The spatial and temporal overlap between the stranded dolphin dataset presented here and those used by Hohn et al. (2017) provided an opportunity to predict the spatial origins (i.e., habitats) of our stranded bottlenose dolphins. If stranded dolphins could be assigned to habitats (e.g., estuarine, barrier island, coastal), we could more effectively explore the spatial variation in Hg reported in dolphins by McCormack et al. (2020a,b). A more detailed investigation of the Hg concentrations in bottlenose dolphins from the nGoM and potential sources of

variation (e.g., trophic position) is warranted as it is related to the behavioral structure of BSE stocks, and elevated Hg concentrations may negatively influence individual and population health.

In this study, we aim to address the limitations of the previous studies by McCormack et al. (2020a,b) by (i) predicting the habitat (e.g., estuarine, barrier island, coastal) of deceased stranded dolphins across locations in the nGoM, (ii) estimating the trophic position of dolphins associated with each habitat, and (iii) determining the influence of trophic position on dolphin THg concentrations. We specifically aim to address these goals by (i) predicting the habitat of stranded dolphins reported by McCormack et al. (2020a,b) using stable isotope ratios ($\delta^{13}\text{C}$ and $\delta^{34}\text{S}$) in stranded dolphin skin and the splitting criteria reported by Hohn et al. (2017), (ii) estimating trophic position of dolphins using $\delta^{15}\text{N}$ values in skin from stranded dolphins and the tissues from primary consumers [e.g., striped mullet (*Mugil cephalus*)], and (iii) comparing the THg concentrations and estimated trophic positions among stranded dolphins assigned to each habitat to determine if the trophic position or foraging habitat helped to explain spatial variation in THg concentrations among bottlenose dolphins from the nGoM.

Methods

Tissue Sampling

Local stranding networks collected skin samples from deceased bottlenose dolphins that stranded along the FL panhandle ($n = 29$) and LA ($n = 72$) coasts between 2011 and 2016. We limited our dataset to dolphins with body lengths ≥ 183 cm to avoid

ontogenetic effects (Knoff et al., 2008). In FL, there were 19 females, 9 males, and 1 dolphin of unknown sex; mean body length \pm standard deviation was 228 ± 25 cm, 223 ± 28 cm, and 247 cm for females, males, and the dolphin of unknown sex, respectively. In LA, there were 19 females, 42 males, and 11 dolphins of unknown sex; mean body length \pm 1 standard deviation was 230 ± 29 cm, 244 ± 28 cm, and 240 ± 25 cm for females, males, and dolphins of unknown sex, respectively. All THg concentrations ($n = 101$) and the majority of ($n = 86$) of stable isotope ratios ($\delta^{13}\text{C}$, $\delta^{15}\text{N}$, and $\delta^{34}\text{S}$) were measured in skin samples from stranded bottlenose dolphins that had been previously published (McCormack et al., 2020a,b). However, in the present study, we also determined the $\delta^{13}\text{C}$, $\delta^{15}\text{N}$, and $\delta^{34}\text{S}$ values in skin for the 15 individual stranded bottlenose dolphins for which only THg concentrations were previously reported in McCormack et al. (2020b). The condition code of individual dolphins sampled ranged from 2 (fresh) to 4 (advanced decomposition) (Geraci and Lounsbury, 2005); however, 50% of samples from FL and 94% of the samples from LA were taken from condition code 4 individuals.

Stable isotope analysis

Detailed methods describing the stable isotope analysis are reported in McCormack et al. (2020a). In summary, skin samples were freeze-dried and lipid extracted using methanol and chloroform. Next, samples were cut into 1 mm x 1 mm pieces, after which between 0.25-3.5 mg and 0.5-1 mg of each skin sample was packaged for $\delta^{34}\text{S}$ analysis and dual $\delta^{13}\text{C}/\delta^{15}\text{N}$ analysis, respectively. Stable isotope analyses were conducted at the UC Davis Stable Isotope Facility (Davis, CA) using an elemental analyzer [$\delta^{13}\text{C}/\delta^{15}\text{N}$ (PDZ Europa ANCA-GSL); $\delta^{34}\text{S}$ (Elementar vario ISOTOPE cube)] that was interfaced to a continuous-flow isotope ratio mass spectrometer [$\delta^{13}\text{C}/\delta^{15}\text{N}$ (PDZ

Europa 20-20; Sercon Ltd., Cheshire, UK); $\delta^{34}\text{S}$ (SerCon 20–22 IRMS; Sercon Ltd., Cheshire, UK)]. Using δ -notation, stable isotope results were expressed using the following equation:

$$\delta_{\text{Sample}} (\text{‰}) = [(R_{\text{Sample}}/R_{\text{Standard}}) - 1] \times 1000$$

where R is the molar ratio of heavier to lighter isotopes ($\text{C}_{13}/\text{C}_{12}$, $\text{N}_{15}/\text{N}_{14}$, or $\text{S}_{34}/\text{S}_{32}$).

Results were expressed relative to the following standards: Vienna Pee Dee Belemnite ($\delta^{13}\text{C}$), atmospheric nitrogen ($\delta^{15}\text{N}$), and Vienna-Canyon Diablo Troilite ($\delta^{34}\text{S}$). For quality control, replicate assays of standard reference materials and duplicate samples were included with every 20 samples analyzed. The relative percent difference between duplicate samples was 4.4%, 3.0%, and 2.6% for $\delta^{13}\text{C}$, $\delta^{15}\text{N}$, and $\delta^{34}\text{S}$, respectively.

Node Assignment

$\delta^{13}\text{C}$ and $\delta^{34}\text{S}$ values in stranded dolphin skin were utilized to assign deceased stranded bottlenose dolphins to habitats using the splitting criteria provided by Hohn et al. (2017). To develop this criterion, Hohn et al. (2017) analyzed the $\delta^{13}\text{C}$ and $\delta^{34}\text{S}$ values in biopsied skin samples from free-ranging bottlenose dolphins off the coast of AL, MS, and LA of known habitats (e.g., estuarine, barrier island, coastal) and performed a recursive partition analysis (i.e., classification/regression tree) to describe the relationship between habitat (used as a proxy for stock) and stable isotope ratios. Currently, NOAA/NMFS includes barrier island habitats within BSE stocks; however, recent telemetry and genetic studies suggest that barrier island populations may represent separate stocks; therefore, Hohn et al. (2017) treated individuals associated with barrier island habitats as potentially distinct stocks (Rosel et al., 2017; Wells et al., 2017; Hayes et al., 2019). In their study, Hohn et al. (2017) analyzed the samples from free-ranging

dolphins from east and west of the Mississippi River Bird's Foot Delta [hereafter referred to as the Mississippi River Delta (MRD)] separately to account for differences between the estuarine systems west and east of the MRD. Both the east and west datasets included samples collected from dolphins in estuarine, barrier island, and coastal habitats. The recursive partition analysis resulted in six terminal nodes corresponding to six different habitats including one coastal node (node 1), one barrier island node (node 2), and one estuarine node (node 3) west of the MRD, and one barrier island (node 4), and two estuarine nodes (nodes 5 and 6) east of the MRD. When Hohn et al. (2017) used the splitting criteria to predict dolphin habitats for free-ranging dolphins of known habitats, it assigned 80.5% of the dolphins to the correct habitat. The authors subsequently assigned deceased stranded dolphins from AL, FL, LA, and MS to predicted habitats using the spitting criteria generated from the recursive partition analysis. First, for both dolphins that stranded east and west of the MRD, dolphins exhibiting $\delta^{34}\text{S} \geq +15\text{‰}$ were assigned to the coastal node (node 1), and dolphins with $\delta^{34}\text{S} < +15\text{‰}$ were retained for future node assignment. Next, for the western group, those with $\delta^{13}\text{C} \geq -18.5\text{‰}$ were assigned to the west barrier island (node 2), and those with $\delta^{13}\text{C} < -18.5\text{‰}$ were assigned to the west estuary (node 3). For the eastern group, dolphins with $\delta^{13}\text{C} < -17.6\text{‰}$ were assigned to the first east estuary (node 6). The remaining dolphins in the eastern group with $\delta^{13}\text{C} \geq -17.6\text{‰}$ were split based on their $\delta^{34}\text{S}$ values; those with $\delta^{34}\text{S} \geq +13.5\text{‰}$ were assigned to the east barrier island (node 4), and those with $\delta^{34}\text{S} < +13.5\text{‰}$ were assigned to the second east estuary (node 5). Overall, Hohn et al. (2017) found some spatial patterns in node assignment among stranded dolphins, particularly related to estuarine habitats east of the MRD. For example, most of the dolphins assigned to the east estuary (node 5)

stranded along the FL panhandle, while those associated with the east estuary (node 6) stranded in AL, MS, and eastern LA (Figure 3.1A).

Statistical analyses for comparing stable isotope ratios and THg concentrations among nodes

We used generalized linear models with a normal distribution and identity link function to determine the influence of node assignment, sex, and stranding year on THg concentration and $\delta^{15}\text{N}$ in dolphin skin. Sample decomposition can influence both THg concentrations and stable isotopes ratios (Payo-Payo et al., 2013; Hohn et al., 2017; Martínez-López et al., 2019); however, condition code was excluded as a predictor of THg concentrations and $\delta^{15}\text{N}$ since the majority (80%) of samples were from condition code 4 individuals (i.e., limited variation in predictor). Node assignment was dependent on $\delta^{13}\text{C}$ and $\delta^{34}\text{S}$ values; therefore, $\delta^{13}\text{C}$ and $\delta^{34}\text{S}$ were excluded from the analyses. Models with all possible combinations of explanatory variables were compared using an Akaike Information Criterion adjusted for small sample sizes (AIC_c) (Akaike, 1973; Symonds and Moussalli, 2011). The model with the lowest AIC_c score has the largest support; however, models within 2 AIC_c units of the top model are considered to be competing and have equal support. If two competing models were nested, we chose the model with the fewest parameters following the principle of parsimony (Burnham and Anderson, 2002). The level of significance was set at $\alpha = 0.05$ and all analyses were performed in R version 4.0.2 (R core team, 2020). We checked the models for assumptions of normality and homoscedasticity by inspecting residual plots (Zurr et al., 2010). When assumptions were violated, response variables were Log_{10} transformed. If node assignment and either sex, body length, or stranding year were significant, we

estimated the marginal mean of the response variable using the emmeans package in R (Length, 2020). To explore the influence of each predictor in the final model, we used the effects package to calculate the effect for one predictor at a time while holding the remaining predictors constant at their mean value (Fox and Hong, 2009).

Statistical analyses for estimating bottlenose dolphin trophic position in each node

After dolphins were assigned to a node corresponding to a predefined habitat, we estimated the trophic position of dolphins in each node utilizing a Bayesian approach. Traditionally, trophic position is estimated using a single point estimate for both the isotopic value of the baseline organism and the trophic enrichment factor (TEF) or the difference in isotopic value between the predator and prey (Quezada-Romegialli et al., 2018a,b; Wild et al., 2020). In the present study, to reflect the variation more accurately in both the isotopic values of primary consumers and the TEF, we utilized the R package tRrophicPosition, which applies a Bayesian model to estimate trophic position (Quezada-Romegialli et al., 2018b). We estimated the trophic position for each dolphin node using $\delta^{15}\text{N}$ values from a single baseline and included the TEF for nitrogen only ($\Delta^{15}\text{N}$), using the following equation:

$$\delta^{15}\text{N}_c = \delta^{15}\text{N}_b + \Delta^{15}\text{N} (\text{TP} - \lambda)$$

where $\delta^{15}\text{N}_c$ = the $\delta^{15}\text{N}$ value in the consumer (dolphins), $\delta^{15}\text{N}_b$ = the $\delta^{15}\text{N}$ in primary consumer, $\Delta^{15}\text{N}$ = the trophic enrichment factor for $\delta^{15}\text{N}$, TP = the trophic position of the consumer (dolphin), and λ = the trophic level of the primary consumer. In this way, tRrophicPosition calculates the trophic position at the population level, combining Markov Chain Monte Carlo simulations through JAGS and statistical analyses (Quezada-Romegialli et al., 2018a,b).

In the model, $\delta^{15}\text{N}$ values of the primary consumers and dolphins, and $\Delta^{15}\text{N}$ are treated as random variables, each with a prior normal distribution. The trophic level (λ) of the primary consumer is treated as a fixed variable. $\delta^{15}\text{N}$ values of primary consumers [striped mullet, white mullet (*Mugil curema*) and Gulf menhaden (*Brevoortia patronus*)], found in areas associated with the stranded dolphin habitats, were taken from the literature (Table 3.1) (Deegan et al., 1990; Senn et al., 2010; Fry and Chumchal, 2012; Worthy et al., 2013). We could not find barrier island-specific data for the primary consumers; therefore, for the east and west barrier island nodes, we utilized data from nearby estuarine habitats. For each node, values for $\delta^{15}\text{N}$ in the primary consumers were simulated from a normal distribution with the same mean and standard deviation (SD) from their respective datasets. The length of the resulting dataset was equal to the number of dolphins assigned to the respective node.

Trophic enrichment factors (Δ) vary depending on the species, dietary sources, and the tissue type investigated (McCutchan et al., 2003; Vanderkluft and Ponsard, 2003; Caut et al., 2009, 2011; Robbins et al., 2005,2010). Generalized TEFs of ≈ 1.0 for $\Delta^{13}\text{C}$ and ≈ 3.4 for $\Delta^{15}\text{N}$ are often applied to marine mammal studies (Post et al., 2002; McCutchan et al., 2003; Caut et al., 2009). However, there are a few controlled dietary studies that estimate the TEF in marine mammals (Hobson et al., 1996; Alves-Stanley et al., 2009; Caut et al., 2011; Browning et al., 2014; Giménez et al., 2016). Two studies estimated the TEF in bottlenose dolphin skin (Browning et al., 2014; Giménez et al., 2016); both studies found that while a $\Delta^{13}\text{C}$ value of 1‰ may be appropriate for bottlenose dolphin skin, the $\Delta^{15}\text{N}$ value for bottlenose dolphin skin may be closer to 1.5‰, which substantially differs from the general literature value of 3.4‰. Therefore,

for this study, we used the variance-weighted mean $\Delta^{15}\text{N}$ and standard error calculated from the raw data of Browning et al. (2014) and Giménez et al. (2016) ($\Delta^{15}\text{N} = 2.12 \pm 0.53\text{‰}$), which was reported by Wild et al. (2020), for trophic level modeling. $\Delta^{15}\text{N}$ values were simulated from a normal distribution of $2.14 \pm 0.53\text{‰}$. To understand the implications of using different values of TEF, the above methods were repeated using the traditional $\Delta^{15}\text{N}$ value of $3.4 \pm 1\text{‰}$ (Post et al. 2002).

In most cases, we were able to find the λ values of primary consumers from the same habitats as the stranded dolphins. The trophic level of Gulf menhaden ($\lambda = 2.5$) was used to estimate dolphin trophic position for the coastal node (node 1), and the trophic level of striped and white mullet combined ($\lambda = 2.6$) was used to estimate the trophic position of dolphins assigned to the west barrier island (node 2), west estuary (node 3), and east estuary (node 6). For the east estuary (node 5), the trophic level of striped mullet was not reported by Worthy et al. (2013) or in other published literature from the region; thus, we used the average trophic level for primary consumers across the above-mentioned studies ($\lambda = 2.55$). After estimating a trophic position for each dolphin habitat (i.e., node) using a mean of $\Delta^{15}\text{N}$ of 2.14‰ and 3.4‰ , we then compared the trophic positions between all combinations of nodes using the compare two distribution functions in the tRophicPosition package.

To put our Hg biomagnification data into a broader context, we estimated the average biomagnification rate of THg, using the $\delta^{15}\text{N}$ and THg concentrations from primary consumers taken from the literature (Senn et al., 2010; Karouna-Renier et al., 2011; Fry and Chumchal, 2012) and our dolphin samples using the following equation:

$$\text{Log}_{10}\text{THg concentration} = a \times \delta^{15}\text{N} + b$$

where a = the slope of the relationship between $\text{Log}_{10}\text{THg}$ concentration and $\delta^{15}\text{N}$ (i.e., the biomagnification rate), and b is the intercept. Next, we calculated the trophic biomagnification factor (TMF), or the average factor change in THg concentration between two trophic positions (Ouédraogo et al., 2015; Masset et al., 2019), using the following equation:

$$\text{TMF} = 10^{a \cdot \text{TEF}}$$

where a is the biomagnification rate or the slope from the relationship between $\text{Log}_{10}\text{THg}$ concentration, and TEF is the trophic enrichment factor for $\delta^{15}\text{N}$. All THg concentrations in the primary consumers taken from the literature were measured in fish sampled within a 5-year period (2003-2007). Although temporal differences were not assessed in the studies, variation in THg concentrations within species was on the level of 3-5 ng/g. We also plotted the relationship between the trophic position and $\text{Log}_{10}\text{THg}$ concentration and the relationship between $\delta^{15}\text{N}$ and $\text{Log}_{10}\text{THg}$ concentration using a $\Delta^{15}\text{N}$ of both 2.14‰ and 3.4‰ to determine the influence of TEF on the estimated trophic position.

Results

Predicted habitat of stranded bottlenose dolphins

We initially separated dolphins into two groups according to their stranding locations; dolphins that stranded east of the MRD were assigned to the eastern group and dolphins that stranded west of the MRD was assigned to the western group. Therefore, the eastern group included all dolphins that stranded in FL ($n = 29$), as well as those that stranded in LA east of the MRD ($n = 14$), while the western group included dolphins that stranded in LA west of the MRD ($n = 58$). Because we did not have samples from AL or

MS, the shortest distance between dolphins assigned to the eastern and western groups was approximately 150 km. We then predicted the habitat of each stranded individual using the splitting criteria generated from the recursive patrician analysis reported in Hohn et al. (2017).

The spatial pattern of node assignment was similar to the spatial pattern observed among stranded bottlenose dolphins reported by Hohn et al. (2017) (Figure 3.1A and 3.11B). Across nodes, the greatest number of dolphins were assigned to the west barrier island (node 2; 41%; $n = 42$), followed by the east estuary (node 5 = 23%; $n = 23$), the coastal node (node 1 = 15%; $n = 15$), the east estuary (node 6 = 11%; $n = 11$), the west estuary (node 3 = 7%; $n = 7$), and the east barrier island (node 4 = 3%; $n = 3$). More stranded dolphins from west of the MRD were assigned to the coastal node (node 1) than east of the MRD ($n = 9$ and 6 , respectively). Dolphins assigned to the western barrier island (node 2) stranded primarily along the barrier islands separating Barataria Bay and the adjoining bays from the GoM. Most dolphins assigned to the west estuary (node 3) stranded just west of the MRD. East of the MRD, the three dolphins assigned to the eastern barrier island (node 4) stranded in eastern LA. Of the two eastern estuarine nodes, the east estuary (node 5) was more associated with dolphins stranded along the FL panhandle whereas, the east estuary (node 6) was more commonly associated with dolphins stranded in eastern LA, with the majority stranding along the shoreline of Lake Pontchartrain.

Stable isotope ratios and THg in relation to predicted habitats

$\delta^{13}\text{C}$, $\delta^{15}\text{N}$, and $\delta^{34}\text{S}$ values varied across nodes (Figure 3.2; Table 3.2). Across all three stable isotopes, the east estuary (node 5) was unique. The east estuary (node 5) was

most $\delta^{13}\text{C}$ enriched, while the east estuary (node 6) and west estuary (node 3) were most $\delta^{13}\text{C}$ depleted. Across nodes, $\delta^{15}\text{N}$ was similar except for the east estuary (node 5), which was $\delta^{15}\text{N}$ depleted compared to the remaining nodes. The coastal node (node 1) was the most enriched in $\delta^{34}\text{S}$, and the east estuary (node 5) was the most $\delta^{34}\text{S}$ depleted. For inferential statistics, we did not include dolphins assigned to the east barrier island (node 4) due to the small sample size ($n = 3$). The model with the most support following AIC_c included node assignment and stranding year as predictors of stranded bottlenose dolphin skin $\delta^{15}\text{N}$ values (Table 3.3). The effect plots for stranding year and node assignment (Figure 3.3A and 3.3B) provide predicted values for a single predictor while holding the remaining predictor constant at their mean value. The estimated marginal mean (± 1 SE) $\delta^{15}\text{N}$ (‰), which accounts for variation in stranding year, was most enriched in the west estuary (node 3 = $+16.7 \pm 0.44$), followed by the coastal node (node 1 = $+16.6 \pm 0.29$), west barrier island (node 2 = $+16.2 \pm 0.18$), east estuary (node 6 = $+15.5 \pm 0.38$), and east estuary (node 5 = $+14.2 \pm 0.24$).

Mean (± 1 SD) THg concentrations [$\mu\text{g/g}$ dry weight (wt)] were greatest in the coastal node (node 1 = 7.70 ± 7.12), followed by the east estuary (node 5 = 5.52 ± 4.34), the east barrier island (node 4 = 3.75 ± 2.94), the west barrier island (node 2 = 1.53 ± 1.41), the east estuary (node 6 = 1.47 ± 1.07), and the west estuary (node 3 = 0.995 ± 0.587) (Figure 3.4). The model with the most support included node assignment, sex, and body length as predictors of THg concentration (Table 3.3). Body length and THg concentration were positively correlated (Figure 3.5A). Holding the other predictors constant, females had greater THg concentrations than males (Figure 3.5C). After accounting for body length and sex, the order of nodes in relation to mean THg

concentration changed; the east estuary (node 5) had the greatest estimated marginal mean (± 1 SE) THg concentration ($\mu\text{g/g}$ dry wt) (4.81 ± 0.84), followed by the coastal node (node 1 = 3.65 ± 0.68), the east estuary (node 6 = 2.59 ± 0.65), the west barrier island (node 2 = 0.993 ± 0.12), and the west estuary (node 3 = 0.675 ± 0.18). However, despite changes in the ranking, the nodes were still separated into two distinct groups (Figure 3.5B). The first group, which included the east estuary (node 5), the coastal node (node 1), and the east estuary (node 6), had greater mean THg concentrations than the second group, which included the west barrier island (node 2) and west estuary (node 3).

Trophic position estimations

When utilizing a $\Delta^{15}\text{N}$ TEF of $2.12 \pm 0.53\text{‰}$, the mean trophic position estimates for each node ranged from 5.24 to 6.06. On average, the trophic position estimate was highest in the east estuary (node 6 = 6.06), followed by the east estuary (node 5 = 5.88), the west estuary (node 3 = 5.61), the west barrier island (node 2 = 5.47), and the coastal node (node 1 = 5.24) (Figure 3.6A). The trophic position of the coastal node (node 1) differed from the trophic position of both the east estuarine nodes [node 5 ($p = 0.042$) and node 6 ($p = 0.021$)]. In contrast, when trophic position estimations were calculated using a $\Delta^{15}\text{N}$ TEF of $3.4 \pm 1\text{‰}$, trophic positions of dolphins across all nodes were approximately one trophic level lower (mean range: 4.21 - 4.77). However, the order of trophic position from highest to lowest according to node assignment remained the same. On average, when utilizing a $\Delta^{15}\text{N}$ of 3.4‰ , trophic position estimates were greatest in the east estuary (node 6 = 4.77), followed by the east estuary (node 5 = 4.64), the west estuary (node 3 = 4.49), the west barrier island (node 2 = 4.39), and the coastal node (node 1 = 4.21) (Figure 3.6B). The only differences in trophic positions were between the

coastal node (node 1) and both the east estuarine nodes [node 5 ($p = 0.046$) and node 6 ($p = 0.024$)].

Next, we explored the relationship between $\text{Log}_{10}\text{THg}$ concentration and $\delta^{15}\text{N}$ values in both the primary consumers and bottlenose dolphins. The slope of the linear regression between $\text{Log}_{10}\text{THg}$ concentration and $\delta^{15}\text{N}$ is equal to the biomagnification rate. We estimated an average biomagnification rate of 0.23 (Figure 3.7A). We then plotted the relationship between the mean estimated trophic position, calculated based on $\Delta^{15}\text{N}$ of 3.4‰ and 2.14‰, and $\text{Log}_{10}\text{THg}$ concentration, and compared the linear regressions in Figure 3.7B and 3.7C, respectively. There was a slightly higher R^2 value for the model that used a $\Delta^{15}\text{N}$ of 2.14‰. There was an expansion of the food web when using a $\Delta^{15}\text{N}$ of 2.14‰. In Figures 3.7D and 3.7E, alongside the relationship between $\delta^{15}\text{N}$ and $\text{Log}_{10}\text{THg}$, we included horizontal lines that coincide with estimated trophic positions based on a $\Delta^{15}\text{N}$ of 3.4‰ and 2.14‰, respectively. These results reinforce that varying inputs of TEF will substantially alter the trophic position estimations, with a $\Delta^{15}\text{N}$ of 2.14‰ leading to higher estimations of trophic position. Finally, the estimated TMF was 3.11 and 6.05 when we applied a $\Delta^{15}\text{N}$ of 2.12‰ and 3.4‰, respectively.

Discussion

Exhibiting long-term residence patterns in nearshore habitats, bottlenose dolphins from the nGoM show spatial patterns of skin THg concentrations that are similar to those found in lower trophic level consumers, which may reflect local Hg sources and environmental conditions (Balmer et al., 2008; Hall et al., 2008; Apeti et al., 2012; Evans et al., 2015; Wells et al., 2017; Toms, 2019; Perrot et al., 2019; McCormack et al.,

2020a,b). However, our study also suggests that differing trophic positions among dolphin populations also contribute to the spatial variability of THg concentrations. Notably, dolphins that stranded east of the MRD and were assigned to estuarine habitats had greater skin THg concentrations and higher estimated trophic positions than dolphins assigned to estuarine or barrier island habitats west of the MRD.

Top pelagic predators are often migratory, and during migration, organisms incorporate chemical signals (including contaminants) across various foraging habitats, in some cases spanning large spatial extents. As a result, an organism's chemical signature (e.g., contaminant concentrations, stable isotope ratios) reflects the influence of multiple foraging habitats, which can mask local signatures (Post et al., 2002; Wilson et al., 2013; Evans et al., 2015). Some bottlenose dolphins in the nGoM display site fidelity towards specific bays, sounds, and estuaries (e.g., <100 km² in Barataria Bay, LA), while others may move between nearby BSE stocks and between BSE and coastal stocks (up to 20 m isobath) within the nGoM (Balmer et al., 2008; Tyson et al., 2011; Würsig, 2017; Wells et al., 2017; Toms, 2019). Compared to other marine predators like Atlantic bluefin tuna (*Thunnus thynnus L.*) (Teo et al., 2007), migration of bottlenose dolphins in the nGoM is comparably small and may allow for the spatial integration of pollution signals.

Previous research reported that blubber, kidney, liver, lung, and skin THg concentrations from bottlenose dolphins stranded along the FL panhandle were greater than dolphins stranded along the LA coast (McCormack et al., 2020a,b). In these studies, differences in THg concentrations between dolphins stranded in FL and LA were addressed within the context of Hg sources and environmental conditions (McCormack et al., 2020a,b). While we will also address these topics, we will first address the focus of

the current study, which is the importance of trophic position in explaining the variation in THg concentrations among bottlenose dolphins. Before estimating trophic position, we first assigned the stranded dolphins to predicted habitats based on their skin $\delta^{13}\text{C}$ and $\delta^{34}\text{S}$ values, according to the splitting criterion reported in Hohn et al. (2017). Categorizing dolphins according to habitats allowed us to explore spatial differences in THg concentrations within stranded dolphins from FL and LA. We were also able to assess whether there were differences in THg concentrations between the estuarine, barrier island, and coastal (from 2 km off the beach to the 20 m isobath) dolphins (Hohn et al., 2017).

However, the spatial and temporal coverage of the Hohn et al. (2017) study did not directly coincide with the present study. Our study included stranded dolphins between 2011 and 2016, while Hohn et al. (2017) analyzed stranded dolphins between 2010 and 2013. We assume that the spatial variation in isotopic signatures is greater than the temporal variation. Although we cannot test the robustness of this assumption, the standard error of the mean reported for $\delta^{13}\text{C}$, $\delta^{34}\text{S}$, and $\delta^{15}\text{N}$ in striped and white mullet caught between July and October across a 5-year study period in Barataria Bay, LA was between 2-7 ‰, suggesting there is minimal temporal variation in isotopic signatures in Barataria Bay (Fry and Chumchal, 2012). Stable isotope ratios may also vary seasonally within a year. In Pensacola Bay, FL, Worthy et al. (2013) reported mean \pm 1 SD $\delta^{15}\text{N}$ (‰) values for striped mullet measured in November (7.05 ± 0.77 ; $n = 14$), February (9.48 ; $n = 1$), April (7.66 ± 0.91 ; $n = 14$), and July (7.17 ± 1.93 ; $n = 5$) between 2010 and 2011. Additionally, while stranded dolphins were sampled by Hohn et al. (2017) from AL, FL, LA, and MS, our study only included those stranded dolphins from FL and LA.

Compared to Hohn et al. (2017), our strandings from FL also occurred further east in the panhandle. As a result, some dolphins analyzed in the present study may have originated from source populations not included in the analysis by Hohn et al. (2017). For example, across nodes, the range of mean $\delta^{13}\text{C}$ values in the present study was greater than the range of mean $\delta^{13}\text{C}$ values reported by Hohn et al. (2017), suggesting that some dolphins in our study may have originated from different habitats. Based on the stable isotope ratios and stranding locations, dolphins in our study may have originated from estuarine systems further east (e.g., St. Andrew Bay, St. Joseph Bay); therefore, they more accurately represent THg concentrations in local dolphin populations in those systems rather than THg concentrations in the resident dolphins of Pensacola/Choctawhatchee Bay system as was suggested by Hohn et al. (2017). Influxes of seasonal migrants may also influence the interpretation of our results, particularly in St. Joseph Bay which receives substantial seasonal migrants in the spring and autumn months (Balmer et al., 2008). Of the ten dolphins that stranded in St. Joseph Bay, eight stranded between December and February, a time when most dolphins present are year-round residents. The remaining two dolphins stranded in November and March and could be either year-round residents or seasonal migrants.

We estimated the trophic position for each node twice, once with a mean ± 1 SD $\Delta^{15}\text{N}$ of $2.12 \pm 0.53\text{‰}$ and once with a $\Delta^{15}\text{N}$ of $3.4 \pm 1\text{‰}$. Trophic position estimates were higher when we used a $\Delta^{15}\text{N}$ of 2.12 (mean trophic position range: 5.24 - 6.06) than a $\Delta^{15}\text{N}$ of 3.14‰ (4.21 - 4.77). However, the ranking of nodes remained the same. Trophic positions were higher in estuarine habitats east of the MRD (nodes 5 and 6) compared to the west barrier island (node 2) and west estuary (node 3). These findings

coincided with THg concentrations; compared to dolphins assigned to the east estuarine habitats, dolphins assigned to western estuarine and barrier island habitats had lower estimated marginal mean THg concentrations and lower trophic positions. However, this was not the case for coastal dolphins; those assigned to the coastal node had the second-highest estimated marginal mean THg concentration among nodes but had the lowest estimated trophic position. The discrepancy between the trophic position and THg concentrations may indicate that the primary consumer applied to the model was inappropriate for these dolphins. The food webs coastal dolphins are relying on may have greater underlying Hg concentrations. Local point sources of $\delta^{15}\text{N}$ (e.g., agriculture runoff from the MS river) can also complicate the interpretation of relative trophic position. Since we utilized baseline primary consumers from each habitat to estimate the trophic position, the differences in baseline nitrogen values were incorporated within the model framework (Valiela et al., 1997; Bricker et al., 2007). However, a lack of barrier island specific baselines is a limitation of the study and may also have influenced our results.

In the nearshore waters of the GoM, dolphins forage on a variety of fishes, particularly soniferous fishes such Atlantic croaker (*Micropogonias undulatus*), pigfish (*Orthopristis chrysoptera*), silver perch (*Bairdiella chrysoura*), spot (*Leiostomus xanthurus*), and spotted sea trout, but also non-soniferous fishes such as pinfish (*Lagodon rhomboides*) and striped mullet (Fish and Mowbray, 1970; Barros and Odell, 1990; Barros, 1993; Beren-McCabe, 2010; Bowen, 2011; Bowens-Stevens et al., 2021). There have been more dietary studies focused on bottlenose dolphin populations in FL compared to LA. While the types of prey items are similar between the habitats, there

may be dietary differences between dolphin populations in FL and LA resulting from differences in fish communities or individual foraging behavior (Barros and Odell, 1990; Barros, 1993; Beren-McCabe, 2010; Bowens-Stevens et al., 2021). For example, Bowens-Stevens et al. (2021) recently reported that the Atlantic croaker was the most abundant prey item found in the stomachs of bottlenose dolphins stranded in Barataria Bay, LA between 2010 and 2012. In contrast, Bowen (2011) found that spot was the most abundant prey item in stranded bottlenose dolphins from the FL panhandle. Furthermore, compared to dolphins that stranded along the FL panhandle, dolphins that stranded in LA had a greater proportion of shrimp and a higher abundance of anchovies in their stomachs (Bowen, 2011; Bowen-Stevens et al., 2021). A greater dependence on lower trophic level prey items in LA may explain the lower trophic positions observed in dolphins stranded in LA in the present study.

Body condition and sample decomposition can also influence THg concentrations. We do not have information on the body condition of the animals before death. Level A data collected from NOAA stranding networks define the condition of a deceased stranded animals from 2-4 (code 2 = fresh, code 3 = moderate decomposition, code 4 = advanced decomposition; Smithsonian Institution Coding System; Geraci and Lounsbury, 2005). Although we did not explore the influence of condition code, McCormack et al. (2020a,b) found that condition code or sample decomposition positively influenced THg concentrations in the blubber, kidney, liver, and skin. However, the inclusion of condition code in the regression models did not improve model fit substantially. We do not have specific data on the body condition of the animals sampled in this study, but many dolphins analyzed in this study stranded during the nGoM cetacean unusual mortality

event (2010-2014) which coincided with the Deepwater Horizon oil spill (DWHOS).

After the oil spill, dolphins were in poor body condition, particularly those studied in LA (Carmichael et al., 2012; Schwacke et al., 2014). A loss of lipids associated with poor body condition can increase observed Hg concentrations (Lavoie et al., 2010).

Additionally, dolphins may have been exposed to Hg from the DWHOS.

Dolphins from estuarine and barrier island habitats in LA (nodes 2 and 3) would be more affected by the DWHOS than those in FL (nodes 5 and 6). Mercury is present in crude oil (Wilhelm et al., 2007); therefore, some dolphins could have been exposed to Hg through the direct ingestion of oil or if they ingested oil-contaminated prey. One might expect to find greater concentrations of Hg in fish near the Deepwater Horizon well-head, and as a result, greater Hg concentrations in dolphins foraging near the well-head.

However, measuring the concentration of Hg in golden tilefish along the nGoM shelf break, Perrot et al. (2019) found the opposite: golden tilefish closer to the well-head (47 km) had lower concentrations of THg than golden tilefish sampled >100 km northeast of the well-head. Based on $\delta^{202}\text{Hg}$, $\delta^{13}\text{C}$, $\delta^{15}\text{N}$, and $\delta^{34}\text{S}$ values, the authors hypothesized that fish closer to the well-head had lower Hg concentrations due to suspended particles from the Mississippi River, which reduced Hg bioavailability.

Houde et al. (2006) estimated the trophic position of bottlenose dolphin populations in Sarasota Bay, FL and in the waters off Charleston, South Carolina at 4.4 and 4.1, respectively. Compared to the trophic position estimations of Houde et al. (2006), our trophic position estimates were elevated, particularly when we applied a $\Delta^{15}\text{N}$ of 2.14‰. Elevated trophic positions may indicate that 2.14‰ is an underestimation of $\Delta^{15}\text{N}$. The $\Delta^{15}\text{N}$ may also be between 2.12‰ and 3.14‰. Hussey et al. (2014) suggest

that applying a single $\Delta^{15}\text{N}$ across the food web may not be appropriate; instead, the authors proposed that there may be a narrowing of $\Delta^{15}\text{N}$ as you move up the food web. As a result, a $\Delta^{15}\text{N}$ of 3.4‰ may be appropriate for some trophic level steps, but a smaller $\Delta^{15}\text{N}$ may be more applicable for higher trophic level steps. Instead of the default value of 2 in the `tRrophicPosition` package in R, we used trophic positions for Gulf menhaden and striped or white mullet from the literature, which were 2.5 and 2.6, respectively. If we used the default value of 2, our trophic position estimates for dolphins would be lower. We estimated a THg magnification rate of 0.23, which is similar to the THg magnification rate reported by Hong et al. (2013) for Sarasota Bay, FL (0.27) and by Lavoie et al. (2013) of (0.19), which reviewed THg magnification rates worldwide for coastal marine systems within 20 km of the coast. We calculated the TMF twice: once using a $\Delta^{15}\text{N}$ of 2.12‰ and once using $\Delta^{15}\text{N}$ of 3.4‰ and estimated a TMF of 3.11 and 6.05, respectfully. Both values are within the range reported in the literature for marine systems (Lavoie et al., 2013). However, the use of bulk $\delta^{15}\text{N}$ to estimate TMF can be misleading, particularly when there is a difference in baseline $\delta^{15}\text{N}$ sources (Eliot et al., 2021).

When interpreting stable isotope ratios, understanding tissue-specific isotopic turnover and the effect of body condition and sample decomposition is also critical. A controlled study by Browning et al. (2014) determined that the mean (\pm SD) isotopic turnover of $\delta^{13}\text{C}$ and $\delta^{15}\text{N}$ in bottlenose dolphin skin was 13.9 ± 4.8 days and 17.2 ± 1.3 days, respectively. Therefore, $\delta^{13}\text{C}$ and $\delta^{15}\text{N}$ isotopic signatures in dolphin skin are only reflective of prey consumed within the previous 6 to 8 weeks (Hohn et al., 2017). Sample decomposition and poor body condition may also lead to enriched nitrogen values (Payo-

Payo et al., 2013; Hertz et al., 2015; Martínez-López et al., 2019). The results of Hohn et al. (2017) suggest that sample decomposition is not a large contributor to the variation in isotopic ratios ($\delta^{13}\text{C}$, $\delta^{15}\text{N}$, and $\delta^{34}\text{S}$) in bottlenose dolphin skin; however, stranded dolphins did have more enriched skin $\delta^{15}\text{N}$ values than free-ranging dolphins. In contrast, McCormack et al. (2020a) determined that condition code positively influenced $\delta^{15}\text{N}$ values in stranded bottlenose dolphin skin. For dolphins stranded in FL, condition code 4 individuals were on average 0.50‰ more enriched in $\delta^{15}\text{N}$ than condition code 2 individuals. For dolphins stranded in LA, condition code 4 individuals were on average 1.5‰ more enriched in $\delta^{15}\text{N}$ compared to condition code 2 individuals. The effects of decomposition were not investigated in the present study. Again, we do not have information on the condition of the animals before death; however, following the DWHOS dolphins were in poor body condition (Carmichael et al., 2012; Schwacke et al., 2014).

Given the data, differences in trophic positions between dolphin populations and differences in Hg sources and deposition between foraging habitats likely both simultaneously contribute to the spatial variability in skin THg concentrations observed among dolphins. Variation in Hg sources and environmental conditions that facilitate Hg methylation have previously been discussed by McCormack et al. (2020a,b). In summary, in the nGoM, Hg sources can include atmospheric deposition, riverine inputs, and the Loop Current transporting Hg from the Atlantic Ocean (Harris et al., 2012a,b). Mercury sources can be further categorized as non-point and point sources. The proportion that each source contributes varies spatially due to differences in Hg sources, uneven mixing, and water circulation patterns. Although it is not within the scope of this study to link Hg

sources to Hg concentrations in bottlenose dolphins, it is relevant to highlight the known point sources of Hg in the region which could influence local Hg conditions. In the coastal counties of the FL panhandle between Escambia County and Franklin County, the greatest contributors to Hg emissions, according to the US EPA 2011 report, were the Gulf Power Company (an electricity-generating plant) in Pensacola (43.9 lbs), the International paper company (12 lbs) in Cantonment, the Gulf Power Company in Lynn Haven (75 lbs), Bay county solid waste (7.79 lbs) in Panama City, and Westrock CP LLC (6.35 lbs) in Panama City, the latter of which are a municipal waste combustor and paper and pulp facility, respectively. The major facilities contributing to Hg emissions in LA occur in the western LA parish of Calcasieu, some of which exceeded 300 lbs. However, the closest Hg-emitting facilities to Barataria Bay were a few parishes away including, petroleum refineries in St. Charles, Plaquemines, and St. Bernard parishes, which contributed 105, 25, 14 lbs, respectively, and a steel mill in St. John the Baptist parish (54 lbs).

Mercury entering the GoM is primarily Hg^{2+} (Fitzgerald et al., 2007; Selin, 2009; Pirrone et al., 2010). Both the source of Hg to the GoM and the local environmental conditions can influence the likelihood of Hg methylation, and as a result, biomagnification in the food web (Rice et al., 2009; Harris et al., 2012a,b; Evans et al., 2015; Lavoie et al., 2013,2015; Harper et a. 2018). Environmental conditions including geochemical factors (e.g., quantity and quality of dissolved organic matter and sulfide concentrations; Liu et al., 2009; Mangal et al., 2018) and microbial factors (e.g., presence of sulfate-reducing organisms; Peterson et al., 2020) can facilitate or inhibit Hg methylation. The biomass of the primary producer may also contribute to overall Hg

concentrations in higher trophic position organisms. For example, Chen et al. (2005) found negative correlations between phytoplankton density and Hg concentrations in zooplankton and between zooplankton density and Hg concentrations in herbivorous and predatory fish. Over time, high concentrations of phytoplankton remove Hg from the water column, which can create a steady-state in which there is less Hg available for uptake and consequently lower Hg concentrations, a process termed biodilution (Evans et al., 2015). Increased nutrient runoff from the Mississippi River may foster increased phytoplankton, decreasing THg concentrations in biota. Also, the seasonally occurring hypoxic zone, which occurs west of the MRD, is characterized by an increase in hydrogen sulfide releases from the sediment, which can inhibit Hg methylation (Benoit et al., 1999; Rabalais et al., 2001; Fitzgerald. et al., 2007; Sluis et al., 2013). In addition to differences in trophic position, the abovementioned differences in Hg sources and environmental conditions may also explain why estuarine and barrier island dolphins that stranded west of the MRD had lower THg concentrations than those that stranded east of the MRD.

Conclusions

Our study suggests that differences in trophic positions among dolphins from the nGoM partially explain the spatial variation in skin THg concentrations observed among deceased bottlenose dolphins that stranded along the LA and FL coasts. However, differences in Hg sources and environmental factors between foraging habitats likely also contribute to the spatial variation of Hg observed in bottlenose dolphins from the nGoM. Finally, we demonstrate that trophic position estimations are sensitive to differences in

TEFs. Additional research on the tissue and species-specific TEFs for marine mammals would benefit future studies.

Table 3.1. $\delta^{15}\text{N}$ values (mean \pm 1 standard deviation or standard error*) for primary consumers used to predict bottlenose dolphin trophic position according to node assignments based on Hohn et al. (2017). Menhaden used for the node 1 were collected in coastal waters outside of Terrebonne Bay, LA (< 20 km from the shoreline); striped mullet used for nodes 4 and 5 were collected within Pensacola Bay, FL; striped mullet for nodes 2 and 3 were sampled in within the lower portions of Barataria Bay, LA; and striped and white mullet for node 6 were sampled in Brenton Sound, LA.

Predicted node	Baseline organism	$\delta^{15}\text{N}$ (‰)	Reference
Coastal (node 1)	Gulf menhaden (<i>Brevoortia patronus</i>)	10.8 \pm 0.80	Senn et al., 2010
West barrier island (node 2)	Striped mullet (<i>Mugil cephalus</i>)	10.1 \pm 1.20*	Fry and Chumchal, 2012
West estuary (node 3)	Striped mullet	10.1 \pm 1.20*	Fry and Chumchal, 2012
East barrier island (node 4)	Striped mullet	7.05 \pm 0.77	Worthy et al., 2013
East estuary (node 5)	Striped mullet	7.05 \pm 0.77	Worthy et al., 2013
East estuary (node 6)	Striped mullet and white mullet (<i>Mugil curema</i>)	8.50 \pm 0.40*	Fry and Chumchal, 2012

Table 3.2. Stable isotope ratios [mean, standard deviation (SD), minimum (Min), maximum (Max), and range] for bottlenose dolphins according to node assignment. n = sample size.

Predicted Habitat	n		Mean (‰)	SD	Min	Max	Range
Coastal (node 1)	15	$\delta^{13}\text{C}$	-15.92	1.91	-20.27	-12.95	7.32
		$\delta^{15}\text{N}$	16.51	1.67	13.55	18.46	4.91
		$\delta^{34}\text{S}$	16.39	1.23	15.05	19.11	4.05
West barrier island (node 2)	42	$\delta^{13}\text{C}$	-16.62	1.01	-18.41	-14.59	3.81
		$\delta^{15}\text{N}$	16.23	1.05	13.77	18.26	4.49
		$\delta^{34}\text{S}$	12.71	1.38	8.16	14.69	6.53
West estuary (node 3)	7	$\delta^{13}\text{C}$	-19.18	0.62	-19.92	-18.51	1.42
		$\delta^{15}\text{N}$	16.51	1.13	15.31	18.19	2.88
		$\delta^{34}\text{S}$	12.42	1.72	10.47	14.86	4.39
East barrier island (node 4)	3	$\delta^{13}\text{C}$	-16.57	0.90	-17.12	-15.53	1.59
		$\delta^{15}\text{N}$	16.85	0.40	16.60	17.31	0.71
		$\delta^{34}\text{S}$	13.92	0.73	13.19	14.66	1.46
East estuary (node 5)	23	$\delta^{13}\text{C}$	-14.87	1.23	-17.17	-12.73	4.44
		$\delta^{15}\text{N}$	14.11	0.91	12.52	15.81	3.30
		$\delta^{34}\text{S}$	10.13	1.51	7.92	13.45	5.53
East estuary (node 6)	11	$\delta^{13}\text{C}$	-19.0	0.88	-20.1	-17.76	2.35
		$\delta^{15}\text{N}$	15.75	1.33	12.99	16.92	3.93
		$\delta^{34}\text{S}$	12.82	2.30	7.96	14.95	6.98

Table 3.3. Results of AIC_c model selection for skin THg and $\delta^{15}\text{N}$ in relation to explanatory variables^{ab}

^aModels are generalized linear models with a normal distribution and identity link function

^bOnly models with the lowest AIC_c or competing models with $\Delta\text{AIC}_c < 2$ are displayed; a complete list of models is provided in the supplementary tables S3.1 and S3.2.

Model	K	AIC _c	ΔAIC_c	weight
Log₁₀ Total Hg				
Body length + Node + Sex	5	57.8	0	0.750
$\delta^{15}\text{N}$				
Node + Year	4	314.7	0	0.467
Body length + Node + Year	5	316.4	1.66	0.203

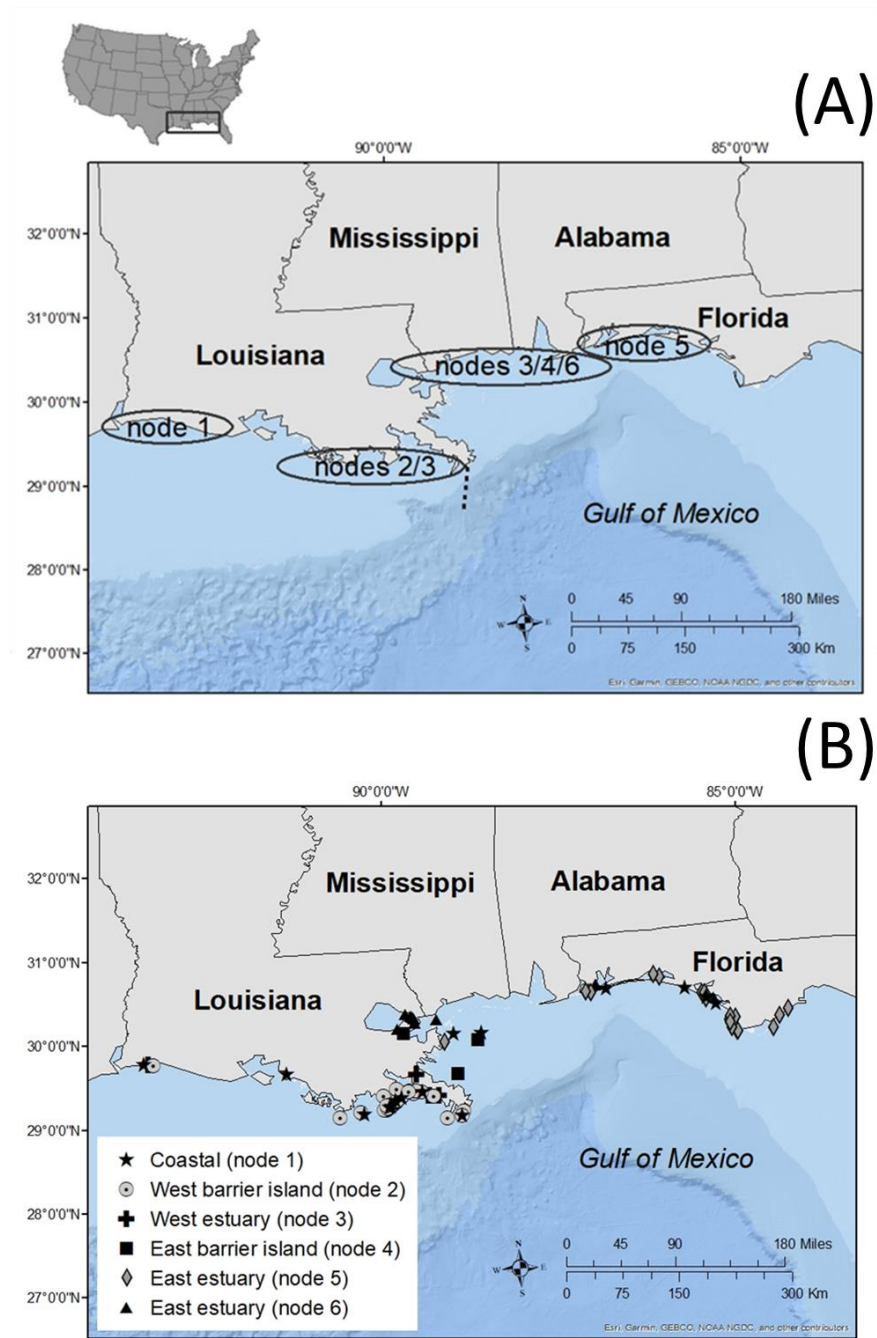


Figure 3.1. Locations where the majority of stranded dolphin in Hohn et al. (2017) were assigned to each habitat (A) and bottlenose dolphin (*Tursiops truncatus*) stranding locations in the present study according to predicted node assignment following the recursive partition analysis of Hohn et al. (2017) (B).

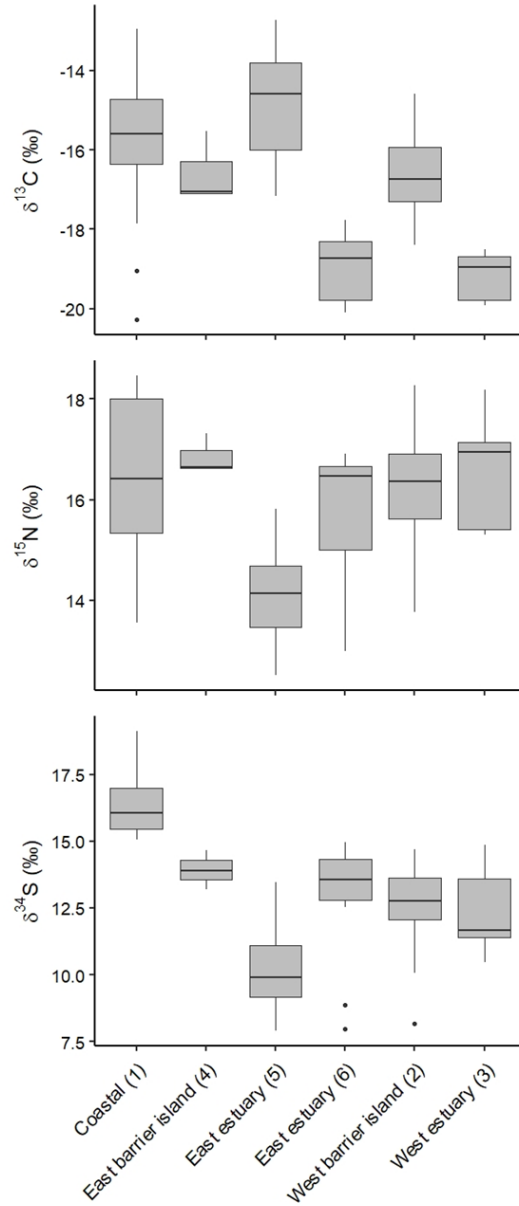


Figure 3.2. Box and whisker plots showing the stable isotope ratios for stranded bottlenose dolphins (*Tursiops truncatus*) according to predicted node assignment (number in parentheses) following the partition analysis by Hohn et al. (2017). Dots represent the outliers which are either 1.5-times the interquartile range above the upper quartile or 1.5-times the interquartile range below the lower quartile.

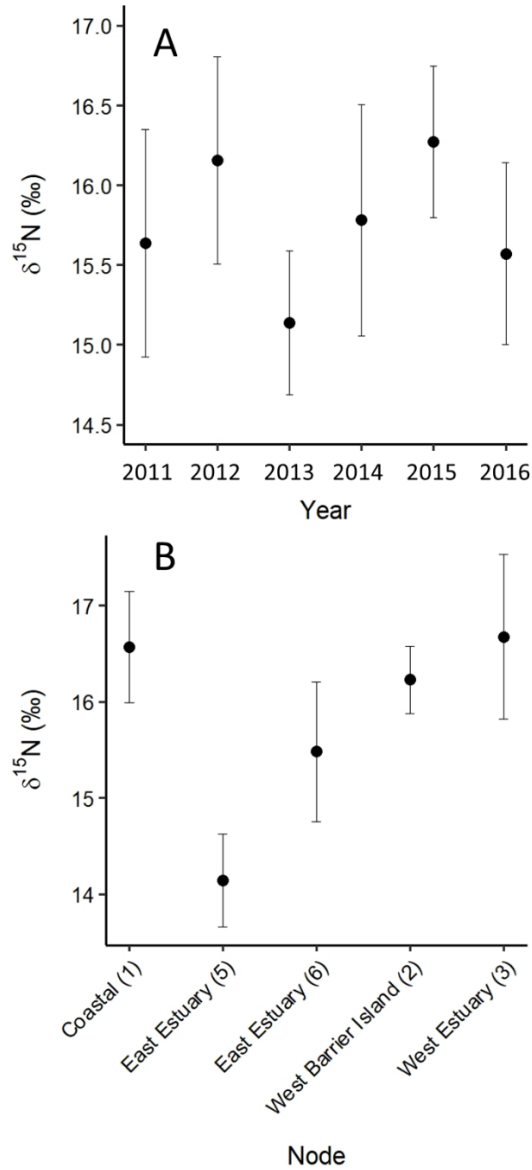


Figure 3.3. Effect plots for the predictors of bottlenose dolphin (*Tursiops truncatus*) skin $\delta^{15}\text{N}$ values. The model includes stranding year and node assignment as predictors of $\delta^{15}\text{N}$. In panel A, model predictions for the effect of stranding year while holding node assignment constant are displayed. In panel B, model predictions of the effect of node assignment (number in parentheses) while holding stranding year constant are displayed. Bars represent 95% confidence intervals of the predictions.

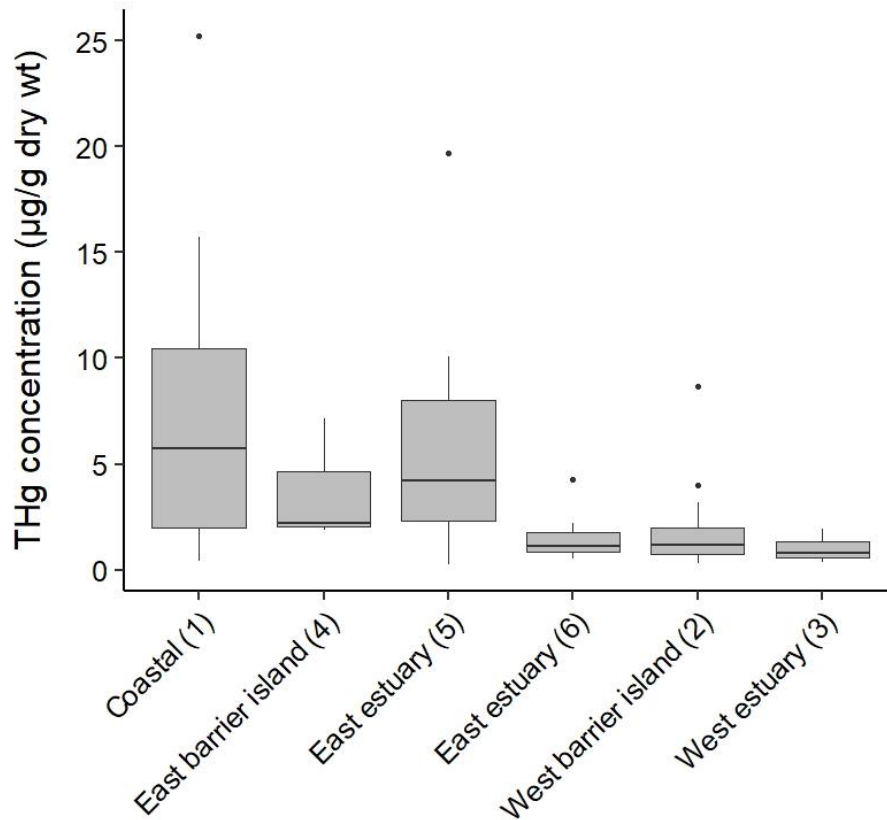


Figure 3.4. Box and whisker plots showing total Hg concentration ($\mu\text{g/g}$ dry wt) in stranded bottlenose dolphin (*Tursiops truncatus*) skin according to the predicted node assignment (number in parentheses) following the recursive partition analysis by Hohn et al. (2017). Dots represent the outliers which are either 1.5-times the interquartile range above the upper quartile or 1.5-times the interquartile range below the lower quartile.

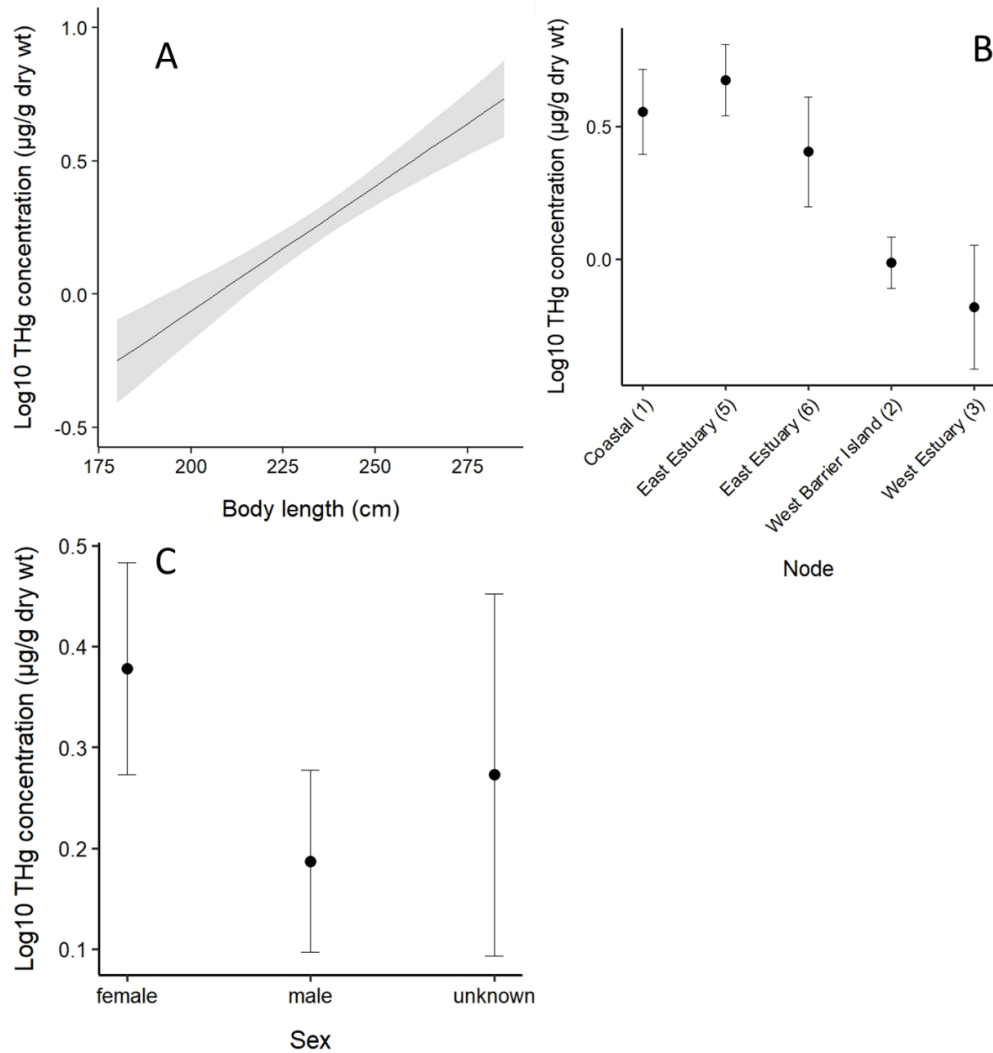


Figure 3.5. Effect plots for the predictors of bottlenose dolphin (*Tursiops truncatus*) skin Log₁₀ THg concentration (μg/g dry wt). The model includes body length, node assignment (number in parentheses), and sex as predictors of Log₁₀ THg concentration (μg/g dry wt). Panel A shows the effect of body length, panel B shows the effect of node assignment, and panel C shows the effect of sex on Log₁₀ THg concentration (μg/g dry wt); in all cases, the other predictors are held constant. Bars represent are 95% confidence intervals of the predictions.

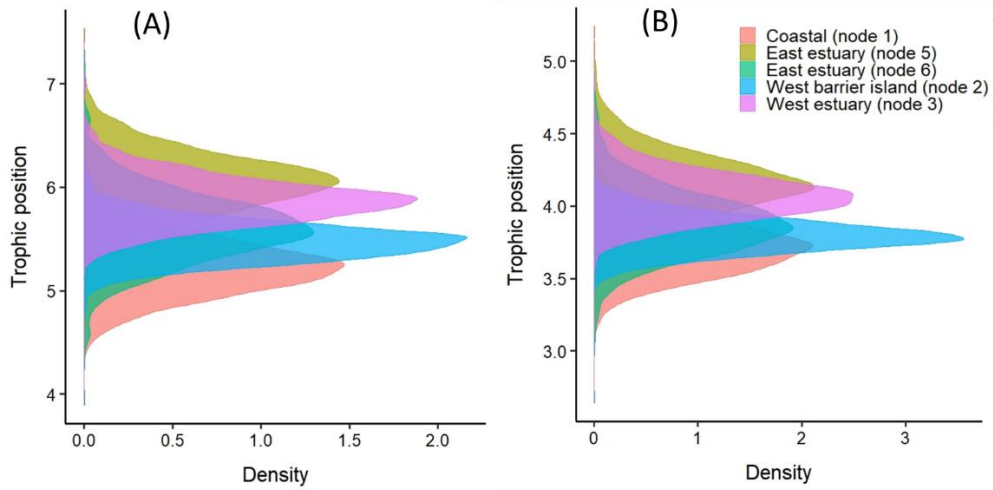


Figure 3.6. Estimated trophic position distribution of bottlenose dolphins (*Tursiops truncatus*) according to node assignment using a mean \pm standard deviation trophic enrichment factor (TEF) for $\delta^{15}\text{N}$ of $2.14 \pm 0.53\text{‰}$ (A) and of $3.4 \pm 1\text{‰}$ (B). Density refers to the posterior estimates of trophic position.

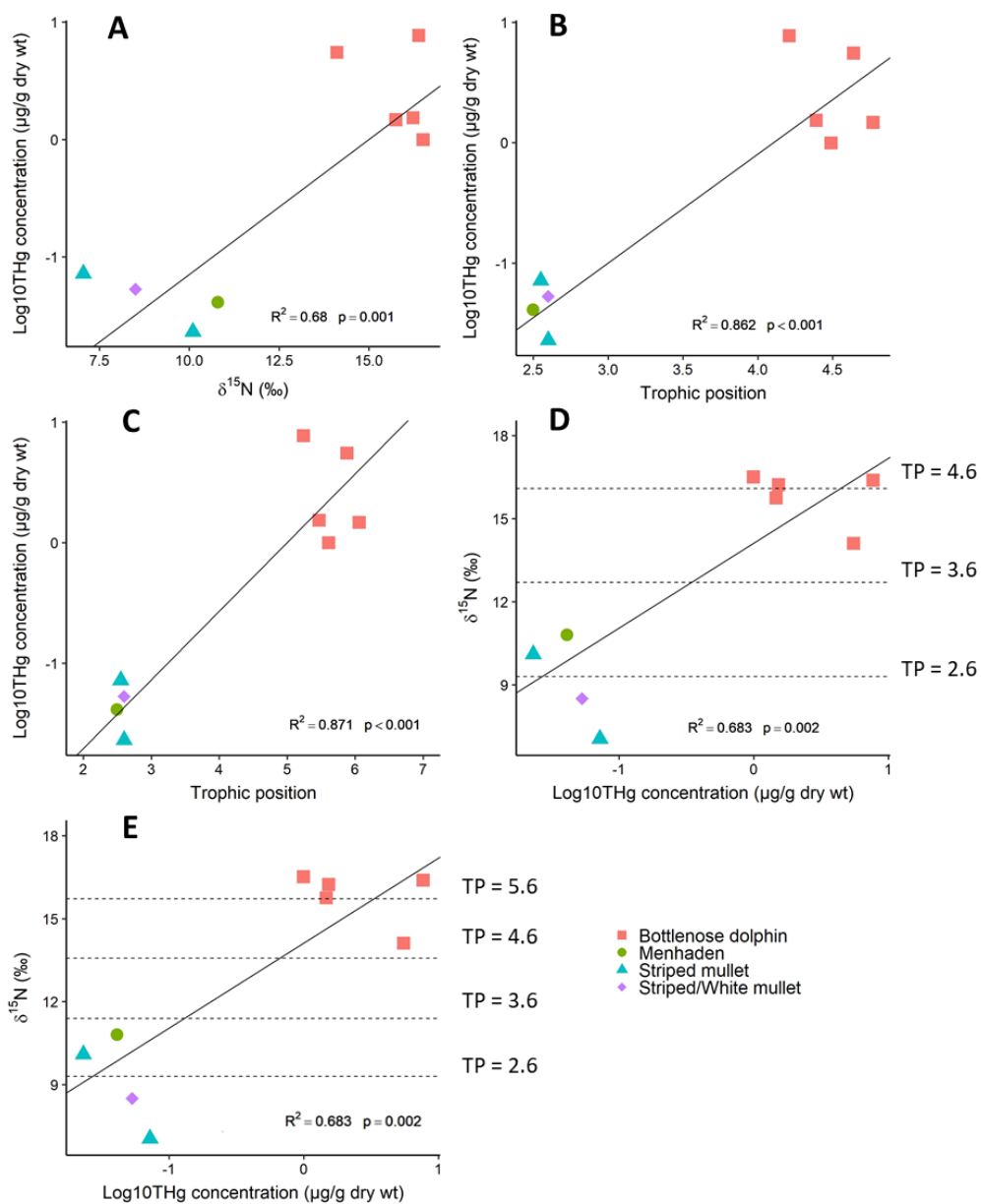


Figure 3.7. Relationship between $\delta^{15}\text{N}$ and Log_{10} THg concentration ($\mu\text{g/g dry wt}$) (A), trophic position and Log_{10} THg concentrations ($\mu\text{g/g dry wt}$) using a mean TEF for $\delta^{15}\text{N}$ of 3.4‰ and 2.14‰, respectively (B and C), and $\delta^{15}\text{N}$ and Log_{10} THg concentration ($\mu\text{g/g dry wt}$) showing trophic position estimated using TEF for $\delta^{15}\text{N}$ of 3.4‰ and of 2.14‰, respectively (D and E) in skin from bottlenose dolphins (*Tursiops truncatus*).

**IV. RELATIONSHIP BETWEEN MERCURY AND SELENIUM
CONCENTRATIONS IN TISSUES FROM STRANDED ODONTOCETES IN
THE NORTHERN GULF OF MEXICO**

Citation: McCormack, M. A., Jackson, B. P., & Dutton, J. (2020). Relationship between mercury and selenium concentrations in tissues from stranded odontocetes in the northern Gulf of Mexico. *Science of The Total Environment*, 749, 141350

Abstract

Odontocetes are apex predators that, despite accumulating mercury (Hg) to high concentrations in their tissues, show few signs of Hg toxicity. One method of Hg detoxification in odontocetes includes the sequestering of Hg in toxically inert mercury selenide (HgSe) compounds. To explore the tissue-specific accumulation of Hg and Se and the potential protective role of Se against Hg toxicity, we measured the concentrations of total mercury (THg) and selenium (Se) in multiple tissues from 11 species of odontocetes that stranded along the northern Gulf of Mexico coast [Florida (FL) and Louisiana (LA)]. Tissues were collected primarily from bottlenose dolphins (*Tursiops truncatus*; n = 93); however, individuals from species in the following 8 genera: *Feresa* (n = 1), *Globicephala* (n = 1), *Grampus* (n = 2), *Kogia* (n = 5), *Mesoplodon* (n = 1), *Peponocephala* (n = 4), *Stenella* (n = 9), and *Steno* (n = 1) were also sampled. In all species, the mean THg concentration was greatest in the liver and lowest in the blubber, lung, or skin. In contrast, in most species, the mean Se concentration was greatest in the liver, lung, or skin, and lowest in the blubber. For all

species, Se:Hg molar ratios decreased with increasing THg concentration in the blubber, kidney, liver, lung, and skin following an exponential decay relationship. In bottlenose dolphins, THg concentrations in the kidney, liver, and lung were significantly greater in FL dolphins compared to LA dolphins. On average, in bottlenose dolphins, Se:Hg molar ratios were approximately 1:1 in the liver and > 1:1 in blubber, kidney, lung, and skin, suggesting that Se likely protects against Hg toxicity. However, more research is necessary to understand the variation in Hg accumulation within and among species, and to assess how Hg, in combination with other environmental stressors, influences odontocete population health.

Introduction

Globally, mercury (Hg) pollution in the marine environment is a pressing environmental issue. Originating from both natural and anthropogenic sources, Hg can be transported long distances in the atmosphere before it is deposited in marine systems (Selin et al., 2009; Pirrone et al., 2010). The cycling of Hg through the marine environment is concerning as Hg is a potent toxin that negatively impacts the health of marine life and humans (Dietz et al., 2013; Rice et al., 2014). Once in the marine environment, through biotic (e.g., sulfate-reducing bacteria) and abiotic processes (e.g., humic matter, methylcobalamin), inorganic Hg (Hg^{2+}) can be methylated into methylmercury (CH_3Hg^+ ; MeHg) which readily enters pelagic and benthic food webs and biomagnifies with increasing trophic position (Compeau and Bartha, 1985; Weber, 1993; Hammerschmidt and Fitzgerald et al., 2006; Fitzgerald et al., 2007; Chen et al., 2009). Furthermore, because MeHg is slowly eliminated from the body, continued dietary

exposure to Hg results in the bioaccumulation of Hg within organisms (Nigro et al., 2002; Hammerschmidt and Fitzgerald et al., 2006). As a result, Hg reaches the highest concentrations in long-lived, apex predators, such as odontocetes (toothed whales) (Das et al., 2003; Hong et al., 2013; Kershaw and Hall, 2019).

Despite accumulating high concentrations of Hg, in some cases greater than 1000 µg/g wet weight in the liver, odontocetes display few signs of Hg toxicity (Law et al., 1996; Storelli et al., 1999; Shoham-Frider et al., 2002; Roditi-Elasar et al., 2003; Bilandžić et al., 2012; Kershaw and Hall, 2019; McCormack et al., 2020a). In the absence of controlled experiments, research focused on identifying potential health effects associated with Hg exposure in odontocetes has been limited to exploring the relationship between tissue Hg concentrations and health-related parameters (Kershaw and Hall, 2019). For example, Rawson et al. (1993) found a positive correlation between liver Hg concentrations and liver abnormalities in stranded bottlenose dolphins (*Tursiops truncatus*), and more recently, Schaefer et al. (2011) reported a positive correlation between blood Hg concentrations in free-ranging bottlenose dolphins and certain hepatic (e.g., gamma-glutamyl transferase) and renal parameters (e.g., blood urea concentration), suggesting that exposure to Hg may result in a reduction of liver and kidney function. However, it has been hypothesized that odontocetes may be able to mitigate the effects of Hg toxicity through two processes: 1) the demethylation of MeHg to inorganic Hg, a less toxic form of Hg, and 2) the binding of Hg with selenium (Se) which results in the formation of toxically inert mercury selenide (HgSe) compounds (Palmisano et al., 1995; Caurant et al., 1996; Wagemann et al., 1998).

In contrast to Hg, which has no biological function, Se is an essential element (Shomburg et al., 2004). Serving as a vital component of some proteins (selenoproteins) and enzymes (selenoenzymes), Se contributes to normal metabolic function in addition to playing an important role in Hg detoxification (Schomburg et al., 2004; Khan and Wang, 2009; Peterson et al., 2009). In odontocetes, HgSe granules were first identified in the liver (Martoja and Viale, 1977); however, more recently, HgSe granules have been identified in several other tissues including the brain, kidney, lung, muscle, pancreas, and spleen (Nakazawa et al., 2011; Gajdosechova et al., 2016). Furthermore, the coaccumulation of Hg and Se in multiple odontocete tissues (e.g., blubber, brain, heart, kidney, liver, lung, muscle, spleen) has also been reported, providing indirect evidence of an interaction between these two elements (Capelli et al., 2008; Cáceres-Saez et al., 2018; Martínez-López et al., 2019a,b; McCormack et al., 2020a). As a result, across a variety of marine vertebrates, including teleosts, sharks, and cetaceans, it has been suggested that if present in molar excess (i.e., Se:Hg molar ratio > 1:1), Se may reduce the likelihood of Hg toxicity. Consequently, the Se:Hg molar ratio has been calculated in numerous toxicology studies focused on teleosts, sharks, and marine mammals to assess the potential health risk of Hg exposure to the animals themselves and human consumers (Ruelas-Inzunza and Páez-Osuna, 2005; Branco et al., 2007; Kaneko and Ralston, 2007; Ralston, 2008; Peterson et al., 2009; Ralston and Raymond, 2010; Bellante et al., 2017; Cáceres-Saez et al., 2018; Azad et al., 2019; McCormack et al., 2020a).

Odontocetes in the Gulf of Mexico occupy diverse habitats including inshore (bay, sound, and estuarine), coastal (< 20 m in depth), and shelf habitats (between 20 and 200 m in depth) [e.g., bottlenose dolphin and Atlantic spotted dolphin (*Stenella*

frontalis]), as well as continental slope and deep ocean habitats (> 200 meters in depth) [e.g., Blainville's beaked whale (*Mesoplodon densirostris*) and melon-headed whale (*Peponocephala electra*)] (Würsig, 2017). Diet and habitat use vary both within and among Gulf of Mexico odontocetes species, and because the diet is the primary source of Hg to odontocetes and environmental conditions influence the biomagnification of Hg in marine food webs, odontocetes can be valuable indicator species to assess how Hg pollution varies spatially throughout the Gulf of Mexico (Hong et al., 2012; Baptista et al., 2016; Damseaux et al., 2017; Würsig, 2017; Hall et al., 2020).

Except for Mackey et al. (2003) and Bryan et al. (2012), which reported the concentrations of Hg and Se in rough-toothed dolphins (*Steno bredanensis*) and pygmy sperm whales, (*Kogia breviceps*), respectively, most studies reporting Hg and or Se concentrations in Gulf of Mexico odontocetes focus solely on inshore bottlenose dolphin populations (Kuehl and Haebler, 1995; Meador et al., 1999; Stein et al., 2003; Bryan et al., 2007; Woshner et al., 2008; Damseaux et al., 2017; McCormack et al., 2020b). Of the abovementioned studies, only Kuehl and Haebler (1995) and Meador et al. (1999) reported the concentrations of Hg in internal tissues (e.g., brain, kidney, liver, gonad); the remaining studies reported Hg concentrations in the blood, blubber, and/or skin (epidermis). In this study, we analyzed multiple tissues collected from stranded odontocetes during and in the two years following the northern Gulf of Mexico Cetacean Unusual Mortality Event (UME; 2010-2014). Obtaining samples from this UME which lasted 48 months and resulted in at least 1,141 cetacean mortalities (Litz et al., 2014; NMFS-OPR, 2019a,b), allowed us to complete a comprehensive assessment of Hg and Se concentrations and Se:Hg molar ratios in bottlenose dolphins from the northern Gulf of

Mexico. In addition, although most tissue samples were collected from bottlenose dolphins, tissue samples were also collected from less commonly sampled species including Atlantic spotted dolphin, Blainville's beaked whale, dwarf sperm whale (*Kogia sima*), melon-headed whale, pantropical spotted dolphin (*Stenella attenuata*), pygmy killer whale (*Feresa attenuata*), pygmy sperm whale, Risso's dolphin (*Grampus griseus*), rough-toothed dolphin, short-finned pilot whale (*Globicephala macrorhynchus*), and an unidentified *Stenella* species. Although the cause of the UME is unknown, it is hypothesized that colder water temperatures, large inputs of fresh water, exposure to petroleum compounds following the *Deepwater Horizon* Oil Spill, and the bacterial infection *brucellosis* may have contributed to the UME (Carmichael et al., 2012; Litz et al., 2014; Schwacke et al., 2014; Venn-Watson et al., 2015a,b, Colegrove et al., 2016).

The objectives of this study were first, to measure the concentration of total mercury (THg) and Se in 11 tissues [blubber (dermis and subcutis), brain, kidney, liver, lung, muscle, placenta, skin (epidermis), spleen, umbilical cord, uterus] from 11 species of stranded odontocetes and one unidentified *Stenella* sp. along the coast of Florida (FL) and Louisiana (LA); second, to calculate and compare the Se:Hg molar ratios across the various tissues and species; third, to explore the relationship between Se:Hg molar ratios and THg concentrations across several tissues and species; and finally, to explore the relationship between THg and Se concentrations as well as the influence of explanatory variables (body length, sex, stranding location [FL, LA], stranding year, and sample decomposition) on THg and Se concentrations, and Se:Hg molar ratios in several bottlenose dolphin tissues.

Methods

Odontocete tissue collection

Tissue samples were collected from 117 odontocetes in total, including 93 bottlenose dolphins, 6 Atlantic spotted dolphins, 4 melon-headed whales, 3 pygmy sperm whales, 2 dwarf sperm whales, 2 pantropical spotted dolphins, 2 Risso's dolphins, 1 Blainville's beaked whale, 1 pygmy killer whale, 1 rough-toothed dolphin, 1 short-finned pilot whale, and 1 unidentified *Stenella* species. In LA, all tissue samples were collected from bottlenose dolphins (n = 41), whereas in FL, tissues were collected from 52 bottlenose dolphins and all the other species (Table 4.1; Figure 4.1). Local stranding networks also recorded the body length, sex, and condition code of each individual at the time of sample collection; a summary is provided in Table 4.1. In FL, the condition of the stranded animals varied, ranging from condition code 1 (alive) to code 4 (advanced decomposition) (Geraci and Lounsbury, 2005) with 18% from code 1 individuals, 44% from code 2 individuals, 29% from code 3 individuals, and 9% from code 4 individuals. Odontocetes that were alive at the time of examination (code 1) were either euthanized, died naturally on the beach, during transportation to the rehabilitation facility, or while at the rehabilitation facility. In LA, all odontocetes sampled were of condition code 3 (moderate decomposition). Samples from less decomposed individuals [e.g., condition code 2 (fresh dead)] are preferable, as decomposition may affect trace element concentrations; however, other studies have found that samples from more heavily decomposed individuals (e.g., condition code 3 and 4) can be utilized for trace element analyses if condition code is considered as a potential confounding variable (Martínez-López et al., 2019a; McCormack et al., 2020b).

Due to stranding networks collecting tissue samples over 7 years, we were able to analyze samples collected from a large number of individual odontocetes. However, sampling was opportunistic, and not every tissue was collected from each odontocete. In total, 59 blubber, 15 brain, 75 kidney, 95 liver, 88 lung, 2 muscle, 1 placenta, 48 skin, 3 spleen, 2 umbilical cord, and 9 uterus samples were available for analysis. All tissue samples were held at -20°C at the National Marine Fisheries Service (NMFS) Southeast National Fisheries Science Center in Pascagoula, MS before being transported to Texas State University (San Marcos, TX) where they were stored at -20°C until further processing. The samples collected for this study were obtained under a NOAA parts authorization letter pursuant to 50 CFR 216.22.

Determination of THg and Se concentrations

First, the surface of all thawed tissues was removed to avoid contamination from external sources. Next, to determine the percentage moisture content in the tissues, which allows for the conversion between dry weight (dry wt) and wet weight (wet wt) THg and Se concentrations, tissue samples were weighed before and after freeze-drying (Labconco Free Zone^{2.5}; Labconco, Kansas City, MO) for 48 hours at -54°C . For all species combined, the percent moisture content [mean \pm standard deviation (SD)] was $42 \pm 15\%$ (range: 22–80%) for blubber, $72 \pm 8\%$ for brain, $76 \pm 6\%$ for kidney, $74 \pm 7\%$ for liver, $79 \pm 4\%$ for lung, 72% for muscle, 85% for placenta, $57 \pm 9\%$ for skin, $77 \pm 1\%$ for spleen, 84% for umbilical cord, and $76 \pm 5\%$ for uterus; a breakdown of the tissue-specific moisture content for each species is provided in the supplementary data (Table S4.1). All tissue samples, except blubber and skin, were then homogenized into a fine

powder. Because blubber and skin samples could not be homogenized, these samples were cut using a clean stainless-steel scalpel into small (~4 x 4 mm) pieces.

Using an ETHOS UP microwave digestion system (Milestone Inc., Shelton, CT), we digested the tissue samples (~0.25 g) in 5 ml of acid (4.5 ml of nitric acid and 0.5 ml of hydrochloric acid) for 75 min. Following digestion, samples were diluted with either 25 ml (blubber and skin) or 45 ml (all other tissues) of Milli-Q water (Millipore, Burlington, MA), resulting in a final sample volume of either 30 ml (dilution factor ~ 120) or 50 ml (dilution factor ~ 200), respectively. Total Hg and Se concentrations were then determined using Inductively Coupled Plasma Mass Spectrometry [ICP-MS (Agilent 7900 and 8900; Agilent Technologies Santa Clara, CA)] analysis at the Trace Element Analysis Core Laboratory at Dartmouth College (Hanover, NH) in accordance with EPA method 6020A (U.S. EPA, 1998). The Se:Hg molar ratios were calculated by dividing the dry wt concentration of THg and Se by the respective atomic weight (Se = 78.96, Hg = 200.59). Next, the ratio was determined by dividing the μmol Se concentration by the μmol THg concentration.

To ensure the accuracy of our measured THg and Se concentrations, blanks (n = 24), duplicate samples (n = 32), spiked samples (n = 22), and certified reference materials [DOLT-5 dogfish liver (n = 10; THg: 0.44 $\mu\text{g/g}$, Se: 8.3 $\mu\text{g/g}$) and DORM-4 fish protein (n = 14; THg: 0.412 $\mu\text{g/g}$, Se: 3.45 $\mu\text{g/g}$); National Research Council Canada] were analyzed for quality control. The ICP-MS analysis was performed in 3 batches, with the kidney and liver analyzed in batch 3, and all other tissues analyzed in batches 1 and 2. In all blanks, THg and Se concentrations were below the detection limit (batches 1 and 2: THg = < 0.024 $\mu\text{g/g}$, Se = < 0.024 $\mu\text{g/g}$; batch 3: THg = < 0.25 $\mu\text{g/g}$, and Se = < 0.10

$\mu\text{g/g}$). Between duplicate samples, on average, there was $\leq 10\%$ relative percent difference for THg in all tissues except skin, kidney, uterus, and muscle for which the mean relative percent difference was 13.2%, 22.2%, 20.5%, and 31.7%, respectively. For Se, on average, there was $\leq 10\%$ relative percent difference between duplicate samples in all tissues except blubber and uterus, for which the mean relative percent difference was 12.7% and 18.9%, respectively. The mean percentage recovery for spiked samples was 80.3% for THg and 86.9% for Se. For DORM-4, the mean percentage recovery for THg was 89.6%, and the mean percentage recovery for Se was 105.0%. For DOLT-5, the mean percentage recovery for THg was 88.2%, and the mean percentage recovery for Se was 81.8%.

Data analysis

Due to sample size limitations, most inferential statistics described below were limited to bottlenose dolphin tissues with >10 samples (blubber, kidney, liver, lung, and skin). To explore what explanatory variables [body length, sample decomposition (condition code), sex, stranding location (FL, LA), and stranding year] influenced THg and Se concentrations, multiple linear regression models were used. In both cases, the response variable (THg or Se concentration), could be influenced by several possible predictors; therefore, multiple models needed to be compared and ranked to determine which combination of predictors best explained the variation in tissue THg and Se concentrations. To compare potential models, we calculated the Akaike Information Criterion (AIC) modified for small sample sizes (AIC_c) (Akaike, 1973; Symonds and Moussalli, 2011). In general, we selected the model with the lowest AIC_c score; however, if the model with the lowest AIC_c score was within 2.2 AIC_c units of the next ranked

model, and the models differed by only one parameter, the models were further investigated. We determined whether or not the additional parameter should be included in the final model by calculating the 85% confidence interval for the parameter; those parameters in which the confidence interval included zero were considered uninformative and removed (Arnold, 2010; Leroux, 2019). An 85% confidence level was used instead of a 95% confidence interval to remain consistent with the AIC model selection process which supports additional parameters when the 85% confidence interval excludes zero (Arnold, 2010). Only final models are reported in text; however, the ranking of all the potential models is included in the supplementary data (Tables S4.2-S4.11). In bottlenose dolphins, body length did not differ among blubber, kidney, liver, lung, and skin datasets from FL [Kruskal-Wallis ANOVA on Ranks (Chi square = 0.359, $p = 0.956$, $df = 4$)] or among kidney, liver, and lung datasets from LA [Kruskal-Wallis ANOVA on Ranks (Chi square = 1.12, $p = 0.571$, $df = 2$)]; therefore, for both stranding locations, we used a one-way ANOVA to determine if mean concentrations of THg and Se and mean Se:Hg molar ratios differed among tissues. If significant differences were found, we used a Tukey's post hoc test to explore which tissues differed from one another. Mean Se:Hg molar ratios were compared between stranding locations using a one-way ANOVA. In each tissue, we explored the relationship between THg and Se using a simple linear regression model. Total Hg and Se concentrations were continuous variables; therefore, a Gaussian distribution was applied. The data was explored for outliers and, in all final general linear models, residual plots were inspected to validate the assumptions of normality and homoscedasticity (Zurr et al., 2010). When assumptions were not met, data was Log10 transformed. If Log10 transformed data still did not meet the assumptions, nonparametric

tests were used (e.g., Kruskal-Wallis ANOVA by Ranks and a Dunn's pairwise comparisons post hoc test). Next, Pearson's correlation coefficients were used to explore the relationship between the Se:Hg molar ratio and body length in bottlenose dolphin tissues. Finally, to explore the relationship between THg concentrations and Se:Hg molar ratios in the blubber, kidney, liver, lung, and skin tissues for all species combined, nonlinear regressions were used. To summarize, a self-starting function was used to estimate initial parameters of an asymptotic regression function; parameter estimates were then used as starting values for the one phase decay model [formula: $y = y_f + (y_0 - y_f) * \exp(-\alpha * x)$; y_0 = average y when $x = 0$, y_f = y value when y reaches an asymptote; α = rate constant]. In all nonlinear models, data points with standardized residuals that were greater than 3 or less than -3 were removed. All statistical analyses were performed in R v.3.4.0 (R Core Team, 2018) using $\mu\text{g/g}$ dry weight concentrations, and the level of significance was set at $\alpha = 0.05$.

Results

Total Hg and Se tissue concentrations, and Se:Hg molar ratios in odontocetes

Descriptive statistics (mean, SD, minimum, and maximum) for dry wt and wet wt THg and Se concentrations and Se:Hg molar ratios are reported in Table 4.2. The following results, discussed on a dry wt basis, are limited to blubber, kidney, liver, lung, and skin, which had the greatest number of samples. The lowest individual THg concentration was reported in a bottlenose dolphin blubber sample ($0.025 \mu\text{g/g}$), and the greatest individual THg concentration was observed in a bottlenose dolphin liver sample ($2059 \mu\text{g/g}$). For all species, mean THg concentrations were greatest in the liver and

lowest in the blubber, lung, or skin. Among species, the Risso's dolphin had the lowest mean blubber, kidney, and liver THg concentration, the single pantropical spotted dolphin had the lowest lung THg concentration, and the single dwarf sperm whale had the lowest skin THg concentration. In contrast, the single Blainville's beaked whale had the greatest kidney, liver, and lung THg concentration, and the melon-headed whale had the greatest mean concentrations of THg in the blubber and skin.

The lowest individual Se concentration was observed in a bottlenose dolphin blubber sample (0.143 $\mu\text{g/g}$), and the greatest individual Se concentration was observed in a bottlenose dolphin liver sample (651 $\mu\text{g/g}$). For all species in this study, on average, the Se concentrations were greatest in the liver, lung, or skin. Except for the Risso's dolphin, when blubber was analyzed, mean Se concentrations were lowest in the blubber. Among species, the Risso's dolphin had the lowest mean Se concentration in the liver, bottlenose dolphins that stranded in LA had the lowest mean Se concentrations in the kidney and lung, the pygmy killer whale had the lowest mean Se concentration in the blubber, and the single pygmy sperm whale had the lowest Se concentration in the skin. In contrast, the Risso's dolphin had the greatest mean blubber and skin Se concentrations, the single short-finned pilot whale had the greatest kidney Se concentration, the pygmy sperm whale had the greatest mean liver Se concentration, and the single Blainville's beaked whale had the greatest lung Se concentration.

For all species except the short-finned pilot whale, mean Se:Hg molar ratios were greatest in either the lung, blubber, or skin and lowest in the liver. In the single short-finned pilot whale, the Se:Hg molar ratio was greatest in the kidney, followed by the lung, and lowest in the liver. Overall, mean Se:Hg molar ratios were $\geq 1:1$ in all tissues

except the placenta (0.981). For all species combined, the relationship between the Se:Hg molar ratio and THg concentration in the blubber, kidney, liver, lung, and skin is shown in Figure 4.2. In each tissue, we modeled a one phase decay model [$y = y_f + (y_0 - y_f) * \exp(-\alpha * x)$]. Between two and three data points were removed from each analysis based on the standardized residual values. All tissues displayed similar trends with high Se:Hg molar ratios at low THg concentrations followed by decreasing Se:Hg molar ratios at greater THg concentrations before reaching an asymptote. The models predicted the asymptote was reached at Se:Hg molar ratios of 1.05, 1.79, 3.28, 3.77, and 10.7 for the liver, kidney, lung, blubber, and skin tissues, respectively.

Variability in THg and Se tissue concentrations, and Se:Hg molar ratios in bottlenose dolphins

In bottlenose dolphins, for both stranding locations combined, mean dry wt THg concentrations were greatest in the liver (227 $\mu\text{g/g}$) followed by the spleen (37.9 $\mu\text{g/g}$), kidney (25.0 $\mu\text{g/g}$), uterus (22.1 $\mu\text{g/g}$), lung (8.65 $\mu\text{g/g}$), brain (8.42 $\mu\text{g/g}$), skin (5.79 $\mu\text{g/g}$), placenta (5.14 $\mu\text{g/g}$), muscle (4.15 $\mu\text{g/g}$), umbilical cord (2.83 $\mu\text{g/g}$), and blubber (2.44 $\mu\text{g/g}$). On average, THg concentrations differed among blubber, kidney, liver, lung, and skin tissues in stranded dolphins from FL (Chi square = 100.3, $p < 0.001$, $df = 4$); the mean concentration of THg differed between all tissues ($p < 0.013$) except between the skin and lung ($p = 0.252$) and between kidney and liver ($p = 0.066$). Similarly, mean THg concentrations differed between kidney, liver, and lung tissues in stranded dolphins from LA (Chi square = 59.1, $p < 0.001$, $df = 2$); mean THg concentrations differed between all tissues ($p \leq 0.001$).

In all final models except for the liver, body length was a significant predictor of THg concentration, positively influencing THg concentrations in the blubber, kidney, lung, and skin (Figures 4.3 and 4.4; Table 4.3). In the abovementioned tissues, compared to smaller dolphins (<225 cm), there was a greater range of THg concentrations observed among larger dolphins (>225 cm) (Figure 4.3). There was no significant relationship between THg concentration and body length in the liver. Bottlenose dolphins stranded along the LA coast had significantly lower THg concentrations in the kidney, liver, and lung compared to those that stranded along the FL coast (Figure 4.4; Table 4.3). There was only one blubber sample from a bottlenose dolphin that stranded in LA and no skin samples from bottlenose dolphins that stranded in LA; therefore, we could not determine if THg concentrations differed between stranding locations in these two tissues. Stranding year was not a significant predictor in any of the final models. Sex significantly influenced THg concentrations in the blubber and lung; in both tissues, males had lower THg concentrations than females (Table 4.3). In both kidney and liver, THg concentrations increased with increasing condition code (Table 4.3). Condition code and sex were not included in the regressions shown in Figure 4.4 because, more than two predictors could not be clearly represented in a two-dimensional figure. Furthermore, condition code and sex did not substantially improve model fit. Instead, we analyzed a model with stranding location and body length as predictors and plotted the fitted lines with the intercepts adjusted for stranding location.

For both stranding locations combined, mean dry wt Se concentrations in bottlenose dolphin tissues were greatest in the liver (89.7 $\mu\text{g/g}$) followed by the kidney (15.6 $\mu\text{g/g}$), skin (15.2 $\mu\text{g/g}$), spleen (12.8 $\mu\text{g/g}$), uterus (8.42 $\mu\text{g/g}$), lung (5.20 $\mu\text{g/g}$),

brain (3.30 $\mu\text{g/g}$), blubber (2.73 $\mu\text{g/g}$), placenta (1.98 $\mu\text{g/g}$), muscle (1.45 $\mu\text{g/g}$), and umbilical cord (1.30 $\mu\text{g/g}$). Mean Se concentrations differed significantly among blubber, kidney, liver, lung, and skin tissues in stranded dolphins from FL (Chi square = 93.1, $p < 0.001$, $df = 4$). Significant differences in mean Se concentrations were observed between all tissues ($p \leq 0.016$), except between skin and kidney ($p = 0.105$) and between kidney and liver ($p = 0.244$). For dolphins stranded in LA, mean Se concentrations differed among kidney, liver, and lung tissues (Chi square = 36.5, $p < 0.001$, $df = 2$); mean Se concentrations differed between all tissues ($p < 0.001$) except between kidney and liver ($p = 0.130$).

Body length positively influenced Se concentrations in the blubber, kidney, lung, and skin (Figures 4.5 and 4.6; Table 4.3). In the liver, there was no relationship between body length and Se concentrations. Compared to dolphins that stranded along the FL coast, dolphins that stranded along the LA coast had significantly lower concentrations of Se in the kidney, liver, and lung (Figures 4.5 and 4.6; Table 4.3). Spatial differences in Se concentrations could not be assessed for blubber and skin samples. Again, stranding year was not a significant predictor of Se concentrations. Sex significantly influenced Se concentrations in blubber, lung, and skin, and in all cases, males had lower Se concentrations than females. Condition code significantly influenced Se concentrations in the liver and skin, with the condition code positively influencing Se concentrations in the liver and negatively influencing Se concentrations in the skin (Table 4.3). Like for Hg, only body length and stranding location were included as predictors in the regressions shown in Figure 4.6. However, the final model regression equations which include condition code and sex, when applicable, are shown in Table 4.3. It should be noted that

the inclusion of sex as a predictor of Se concentration in the blubber, lung, and skin models improved the model fit by 10%, 4%, and 16%, respectively.

For both stranding locations combined, mean Se:Hg molar ratios were greatest in bottlenose dolphin lung (10.2) followed by skin (9.6), blubber (6.9), kidney (5.0), spleen (2.1), uterus (1.6), brain and muscle (1.4), liver and umbilical cord (1.2), and placenta (0.98). In dolphins that stranded in FL, mean Se:Hg molar ratios differed among blubber, kidney, liver, lung, and skin tissues (Chi square = 85.6, $p < 0.001$, $df = 4$); differences in mean Se:Hg molar ratios were significant for all combinations of tissues except between skin and blubber ($p = 0.200$) and lung and kidney ($p = 0.711$). In dolphins stranded in LA, mean Se:Hg molar ratios differed among kidney, liver, and lung tissues (Chi square = 68.7, $p < 0.001$, $df = 2$); the mean Se:Hg molar ratio in the liver differed from the mean Se:Hg molar ratios in the kidney and lung ($p < 0.001$), but the mean Se:Hg molar ratio in the kidney did not differ from the mean Se:Hg molar ratio in the lung ($p = 0.08$).

The relationship between THg and Se concentrations, on a molar basis, in bottlenose dolphin blubber, brain, kidney, liver, lung, and skin are shown in Figure 4.7. Linear regressions revealed there was a significant positive relationship between THg and Se concentrations in all tissues; however, statistical results for brain should be taken with caution due to the small sample size. The relationship between Se and THg concentration was stronger in the brain, liver, and kidney ($R^2 = 0.844 - 0.976$) compared to the blubber, lung, and skin ($R^2 = 0.202 - 0.681$). In liver and brain, Se:Hg molar ratios were approximately 1:1; in blubber and skin, Se:Hg molar ratios were $\geq 1:1$; and in kidney and lung, Se:Hg concentrations were $>1:1$ at lower THg concentrations but approached a 1:1 ratio at greater THg concentrations ($> 35.5 \mu\text{g/g}$ dry wt in the kidney and $> 15.8 \mu\text{g/g}$ dry

wt in the lung). Bottlenose dolphins that stranded along the FL coast had a significantly lower mean Se:Hg molar ratio in the kidney (Chi square = 29.1, $p < 0.001$, $df = 1$) and lung (Chi square = 27.3, $p < 0.001$, $df = 1$) compared to dolphins that stranded along the LA coast. Mean Se:Hg molar ratios did not differ between stranding locations in the liver (Chi square = 1.73, $p = 0.188$, $df = 1$). The relationship between the Se:Hg molar ratio and body length in each tissue is shown in Figure 4.8. There was a significant negative relationship between the Se:Hg molar ratio and body length in the kidney for both stranding locations; however, there were no significant relationships between the Se:Hg molar ratio and body length in the other tissues.

Discussion

To interpret tissue Hg concentrations in odontocetes, it is important to consider the ecological, physiological, and biological variables that can influence tissue Hg concentrations (Chételat et al., 2020). The diet is the primary source of exposure to Hg for odontocetes; therefore, ecological variables including the trophic position of prey, the foraging habitat, and the associated environmental conditions that dictate Hg methylation and biomagnification within the food web can influence tissue Hg concentrations (Stavros et al., 2007, 2011; Hong et al., 2012; Baptista et al., 2016; Monterio et al., 2016; Damseaux et al., 2017; Chételat et al., 2020; McCormack et al., 2020b). In addition to ecological processes, within an organism, tissue-specific physiological processes influence the assimilation, metabolism, and excretion of Hg (Bolea-Fernandez et al., 2019; Ewald et al., 2019; Chételat et al., 2020). Finally, certain biological variables (e.g., age, body length, sex, energetic requirements) and life history events (e.g., ontogenetic

shifts in the diet, pregnancy, fasting) can affect tissue Hg concentrations (Woshner et al., 2008; Peterson et al., 2018; Chételat et al., 2020; McCormack et al., 2020b).

Total Hg concentrations and tissue distribution among odontocete species

During digestion, Hg (primarily as MeHg) binds to cysteine and crosses the gastrointestinal tract, where it can be remobilized around the body and accumulate in other tissues (Clarkson, 1993, 1997; Oliveira Ribeiro et al., 1999; Leaner and Mason, 2002; Chételat et al., 2020). Methylmercury from the diet is first distributed to the visceral organs (liver, kidney, spleen), where it can be metabolized, before being transported to other vascularized tissues via the circulatory system (Oliveira Ribeiro et al., 1999; Ewald et al., 2019). In odontocete liver, MeHg only accounts for between 1-12% of THg, suggesting that MeHg is slowly demethylated to inorganic Hg (Wagemann et al., 1998; Lemes et al., 2011; Bolea-Fernandez et al., 2019). The liver is the primary site of MeHg detoxification; consequently, the liver is the target organ for Hg accumulation in odontocetes (Frodello et al. 2000; Cardellicchio et al., 2002; Carvalho et al., 2002; Roditi-Elasar et al., 2003; Capelli et al., 2008; Nakazawa et al., 2011; Aubail et al., 2013; Cáceres-Saez et al., 2018; Bolea-Fernandez et al., 2019; McCormack et al., 2020a). The kidney and spleen are also important sites of Hg storage, detoxification, and excretion; as a result, these tissues can also accumulate high concentrations of Hg (Leonzio et al., 1992; Augier et al., 1993; Frodello et al., 2000; Capelli et al., 2008; Nakazawa et al., 2011; Bolea-Fernandez et al., 2019). Our results support the findings of previous studies, reporting THg in greatest concentrations in the liver, followed by the spleen and kidney.

Although the greatest concentrations of Hg are found in tissues associated with Hg storage, transformation, or excretion (e.g., liver, kidney, and spleen), other tissues can

also accumulate Hg (e.g., blubber, brain, lung, muscle, skin, uterus) (Storelli and Marcotrigiano, 2000, Capelli et al., 2008; Bolea-Fernandez et al., 2019; Chételat et al., 2020; McCormack et al., 2020b). Of these tissues, the accumulation of Hg in the brain is the most concerning because Hg can cross the blood-brain barrier (Lemes et al., 2011). In an odontocete brain, between 16-22 % of THg is present as MeHg (Lemes et al., 2011; Krey et al., 2015). Krey et al. (2015) determined that the concentration of THg in beluga whale (*Delphinapterus leucas*) brain tissues exceed thresholds identified in laboratory animals (small mammals such as mice, minks, and rats) known to cause deleterious neurobehavioral, neuropathological, and neurochemical changes. In summarizing pre-existing laboratory studies and field observations, Krey et al. (2015) determined that clinical signs (e.g., clonic convulsions, vomiting, recumbency, and gait disorders) of Hg neurotoxicity are generally observed in mammals [laboratory studies (mice, minks, rats); field observations (cats, dogs, minks, river otters, polar bears)] when brain THg concentrations exceed 6.75 µg/g wet wt, but neuropathological signs and neurochemical disruptions are observed at lower concentrations (> 4 µg/g wet wt and > 0.4 µg/g wet wt, respectively). The THg concentrations measured in the beluga whale brain samples reported by Krey et al. (2015) exceeded all the above-mentioned neurotoxicity thresholds. In the present study, the average brain THg concentration for all species combined was 6.40 µg/g wet wt. Based on the results of Krey et al. (2015), 66.7% of brain samples (n = 10) had THg concentrations that exceeded concentrations known to cause negative neurochemical and neuropathological effects, and 20% of samples (n = 3) had THg concentrations that exceeded concentrations known to cause clinical

effects. However, these conclusions are based on a small number of samples and may not be representative of free-ranging populations.

The accumulation of Hg in odontocete lungs has also previously been reported; however, it has been hypothesized that the pathway of Hg accumulation in the lung is different from other tissues (Leonzio et al., 1992; Augier et al., 1993; Rawson et al., 1995; Frodello et al., 2000; Cáceres-Saez et al., 2018). Cáceres-Saez et al. (2018) determined that while there were significant positive relationships between liver, muscle, and spleen THg concentrations in false killer whales (*Pseudorca crassidens*), there was no relationship between liver and lung THg concentrations in false killer whales. The authors suggest that inhalation of atmospheric Hg, rather than Hg derived from dietary sources, may lead to the accumulation of Hg in the lung. Furthermore, Rawson et al. (1995) reported that HgSe granules in the bottlenose dolphin lung were associated with airborne particles, suggesting that the HgSe granules in the lung did not originate from the liver.

In contrast to the lung, the accumulated THg in odontocete muscle is thought to originate from dietary sources. In the muscle, Hg, particularly MeHg, forms strong bonds with sulfhydryl groups present in proteins and accumulates over time; between 32-84 % of the THg in odontocete muscle has been reported as MeHg (Bloom, 1992; Endo et al., 2005; Capelli et al., 2008; Lemes et al., 2011). Muscle samples analyzed in the present study were taken from two relatively small bottlenose dolphins [170 cm (LA) and 197 cm (FL)]; therefore, the reported muscle THg concentrations are likely an underestimation of the mean THg muscle concentration in both locations.

Like the muscle, the majority of THg in odontocete skin is present as MeHg (72-100%; Stavros et al., 2007; Woshner et al., 2008). Previous studies have reported that THg concentrations in odontocete skin are lower than concentrations found in the internal tissues (e.g., liver, kidney, muscle), but greater than concentrations found in the blubber (Frodello et al., 2000; Carvalho et al., 2002; Roditi-Elasar et al., 2003; Aubail et al., 2013; McCormack et al., 2020b). In blubber, Hg does not accumulate to high concentrations (Cardellicchio et al., 2002; Carvalho et al., 2002; Aubail et al., 2013; McCormack et al., 2020a,b). Compared to the octanol-water partition coefficient of organic contaminants [e.g., polychlorinated biphenyls (PCBs)], the octanol-water partition coefficient of inorganic Hg and MeHg is lower indicating that Hg is not as lipid-soluble as organic contaminants; therefore, Hg does not accumulate to high concentrations in fat (Mason et al., 1996; Gerofke et al., 2005; Voutsas, 2007).

Finally, while sample sizes were small, we found measurable concentrations of THg in all uterus, placenta, and umbilical cord samples. The transfer of Hg from the mother to the fetus via the placenta has been reported in odontocetes (Itano et al., 1984; Storelli and Marcotrigiano, 2000; Lahaye et al., 2007). The uterus, placenta, and umbilical cord are not commonly analyzed in toxicology studies; however, the single THg concentration reported in a bottlenose dolphin uterus (50.8 $\mu\text{g/g}$ dry wt) reported by Storelli and Marcotrigiano (2000) was within the range of THg concentrations determined for the six uterus samples from bottlenose dolphins in the present study (range: 2.02 – 73.8 $\mu\text{g/g}$ dry wt). In contrast, the THg concentration in the single bottlenose dolphin placenta analyzed in the present study (5.14 $\mu\text{g/g}$ dry wt) was lower

than the THg concentration reported in the single bottlenose dolphin placenta (13.2 µg/g dry wt) by Storelli and Marcotrigiano (2000).

Overall, among species, we found that the Risso's dolphin, pantropical spotted dolphin, and dwarf sperm whale had the lowest mean tissue THg concentrations whereas, for most tissues, the single Blainville's beaked whale had the greatest THg concentrations. The Risso's dolphin, pantropical spotted dolphin, and dwarf sperm whale are all small delphinidae species, reaching approximately 300 cm in length, that forage primarily on fish and squid (Würsig, 2017). In addition, the Risso's dolphins sampled in the present study were relatively small, between 155 and 213 cm, which may have contributed to the low THg concentrations determined in this species. In contrast, Blainville's beaked whales can reach 470 cm (Würsig, 2017). The single Blainville beached whale analyzed was a 411 cm indicating it was an adult. Its size, combined with a diet of deep-water fishes and squid, may have contributed to the high THg concentration determined in this species (Choy et al., 2009; Würsig, 2017). That being said, our analyses for the abovementioned species were limited to between 1 and 4 individuals, and a larger sample size is needed to confirm these findings. Estimating potential dietary sources and trophic positions using carbon and nitrogen stable isotope analyses would also be beneficial to compare THg concentrations across odontocete species (Capelli et al., 2008).

Influence of explanatory variables on bottlenose dolphin THg and Se concentrations

Continuous dietary exposure to Hg, coupled with low excretion rates, results in the bioaccumulation of Hg in odontocete tissues (Nigro et al., 2002; Monteiro et al.,

2016; McCormack et al., 2020b). In addition, prey selection may vary with body size, and larger individuals may consume prey with greater THg concentrations, which could also explain why larger individuals have greater tissue THg concentrations (Loseto et al., 2008; Miller et al., 2011). We found a positive relationship between THg concentration and body length in bottlenose dolphin blubber, kidney, lung, and skin; in smaller dolphins (<225 cm), growth dilution limits the amount of Hg that is accumulated, whereas, in larger dolphins (>225 cm), which have slower growth rates, Hg bioaccumulates. Similar results have been reported for blubber, liver, muscle, and skin in bottlenose dolphins and striped dolphins (*Stenella coeruleoalba*) (Andre et al., 1991; Monteiro et al., 2016; McCormack et al., 2020b). However, we found no relationship between liver THg concentration and body length, which does not support the finding of previous studies that reported a positive relationship between liver THg concentration and body length in bottlenose dolphins (Durden et al., 2007; Monteiro et al., 2016). The reason for the lack of relationship between body length and THg concentration in the liver in our study is not apparent.

In all tissues for which stranding location was included as an explanatory variable, bottlenose dolphins that stranded along the LA coast had lower tissue THg concentrations compared to bottlenose dolphins that stranded along the coast of the FL panhandle when body length was included as a covariate. These results are consistent with the spatial patterns of THg concentrations reported in previous studies from bottlenose dolphins in the northern Gulf of Mexico. Dolphins sampled along the FL panhandle and FL peninsula had greater skin THg concentrations (mean skin THg range: 4.36 - 5.79 $\mu\text{g/g}$ dry wt; Bryan et al., 2007; McCormack et al., 2020b; this study)

compared to bottlenose dolphins sampled along the LA coast (1.94 $\mu\text{g/g}$ dry wt; McCormack et al., 2020b). Similarly, dolphins that stranded along the Gulf coast of FL had greater liver THg concentrations (mean liver THg range: 223 -399 $\mu\text{g/g}$ dry wt; Meador et al., 1999; Stein et al., 2003, this study) compared to those stranded along the LA (74.4 $\mu\text{g/g}$ dry wt; this study) and Texas coast (mean liver THg range: 114 – 212 $\mu\text{g/g}$ dry wt; Kuehl and Haebler, 1995; Meador et al., 1999; Stein et al., 2003). These spatial distributions are similar to those found in oysters [e.g., American oyster (*Crassostrea virginica*)] and fish [e.g., spotted sea trout (*Cynoscion nebulosus*)] in the northern Gulf of Mexico and likely reflect differences in Hg methylation, Hg sources, and transport of Hg by ocean currents within the Gulf of Mexico (Ache et al., 2000; Evans et al., 2000; Apeti et al., 2012; Harris et al., 2012). Compared to dolphins sampled along the northern Gulf of Mexico, free-ranging dolphins sampled in the FL coastal Everglades were shown to have greater concentrations of THg in the skin (11.1 $\mu\text{g/g}$ dry wt) (Damseaux et al., 2017). The authors suggest that the environmental conditions of mangrove ecosystems in the coastal Everglades (e.g., acidic mud), coupled with high organic content, may facilitate the methylation of Hg, which in turn can be biomagnified up the food web (Bergamaschi et al., 2012). Liver THg concentrations were not reported in the study; however, high concentrations of THg would likely also be observed in the liver of dolphins from the FL coastal Everglades.

In adult female dolphins, maternal transfer can serve as an excretory route for Hg; therefore, one might expect that THg concentrations would be greater in adult males compared to adult females (Storelli and Martotrigiano, 2000; Frodello et al., 2002). However, in the blubber and lung, males had lower THg concentrations than females. If

females are consuming greater amounts of fish to meet the energetic demands associated with lactation it would be reasonable to expect that tissue THg concentrations in females would be greater than males (Cheal and Gales, 1991; Worthy, 2001; Bryan et al., 2007; Kastelein et al., 2002, 2003). In both kidney and liver tissues, THg concentrations increased with increasing condition code. Decomposition or poor body condition can lead to lipid loss; because there is not a strong binding affinity between Hg and lipids, a loss of lipids would increase observed Hg concentrations as lipids dilute Hg concentrations (Lavoie et al., 2010).

Unlike Hg, within mammalian systems, Se, like other essential trace elements, is regulated within the body (Khan and Wang, 2009; Cáceres-Saez et al., 2018). However, the coaccumulation of Hg and Se in marine mammal tissues is well documented, and as a result, Se concentrations can exceed the limit of homeostatic control (e.g., 0.40 - 40 $\mu\text{g/g}$ dry wt in the liver) (Mackey et al., 1996; Cardellicchio et al., 2002; Capelli et al., 2008; Cáceres-Saez et al., 2013, 2015, 2018). Similar to THg, we found that Se concentrations were positively correlated with body length in all tissues except the liver. In addition, Se concentrations were greater in dolphins that stranded along the FL coast compared to those that stranded along the LA coast. Differences in tissue Se concentrations may be due to differences in Se concentrations between dolphin prey, but may also be due to the coaccumulation of Hg and Se (Seixas et al., 2007; Kehrig et al., 2009). In the blubber and skin, males had lower Se concentrations than females; if females are lactating and consuming more fish, they may also be exposed to greater amounts of Se (Kehrig et al., 2009). Increased Se concentrations in the blubber may also be due to the coaccumulation of Hg with Se, as females also had greater blubber THg concentrations. The reason for

elevated Se concentrations in female skin is not apparent, but the accumulation of Se in the skin is consistent with previous odontocete studies (Yang et al., 2002; Stavros et al., 2007; Savery et al., 2013). Finally, condition code positively influenced Se concentrations in the liver and negatively influenced Se concentrations in the skin. The reason for the negative correlation between condition code and skin Se concentration is not apparent.

An important caveat of this study is that the body condition of the animals and the cause of death was unknown. Following the *Deepwater Horizon* oil spill in 2011, Schwake et al. (2014) reported that free-ranging bottlenose dolphins in Barataria Bay, LA, which is within the spatial and temporal extent of this study, were in poor body condition. If animals were experiencing chronic stressors and were in poor body condition, there may have been an increase in Hg and Se concentrations. Ketone metabolism— which occurs during starvation—requires Se; therefore, if dolphins were in poor body condition as a result of starvation one may expect to observe elevated concentrations of Se (Olsson, 1985; Dehn et al., 2006; Cáceres-Saez et al., 2013). Similarly, previous studies have found that Hg concentrations in polar bear hair (*Ursus maritimus*) are negatively correlated with body mass index; the authors suggest that catabolism of protein rich tissues during times of fasting or starvation may release Hg into circulation which leads to differences in the deposition of Hg throughout the body (McKinney et al., 2017; Chételat et al., 2020). Finally, odontocetes in this study may have been exposed to oil from the *Deepwater Horizon* oil spill; however, exposure to Hg through ingestion, inhalation, or dermal contact with oil is considered unlikely as Hg was

not listed as a component of the MC252 crude oil from the *Deepwater Horizon* oil spill (Steffy et al., 2013; Godard-Codding and Collier, 2018).

Total Hg and Se relationships within and among tissues

Although the mechanisms of Hg-Se antagonism remain unclear, it has long been recognized that, if present in molar excess, Se may reduce the direct toxic effects of Hg exposure (Berry and Ralston, 2008; Khan and Wang, 2009). The demethylation of MeHg is aided by Se; also, through the formation of HgSe compounds, Se sequesters, and stores Hg in a toxicologically inert phase (Khan and Wang, 2009). Selenium:mercury molar ratios $> 1:1$ may reflect conditions in which Se protects against Hg toxicity, whereas Se:Hg molar ratios $< 1:1$ may reflect conditions in which Se is not in high enough molar concentration to protect against Hg toxicity (Kaneko and Ralston, 2007; Ralston, 2008; Peterson et al., 2009; Ralston and Raymond, 2010). Nakazawa et al. (2011) identified HgSe granules in several odontocete tissues (brain, kidney, liver, lung, muscle, pancreas, spleen) which suggests that Se mediated detoxification of Hg may occur in several tissues; however, based on the amount of HgSe granules identified in the tissues, the authors suggest that Se mediated detoxification of Hg occurs primarily in the liver and spleen.

Differences in Se:Hg molar ratios between tissues are driven largely by the distribution and deposition of Hg within the body. Of the tissues analyzed in the present study, the strongest correlation between THg and Se concentrations was determined in the liver. The liver is the target site of Hg accumulation and the primary organ for Se mediated detoxification of Hg; consequently, in the liver, Se:Hg molar ratios are approximately 1:1. In beluga whales, MeHg in the brain is found predominantly as

methylmercuric cysteinate (CH_3HgSCys), which can cause negative neurological effects (Lemes et al., 2011). In the brain, the mean Se:Hg molar ratio for all species was 2.2 (range: 0.756 – 14); four out of fifteen samples had Se:Hg molar ratios < 1 suggesting that some odontocetes analyzed in this study may be at risk for neurotoxicity. In contrast, in other tissues where Hg does not accumulate to as high concentrations [e.g., blubber, lung, skin], Se is often present in molar excess. That being said, the Se:Hg molar ratio can also be influenced by the distribution and deposition of Se; for example, among tissues, following the liver, odontocete skin often had the second greatest Se concentration. High Se concentrations in the skin, which is thought to be associated with UV protection, in combination with low THg concentrations in the skin result in Se:Hg molar ratios $> 1:1$ (McKenzie, 2000; Stavros et al., 2011; Cáceres-Saez et al., 2015).

Consistent with the literature, in the present study, we also found that Se:Hg molar ratios decreased with increasing THg concentrations following an exponential decay model (Cáceres-Saez et al., 2013; Krey et al., 2015; Bellante et al., 2017). Mercury biomagnifies up the food web to a greater extent than Se, and because dietary uptake rates of Hg exceed Hg excretion rates, Hg accumulates over time while the physiological requirements of Se remain relatively stable (Nigro et al., 2002; Hong et al., 2013; Kehrig et al., 2013; Kershaw and Hall, 2019). In addition, in bottlenose dolphins, we found that there was a negative relationship between the Se:Hg molar ratio and body length in the kidney. As THg accumulates in larger individuals, Se is not maintained at equal molar concentrations, and Se:Hg molar ratios decrease as a result. Although not statistically significant, there appeared to be a negative relationship between Se:Hg molar ratios and body length in the skin of bottlenose dolphins stranded along the FL coast as well. In

contrast, for both stranding locations, body length did not influence liver Se:Hg molar ratios. This may be because, even in young dolphins, Hg is accumulating in liver because once Hg crosses the gastro-intestinal tract it can be metabolized in the liver, therefore reducing the amount of Hg that enters the circulatory system and is remobilized around the body.

Palmisano et al (1995) suggested a 1:1 Se:Hg molar ratio in the liver of odontocetes only occurs after a threshold concentration of Hg (100 $\mu\text{g/g}$ wet wt) has been exceeded. Others studies have suggested a 1:1 Se:Hg molar ratio occurs in the liver at lower concentrations (e.g., 50 $\mu\text{g/g}$ wet wt) (Caurant et al., 1996; Meador et al., 1999; Lailson-Brito et al., 2012). Our results are consistent with the latter studies and suggest a 1:1 Se:Hg molar ratio in the liver occurs at THg concentrations around 50 $\mu\text{g/g}$ wet wt.

The Se:Hg molar ratios reported in this study suggest that the molar concentrations of Se are great enough that Se may have a protective effect against Hg toxicity in Gulf of Mexico odontocetes. However, the protective effect of Se can only occur if individuals with high molar concentrations of Hg can maintain equally high molar concentrations of Se. If Hg concentrations exceed Se concentrations, on a molar basis, Se:Hg molar ratios would fall below 1:1; in the present study, Se:Hg molar ratios were < 1:1 in some brain, muscle, kidney, liver, lung, spleen, placenta, and uterus samples. Furthermore, it is assumed that in a 1:1 Se:Hg molar ratio, all Se is bound to Hg, but Se is also necessary for physiological processes, and Se deficiencies can cause negative health effects (Khan and Wang, 2009; Gajdosechova et al., 2016). For example, Gajdosechova et al. (2016) reported that compared to juvenile long-finned pilot whales, adults had lower concentrations of Se-methionine (the biological pool of Se), but greater

concentrations of Se-cysteine and inorganic Se, suggesting that in response to MeHg detoxification, concentrations of Se-methionine are reduced to maintain adequate concentrations of Se-cysteine. Therefore, it has been suggested that to protect against Hg toxicity a Se:Hg molar ratio > 5:1 may be necessary (Burger and Gochfeld, 2013). If we use the more conservative estimate, more than half the tissue samples in the present study would have Se:Hg molar ratios < 5:1 suggesting that northern Gulf of Mexico odontocetes might be at risk of Hg toxicity. There are no controlled experiments to determine Hg toxicity thresholds in odontocetes; however, Rawson et al. (1993) determined that liver abnormalities were present in stranded bottlenose dolphins when liver THg concentrations $\geq 61 \mu\text{g/g}$ wet wt; in the present study, 35% of the liver samples exceeded $61 \mu\text{g/g}$ wet wt.

Conclusions

The present study is the first to report THg and Se concentrations in multiple tissues from several species of odontocetes in the Gulf of Mexico. This paper expands upon previous research focusing on Hg and Se concentrations in bottlenose dolphin from the Gulf of Mexico, exploring the influence of sample decomposition (condition code), body length, stranding location, and sex on THg and Se concentrations in multiple tissues. Our results support the findings of previous studies reporting THg in the greatest concentrations in the liver, followed by the spleen and kidney. Overall, the Se:Hg molar ratios in the tissues analyzed in the present study suggest that Se may protect against Hg toxicity in odontocetes inhabiting the northern Gulf of Mexico. However, as our results showed, in some odontocetes, Se does not accumulate to the same extent as Hg, and, as a

result, Se:Hg molar ratios fall below 1:1. The spatial variability in THg observed among bottlenose dolphins suggests that Hg accumulation may vary across habitats. Future research should focus on identifying differences in Hg accumulation among food webs within the northern Gulf of Mexico and explore whether certain odontocete species or population stocks may be at greater risk of Hg toxicity. In addition, odontocetes are long-lived, high trophic level organisms, often consuming similar fish species to humans, making them important environmental biomonitoring species, and elevated Hg concentrations, particularly those reported in bottlenose dolphins stranded along the Florida coast, warrants further investigation to determine potential routes of Hg exposure to human consumers.

Table 4.1. Sex, number of individuals sampled (n), and body length [mean \pm standard deviation; range in parentheses], for odontocete species stranded along the coast of Florida and Louisiana. ND = not determined due to small sample size.

Species	Location	Sex	N	Body length (cm)
Atlantic spotted dolphin	Florida	Female	3	212 \pm 2 (210 - 214)
		Male	3	182 \pm 54 (119 - 213)
Blainville's beaked whale		Female	1	411 \pm ND
Bottlenose dolphin		Female	25	215 \pm 38 (111 - 278)
		Male	25	213 \pm 61 (98 - 276)
		Unknown	2	175 \pm ND (102 - 247)
Dwarf sperm whale		Female	2	182 \pm ND (133 - 231)
Melon-headed whale		Female	1	233 \pm ND
		Male	3	253 \pm 6 (247 - 258)
Pantropical spotted dolphin		Female	2	185 \pm ND (155 - 213)
Pygmy killer whale		Female	1	198 \pm ND
Pygmy sperm whale		Male	3	278 \pm 67 (205 - 336)
Risso's dolphin		Female	2	172 \pm ND (165 - 180)
Rough-toothed dolphin		Male	1	183 \pm ND
Short-finned pilot whale		Male	1	267 \pm ND
<i>Stenella</i> sp.		Female	1	215 \pm ND
Bottlenose dolphin	Louisiana	Female	21	176 \pm 61 (91 - 248)
		Male	20	195 \pm 58 (86 - 272)

Table 4.2. Dry and wet weight THg and Se concentrations, and Se:Hg molar ratios (mean \pm standard deviation; range in parentheses) in each tissue and species. n = sample size of each tissue. ND = not determined.

Specimen	n	THg ($\mu\text{g/g}$ dry wt)	THg ($\mu\text{g/g}$ wet wt)	Se ($\mu\text{g/g}$ dry wt)	Se ($\mu\text{g/g}$ wet wt)	Se:Hg molar ratio
Blubber						
Atlantic spotted dolphin	6	3.07 \pm 3.15 (0.202 - 9.17)	1.75 \pm 1.42 (0.156 - 4.29)	7.07 \pm 6.15 (1.60 - 18.2)	4.23 \pm 2.89 (0.893 - 8.52)	9.69 \pm 9.23 (2.01 - 27.3)
Blainville's beaked whale	1	2.25 \pm ND	1.75 \pm ND	1.51 \pm ND	1.18 \pm ND	1.71 \pm ND
Bottlenose dolphin (FL)	36	2.47 \pm 3.93 (0.025 - 17.6)	1.15 \pm 1.50 (0.019 - 8.32)	2.74 \pm 3.37 (0.143 - 13.0)	1.31 \pm 1.31 (0.010 - 6.79)	6.98 \pm 9.27 (1.07 - 45.3)
Bottlenose dolphin (LA)	1	1.21 \pm ND	0.516 \pm ND	2.34 \pm ND	0.997 \pm ND	4.92 \pm ND
Dwarf sperm whale	2	0.223 \pm ND (0.040 - 0.407)	0.162 \pm ND (0.017 - 0.307)	1.07 \pm ND (0.756 - 1.39)	0.581 \pm ND (0.572 - 0.590)	46.7 \pm ND (4.72 - 88.7)
Melon-headed whale	4	7.27 \pm 1.91 (4.59 - 8.71)	2.88 \pm 0.742 (2.01 - 3.80)	9.01 \pm 5.55 (4.55 - 16.4)	3.41 \pm 1.61 (1.92 - 5.16)	3.04 \pm 1.35 (1.61 - 4.87)
Pantropical spotted dolphin	2	4.92 \pm ND (4.18 - 5.67)	2.41 \pm ND (1.68 - 3.15)	4.72 \pm ND (4.63 - 4.82)	2.26 \pm ND (1.94 - 2.57)	2.5 \pm ND (2.08 - 2.93)
Pygmy killer whale	1	1.85 \pm ND	1.06 \pm ND	1.42 \pm ND	0.813 \pm ND	1.95 \pm ND
Pygmy sperm whale	3	0.439 \pm 0.533 (0.088 - 1.07)	0.278 \pm 0.346 (0.053 - 0.678)	0.891 \pm 0.180 (0.760 - 1.10)	0.558 \pm 0.119 (0.488 - 0.695)	12.7 \pm 10.5 (2.61 - 23.0)
Risso's dolphin	2	0.197 \pm ND (0.193 - 0.202)	0.087 \pm ND (0.080 - 0.094)	12.0 \pm ND (9.85 - 14.1)	5.21 \pm ND (4.59 - 5.83)	155 \pm ND (124 - 186)
Rough-toothed dolphin	1	1.60 \pm ND	0.604 \pm ND	3.80 \pm ND	1.43 \pm ND	6.03 \pm ND

Brain						
Atlantic spotted dolphin	1	15.5 ± ND	6.84 ± ND	7.07 ± ND	3.13 ± ND	1.16 ± ND
Blainville's beaked whale	1	106 ± ND	37.5 ± ND	34.4 ± ND	12.1 ± ND	0.823 ± ND
Bottlenose dolphin (FL)	9	8.42 ± 13.1 (1.56 – 43.0)	2.33 ± 3.66 (0.352 – 12.0)	3.30 ± 3.59 (1.63 – 12.8)	0.914 ± 1.01 (0.404 – 3.58)	1.44 ± 0.694 (0.756 – 0.291)
Melon-headed whale	2	52.3 ± ND (32.6 – 71.9)	13.4 ± ND (6.51 – 20.3)	18.6 ± ND (14.1 – 23.1)	4.67 ± ND (2.82 – 6.51)	0.958 ± ND (0.816 – 1.10)
Risso's dolphin	1	1.41 ± ND	0.280 ± ND	7.86 ± ND	1.56 ± ND	14.2 ± ND
<i>Stenella</i> sp.	1	15.1 ± ND	3.70 ± ND	7.77 ± ND	1.90 ± ND	1.31 ± ND
Kidney						
Atlantic spotted dolphin	5	29.8 ± 16.3 (1.93 – 41.4)	7.35 ± 3.80 (1.39 – 11.2)	21.6 ± 8.80 (6.27 – 28.2)	5.78 ± 1.23 (4.51 – 7.53)	3.07 ± 2.91 (1.63 – 8.26)
Blainville's beaked whale	1	58.5 ± ND	15.1 ± ND	36 ± ND	9.33 ± ND	1.57 ± ND
Bottlenose dolphin (FL)	28	46.4 ± 45.0 (0.693 – 172)	10.8 ± 10.1 (0.178 – 39.7)	23.8 ± 17.7 (3.47 – 76.0)	5.53 ± 3.93 (0.890 – 17.1)	2.14 ± 2.27 (0.991 – 12.7)
Bottlenose dolphin (LA)	33	6.85 ± 7.61 (0.295 – 26.3)	1.59 ± 1.76 (0.057 – 6.86)	8.65 ± 4.85 (1.98 – 17.0)	2.00 ± 1.16 (0.343 – 4.48)	7.45 ± 5.52 (1.56 – 21.2)
Melon-headed whale	3	32.6 ± 5.72 (27.1 – 38.5)	7.64 ± 1.39 (6.22 – 8.99)	22.7 ± 3.33 (19.6 – 26.2)	5.33 ± 0.722 (4.70 – 6.11)	1.80 ± ND (1.55 – 2.11)
Pygmy sperm whale	2	17.9 ± ND (13.2 – 22.6)	4.07 ± ND (2.78 – 5.35)	29.4 ± ND (20.7 – 38.2)	6.47 ± ND (4.91 – 8.04)	4.82 ± ND (2.33 – 7.34)

Risso's dolphin	1	4.22 ± ND	0.966 ± ND	9.51 ± ND	2.17 ± ND	5.72 ± ND
Rough-toothed dolphin	1	29.1 ± ND	6.98 ± ND	23.9 ± ND	5.72 ± ND	2.08 ± ND
Short-finned pilot whale	1	46.6 ± ND	11.3 ± ND	53.3 ± ND	12.9 ± ND	2.91 ± ND
Liver						
Atlantic spotted dolphin	6	584 ± 443	180 ± 126	235 ± 156	73.3 ± 45.6	1.23 ± 0.395
		(8.20 – 1294)	(2.51 – 349)	(6.41 – 467)	(1.96 – 126)	(0.916 – 1.99)
Blainville's beaked whale	1	832 ± ND	282 ± ND	315 ± ND	107 ± ND	0.963 ± ND
Bottlenose dolphin (FL)	33	407 ± 490	129 ± 146	160 ± 176	50.1 ± 54.3	1.05 ± 0.141
		(4.79 – 2059)	(0.175 – 555)	(1.84 – 651)	(0.067 – 176)	(0.742 – 1.46)
Bottlenose dolphin (LA)	39	74.4 ± 139	21.3 ± 39.8	30.6 ± 53.9	8.81 ± 15.5	1.28 ± 0.497
		(4.81 – 815)	(1.04 – 232)	(2.14 – 321)	(0.492 – 91.3)	(0.609 – 2.80)
Dwarf sperm whale	2	14.1 ± ND	4.53 ± ND	11.7 ± ND	3.52 ± ND	4.72 ± ND
		(2.62 – 25.6)	(0.655 – 8.41)	(8.18 – 15.2)	(2.04 – 4.99)	(1.51 – 7.92)
Melon-headed whale	4	726 ± 361	222 ± 109	275 ± 106	84.7 ± 32.5	1.01 ± 0.175
		(411 – 1213)	(134 – 373)	(196 – 427)	(58.5 – 131)	(0.894 – 1.27)
Pantropical spotted dolphin	1	21 ± ND	5.85 ± ND	13.6 ± ND	3.78 ± ND	1.64 ± ND
Pygmy killer whale	1	441 ± ND	125 ± ND	231 ± ND	65.5 ± ND	1.33 ± ND
Pygmy sperm whale	3	38.8 ± 39.9	13.4 ± 14.7	384 ± 94.1	12.0 ± 4.62	0.895 ± 0.003
		(8.50 – 83.4)	(2.70 – 30.1)	(276 – 449)	(6.75 – 15.5)	(0.894 – 0.898)
Risso's dolphin	2	6.16 ± ND	2.36 ± ND	6.35 ± ND	2.3 ± ND	2.65 ± ND
		(5.95 – 6.38)	(1.89 – 2.84)	(4.54 – 8.17)	(2.02 – 2.59)	(1.8 – 3.49)

Rough-toothed dolphin	1	317 ± ND	101 ± ND	150 ± ND	47.7 ± ND	1.2 ± ND
Short-finned pilot whale	1	199 ± ND	60.1 ± ND	120 ± ND	36.2 ± ND	1.53 ± ND
<i>Stenella</i> sp.	1	261 ± ND	196 ± ND	113 ± ND	84.7 ± ND	1.1 ± ND
Lung						
Atlantic spotted dolphin	6	13.2 ± 8.09	7.19 ± 5.91	7.21 ± 4.52	4.78 ± 2.45	1.39 ± 0.114
		(5.32 – 22.3)	(0.277 – 15.1)	(2.92 – 12.8)	(0.688 – 7.28)	(1.21 – 1.54)
Blainville's beaked whale	1	116 ± ND	10.3 ± ND	44.9 ± ND	3.97 ± ND	0.981 ± ND
Bottlenose dolphin (FL)	35	14.7 ± 21.4	3.36 ± 5.21	7.46 ± 8.79	1.70 ± 2.16	3.71 ± 6.20
		(0.128 – 115)	(0.030 – 28.9)	(1.31 – 50.8)	(0.267 – 12.8)	(0.893 – 34.6)
Bottlenose dolphin (LA)	29	1.11 ± 1.57	0.256 ± 0.352	2.85 ± 1.03	0.655 ± 0.245	17.9 ± 20.3
		(BDL – 8.01)	(BDL – 1.75)	(1.37 – 5.13)	(0.282 – 1.19)	(1.42 – 75.9)
Dwarf sperm whale	2	2.18 ± ND	0.483 ± ND	13.2 ± ND	3.02 ± ND	10.4 ± ND
		(BDL – 2.18)	(BDL – 0.483)	(8.94 – 17.5)	(1.96 – 4.05)	
Melon-headed whale	4	25.0 ± 6.85	5.78 ± 1.77	14.3 ± 3.55	3.32 ± 0.967	1.48 ± 0.313
		(20.0 – 34.6)	(4.02 – 8.09)	(10.5 – 18.7)	(2.11 – 4.39)	(1.27 – 1.95)
Pantropical spotted dolphin	1	0.978 ± ND	0.233 ± ND	14.0 ± ND	3.35 ± ND	36.5 ± ND
Pygmy killer whale	1	67.8 ± ND	16.3 ± ND	39.8 ± ND	9.57 ± ND	1.49 ± ND
Pygmy sperm whale	3	2.16 ± 0.615	0.556 ± 0.121	16.7 ± 9.24	4.39 ± 2.39	21.9 ± 14.2
		(1.46 – 2.63)	(0.427 – 0.667)	(6.40 – 24.3)	(1.63 – 5.84)	(6.19 – 33.8)
Risso's dolphin	2	1.03 ± ND	0.205 ± ND	16.9 ± ND	3.27 ± ND	44.7 ± ND
		(0.821 – 1.24)	(0.147 – 0.263)	(14.4 – 19.4)	(3.06 – 3.50)	(29.5 – 60.0)

Rough-toothed dolphin	1	44.4 ± ND	9.61 ± ND	27.4 ± ND	5.93 ± ND	1.57 ± ND
Short-finned pilot whale	1	24.4 ± ND	5.08 ± ND	19.3 ± ND	4.00 ± ND	2.00 ± ND
<i>Stenella</i> sp.	1	11.2 ± ND	2.92 ± ND	20.1 ± ND	5.24 ± ND	4.56 ± ND
Muscle						
Bottlenose dolphin (FL)	1	7.09 ± ND	2.20 ± ND	1.92 ± ND	0.595 ± ND	0.687 ± ND
Bottlenose dolphin (LA)	1	1.21 ± ND	0.322 ± ND	0.989 ± ND	0.263 ± ND	2.08 ± ND
Placenta						
Bottlenose dolphin (FL)	1	5.14 ± ND	0.762 ± ND	1.98	0.294 ± ND	0.981 ± ND
Skin						
Atlantic spotted dolphin	5	7.16 ± 3.60 (0.849 – 9.72)	3.10 ± 1.42 (0.581 – 4.01)	44.8 ± 16.6 (17.8 – 63.0)	20.4 ± 7.22 (12.2 – 31.2)	22.8 ± 17.3 (12.5 – 53.3)
Blainville's beaked whale	1	7.65 ± ND	4.78 ± ND	20.6 ± ND	12.8 ± ND	6.82 ± ND
Bottlenose dolphin (FL)	31	5.79 ± 4.32 (0.274 – 19.7)	(2.45 ± 1.83) (0.120 – 7.14)	15.2 ± 14.6 (2.21 – 80.9)	6.34 ± 5.83 (0.849 – 32.1)	9.64 ± 8.22 (1.07 – 32.0)
Dwarf sperm whale	1	0.129 ± ND	0.048 ± ND	9.70 ± ND	3.58 ± ND	191 ± ND
Melon-headed whale	3	11.1 ± 4.04 (7.46 – 15.4)	4.04 ± 1.59 (2.98 – 5.87)	26.4 ± 1.57 (25.9 – 28.0)	9.67 ± 1.17 (8.38 – 10.7)	6.54 ± 1.93 (4.62 – 8.48)
Pantropical spotted dolphin	2	6.06 ± ND	2.33 ± ND	80.7 ± ND	32.7 ± ND	78.8 ± ND

		(0.962 – 11.2)	(0.449 – 4.20)	(50.1 – 111)	(22.4 – 41.9)	(25.3 – 132)
Pygmy sperm whale	1	0.847 ± ND	0.366 ± ND	4.62 ± ND	2.00 ± ND	13.9 ± ND
Risso's dolphin	2	1.01 ± ND	0.364 ± ND	134 ± ND	48.0 ± ND	337 ± ND
		(0.865 – 1.16)	(0.321 – 0.480)	(122 – 145)	(45.1 – 50.9)	(318 – 357)
Rough-toothed dolphin	1	7.04 ± ND	2.38 ± ND	82.6 ± ND	27.9 ± ND	29.8 ± ND
<i>Stenella</i> sp.	1	5.30 ± ND	2.89 ± ND	73.1 ± ND	39.8 ± ND	35.1 ± ND
Spleen						
Bottlenose dolphin (FL)	3	37.9 ± 45.5	8.55 ± 9.97	12.8 ± 11.3	2.93 ± 2.45	2.09 ± 2.08
		(2.09 – 89.0)	(0.498 – 19.7)	(3.69 – 25.4)	(0.880 – 5.63)	(0.727 – 4.49)
Umbilical cord						
Bottlenose dolphin (FL)	1	2.83 ± ND	0.504 ± ND	1.30 ± ND	0.232 ± ND	1.17 ± ND
<i>Stenella</i> sp.	1	6.43 ± ND	0.865 ± ND	2.73 ± ND	0.368 ± ND	1.08 ± ND
Uterus						
Bottlenose dolphin (FL)	6	22.1 ± 28.5	4.92 ± 6.31	8.42 ± 8.73	1.89 ± 1.94	1.65 ± 0.887
		(2.02 – 73.8)	(0.330 – 16.3)	(1.64 – 23.1)	(0.268 – 5.10)	(0.795 – 3.10)
Dwarf sperm whale	1	1.60 ± ND	0.378 ± ND	3.93 ± ND	0.929 ± ND	6.25 ± ND
Risso's dolphin	1	1.11 ± ND	0.366 ± ND	4.71 ± ND	1.55 ± ND	10.8 ± ND
<i>Stenella</i> sp.	1	22.8 ± ND	5.94 ± ND	11.7 ± ND	3.05 ± ND	1.31 ± ND

Table 4.3 Final models fitted to THg and Se concentrations in bottlenose dolphin blubber, kidney, liver, lung, and skin. Le = body length; Lo = stranding location; Co = condition code. *Stranding location was included as a predictor in liver, kidney, and lung models

THg models				Se models			
Blubber				Blubber			
Log10(Hg) = b ₀ + b ₁ (Le) + b ₂ (Sex)		R ² = 0.481 p < 0.001		Log10(Se) = b ₀ + b ₁ (Le) + b ₂ (Sex)		R ² = 0.433 p < 0.001	
Coefficients	Estimate	Std. Error	p value	Coefficients	Estimate	Std. Error	p value
Intercept	-1.835	0.366	<0.001	Intercept	-0.86	0.271	<0.001
Body length	0.009	0.002	<0.001	Body length	0.006	0.001	<0.001
Sex:male	-0.266	0.160	0.106	Sex:male	-0.311	0.118	0.013
Kidney		R ² = 0.799 p < 0.001		Kidney		R ² = 0.756 p < 0.001	
Log10(Hg) = b ₀ + b ₁ (Le) + b ₂ (Lo) + b ₃ (Co)		R ² = 0.799 p < 0.001		Log10(Se) = b ₀ + b ₁ (Le) + b ₂ (Lo)		R ² = 0.756 p < 0.001	
Coefficients	Estimate	Std. Error	p value	Coefficients	Estimate	Std. Error	p value
Intercept	-0.786	0.333	0.022	Intercept	0.341	0.096	<0.001
Body length	0.008	0.001	<0.001	Body length	0.004	0.0004	<0.001
Location:LA	-0.806	0.110	<0.001	Location:LA	-0.290	0.049	<0.001
Condition code	0.192	0.113	0.093				
Liver		R ² = 0.246 p < 0.001		Liver		R ² = 0.218 p < 0.001	
Log10(Hg) = b ₀ + b ₁ (Lo) + b ₂ (Co)		R ² = 0.246 p < 0.001		Log10(Se) = b ₀ + b ₁ (Lo) + b ₂ (Co)		R ² = 0.218 p < 0.001	
Coefficients	Estimate	Std. Error	p value	Coefficients	Estimate	Std. Error	p

							value
Intercept	1.19	0.473	0.014	Intercept	0.826	0.459	0.076
Location:LA	-1.012	0.214	<0.001	Location:LA	-0.945	0.207	<0.001
Condition code	0.429	0.202	0.037	Condition code	0.418	0.196	0.036
Lung				Lung			
Log10(Hg) = b ₀	R ² = 0.700	p < 0.001		Log10(Se) = b ₀	R ² = 0.535	p < 0.001	
+b ₁ (Le)+ b ₂ (Lo) +				+b ₁ (Le)+ b ₂ (Lo) +			
b ₃ (Sex)				b ₃ (Sex)			
Coefficients	Estimate	Std. Error	p value	Coefficients	Estimate	Std. Error	p value
Intercept	-0.515	0.248	0.042	Intercept	0.197	0.122	0.114
Body length	0.007	0.001	<0.001	Body length	0.003	0.0005	<0.001
Location:LA	-0.984	0.109	<0.001	Location:LA	-0.285	0.054	<0.001
Sex:male	-0.277	0.11	0.015	Sex:male	-0.144	0.054	0.011
Skin				Skin			
Log10(Hg) = b ₀	R ² = 0.474	p < 0.001		Log10(Se) = b ₀	R ² = 0.634	p < 0.001	
+b ₁ (Le)				+b ₁ (Le)+ b ₂ (Sex)+			
				b ₃ (Co)			
Coefficients	Estimate	Std. Error	p value	Coefficients	Estimate	Std. Error	p
Intercept	-0.432	0.206	0.045	Intercept	0.557	0.204	0.0114
Length	0.004	0.0009	<0.001	Body length	0.004	0.007	<0.001
				Sex:male	-0.242	0.082	0.006
				Condition code	-0.105	0.048	0.0402

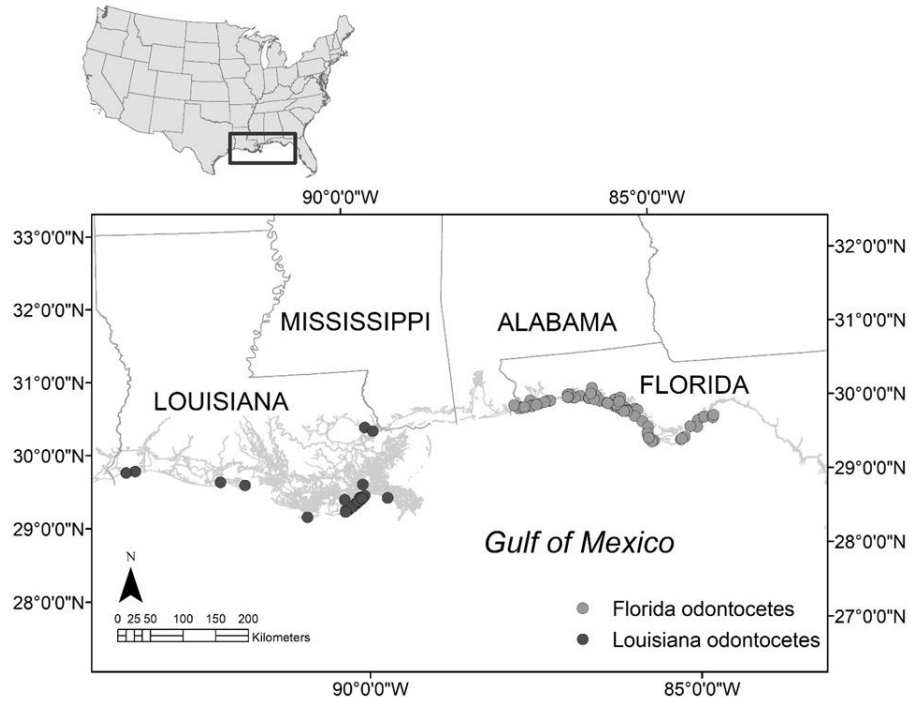


Figure 4.1. Stranding locations of odontocetes sampled in this study.

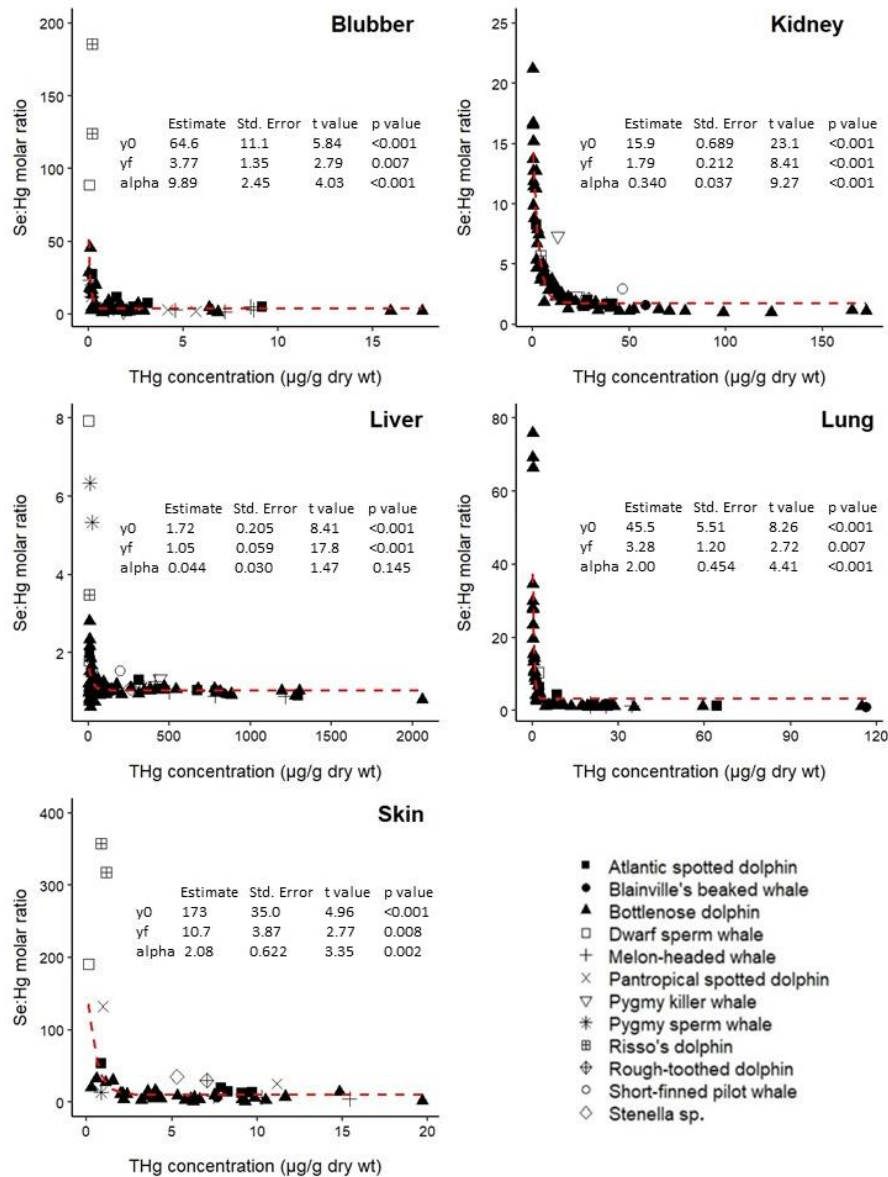


Figure 4.2. Relationship between Se:Hg molar ratio and THg concentration ($\mu\text{g/g}$ dry wt) in the blubber, kidney, liver, lung, and skin of odontocetes. The red dashed lines represent the one-phase decay model [formula: $y = y_f + (y_0 - y_f) \cdot \exp(-\alpha \cdot x)$; y_0 = average y when $x = 0$, y_f = y value when y reaches an asymptote; α = rate constant].

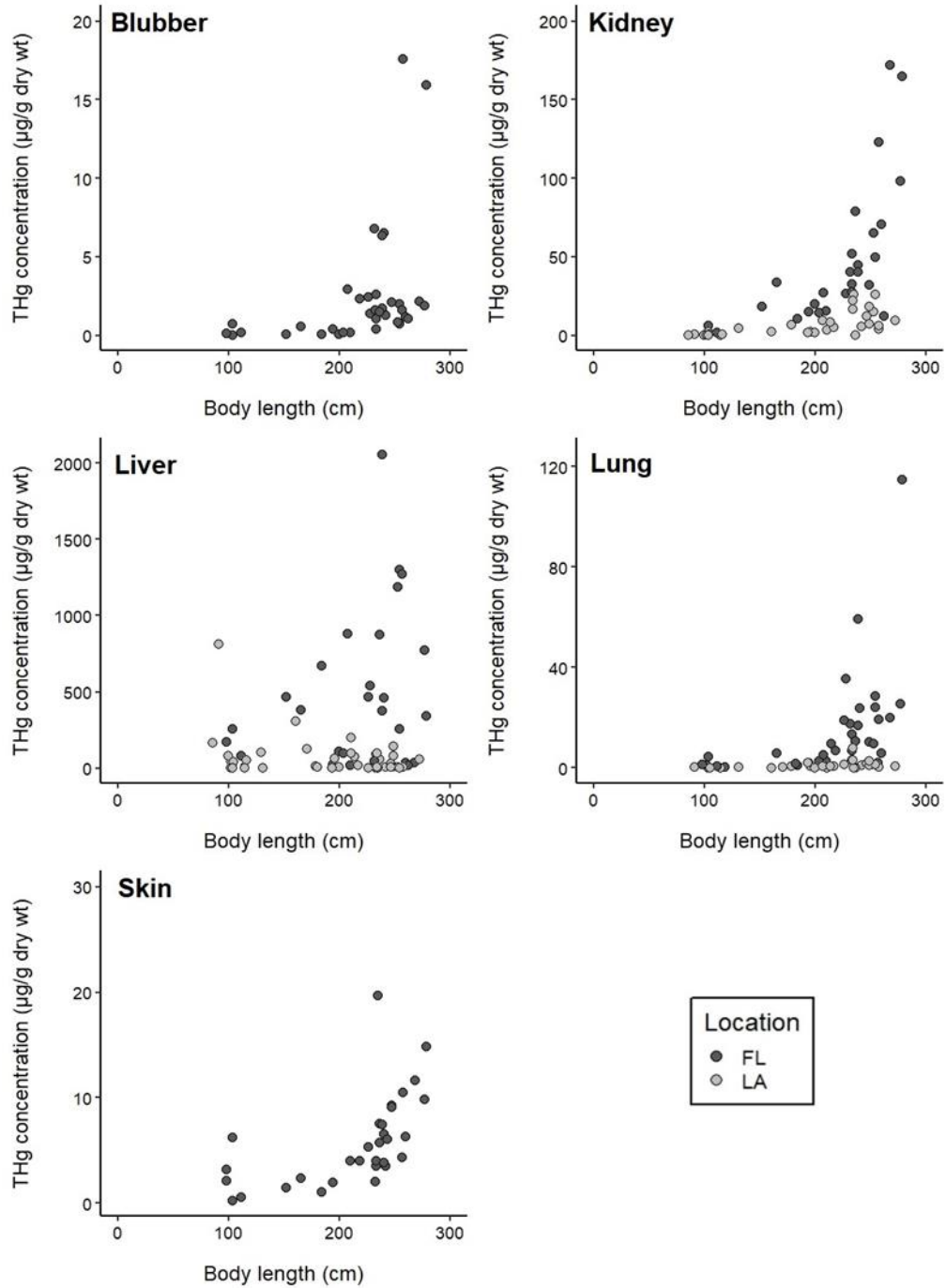


Figure 4.3. Relationship between THg concentration ($\mu\text{g/g dry wt}$) and body length (cm) in the blubber, kidney, liver, lung, and skin of stranded bottlenose dolphins.

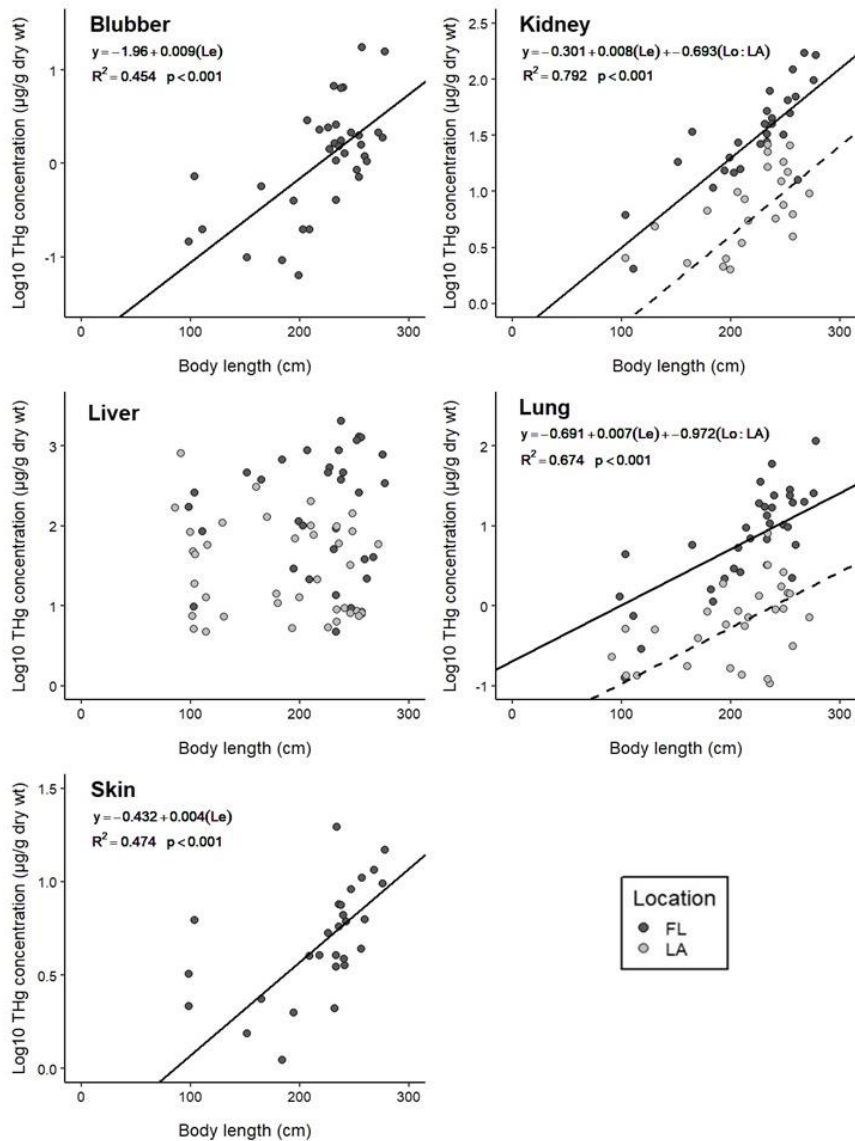


Figure 4.4. Scatterplots and linear regression lines showing the relationship between Log₁₀ THg concentrations (µg/g dry wt), body length (cm), and stranding location, when applicable, in the blubber, kidney, liver, lung, and skin of stranded bottlenose dolphins (Le = length; Lo = location). Solid regression lines correspond to Florida (FL) dolphins and dashed regression lines correspond to Louisiana (LA) dolphins. Body length was not a significant predictor of THg concentration in the liver; therefore, in the liver plot, the linear regression lines were not included.

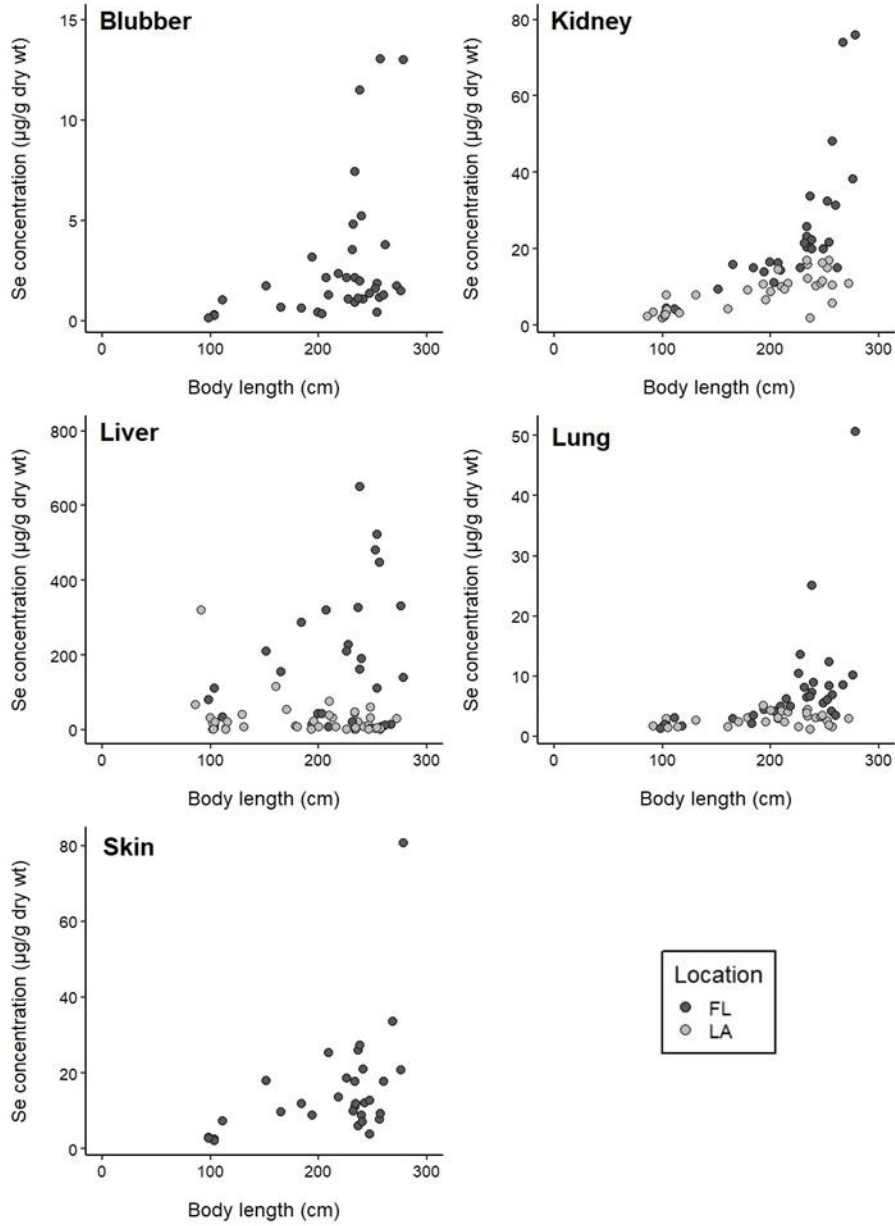


Figure 4.5. Relationship between Se concentration (µg/g dry wt) and body length (cm) in the blubber, kidney, liver, lung, and skin of stranded bottlenose dolphins.

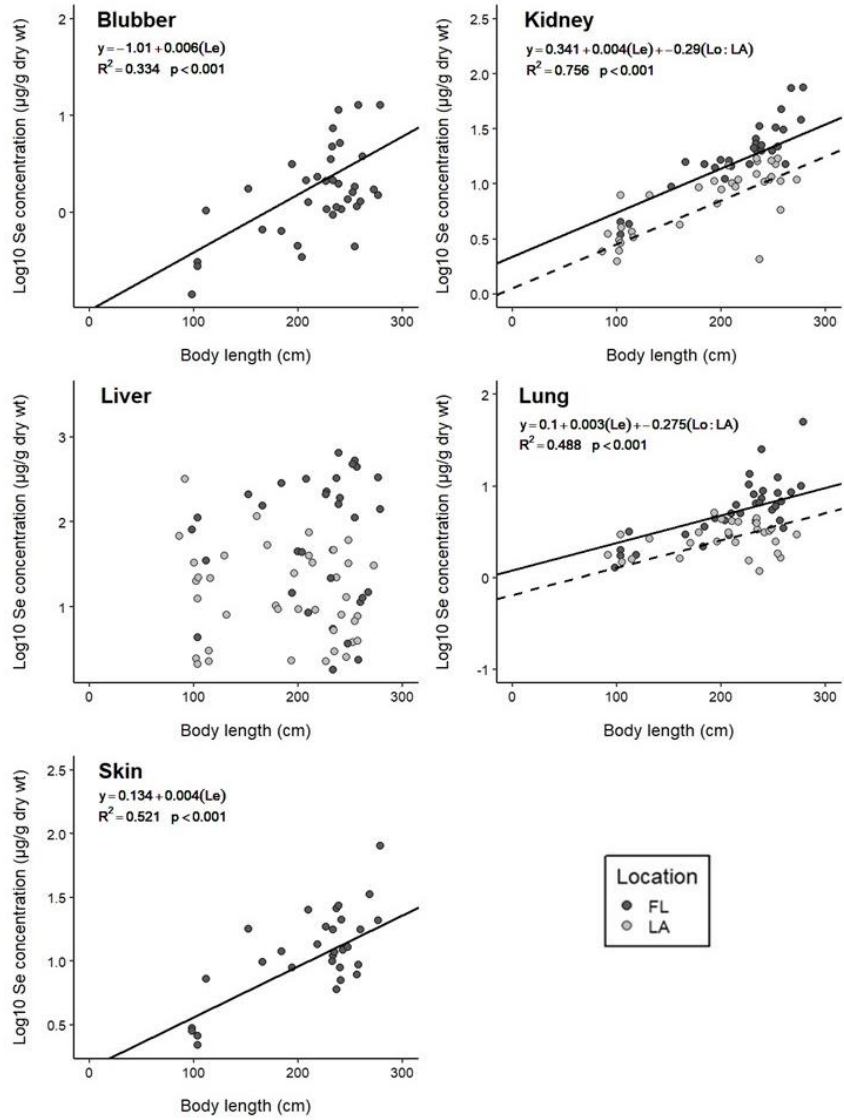


Figure 4.6. Scatterplots and linear regression lines showing the relationship between Log₁₀ Se concentrations (µg/g dry wt), body length (cm), and stranding location, when applicable, in the blubber, kidney, liver, lung, and skin of stranded bottlenose dolphins (Le = length; Lo = location). Solid regression lines correspond to Florida (FL) dolphins and dashed regression lines correspond to Louisiana (LA) dolphins. Body length was not a significant predictor of Se concentration in the liver; therefore, in the liver plot, the linear regression lines were not included.

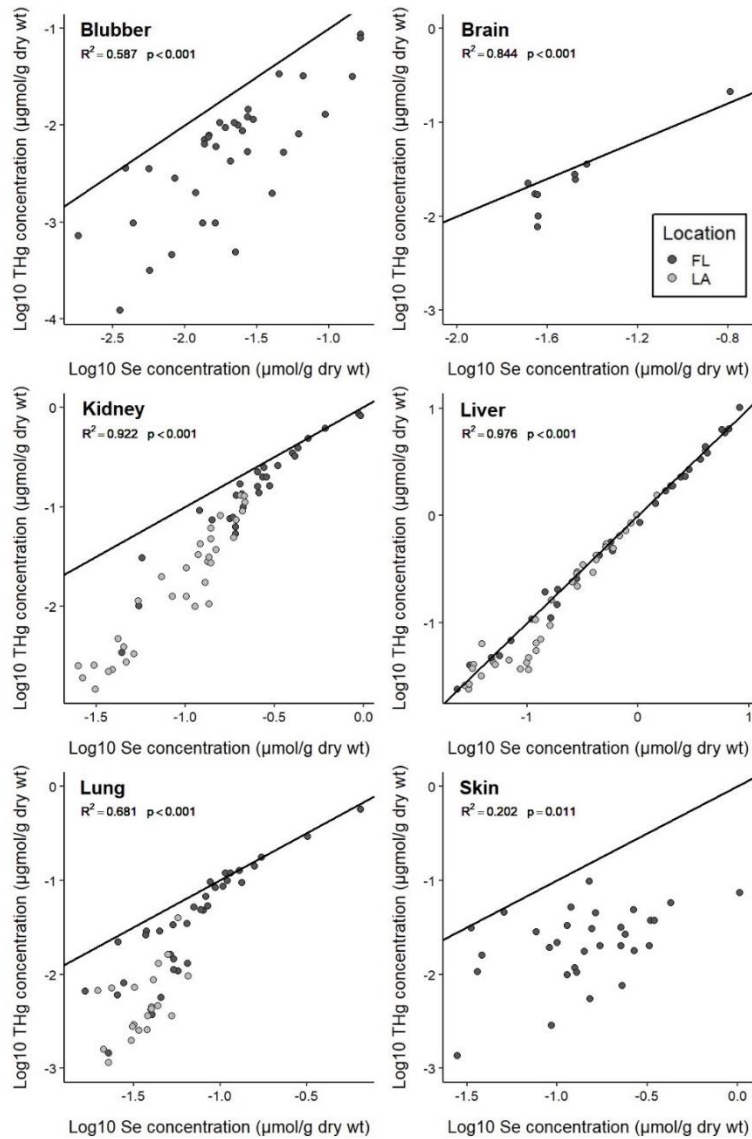


Figure 4.7. Relationship between Log₁₀ THg concentration (μmol/g dry wt) and Log₁₀ Se concentration (μmol/g dry wt) in tissues from stranded bottlenose dolphins. The solid line represents the 1:1 Se:Hg molar ratio. The R² and p values from the simple linear regression between Log₁₀ THg concentration (μmol/g dry wt) and Log₁₀ Se concentration (μmol/g dry wt) is provided in each plot.

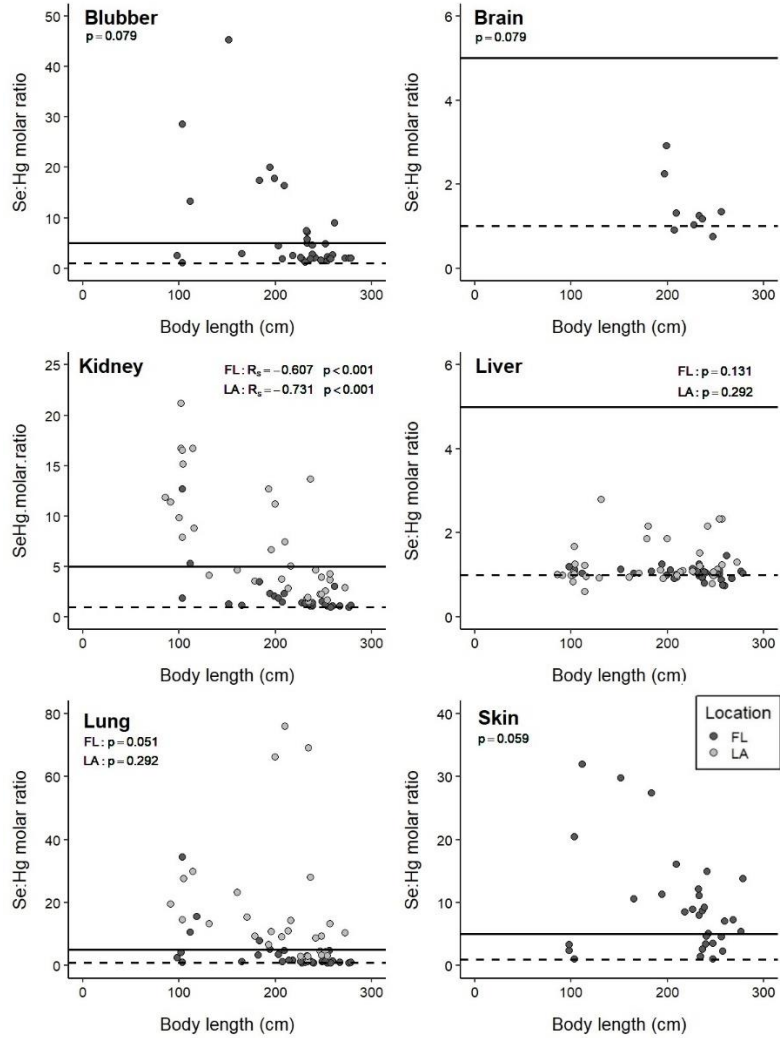


Figure 4.8. Relationship between the Se:Hg molar ratio and body length (cm) in the blubber, brain, kidney, liver, lung, and skin of stranded bottlenose dolphins. The solid horizontal line represents the 5:1 Se:Hg molar ratio and the broken horizontal line represents the 1:1 Se:Hg molar ratio.

**V. EFFECTS OF FORMALIN FIXATION ON TRACE ELEMENT
CONCENTRATIONS IN BOTTLENOSE DOLPHIN (*TURSIOPS TRUNCATUS*)
TISSUES**

Citation: McCormack, M. A., Jackson, B. P., & Dutton, J. (2020). Effects of formalin fixation on trace element concentrations in bottlenose dolphin (*Tursiops truncatus*) tissues. *Environmental Toxicology and Chemistry*, 39(6), 1149-1164.

Abstract

Odontocetes are considered ideal sentinel species to monitor environmental trace element concentrations. While frozen tissues are preferable for trace element analysis, often formalin-fixed tissues are the only samples available; however, it is uncertain if formalin fixation alters tissue trace element concentrations. To explore whether formalin-fixed tissues could be utilized for toxicology studies, concentrations of 14 trace elements (As, Cd, Co, Cr, Cu, Fe, Hg, Mn, Ni, Pb, Se, Sn, V, and Zn) were measured in frozen and formalin-fixed bottlenose dolphin (*Tursiops truncatus*) tissues following short-term (6 weeks; tissues: blubber, liver, lung) and long-term preservation (3-7 years; tissues: blubber, brain, kidney, liver, lung, skin) using Inductively Coupled Plasma Mass Spectrometry (ICP-MS). Following both short-term and long-term preservation, there were significant differences in tissue trace element concentrations between preservation methods. Some trace elements were found in greater concentrations in frozen tissues compared to formalin-fixed tissues suggesting leaching (e.g., mean As concentrations were between 1.4 and 7.6-times greater in frozen tissues). In contrast, other trace

elements were found in greater concentrations in formalin-fixed tissues compared to frozen tissues suggesting contamination (e.g., mean Zn concentrations were up to 8.7-times higher in some formalin-fixed tissues). Our results suggest that it may be possible to account for the effects of formalin fixation for some trace elements but leaching and contamination should be carefully considered.

Introduction

Marine mammals, including odontocetes, are long-lived, high trophic level organisms, and as such, can accumulate high concentrations of trace elements [e.g., cadmium (Cd), mercury (Hg)] in their tissues (Das et al. 2003; Monteiro et al. 2020). In addition, marine mammals are often long-term residents of coastal environments and consume similar fish to human populations, making them ideal sentinel species for ecosystem and public health (Bossart 2011; Reif et al. 2015). Because of these characteristics, trace element concentrations in marine mammal tissues have been increasingly utilized to understand their population structure and ecology, to identify population-level threats due to contaminant exposure, to assess temporal changes in environmental trace element concentrations, and to identify public health hazards (Parsons et al. 2004; García-Alvarez et al. 2015; Reif et al. 2015; Romero et al. 2017).

When measuring trace element concentrations in animal tissues, it is imperative that sample collection, preservation, and processing does not alter tissue trace element concentrations (Campbell and Drevnick 2015). While fresh or frozen tissues are preferable for trace element analysis, often formalin-fixed tissues are the only samples available (Bush et al. 1995; Bischoff et al. 2008; Gellein et al. 2008). Formalin, which is

commonly used to preserve marine mammal tissues for histopathological examination and museum collections, has the potential to alter trace element concentrations; however, relatively few controlled experiments have been performed to determine the effects of formalin fixation on trace element concentrations in animal tissues and results have been variable. Some studies have found that formalin fixation does not alter tissue trace element concentrations, while other studies have found that formalin fixation significantly alters tissue trace element concentrations, either by increasing or decreasing concentrations suggesting issues of contamination and leaching, respectively (Gibbs et al. 1974; Theron et al. 1974; Sullivan et al. 1993; Koizumi et al. 1994; Bush et al. 1995; Renaud et al. 1995; Meldrum 2001; Quan et al. 2002; Sato et al. 2006; Bischoff et al. 2008; Gellein et al. 2008; Hill et al. 2010; Pouloupoulos 2013). If formalin fixation does not impact tissue trace element concentrations or it has consistent and predictable effects, such that trace element concentrations in unpreserved tissues can be predicted from trace element concentrations in formalin-fixed tissues; formalin-fixed tissues may be useful not only histopathological examination but also for toxicology studies (Renaud et al. 1995; Sato et al. 2006; Pouloupoulos 2013; Campbell and Drevnick 2015).

In the present study, we investigated the effects of long-term (3–7 years) and short-term (6 weeks) formalin fixation on trace element concentrations in bottlenose dolphin (*Tursiops truncatus*) tissues. By chance, we obtained *T. truncatus* tissues [blubber (dermis and subcutis), brain, kidney, liver, lung, and skin (epidermis)], which had been subsampled from the same individual dolphin, with one subsample frozen and the other subsample preserved in formalin for between 3 and 7 years. Our objectives for the long-term study were to measure the concentration of 9 essential trace elements

[cobalt (Co), chromium (Cr), copper (Cu), iron (Fe), manganese (Mn), nickel (Ni), selenium (Se), vanadium (V), and zinc (Zn)] and 5 nonessential elements [arsenic (As), Cd, Hg, lead (Pb), and tin (Sn)] in formalin-fixed and frozen *T. truncatus* tissues using Inductively Coupled Plasma Mass Spectrometry (ICP-MS) analysis, determine if formalin fixation altered tissue trace element concentrations and if so, determine if the effects were predictable. In the long-term study, formalin-fixed tissue trace element concentrations differed significantly from frozen tissue trace element concentrations; therefore, to determine if the effects of formalin fixation were similar following short-term preservation, we performed an additional laboratory study. In the short-term study, *T. truncatus* tissues (blubber, liver, lung) were subsampled, either frozen or preserved in formalin for six weeks, and analyzed for all the above-mentioned trace elements except for V. Finally, to assess if the effects of formalin fixation were time-dependent, we compared the absolute percent differences in tissue trace element concentrations between formalin-fixed and frozen tissue pairs from the long-term and short-term studies.

Methods

Long-term formalin fixation

Frozen and formalin-fixed *T. truncatus* tissues were obtained from the National Oceanographic and Atmospheric Administration (NOAA) under a NOAA parts authorization letter pursuant to 50 CFR 216.22. Tissue samples were collected from dolphins that stranded along the Florida (FL) panhandle between 2011 and 2015 by local stranding networks. All samples were collected from code 2 (fresh) or code 3 (moderate decomposition) animals [Smithsonian Institution Coding System] (Geraci and Lounsbury

2005). Samples were transferred to Texas State University and analyzed in 2018; therefore, at the time of analysis, samples had either been frozen or preserved in formalin for approximately between 3 and 7 years. Frozen tissue samples were individually wrapped in aluminum foil and sealed in Ziplock bags. In contrast, all formalin-fixed tissues from a single dolphin were packaged together wrapped in paper towels and sealed in Ziplock bags. The edges of all tissues were removed using a clean ceramic knife or stainless-steel scalpel to avoid contamination. In total, 56 tissue pairs [blubber (n = 10), brain (n = 6), kidney (n = 10), liver (n = 10), lung (n = 10), and skin (n = 10)] were analyzed.

Tissues were soaked in approximately 60 mL of Milli-Q water (Milli-Q Academic; Millipore) for 48 hours in trace metal clean 100 mL glass beakers, with the water changed once after 24 hours to remove formalin (Hill et al. 2010). Both formalin-fixed tissues and thawed frozen tissues were then blot dried to remove excess water, weighed to determine the wet weight (wet wt), freeze-dried (Labconco FreeZone 2.5; Labconco) for 48 hours, and weighed again to determine the dry weight (dry wt). Blubber and skin samples were cut into approximately 4 x 4 mm pieces using a stainless-steel scalpel, whereas all other tissues were homogenized into a fine powder. The mean percentage moisture content [\pm standard deviation (SD)] for formalin-fixed tissues was $54 \pm 13\%$, $77 \pm 5\%$, $83 \pm 3\%$, $79 \pm 5\%$, $84 \pm 1\%$, and $66 \pm 3\%$ for blubber, brain, kidney, liver, lung, and skin, respectively. For frozen tissues, the mean percentage moisture content \pm SD was $42 \pm 14\%$, $76 \pm 3\%$, $76 \pm 3\%$, $72 \pm 3\%$, $77 \pm 1\%$, and $58 \pm 6\%$ for blubber, brain, kidney, liver, lung, and skin, respectively.

Trace element concentrations were determined using microwave-assisted acid digestion and ICP-MS analysis. In summary, between 0.20 to 0.25 g of each sample was digested in a microwave digestion system (Ethos-UP; Milestone Inc.) in 5 mL of nitric acid:hydrochloric acid (9:1, v/v) for 75 minutes (25 minute ramp time to 200°C, 20 minute hold time at 200°C, and 30 minute cool down time). Once cool, blubber and skin samples were diluted with 25 mL of Milli-Q water, while all other tissues were diluted with 45 mL of Milli-Q water, to obtain a final sample volume of 30 mL (dilution factor ~ 120) and 50 mL (dilution factor ~ 200), respectively. Samples were then sent to the Trace Element Analysis Core Laboratory at Dartmouth College (Hanover, NH) for ICP-MS analysis (Agilent 7900 and 8900; Agilent Technologies) following EPA Method 6020A (U.S. EPA 1998). For quality control, blanks (acid with no sample; n = 27), certified reference materials [CRM; DORM-4, fish protein (n = 16) and DOLT-5, dogfish liver (n = 12) from the National Research Council Canada], spiked samples (n = 25), and duplicate samples (n = 34) were included. Blanks were below the detection limit (BDL) for all trace elements. For DORM-4, the mean percentage recovery was between 82 and 106% for all trace elements. For DOLT-5, the mean percentage recovery was between 81 and 108% for all trace elements, except Sn which was 75%. The mean percentage spike recovery was between 80 and 98% for all trace elements. For all tissues combined, mean relative percent differences between duplicate samples were $\leq 15\%$ for Cu, Hg, Mn, Ni, Se, and Zn, between 15 and 25% for As, Cd, Co, Fe, Sn and V, 31% for Cr, and 35% for Pb.

Short-term formalin fixation

Blubber (n = 5), liver (n = 5), and lung (n = 5) samples from *T. truncatus* that stranded along the Texas (TX) coast between 2011 and 2017 were collected by the Texas Marine Mammal Stranding Network (TMMSN; Galveston, TX). All samples were collected from code 2 or code 3 individuals. Samples were held at -20°C at the TMMSN and transported to Texas State University, under a NOAA parts authorization letter pursuant to 50 CFR 216.22, where they remained at -20°C until the start of the experiment. Tissues were thawed, and the edges were removed using a trace metal clean ceramic knife to avoid contamination. Samples were then split into two approximately 2 cm x 1 cm x 1 cm cubes. One subsample was blot dried, weighed to determine the wet weight, placed in a 50 mL trace metal clean plastic tube, and stored at -20°C for 6 weeks. The other subsample was blot dried, placed in a trace metal clean glass jar which was then filled with 35 mL of 10% neutral buffered formalin, capped, and stored at room temperature (22°C) for 6 weeks. 10% neutral buffered formalin was made by combining 4 g ACS reagent grade sodium phosphate monobasic, 6.5 g reagent grade sodium phosphate dibasic, 100 mL of 37% (w/w) reagent grade formaldehyde (all chemicals purchased from Fisher Scientific), and 900 mL of Milli-Q water. After six weeks, formalin-fixed tissues were transferred to 50 mL trace metal clean plastic tubes, and the formalin was removed by soaking tissues in 40 mL of Milli-Q water for 48 hours, with the water changed once after 24 hours. The formalin-fixed tissues were then blot dried to removed excess water and weighed to determine a wet weight. Next, both the formalin-fixed and frozen tissues were freeze-dried and either cut or homogenized following the procedure described for the long-term study. For formalin-fixed tissues, the mean

percentage moisture content (\pm SD) was $53 \pm 24\%$ (range: 22-76%), $80 \pm 3\%$, and $90 \pm 14\%$ for the blubber, liver, and lung, respectively. For frozen tissues, the mean percentage moisture content (\pm SD) was $40 \pm 25\%$ (range: 17-71%), $69 \pm 4\%$, and $75 \pm 3\%$ for the blubber, liver, and lung, respectively. All samples were digested and analyzed to determine the concentration of trace elements following the method described for the long-term study, with the exception that in short-term study, blubber was diluted with 20 mL of Milli-Q water and the liver and lung tissues with 25 mL of Milli-Q water, to obtain a final volume of 25 mL (dilution factor \sim 100) and 30 mL (dilution factor \sim 120), respectively. For quality control, blanks ($n = 2$), certified reference materials (DORM-4; $n = 2$), spiked samples ($n = 2$), and duplicate samples ($n = 3$) were included. All blanks were BDL for all trace elements. For all trace elements, the mean percentage recovery for DORM-4 ranged from 80 to 102%, and the mean percentage spiked recovery was between 86% and 94%. For all tissues combined, the mean relative percent difference between duplicate samples was $<14\%$ for all trace elements except Ni which was 118%. The reason for the high relative percent difference in Ni concentrations between duplicate samples is not apparent. All samples were processed at the same time using trace metal clean procedures; therefore, we have included the Ni data in the results, but concentrations should be taken with caution.

Statistical analysis

In both the long-term and short-term studies, for each trace element and tissue type, two-sided paired t-tests were used to determine if there were significant differences between formalin-fixed and frozen tissue trace element concentrations. When the data was not normally distributed (Shapiro-Wilk test $p < 0.05$), non-parametric Wilcoxon

signed-rank tests were used. Bland-Altman plots were used to graphically display the agreement between formalin-fixed and frozen tissue trace element concentrations, to calculate the mean within-pair difference between formalin-fixed and frozen tissue trace element concentrations (i.e., mean bias), and to visually assess if there were consistent effects of formalin fixation on trace element concentrations. In traditional Bland-Altman plots, the difference between two paired measurements is displayed on the y-axis, and the average of the paired measurements is displayed on the x-axis (Bland and Altman 1986). Plotting the average of two measurements on the x-axis is appropriate when neither method of measurement is considered standard; however, because freezing is the standard preservation method for trace element analysis, we plotted only the frozen tissue trace element concentration on the x-axis (Krouwer, 2008).

In each tissue type, if trace element concentrations in formalin-fixed tissues differed significantly from trace element concentrations in frozen tissues ($p < 0.05$), a linear regression with formalin-fixed tissue trace element concentration as the independent variable and frozen tissue trace element concentration as the dependent variable was analyzed. Regression models were checked for assumptions of normality and homoscedasticity through the visual inspection of residual plots. If the linear regression was significant ($p < 0.05$) and the R^2 value was ≥ 0.80 , we determined that for that trace element and tissue, concentrations of trace elements in formalin-fixed tissues may be useful to predict concentrations of trace elements in frozen tissues. However, additional controlled experiments would be needed to confirm these findings.

While it is common in toxicological studies to assign values of 50% the detection limit to samples which are BDL (e.g., Adams and Engel 2014), we excluded values that

were BDL from both descriptive and inferential statistics. If 50% of the detection limit was assigned to samples which were BDL, within tissue pairs, if both formalin-fixed and frozen samples were BDL for a particular trace element it would appear that there was no difference between preservation methods; however, because the concentration of the trace element lies somewhere between zero and the detection limit, although they cannot be detected, differences between preservation methods may still exist. Furthermore, because samples were sent for ICP-MS analysis in multiple batches, detection limits for trace elements differed both within the long-term study and between the long-term and short-term studies; therefore, we could only compare tissue trace element concentrations which were above the detection limit.

In addition to the above analyses, we also calculated the absolute percent difference in trace element concentrations between formalin-fixed and frozen tissue pairs as small changes in concentrations may not influence the interpretation of results for trace elements normally found in high concentrations (e.g., Fe, Zn), but may influence the interpretation of results for trace elements normally found in low concentrations (e.g., Cr, Ni). Given that freezing is the standard preservation method for trace element analyses, we calculated the absolute percent difference in trace element concentration between formalin-fixed and frozen tissue pairs using the following equation:

$$\text{ABS} [(\text{Formalin-fixed X} - \text{Frozen X}) / (\text{Frozen X})] \times 100 \quad (1)$$

where X is the concentration of a trace element in $\mu\text{g/g}$ dry wt. T-tests were used to determine if the mean absolute percent difference in trace element concentrations between formalin-fixed and frozen tissue pairs differed between the long-term and short-term studies. If the data violated the assumptions of the t-test, Mann-Whitney U tests were

utilized. All analyses were performed in Sigma plot version 13, and the level of significance was set at $\alpha = 0.05$. All concentrations were reported on a dry wt basis.

Results

Long-term formalin fixation

For several samples, trace element concentrations were below the detection limit; a breakdown of the number of samples that were above the detection limit is shown in Table 5.1. The detection limit for each trace element is reported in Supplementary Table 5.1. For each tissue type, the mean, standard deviation, minimum, and maximum trace element concentrations for formalin-fixed and frozen tissues are reported in Table 5.2. The effects of formalin fixation varied among trace elements and tissue types. Overall, we identified four general patterns: 1) formalin-fixed tissues had consistently lower trace element concentrations compared to frozen tissues; 2) formalin-fixed tissues had consistently greater trace element concentrations compared to frozen tissues; 3) differences between trace element concentrations in formalin-fixed and frozen tissue pairs were small, and concentrations were not consistently greater in either formalin-fixed or frozen tissues, and 4) differences in trace element concentrations between formalin-fixed and frozen tissue pairs were large, but concentrations were not consistently greater in either formalin-fixed or frozen tissues.

Compared to frozen tissues, formalin-fixed tissues had significantly lower concentrations of As in all tissues, Se in the blubber, Cd, Cu, and Se in the kidney, Cd, Cu, Fe, Hg, Mn, and Se in the liver, Hg in the lung, and Se and Zn in the skin (Table 5.3). In contrast, formalin-fixed tissues had significantly greater concentrations of Cu and Fe

in the blubber, Cu and Zn in the lung, and Cu, Fe, Mn, and V in the skin (Table 5.3). Additionally, although the majority of frozen tissues had Ni concentrations that were BDL, those which had concentrations above the detection limit were consistently lower than concentrations in formalin-fixed tissues. The Bland-Altman plots for As and Hg are shown in Figures 5.1 and 5.2, respectively, while the remaining Bland-Altman plots can be found in Supplementary Figures S5.1- S5.11. Nickel was excluded from the Bland-Altman plots due to the low sample size.

In cases where formalin-fixation significantly influenced tissue trace element concentrations, simple linear regression analysis determined that it may be possible to predict frozen blubber As concentrations from formalin-fixed blubber As concentrations ($p < 0.001$; $R^2 = 0.884$), frozen brain As concentrations from formalin-fixed brain As concentrations ($p = 0.008$; $R^2 = 0.858$), frozen kidney Cd concentrations from formalin-fixed kidney Cd concentrations ($p < 0.001$; $R^2 = 0.938$), frozen kidney Se concentrations from formalin-fixed kidney Se concentrations ($p < 0.001$; $R^2 = 0.99$), and frozen lung Hg concentrations from formalin-fixed lung Hg concentrations ($p < 0.001$; $R^2 = 0.99$) (Figures not shown). Using the regression equations to predict frozen tissue trace element concentrations from formalin-fixed tissue trace element concentrations, on average, the absolute difference between measured frozen tissue trace element concentrations and the predicted frozen tissue trace element concentrations was 0.180 $\mu\text{g/g}$ dry wt for As in the blubber, 0.584 $\mu\text{g/g}$ dry wt for As in the brain, 1.90 $\mu\text{g/g}$ dry wt for Cd in the kidney, 1.31 $\mu\text{g/g}$ dry wt for Se in the kidney, and 0.936 $\mu\text{g/g}$ dry wt for Hg in the lung,. The regression equations are provided below:

$$\text{Frozen blubber As concentration} = 0.281 + 2.18(\text{Formalin blubber As concentration}) \quad (2)$$

$$\text{Frozen brain As} = 0.065 + 2.29(\text{Formalin brain As concentration}) \quad (3)$$

$$\text{Frozen kidney Cd concentration} = -0.300 + 3.25(\text{Formalin kidney Cd concentration}) \quad (4)$$

$$\text{Frozen kidney Se concentration} = -0.391 + 1.17(\text{Formalin kidney Se concentration}) \quad (5)$$

$$\text{Frozen lung Hg} = 0.148 + 1.15(\text{Formalin lung Hg concentration}) \quad (6)$$

In contrast to the patterns described above, in some cases, no significant effects of formalin fixation were determined (Table 5.3). Non-significant results could arise from two scenarios: 1) differences between trace element concentrations in formalin-fixed and frozen tissue pairs were small, and concentrations were not consistently greater in either formalin-fixed or frozen tissues suggesting good agreement between preservation methods (e.g., within-pair differences for Co were ≤ 0.040 ; Supplementary Figure S5.2); or 2) differences in trace element concentrations between formalin-fixed and frozen tissue pairs were large, but concentrations were not consistently greater in either formalin-fixed or frozen tissues; therefore, differences could not be attributed to preservation method (e.g., within-pair differences for Fe were upwards of $50 \mu\text{g/g}$ dry wt; Supplementary Figure S5.5). However, despite some trace elements such as Co displaying relatively good agreement between measurements, only skin Cr and Pb mean absolute percent differences between formalin-fixed and frozen tissue trace element concentrations were $<10\%$, both of which were limited to a single tissue pair (Table 5.4).

Short-term formalin fixation

The mean, standard deviation, minimum, and maximum trace element concentrations for formalin-fixed and frozen tissues are reported in Table 5.5. Detection limits for each trace element and tissue type are reported in Supplementary Table 5.1. Like the long-term study, some trace elements were found in greater concentrations in frozen tissues, while

other trace elements were found in greater concentrations in formalin-fixed tissues. Compared to formalin-fixed tissues, frozen tissues had significantly greater concentrations of Zn in the blubber, As and Mn in the liver, and Cu in the lung (Table 5.6). Additionally, while not differing significantly between preservation methods, the majority of As and Se concentrations in the blubber, and As concentrations in the lung were greater in frozen tissues compared to formalin-fixed tissues (Figure 5.3 and Supplementary Figure S5.19). In contrast, formalin-fixed tissues had significantly greater concentrations of Ni in the blubber, Cd, Hg, and Se in the liver, and Cd, Cr, and Ni in the lung (Table 5.6). Bland-Altman plots and linear regressions between formalin-fixed and frozen tissue trace element concentrations for As, Cd, and Hg, can be found in Figures 5.3, 5.4, and 5.5, respectively, while figures for the remaining trace elements can be found in Supplementary Figures S5.12-S5.21.

In cases in which preservation method significantly influenced trace element concentrations, linear regressions between formalin-fixed and frozen tissue trace element concentrations indicated that formalin-fixed tissues may be useful in predicting trace element concentrations in unpreserved tissues for Zn in the blubber ($p = 0.006$; $R^2 = 0.942$), As ($p = 0.037$; $R^2 = 0.813$), Hg ($p = 0.003$ $R^2 = 0.965$), and Se ($p = 0.009$ $R^2 = 0.927$) in the liver, and Cu ($p = < 0.001$, $R^2 = 0.992$) and Ni ($p = 0.030$; $R^2 = 0.835$) in the lung (Figures 5.3 and 5.5; Supplementary Figures S5.14, S5.17, S5.19, and S5.21). Using the regression equations to predict frozen tissue trace element concentrations from formalin-fixed tissue trace element concentrations, on average, the absolute difference between measured frozen tissue trace element concentrations and the predicted frozen tissue trace element concentrations was 3.52 $\mu\text{g/g}$ dry wt for Zn in the blubber, 0.178

$\mu\text{g/g}$ dry wt for As in the liver, $3.50 \mu\text{g/g}$ dry wt for Hg in the liver, $1.99 \mu\text{g/g}$ dry wt for Se in the liver, $0.295 \mu\text{g/g}$ dry wt for Cu in the lung, and $0.010 \mu\text{g/g}$ dry wt for Ni in the lung. The regression equations are provided below:

$$\text{Frozen blubber Zn concentration} = 1.74 + 1.29(\text{Formalin blubber Zn concentration}) \quad (7)$$

$$\text{Frozen liver As concentration} = 0.318 + 1.07(\text{Formalin liver As concentration}) \quad (8)$$

$$\text{Frozen liver Hg concentration} = 0.062 + 0.694(\text{Formalin liver Hg concentration}) \quad (9)$$

$$\text{Frozen liver Se concentration} = 1.50 + 0.691(\text{Formalin liver Se concentration}) \quad (10)$$

$$\text{Frozen lung Cu concentration} = 0.611 + 1.21(\text{Formalin lung Cu concentration}) \quad (11)$$

$$\text{Frozen lung Ni concentration} = -0.019 + 0.334(\text{Formalin lung Ni concentration}) \quad (12)$$

Like the long-term study, for some trace elements, the effects of formalin fixation were not significant (Table 5.6). The smallest absolute mean within-pair differences in trace element concentrations ($\leq 0.20 \mu\text{g/g}$ dry wt) were determined for Cd, Co, Cr, Cu, Hg, Ni, Pb, and Sn in the blubber, Co, Ni, Pb, and Sn in the liver, and Co, Ni, Pb, and Sn in the lung. Intermediate mean absolute within-pair differences in trace element concentrations ($0.21 < x < 6 \mu\text{g/g}$ dry wt) were determined for As, Mn, Fe, and Se in the blubber, As, Cr, Cd, and Mn in the liver, and As, Cd, Cr, Cu, Mn, and Se in the lung. The largest mean absolute within-pair differences in trace element concentrations were determined for Zn in the blubber ($7.69 \mu\text{g/g}$ dry wt), Cu ($6.67 \mu\text{g/g}$ dry wt), Fe ($167 \mu\text{g/g}$ dry wt), Hg ($21.5 \mu\text{g/g}$ dry wt), Se ($8.96 \mu\text{g/g}$ dry wt) and Zn ($12.6 \mu\text{g/g}$ dry wt) in the liver, and Fe ($69.5 \mu\text{g/g}$ dry wt), Hg ($13.0 \mu\text{g/g}$ dry wt), and Zn ($10.8 \mu\text{g/g}$ dry wt) in the lung. Less than 10% mean absolute percent differences were determined for Fe in the lung and Zn in the liver (Table 5.7).

On average, absolute percent differences between formalin-fixed and frozen tissue pairs differed significantly between the long-term and short-term studies for As ($p = 0.002$), Fe ($p = 0.003^\dagger$), and Mn ($p = 0.036^\dagger$) in the blubber, As ($p = 0.001$), Cd ($p = 0.015$), Co ($p = 0.003$), Cu ($p = 0.019^\dagger$), Mn ($p = 0.008^\dagger$), and Zn ($p = 0.017^\dagger$) in the liver, and As ($p = 0.011$) and Cu ($p = 0.011$) in the lung († denotes p values that were estimated from Mann-Whitney U Tests). Except for Cd in the liver, the percent differences were more pronounced following long-term preservation compared to the short-term preservation.

Discussion

Recognizing the benefits of measuring trace element concentrations in marine mammal tissues, several countries have established protocols for the collection and preservation of tissues from stranded marine mammals (Becker et al. 1994; Ballarin et al. 2005). When collecting and preserving tissues for trace element analysis, the aim is to minimize contamination, ideally, samples should be collected using a clean titanium or stainless-steel knife, placed in a clean bag, and frozen until analysis (Geraci and Lounsbury 2005). In contrast, when collecting and preserving tissues for future histopathological examination or museum collections, the aim is to preserve the appearance and structural integrity of the tissues; in such cases, preservation in 10% neutral buffered formalin is preferable over freezing (Geraci and Lounsbury 2005). Although not originally intended for trace element analyses, formalin-fixed tissues may provide valuable opportunities for trace element analysis if the effects of formalin fixation on tissue trace element concentrations are negligible or predictable.

Formalin, which consists of 37-40% formaldehyde (CH₂O) and 60-63% water (w/w), is an effective fixative because it quickly penetrates tissues, prevents autolysis, and preserves cellular structure (Buesa 2008; Kiernan 2000). When dissolved in water, the aldehyde groups (-CHO) in formaldehyde form bonds with the nitrogen atoms found in proteins; the resultant bound formaldehyde can then react with other nearby protein molecules to form a cross-links (-CH₂) between proteins called a methylene bridges which allows the structure of the tissue to be preserved (Kiernan 2000). If trace element concentrations are lower in formalin-fixed tissues compared to concentrations in frozen tissues, it is likely because trace elements were leached from tissues into the preservative. In contrast, if trace elements concentrations in formalin-fixed tissues are greater than concentrations in frozen tissues, it is likely the sample was contaminated. Our results suggest that it may be possible to account for the effects of formalin for some trace elements including As, Cd, Cu, Hg, Ni, Se, and Zn following short-term and/or long-term preservation, but leaching and contamination should be carefully considered when using formalin preserved tissues for trace element analysis.

Leaching of trace elements from formalin-fixed tissues

In the present study, we found greater concentrations of As, Cd, Cu, Fe, Mn, and Zn in frozen tissues compared to formalin-fixed tissues suggesting that these elements leached from the specimens into the preservative. Our results are consistent with Gellein et al. (2008), which reported greater concentrations of the abovementioned trace elements in formalin following preservation of human and rat brains compared to fresh formalin. Leaching of Mn in a variety of human tissues, Cu in antelope (*Damaliscus pygargus phillipsi*) liver, Co in bovine liver, and Se in swine liver has been reported by Bush et al.

(1995), Quan et al. (2002), Meldrum et al. (2001), and Sullivan et al. (1993), respectively. The degree of leaching varied among trace elements; like Gellein et al. (2008), we determined that the leaching of trace elements is not simply a function of trace element concentration. For example, some trace elements found in low tissue concentrations consistently leached from tissues (e.g., As) while other trace elements found in high tissue concentrations did not show consistent leaching patterns (e.g., Hg, except in the liver following long-term preservation).

The degree of leaching may be influenced by the chemical form of the trace element and the binding strength between trace elements and tissues (Gellein et al. 2008). Arsenobetaine—the predominant species of As found in marine mammal liver, kidney, and muscle tissues—does not bind to any specific macromolecules (e.g., proteins) (Vahter et al. 1983; Ebisuda et al. 2002; Kunito et al. 2008); this may explain why arsenic was readily leached from tissues. In contrast, methylmercury (MeHg)—the predominant species of Hg found in odontocete muscle, brain, and skin tissues—has a strong binding affinity for sulfuryl groups present in proteins which may explain why Hg was not readily leached from most tissues (Bloom 1992, Storelli and Marcotrigiano 2000; Endo et al., 2006; Stavros et al. 2007). Similarly, and consistent with Gellein et al. (2008), we did not observe consistent leaching of Ni and Pb, which are also known to form bonds with sulfhydryl groups. However, in the liver following long-term preservation, we found that Hg concentrations in formalin-fixed tissues were significantly lower than Hg concentrations in frozen tissues, which suggests leaching. In odontocete liver, Hg is found predominantly in its inorganic form or as HgSe complexes, which may be more

readily leached from tissues compared to MeHg (Storelli and Marcotrigiano 2000; Kehrig et al. 2008).

Also consistent with Gellein et al. (2008), our results suggest that the degree of leaching is time-dependent, with more pronounced leaching following long-term storage. In the present study, on average, following short-term preservation, As concentrations were 1.4-, 1.6-, and 2.4-times lower than frozen blubber, liver, and lung concentrations, respectively. Following long-term preservation, on average, As concentrations in formalin-fixed tissues were 2.6-, 5.1-, 4.0-times lower than frozen blubber, liver, and lung samples, respectively. One possibility suggested by Sato et al. (2006) that was not explored in the present study is that the leaching of some trace elements may be limited to the surface of the specimen which suggests that if the tissue is large enough to remove the surface preserved tissues may be useful for trace element analyses.

Contamination of formalin-fixed tissues

Formalin fixation also has the potential to introduce trace elements to tissues; higher concentrations of trace elements in formalin-fixed tissues compared to frozen tissues suggest that tissues were contaminated either by the formalin itself and/or by other sources during sample collection, processing, and preservation. The original brand of formalin used for the long-term study was unknown; however, the use of 10% neutral buffered formalin is common practice for marine mammal stranding networks. We also did not measure the concentration of trace elements in the fresh formalin used for the short-term study. However, Gellein et al. (2008) measured the concentration of various trace elements in fresh formalin (Baker, reagent grade) [e.g., Cr (1.9 µg/L), Cu (5.2 µg/L), Fe (31 µg/L), Ni (3.0 µg/L), Pb (0.11 µg/L), Zn (19 µg/L)]. Based on the

concentrations reported by Gellein et al. (2008) in off the shelf formalin, formalin may have introduced Cu, Fe, Ni, and Zn to samples in the long-term study and Cr and Ni in the short-term study. However, we also determined higher concentrations of Mn and V in formalin-fixed tissues compared to frozen tissues following long-term preservation and higher concentrations of Cd, Hg, and Se in formalin-fixed tissues compared to frozen tissues following short-term preservation. Gellein et al. (2008) did not report Se and Mn concentrations in off the shelf formalin but did report Cd (0.01 µg/L), Hg (0.07 µg/L), and V (0.01 µg/L) in low concentrations suggesting that formalin may not have been the source of contamination for these elements.

In addition to the formalin preservative itself, other sources of contamination during sample handling and processing could have occurred. In both the short-term and long-term studies, samples were not originally collected for trace element analyses. Therefore, trace metal clean procedures were likely not followed during sample collection and preservation. Renaud et al. (1995) attempted to account for sources of contamination in formalin preserved fish samples (e.g., container jars, sample tags/labels, etc.). However, the authors concluded that because many sources of contamination could not be accurately measured formalin preserved fish should not be utilized to measure trace element concentrations. Additionally, although unlikely, frozen and formalin-fixed tissue pairs utilized in the long-term study may have been taken from different parts of the body/organ which could influence trace element concentrations.

Predicting trace element concentrations in frozen tissues

Other studies have suggested that if the effects of wet preservation (e.g., formalin, ethanol) are minimal and/or consistent, fluid preserved tissues can be utilized for trace

element analyses if the effects of the preservative are properly considered. This has been the argument in favor of utilizing museum preserved fish to determine historical changes in Hg concentrations. For example, Hill et al. (2010) performed experiments to quantify the effects of fluid preservation on fish muscle Hg concentrations and found that following formalin fixation for 2 days and transference to isopropanol for 5.5 months, Hg concentrations increased 18% reaching an asymptote after 40 days. Because the increase in Hg concentration plateaued after 40 days, the authors suggested that fluid-preserved fish specimens could be used to measure Hg concentrations. The authors suggested that the observed increase in Hg concentrations may be due to lipid loss following preservation in isopropanol (Hill et al. 2010). In the present study, we did not measure tissues throughout the preservation period but rather compared the final trace element concentrations in frozen and formalin-fixed tissues to determine if concentrations in formalin-fixed tissues could be used to predict concentrations in frozen tissues.

If formalin-fixed and frozen tissue trace element concentrations differ, but there is a strong correlation between the preservation methods, it suggests that the effects of formalin are predictable. By determining the formula of the regression line between formalin-fixed tissue trace element concentrations and frozen tissue trace element concentrations, it may be possible to predict trace element concentrations in unpreserved tissues from formalin-fixed tissue trace element concentrations. In the long-term study, we determined that it may be possible to account for the leaching of As in the blubber and brain, Hg in the lung, Cd in the kidney, and Se in the kidney. In the short-term study, we determined that it may be possible to account for the leaching of Zn in the blubber, As

in the liver, and Cu in the lung. In addition, we determined it may be possible to account for contamination of Hg and Se in the liver, and Ni in the lung.

While we determined that it may be possible to account for leaching and contamination of some trace elements, it should be stressed that these results are specific to the present study. Several factors could influence these findings including the tissue collection and processing procedures, the size and surface area of the tissues, the ratio of preservative to tissue, the length of time in formalin, the type of buffer used (if any), and the batch of formalin used to fix the sample. Measuring trace element concentrations in preserved tissues, especially from museum collections, is appealing to researchers because it allows for the evaluation of temporal changes in environmental contaminant concentrations (Campbell and Drevnick, 2015). The key assumption in using preserved tissues for trace element analyses is that the preservative does not impact trace element concentrations or that its effects on trace element concentrations are consistent (Poulopoulos, 2013). Our results demonstrate that trace element concentrations are altered by formalin fixation. While our data suggests that for some trace elements the effects of formalin fixation can be accounted for, because of the many sources of variability described above, it is unlikely these relationships could be applied on a larger scale. To eliminate as many sources of variation as possible, and to aid in the interpretation of data collected from formalin-fixed tissues, it would be beneficial for research laboratories to determine their own correction factors for formalin fixation. More rigorous laboratory studies would be required to confirm these results.

Conclusions

Our results demonstrate that both short-term and long-term preservation in formalin has the potential to substantially alter tissue trace element concentrations both by leaching trace elements from tissues into the preservative and by introducing trace elements to tissues. Unless more laboratory studies are conducted which determine that certain trace elements are either not altered by formalin fixation or are altered in a predictable way that can be accounted for, we recommend that formalin preserved marine mammal tissues not be used for trace element analyses.

Table 5.1. Number of samples above the detection limit for formalin-fixed and frozen *Tursiops truncatus* tissues in the long-term study. As = arsenic; Cd = cadmium; Co = cobalt; Cr = chromium; Cu = copper; Fe = iron; Hg = mercury; Mn = manganese; Ni = nickel; Pb = lead; Se = selenium; Sn = tin; V = vanadium; Zn = zinc.

Trace Element	Preservation	Blubber	Brain	Kidney	Liver	Lung	Skin
As	Formalin	9	6	10	10	10	10
	Frozen	10	6	10	10	10	10
Cd	Formalin	8	4	7	8	9	7
	Frozen	3	4	8	7	5	2
Co	Formalin	1	0	6	4	7	1
	Frozen	5	4	10	10	8	1
Cr	Formalin	10	4	6	6	9	10
	Frozen	6	1	2	0	2	1
Cu	Formalin	9	6	10	10	10	10
	Frozen	10	6	10	10	10	10
Fe	Formalin	10	6	10	8	10	10
	Frozen	10	6	10	10	10	10
Hg	Formalin	10	6	10	10	10	10
	Frozen	10	6	10	10	10	10
Mn	Formalin	5	6	10	10	10	10
	Frozen	6	6	10	10	10	9
Ni	Formalin	8	5	7	10	9	10

	Frozen	1	1	2	1	1	0
Pb	Formalin	3	4	7	8	9	7
	Frozen	4	5	7	5	1	1
Se	Formalin	10	6	10	10	10	10
	Frozen	10	6	10	10	10	10
Sn	Formalin	10	4	6	9	8	10
	Frozen	6	4	1	1	2	1
V	Formalin	10	4	10	10	10	10
	Frozen	10	0	4	2	1	7
Zn	Formalin	10	6	10	10	10	10
	Frozen	10	6	10	10	10	10

Table 5.2. Trace element concentrations [mean \pm standard deviation; $\mu\text{g/g}$ dry wt] in frozen and formalin-fixed *Tursiops truncatus* tissues following long-term (3-7 years) preservation^a

^a Minimum and maximum concentrations are shown in parentheses

^b Detection limits for the abovementioned BDL samples were 0.006, 1.00, 0.120, and 0.012 $\mu\text{g/g}$ dry wt for Co, Cr, Ni and V, respectively

For trace element abbreviations see Table 1; BDL = below detection limit; ND = not determined due to small sample size

Trace Element	Preservation	Blubber	Brain	Kidney	Liver	Lung	Skin
As	Formalin	0.422 \pm 0.323 (0.031 - 0.950)	0.291 \pm 0.111 (0.110 - 0.439)	0.192 \pm 0.085 (0.069 - 0.320)	0.176 \pm 0.078 (0.068 - 0.271)	0.152 \pm 0.064 (0.074 - 0.255)	0.135 \pm 0.069 (0.039 - 0.207)
	Frozen	1.10 \pm 0.780 (0.158 - 2.54)	0.732 \pm 0.276 (0.265 - 1.12)	0.939 \pm 0.547 (0.172 - 1.87)	0.892 \pm 0.584 (0.249 - 1.95)	0.614 \pm 0.200 (0.300 - 0.945)	1.03 \pm 0.509 (0.238 - 1.69)
Cd	Formalin	0.172 \pm 0.232 (0.019 - 0.729)	0.177 \pm 0.143 (0.054 - 0.383)	2.06 \pm 3.55 (0.044 - 9.12)	0.272 \pm 0.348 (0.034 - 1.02)	0.342 \pm 0.461 (0.073 - 1.46)	0.549 \pm 0.928 (0.039 - 2.56)
	Frozen	0.013 \pm 0.004 (0.010 - 0.018)	0.012 \pm 0.005 (0.009 - 0.019)	5.61 \pm 11.2 (0.070 - 32.5)	1.11 \pm 1.90 (0.071 - 5.30)	0.091 \pm 0.151 (0.017 - 0.362)	0.031 \pm 0.019 (0.017 - 0.044)
Co	Formalin	0.035	BDL ^b	0.150 \pm 0.131 (0.055 - 0.390)	0.063 \pm 0.016 (0.047 - 0.078)	0.122 \pm 0.128 (0.052 - 0.410)	0.030
	Frozen	0.011 \pm 0.004 (0.007 - 0.017)	0.015 \pm 0.006 (0.010 - 0.024)	0.108 \pm 0.131 (0.008 - 0.440)	0.019 \pm 0.007 (0.007 - 0.030)	0.110 \pm 0.060 (0.016 - 0.209)	0.009
Cr	Formalin	0.352 \pm 0.768 (0.032 - 2.52)	0.113 \pm 0.052 (0.064 - 0.159)	0.461 \pm 0.798 (0.105 - 2.09)	0.224 \pm 0.200 (0.114 - 0.628)	0.197 \pm 0.124 (0.092 - 0.464)	1.06 \pm 2.32 (0.083 - 7.55)

	Frozen	0.170 ± 0.102 (0.072 - 0.304)	0.510	0.395 ± 0.324 (0.166 - 0.624)	BDL ^b	0.251 ± 0.211 (0.102 - 0.400)	0.094
Cu	Formalin	1.53 ± 1.03 (0.500 - 3.30)	10.9 ± 3.51 (6.22 - 17.1)	13.6 ± 8.47 (5.77 - 29.2)	13.7 ± 6.46 (6.52 - 25.7)	11.5 ± 6.19 (6.01 - 26.2)	3.50 ± 1.92 (1.45 - 7.50)
	Frozen	0.705 ± 0.337 (0.264 - 1.32)	12.1 ± 1.97 (8.96 - 15.1)	25.2 ± 17.3 (14.3 - 71.7)	64.7 ± 113 (14.6 - 386)	4.53 ± 1.59 (2.97 - 7.99)	2.16 ± 0.402 (1.36 - 2.76)
Fe	Formalin	55.7 ± 34.3 (14.0 - 124)	144 ± 62.5 (93.8 - 223)	330 ± 107 (192 - 555)	601 ± 466 (3.27 - 1476)	548 ± 125 (318 - 683)	142 ± 57.0 (54.0 - 248)
	Frozen	15.2 ± 14.8 (3.12 - 54.2)	114 ± 26.6 (75.1 - 152)	324 ± 112 (218 - 606)	1005 ± 542 (442 - 2085)	745 ± 334 (394 - 1468)	12.4 ± 4.87 (4.82 - 19.3)
Hg	Formalin	1.90 ± 1.47 (0.476 - 5.60)	4.79 ± 1.61 (1.90 - 6.50)	38.0 ± 45.9 (1.29 - 155)	202 ± 271 (2.48 - 683)	14.9 ± 30.0 (0.630 - 99.0)	3.07 ± 2.68 (0.435 - 10.1)
	Frozen	2.33 ± 2.45 (0.196 - 6.83)	4.55 ± 1.93 (1.56 - 7.22)	40.4 ± 49.2 (0.693 - 165)	453 ± 646 (9.93 - 2059)	17.4 ± 34.7 (0.753 - 115)	3.71 ± 2.74 (0.274 - 9.85)
Mn	Formalin	1.21 ± 1.88 (0.313 - 4.56)	3.46 ± 3.76 (0.616 - 10.5)	1.76 ± 1.07 (0.519 - 3.73)	1.33 ± 1.51 (0.123 - 5.47)	3.09 ± 2.28 (0.781 - 7.07)	1.62 ± 1.38 (0.386 - 5.13)
	Frozen	0.086 ± 0.016 (0.069 - 0.114)	1.21 ± 0.206 (0.890 - 1.44)	2.61 ± 0.684 (1.59 - 3.64)	11.1 ± 4.62 (4.09 - 17.6)	1.51 ± 2.55 (0.259 - 8.65)	0.194 ± 0.149 (0.082 - 0.541)
Ni	Formalin	0.178 ± 0.286 (0.030 - 0.877)	0.358 ± 0.321 (0.108 - 0.909)	0.134 ± 0.084 (0.030 - 0.279)	0.307 ± 0.292 (0.049 - 0.935)	0.231 ± 0.205 (0.076 - 0.725)	0.251 ± 0.250 (0.084 - 0.935)

	Frozen	0.021	0.153	0.078 ± ND (0.049 - 0.106)	0.056	0.223	BDL ^b
Pb	Formalin	0.083 ± 0.056 (0.047 - 0.148)	0.071 ± 0.023 (0.054 - 0.104)	0.122 ± 0.058 (0.052 - 0.207)	0.222 ± 0.116 (0.053 - 0.369)	0.196 ± 0.126 (0.071 - 0.449)	0.095 ± 0.051 (0.046 - 0.171)
	Frozen	0.040 ± 0.021 (0.020 - 0.068)	0.065 ± 0.085 (0.014 - 0.210)	0.084 ± 0.034 (0.054 - 0.148)	0.195 ± 0.088 (0.109 - 0.330)	0.165	0.044
Se	Formalin	1.16 ± 0.707 (0.290 - 2.63)	1.93 ± 0.660 (1.04 - 2.75)	19.1 ± 17.9 (3.50 - 64.6)	85.9 ± 117 (1.87 - 305)	7.71 ± 12.2 (1.91 - 42.1)	4.77 ± 2.60 (1.31 - 8.38)
	Frozen	2.58 ± 2.31 (0.306 - 7.44)	2.23 ± 0.563 (1.63 - 2.96)	21.9 ± 21.0 (3.47 - 76.0)	166 ± 210 (4.42 - 651)	9.05 ± 14.8 (2.02 - 50.8)	13.2 ± 7.92 (2.21 - 25.5)
Sn	Formalin	0.081 ± 0.052 (0.022 - 0.172)	0.259 ± 0.135 (0.105 - 0.380)	0.051 ± 0.016 (0.023 - 0.070)	0.084 ± 0.074 (0.022 - 0.246)	0.082 ± 0.080 (0.260 - 0.269)	0.085 ± 0.125 (0.014 - 0.423)
	Frozen	0.069 ± 0.028 (0.039 - 0.114)	0.164 ± 0.081 (0.046 - 0.227)	0.051	0.724	0.391 ± ND (0.175 - 0.607)	0.402
V	Formalin	0.077 ± 0.136 (0.016 - 0.462)	0.151 ± 0.128 (0.039 - 0.310)	0.174 ± 0.159 (0.022 - 0.505)	0.149 ± 0.180 (0.035 - 0.531)	0.159 ± 0.162 (0.037 - 0.462)	0.346 ± 0.402 (0.070 - 1.42)
	Frozen	0.022 ± 0.006 (0.017 - 0.036)	BDL ^b	0.090 ± 0.096 (0.026 - 0.232)	0.435 ± 0.214 (0.283 - 0.586)	0.313	0.021 ± 0.015 (0.009 - 0.053)
Zn	Formalin	44.2 ± 50.1 (9.59 - 178)	623 ± 701 (31.9 - 1790)	379 ± 649 (62.7 - 1925)	902 ± 1348 (62.0 - 3913)	560 ± 695 (70.3 - 1767)	155 ± 153 (35.8 - 442)

Frozen	22.5 ± 16.4	71.5 ± 10.5	109 ± 44.5	214 ± 197	87.1 ± 20.6	434 ± 133
	(4.06 - 51.9)	(58.4 - 86.7)	(73.8 - 221)	(75.8 - 758)	(57.4 - 120)	(273 - 608)

Table 5.3. P-values from the paired t-tests or Wilcoxon signed rank tests (†) comparing the effects of preservation method (formalin fixation, freezing) on *Tursiops truncatus* tissue trace element concentrations following long-term (3-7 years) preservation and the mean bias between preservation methods^a.

^aBias refers to the mean within-pair difference between formalin-fixed and frozen *T. truncatus* tissue trace element concentrations; negative values indicate that formalin-fixed samples had lower trace element concentrations than frozen samples. For trace element abbreviations see Table 1; ND = not determined due to low sample size.

Trace element	Blubber		Brain		Kidney		Liver		Lung		Skin	
	p-value	Bias										
As	<0.001	-0.780	0.002	-0.441	<0.001	-0.747	0.002	-0.715	<0.001	-0.462	<0.001	-0.893
Cd	0.215	0.340	0.128	0.208	0.031†	-4.33	0.031†	-0.812	0.063†	0.320	ND	1.65
Co	ND	ND	ND	ND	0.211	-0.013	1†	0.040	1.00†	-0.020	ND	ND
Cr	0.469	-0.038	ND	ND	ND	0.711	ND	ND	ND	0.076	ND	-0.004
Cu	0.044	0.777	0.386	-1.13	0.002†	-11.6	0.002†	-51.0	0.003	6.98	0.040	1.34
Fe	0.001	40.5	0.345	30.8	0.697	6.75	0.019	-464	0.093	-196	<0.001	130
Hg	1†	-0.432	0.457	0.241	0.132	-2.36	0.010†	-251	0.010†	-2.45	0.168	-0.638
Mn	0.125	1.68	0.438†	2.26	0.061	-0.851	0.0002	-9.82	0.091	1.58	0.002†	1.44
Ni	ND	ND	ND	0.082	ND	0.152	ND	0.160	ND	0.089	ND	ND
Pb	ND	ND	0.896	0.008	0.141	0.047	0.389	0.064	ND	0.284	ND	0.003

Se	0.027 [†]	-1.42	0.433	-0.307	0.014 [†]	-2.77	0.002 [†]	-79.6	0.064 [†]	-1.34	0.001	-8.46
Sn	0.110	0.034	0.136	0.095	ND	0.006	ND	-0.562	ND	-0.242	ND	-0.295
V	0.084 [†]	0.055	ND	ND	0.697	0.024	ND	-0.365	ND	-0.181	0.002 [†]	0.329
Zn	0.193 [†]	21.7	0.109	552	0.432 [†]	270	0.625 [†]	688	0.027 [†]	473	0.002	-279

Table 5.4. Absolute percent differences [mean \pm standard deviation] in trace element concentrations between frozen and formalin-fixed *Tursiops truncatus* tissues following long-term preservation (3-7 years)^a.

^a Minimum and maximum absolute percent differences are shown in parentheses.

For trace element abbreviations see Table 1; ND = not determined due to small sample size.

Trace Element	Blubber	Brain	Kidney	Liver	Lung	Skin
As	68.3 \pm 12.8 (45.0 - 91.9)	59.9 \pm 6.08 (49.5 - 68.3)	75.8 \pm 10.2 (54.0 - 84.9)	75.2 \pm 14.2 (44.1 - 88.7)	74.3 \pm 11.1 (51.2 - 84.0)	86.2 \pm 4.30 (78.3 - 92.5)
Cd	2976 \pm 3211 (1002 - 6682)	1966 \pm 1096 (1126 - 3206)	104 \pm 68.6 (46.2 - 255)	43.4 \pm 29.7 (11.5 - 95.2)	461 \pm 181 (302 - 681)	5187 \pm 657 (4722 - 5652)
Co	ND	ND	11.1 \pm 6.75 (4.82 - 24.0)	204 \pm 99.4 (67.3 - 293)	49.9 \pm 26.6 10.9 - 95.6	ND
Cu	126 \pm 115 (0.069 - 350)	17.5 \pm 16.5 (3.34 - 50.4)	43.4 \pm 21.4 (13.1 - 69.0)	57.2 \pm 23.3 (19.0 - 93.3)	160 \pm 95.0 (2.41 - 306)	66.7 \pm 68.5 (6.47 - 201)
Cr	42.9 \pm 28.0 (8.92 - 81.7)	ND	129 \pm 149 (24.4 - 235)	ND	204 \pm 214 (52.5 - 356)	4.54
Fe	522 \pm 690 (98.7 - 2328)	52.3 \pm 49.3 (5.67 - 127)	14.5 \pm 7.70 (0.036 - 26.2)	46.5 \pm 32.4 (5.65 - 99.4)	31.8 \pm 23.2 (5.20 - 67.8)	1110 \pm 367 (439 - 1743)
Hg	78.8 \pm 73.8 (2.58 - 186)	16.7 \pm 5.37 (9.96 - 21.7)	19.1 \pm 24.4 (6.08 - 85.7)	51.4 \pm 35.0 (1.16 - 93.0)	17.9 \pm 12.1 (2.06 - 44.0)	28.9 \pm 23.2 (2.09 - 58.6)
Mn	2293 \pm 3308 (296 - 6112)	185 \pm 261 (13.4 - 691)	41.9 \pm 28.3 (0.813 - 81.8)	85.5 \pm 20.2 (29.3 - 98.5)	499 \pm 791 (22.5 - 2627)	1016 \pm 752 (166 - 2297)

Ni	ND	53.6	268 ± 278 (71.0 - 464)	286	40.1	ND
Pb	ND	336 ± 216 (73.0 - 593)	77.6 ± 75.1 (0.672 - 186)	75.3 ± 77.1 (1.28 - 202)	172	6.43
Se	41.7 ± 24.6 (15.6 - 84.0)	38.1 ± 10.8 (22.9 - 53.3)	12.7 ± 9.47 (0.805 - 33.5)	49.9 ± 34.6 (3.16 - 95.6)	18.0 ± 6.43 (5.66 - 28.9)	58.8 ± 12.6 (40.8 - 82.9)
Sn	76.5 ± 56.2 (4.19 - 137)	77.4 ± 54.9 (7.99 - 130)	12.1	77.6	69.4 ± 19.3 (55.8 - 83.1)	73.4
V	306 ± 710 (2.73 - 2316)	ND	182 ± 192 (24.0 - 445)	81.2 ± 10.9 (73.5 - 89.0)	57.8	2619 ± 2817 (32.6 - 7362)
Zn	195 ± 297 (1.48 - 997)	739 ± 823 (34.7 - 2153)	351 ± 696 (2.05 - 1804)	505 ± 780 (2.86 - 2243)	598 ± 950 (2.28 - 2695)	62.4 ± 35.8 (7.97 - 92.3)

Table 5.5. Trace element concentrations [mean \pm standard deviation; $\mu\text{g/g}$ dry wt] in frozen and formalin-fixed *Tursiops truncatus* tissues following short-term (6 weeks) preservation^a

^a Minimum and maximum concentrations are shown in parentheses; n = 5 for all samples except Cr in formalin-fixed lung samples n = 4.
For trace element abbreviations see Table 1.

Trace Element	Preservation	Blubber	Liver	Lung
As	Formalin	1.23 \pm 0.563 (0.397 - 1.82)	0.565 \pm 0.482 (0.188 - 1.40)	0.184 \pm 0.040 (0.141 - 0.250)
	Frozen	1.73 \pm 1.01 (0.577 - 3.28)	0.920 \pm 0.570 (0.284 - 1.70)	0.435 \pm 0.127 (0.306 - 0.644)
Cd	Formalin	0.137 \pm 0.119 (0.018 - 0.305)	0.672 \pm 0.223 (0.344 - 0.878)	0.374 \pm 0.173 (0.218 - 0.642)
	Frozen	0.001 \pm 0.0005 (0.0008 - 0.002)	0.318 \pm 0.142 (0.100 - 0.474)	0.058 \pm 0.041 (0.022 - 0.127)
Co	Formalin	0.011 \pm 0.006 (0.003 - 0.018)	0.037 \pm 0.007 (0.031 - 0.047)	0.158 \pm 0.109 (0.047 - 0.310)
	Frozen	0.011 \pm 0.008 (0.003 - 0.022)	0.034 \pm 0.007 (0.025 - 0.043)	0.168 \pm 0.115 (0.044 - 0.280)
Cr	Formalin	0.173 \pm 0.107 (0.078 - 0.333)	0.267 \pm 0.143 (0.143 - 0.446)	0.444 \pm 0.029 (0.405 - 0.470)
	Frozen	0.100 \pm 0.070 (0.045 - 0.222)	0.027 \pm 0.025 (0.014 - 0.072)	0.049 \pm 0.047 (0.023 - 0.132)
Cu	Formalin	0.503 \pm 0.287 (0.179 - 0.857)	18.3 \pm 7.99 (12.5 - 32.3)	4.06 \pm 3.52 (1.23 - 9.96)
	Frozen	0.526 \pm 0.330 (0.140 - 0.895)	24.6 \pm 10.3 (15.7 - 36.0)	5.52 \pm 4.28 (2.43 - 12.8)
Fe	Formalin	16.1 \pm 7.02 (9.52 - 26.4)	609 \pm 275 (347 - 1065)	836 \pm 460 (524 - 1650)
	Frozen	17.7 \pm 8.07 (8.46 - 28.8)	599 \pm 178 (430 - 836)	874 \pm 430 (635 - 1641)
Hg	Formalin	0.362 \pm 0.198	70.3 \pm 39.7	31.3 \pm 65.1

		(0.049 - 0.574)	(14.3 - 123)	(0.507 - 148)
	Frozen	0.350 ± 0.228	48.8 ± 28.0	18.4 ± 36.8
		(0.059 - 0.602)	(9.61 - 84.0)	(0.332 - 84.2)
Mn	Formalin	0.090 ± 0.049	9.08 ± 3.65	2.24 ± 2.03
		(0.020 - 0.153)	(5.10 - 12.7)	(0.270 - 5.38)
	Frozen	0.374 ± 0.505	12.4 ± 3.18	2.17 ± 2.77
		(0.050 - 1.26)	(9.37 - 17.5)	(0.327 - 7.04)
Ni	Formalin	0.147 ± 0.099	0.220 ± 0.067	0.277 ± 0.098
		(0.059 - 0.268)	(0.124 - 0.299)	(0.146 - 0.373)
	Frozen	0.046 ± 0.037	0.153 ± 0.009	0.074 ± 0.036
		(0.008 - 0.102)	(0.054 - 0.296)	(0.030 - 0.117)
Pb	Formalin	0.010 ± 0.005	0.114 ± 0.039	0.154 ± 0.106
		(0.004 - 0.015)	(0.058 - 0.154)	(0.055 - 0.301)
	Frozen	0.011 ± 0.007	0.097 ± 0.033	0.084 ± 0.078
		(0.003 - 0.018)	(0.048 - 0.140)	(0.022 - 0.205)
Se	Formalin	1.22 ± 0.777	33.8 ± 15.8	15.4 ± 27.1
		(0.325 - 2.06)	(7.74 - 50.8)	(2.59 - 64.0)
	Frozen	1.65 ± 1.16	24.9 ± 11.4	10.7 ± 15.4
		(0.454 - 3.24)	(6.67 - 35.4)	(2.89 - 38.2)
Sn	Formalin	0.034 ± 0.022	0.210 ± 0.154	0.199 ± 0.408
		(0.019 - 0.073)	(0.067 - 0.430)	(0.011 - 0.928)
	Frozen	0.041 ± 0.028	0.169 ± 0.124	0.120 ± 0.242
		(0.019 - 0.088)	(0.056 - 0.325)	(0.009 - 0.552)
Zn	Formalin	20.8 ± 13.9	153 ± 82.9	78.1 ± 27.8
		(5.21 - 36.6)	(68.7 - 257)	(52.0 - 121)
	Frozen	28.5 ± 18.4	141 ± 73.6	72.4 ± 21.2
		(7.76 - 53.3)	(71.8 - 245)	(58.4 - 109)

Table 5.6. P-values from the paired t-tests or Wilcoxon signed rank tests ([†]) comparing the effects of preservation method (formalin fixation, freezing) on *Tursiops truncatus* tissue trace element concentrations following short-term (6 weeks) preservation and the mean bias between preservation methods^a.

^a Bias refers to the mean within-pair difference between formalin-fixed and frozen *T. truncatus* tissue trace element concentrations; negative values indicate that formalin-fixed samples had lower trace element concentrations than frozen samples; n = 5 for all samples except Cr in formalin-fixed lung samples n = 4.

For trace element abbreviations see Table 5.1.

Trace element	Blubber		Liver		Lung	
	p value	Bias	p value	Bias	p value	Bias
As	0.137	-0.503	0.033	-0.356	0.063 [†]	-0.250
Cd	0.063	0.136	0.003	0.354	0.017	0.315
Co	0.625 [†]	0.0003	0.089	0.003	0.591	-0.010
Cr	0.053	0.072	0.063	0.240	0.0001	0.416
Cu	0.639	-0.024	0.188 [†]	-6.28	0.017	-1.46
Fe	0.610	-1.56	0.930	9.98	0.471	-38.0
Hg	0.775	0.012	0.002	21.5	0.063	13.0
Mn	0.063 [†]	-0.284	0.025	-3.37	0.901	0.066
Ni	0.035	0.101	0.208	0.066	0.002	0.203
Pb	0.226	-0.001	0.214	0.016	0.063 [†]	0.071
Se	0.098	-0.436	0.026	8.96	0.813 [†]	4.72
Sn	0.317	0.071	0.063 [†]	0.041	0.063 [†]	0.079
Zn	0.045	-7.69	0.150	11.4	0.313	5.65

Table 5.7. Absolute percent differences [mean \pm standard deviation] in trace element concentrations between frozen and formalin-fixed *Tursiops truncatus* tissues following short-term preservation (6 weeks)^a.

^a Minimum and maximum absolute percent differences are shown in parentheses; n = 5 for all samples except Cr in formalin-fixed lung samples n = 4.

For trace element abbreviations see Table 5.1.

Trace Element	Blubber	Liver	Lung
As	25.0 \pm 19.0 (1.81 - 44.5)	40.6 \pm 16.3 (17.9 - 58.5)	54.8 \pm 13.9 (43.4 - 78.0)
Cd	9886 \pm 7096 (840 - 20210)	134 \pm 76.2 (69.4 - 244)	901 \pm 1103 (245 - 2860)
Co	85.2 \pm 142 (9.38 - 337)	11.2 \pm 9.48 (2.99 - 25.7)	14.5 \pm 7.10 (7.98 - 25.9)
Cu	19.6 \pm 11.1 (0.892 - 28.2)	22.2 \pm 25.1 (5.32 - 64.8)	30.7 \pm 13.5 (17.6 - 49.6)
Cr	91.3 \pm 79.3 (7.38 - 192)	1359 \pm 1002 (165 - 2602)	1508 \pm 386 (1080 - 1885)
Fe	22.6 \pm 11.6 (12.5 - 37.1)	24.9 \pm 18.6 (4.57 - 53.0)	9.62 \pm 11.4 (0.589 - 29.4)
Hg	26.1 \pm 33.6 (4.60 - 85.4)	45.9 \pm 13.0 (24.1 - 58.8)	33.3 \pm 29.8 (4.84 - 75.5)
Mn	54.7 \pm 26.8 (14.0 - 87.9)	29.1 \pm 18.6 (1.40 - 46.3)	37.7 \pm 37.6 (0.011 - 96.1)
Ni	328 \pm 319 (91.8 - 874)	113 \pm 149 (0.727 - 286)	303 \pm 97.6 (218 - 431)
Pb	24.5 \pm 8.60 (15.4 - 38.1)	23.8 \pm 19.6 (9.77 - 58.1)	149 \pm 190 (46.6 - 488)
Se	23.8 \pm 18.0 (1.07 - 45.7)	34.0 \pm 17.6 (16.0 - 56.9)	26.5 \pm 23.3 (8.07 - 67.3)
Sn	22.5 \pm 21.6 (4.34 - 59.8)	25.5 \pm 10.9 (11.3 - 39.5)	51.4 \pm 32.3 (18.1 - 96.2)
Zn	28.8 \pm 15.3	8.30 \pm 6.40	15.5 \pm 6.77

| (8.38 - 49.7) (2.97 - 18.1) (10.4 - 25.0)

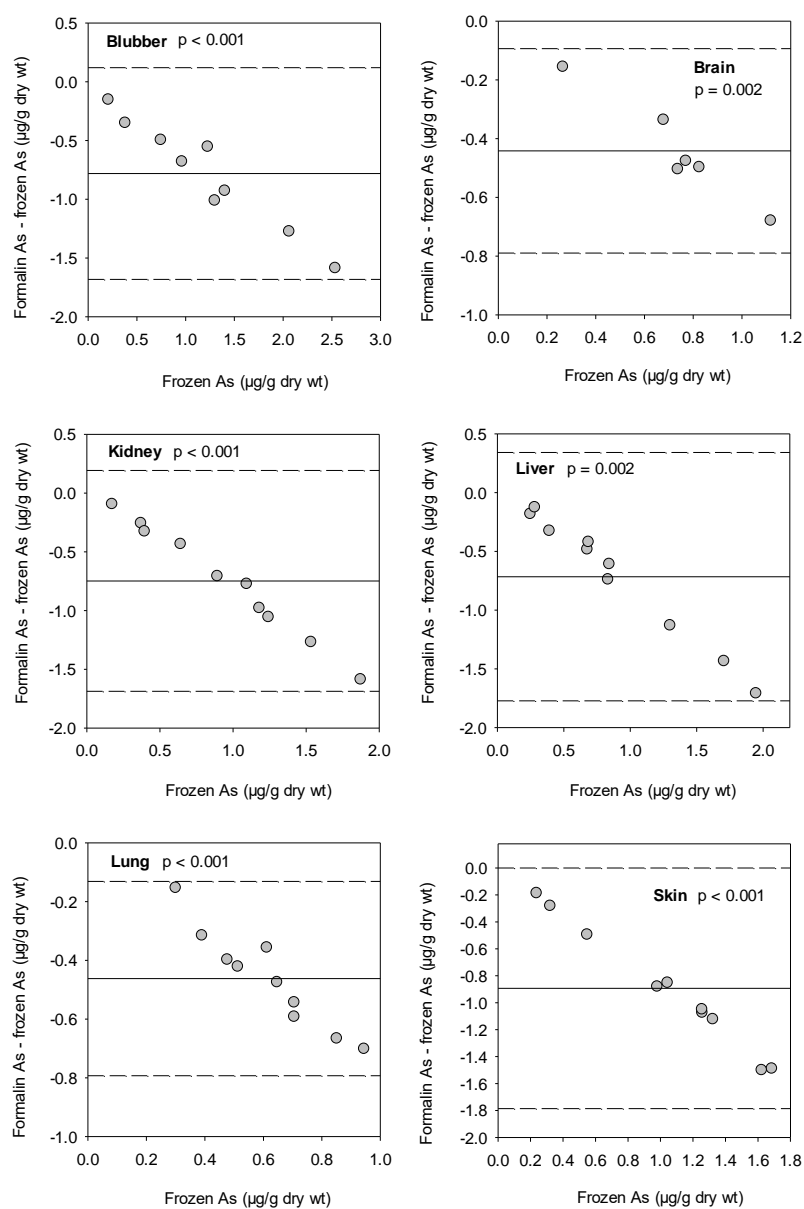


Figure 5.1. Bland-Altman plots comparing arsenic (As) concentrations ($\mu\text{g/g dry wt}$) in formalin-fixed and frozen *Tursiops truncatus* tissues following long-term preservation and p values from the paired t-tests. The solid line represents the mean within-pair difference and the dashed lines represent ± 1.96 standard deviations of the mean within-pair difference.

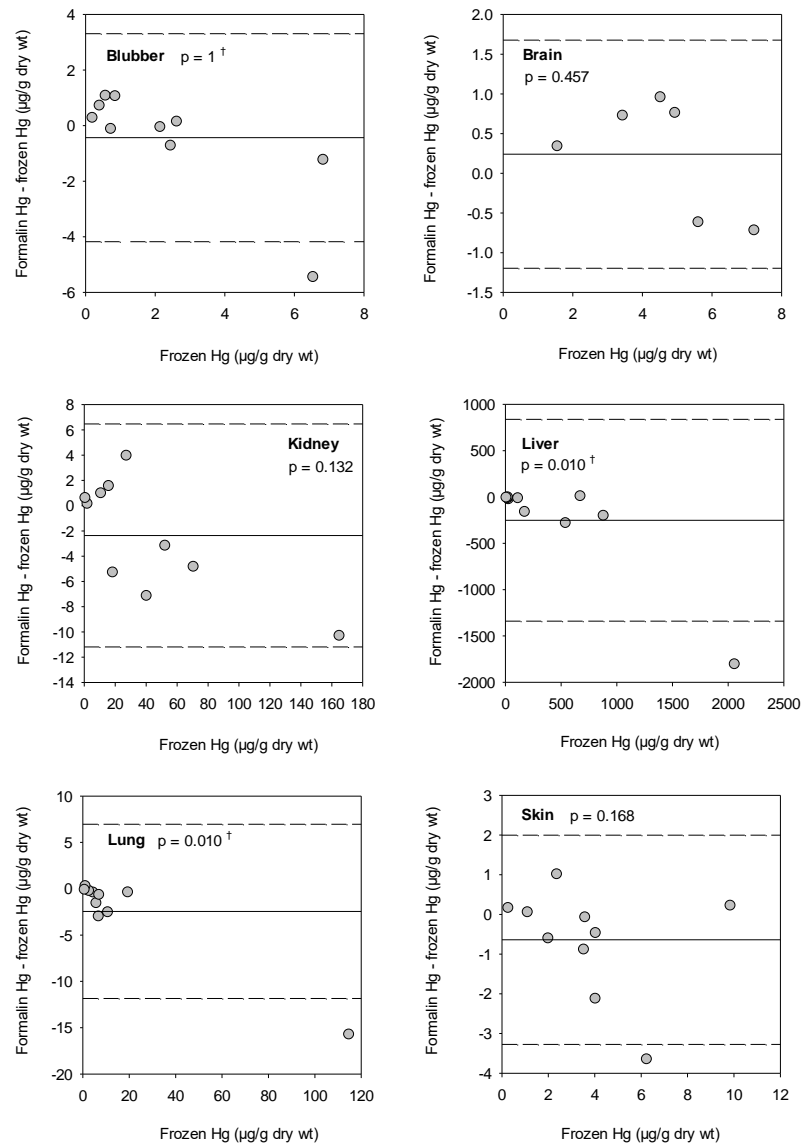


Figure 5.2. Bland-Altman plots comparing mercury (Hg) concentrations ($\mu\text{g/g}$ dry wt) in formalin-fixed and frozen *Tursiops truncatus* tissues following long-term preservation and p values from the paired t-tests or Wilcoxon signed-rank tests (\dagger). The solid line represents the mean within-pair difference and the dashed lines represent ± 1.96 standard deviations of the mean within-pair difference.

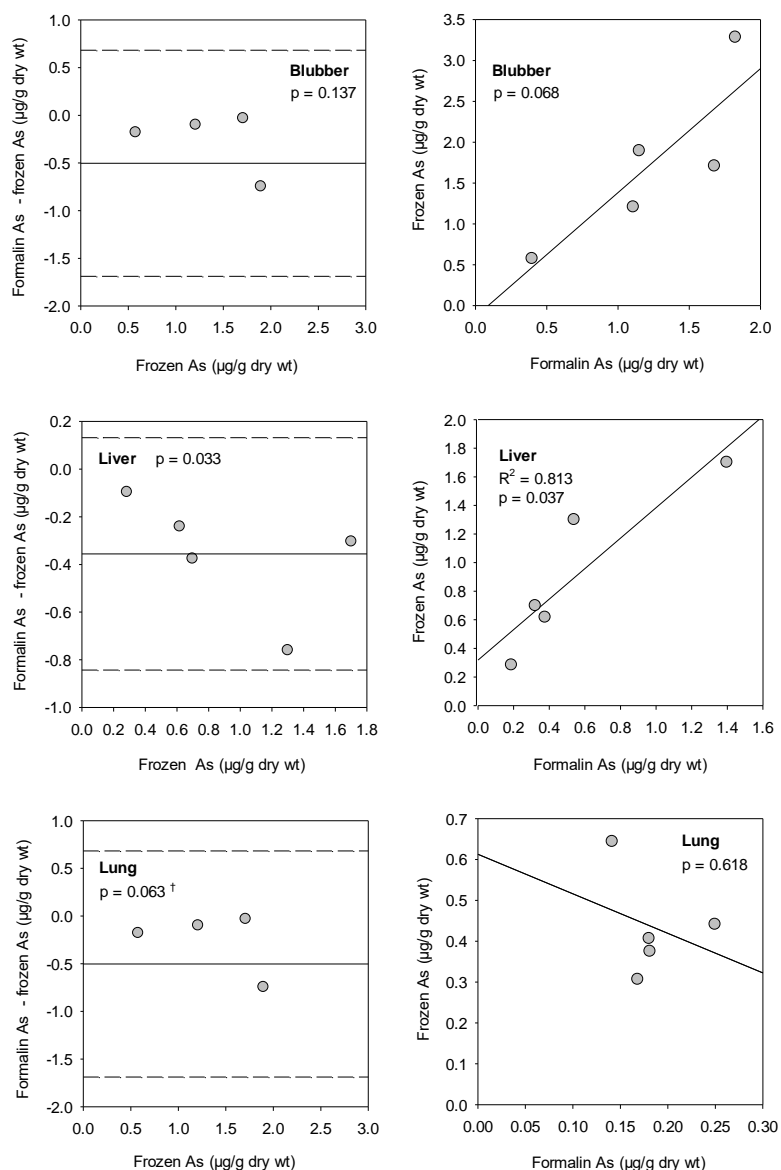


Figure 5.3. Bland-Altman plots comparing arsenic (As) concentrations ($\mu\text{g/g dry wt}$) in formalin-fixed and frozen *Tursiops truncatus* tissues following short-term preservation and p values from the paired t-tests or Wilcoxon signed-rank tests (†) (left panel) and linear regressions between As concentrations ($\mu\text{g/g dry wt}$) in formalin-fixed and frozen *T. truncatus* tissues (right panel). In the Bland-Altman plots, the solid line represents the mean within-pair difference and the dashed lines represent ± 1.96 standard deviations of the mean within-pair difference.

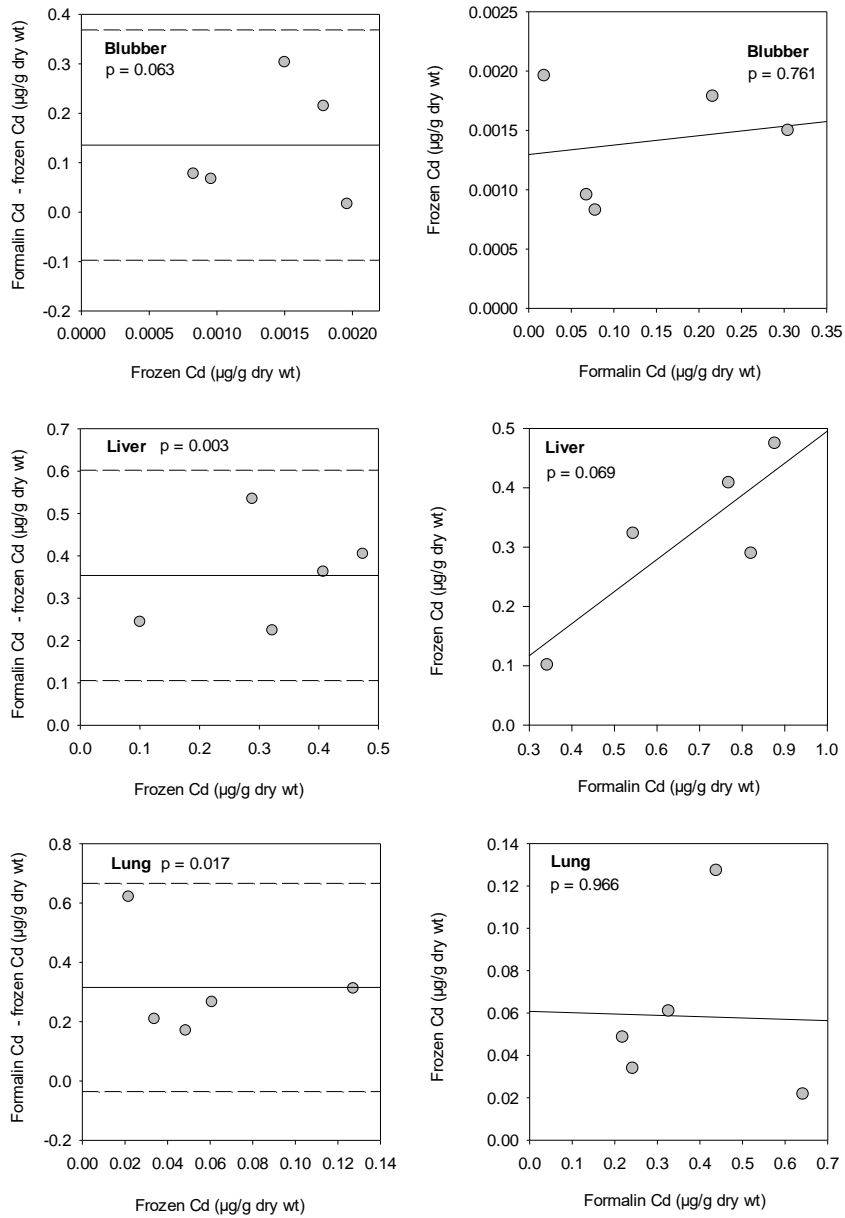


Figure 5.4. Bland-Altman plots comparing cadmium (Cd) concentrations ($\mu\text{g/g dry wt}$) in formalin-fixed and frozen *Tursiops truncatus* tissues following short-term preservation and p values from the paired t-tests (left panel) and linear regressions between Cd concentrations ($\mu\text{g/g dry wt}$) in formalin-fixed and frozen *T. truncatus* tissues (right panel). In the Bland-Altman plots, the solid line represents the mean within-pair difference and the dashed lines represent ± 1.96 standard deviations of the mean within-pair difference.

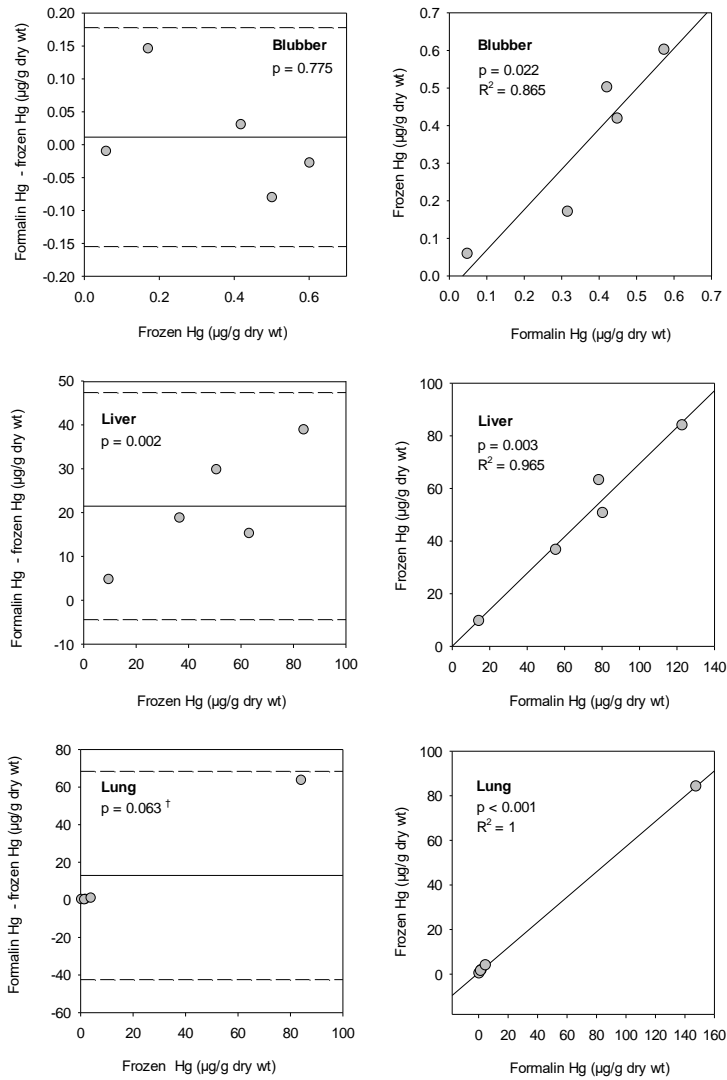


Figure 5.5. Bland-Altman plots comparing mercury (Hg) concentrations ($\mu\text{g/g}$ dry wt) in formalin-fixed and frozen *Tursiops truncatus* tissues following short-term preservation and p values from paired t-tests or Wilcoxon signed-rank tests (†) (left panel) and linear regressions between Hg concentrations ($\mu\text{g/g}$ dry wt) in formalin-fixed and frozen *T. truncatus* tissues (right panel). In the Bland-Altman plots, the solid line represents the mean within-pair difference and the dashed lines represent ± 1.96 standard deviations of the mean within-pair difference.

**VI. EXPLORING THE USE OF SEM-EDS ANALYSIS TO MEASURE THE
DISTRIBUTION OF MAJOR, MINOR, AND TRACE ELEMENTS IN
BOTTLENOSE DOLPHIN (*TURSIOPS TRUNCATUS*) TEETH**

Abstract

Dolphin teeth contain enamel, dentin, and cementum. In dentin, growth layer groups (GLG's), deposited at incremental rates (e.g., annually), are used for aging. Major, minor, and trace elements are incorporated within teeth; their distribution within teeth varies, reflecting tooth function and temporal changes in an individual's exposure. This study used a scanning electron microscope (SEM) equipped with energy dispersive X-ray spectroscopy (EDS) to determine the distribution of major (e.g., Ca, P), minor (e.g., Cl, Mg, Na), and trace elements (e.g., Cd, Hg, Pb, Zn) in teeth from 12 bottlenose dolphins (*Tursiops truncatus*). The objective was to compare elemental distributions between enamel and dentin and across GLG's. Across all dolphins and point analyses, the following elements were detected in descending weight percentage (wt %; mean \pm SE): O (40.8 ± 0.236), Ca (24.3 ± 0.182), C (14.3 ± 0.409) P (14.0 ± 0.095), Al (4.28 ± 0.295), Mg (1.89 ± 0.047), Na (0.666 ± 0.008), Cl (0.083 ± 0.003). Chlorine and Mg differed between enamel and dentin; Mg increased from the enamel towards the dentin while Cl decreased. The wt % of elements did not vary significantly across the approximate location of the GLG's. Except for Al, which may be due to backscatter from the SEM stub, we did not detect trace elements. Other trace elements, if present, are below the detection limit. Technologies with lower detection limits [e.g., laser ablation inductively

coupled plasma mass spectrometry (LA-ICP-MS)] would be required to confirm the presence and distribution of trace elements in bottlenose dolphin teeth.

Introduction

Dolphins have evolved homodont dentition; their simplified cone shaped teeth are also greater in number compared to terrestrial mammals (Myrick, 1999; Werth, 2000; Ungar, 2010; Armfield et al., 2014). The evolution of dolphin dentition is likely a consequence of their foraging behavior and the absence of mastication (Werth, 2000). Further, in contrast to most terrestrial mammals, which are diphyodonts and produce two sets of teeth (deciduous and permanent), dolphins are monophyodonts and develop only one set of teeth (Myrick, 1991; Berta et al., 2006; Wang et al., 2019). In marine mammals, teeth grow incrementally, and once incorporated within the tooth structure, major [e.g., calcium (C), phosphorous (P)], minor [e.g., chlorine (Cl) magnesium (Mg), sodium (Na)], and trace elements [e.g., cadmium (Cd), mercury (Hg), lead (Pb), zinc (Zn)] remain unaltered, thereby reflecting an organism's physiology, ambient environmental conditions, dietary intake, and exposure to trace elements including contaminants [e.g., Cd, chromium (Cr), Pb, Hg] (Evans et al., 1995; Outridge et al., 1995; Wenthrup-Bryne et al., 1997; Ando et al., 2005; Kinghorn et al., 2008; Botta et al., 2015; Zheng et al., 2018; Clark et al., 2020ab; Clark et al., 2021; De María et al., 2021). The chemical composition of teeth and the spatial distribution of major and minor elements within teeth influences tooth function (Loch et al., 2013, 2014). For example, in human teeth, a decrease in tooth hardness has been associated with increases in the weight percentage (wt %) of Na₂O and MgO and decreases in the wt % of P₂O₅ and CaO (Cuy et

al., 2002). Additionally, the pattern of trace element deposition within dolphin teeth may reflect the maternal transfer of contaminants, the timing of life-history events [e.g., Zn to estimate age at maturity], and habitat use [e.g., barium (Ba) as a proxy for salinity] (Evans et al., 1995; Botta et al., 2015; Clark et al., 2020a).

Like other mammalian teeth, dolphin teeth consist of three primary components: enamel, dentin, and cementum (Myrick, 1991; Berta et al., 2006; Ungar, 2010; Armfield et al., 2013; Loch et al., 2014). Structurally, the tooth consists of nested layers. On the exterior, the enamel and cementum line the tooth crown and root, respectively. Following the enamel and cementum is the dentin, which surrounds the central pulp cavity (Myrick et al., 1983). Development of the enamel and dentin begins while the dolphin is *in utero*, while cementum begins developing after birth (Myrick, 1991). In dolphins, dentin layers accumulate along the edges of the pulp cavity at predictable rates (e.g., annually), slowly decreasing the volume of the pulp cavity; collectively, the layers of dentin are referred to as growth layer groups (GLG's) (Myrick et al., 1983; Hohn et al., 1989; Hohn, 2009; Bowen and Northridge, 2010).

Enamel, dentin, and cementum are comprised of water, inorganic components, primarily hydroxyapatite [$\text{Ca}_{10}(\text{PO}_4)_6(\text{OH})_2$], and organic components (e.g., proteins) (Loch et al., 2013, 2014; Vallet-Regí et al., 2016; Wang et al., 2020). Although these three dental tissues have a similar mineral composition, the proportion of inorganic and organic materials varies among the tissues; notably, the enamel is the hardest of the tissues, comprised of 95-96% inorganic material, while the dentin and cementum are softer tissues comprised of a lower percentage of inorganic material (e.g., 70% inorganic material in dentin) (Simmer and Fincham, 1995; Duckworth, 2006; Goldberg et al.,

2011). Calcium and P are the main components of hydroxyapatite and, as a result, are the major elements present in teeth. The structure of hydroxyapatite includes several cationic and anionic sites; therefore, a variety of minor and trace elements can be incorporated within its chemical structure (Kang et al., 2004; Brüggmann et al., 2012). For example, cations such as Cd^{2+} , Cu^{2+} , K^+ , Mg^{2+} , Na^+ , Ni^{2+} , Pb^{2+} , or Zn^{2+} may substitute for Ca^{2+} , while anions such as CO_3^{2-} and SiO_4^{4-} , or Cl^- and F^- may replace PO_4^{3-} and OH^- , respectively (Curzon and Featherstone, 1983; Dorozhkin and Epple, 2002; Kang et al., 2004; Yasukawa et al., 2007; Rautray et al., 2010; Brüggmann et al., 2012; de Dios Teruel et al., 2015). In addition to being incorporated within the mineral structure itself, elements (e.g., Zn) associated with macromolecules on the surface of the crystalline lattice may become trapped as new mineral layers are deposited (Stock et al., 2017). In marine mammals, more than 20 elements have been reported in dental tissues including Ba, carbon (C), Ca, Cd, Cl, copper (Cu), Cr, cobalt (Co), fluorine (F), iron (Fe), Pb, Mg, Hg, P, selenium (Se), Na, strontium (Sr), vanadium (V), and Z (Cruwys et al., 1994; Evans et al., 1995; Ando et al., 2005; Ando-Mizobata et al., 2006; Kinghorn et al., 2008; Loch et al., 2014; Murphy et al., 2014; Botta et al., 2015; Nganvongpanit et al., 2017; Zheng et al., 2018; Clark et al., 2020ab; Clark et al., 2021; De María et al., 2021).

To determine the elemental composition within the tooth structure, several *in situ* analytical methods are currently available. Some techniques involve the use of electron or proton microprobes with X-ray emission detectors, such as scanning electron microscopes (SEM) equipped with energy dispersive X-ray detection (EDS) and particle-induced X-ray fluorescence (PIXE), respectively (Cruwys et al., 1994; Ando-Mizobata et al., 2006; Loch et al., 2014; Murphy et al., 2014). These techniques are advantageous

because they require little sample preparation and have the spatial resolution necessary to measure the concentration or wt % of elements within GLG's. Further, for studies with methodologies that do not require tooth sectioning or studies that utilize teeth that have been previously sectioned, the methods are non-destructive. However, they often lack the sensitivity to detect elements present at low concentrations, although technologies have improved and detection limits can be optimized with proper sample preparation and analytical settings (Cáceres-Saez et al., 2016; Sforza and Lugli, 2017; Ellingham et al., 2018; Wang et al., 2020). An alternative approach combines the use of laser ablation and inductively coupled plasma mass spectrometry (LA-ICP-MS), which allows for fine-scale spatial resolution (e.g., tens of microns) and high levels of sensitivity (< 1 ppm) but is destructive as it requires ablating the surface of the sample (Cáceres-Saez et al., 2016; Sforza and Lugli, 2017).

In this study, we used SEM-EDS analysis to explore the distribution of major, minor, and trace elements within teeth from twelve bottlenose dolphins (*Tursiops truncatus*) that stranded along the northern Texas coast in Galveston County between 1987 and 2014. The primary objectives were to explore whether the distribution of major, minor, and trace elements in dolphin teeth 1) differed between the enamel and pre-natal dentin and 2) varied across the dentin GLG's within individuals, which may reflect physiological changes and exposure to major, minor, and trace elements over time. Finally, although our sample size was limited, we sought to qualitatively assess multi-decadal temporal trends in the wt % of trace elements, particularly those of anthropogenic origin (e.g., Cd, Hg, Pb).

Methods

Teeth collection and preservation

We analyzed teeth from six male and six female bottlenose dolphins that stranded between 1987 and 2014 in Galveston County, TX (Table 6.1). We preferentially chose individuals with straight-line body lengths between 221 cm and 245 cm. In doing so, we aimed to study dolphins that were at least five years old so we could analyze dolphins that had several GLG's but had not yet reached their asymptotic body length (McCormack et al., 2020). In older dolphins, GLG's become increasingly irregular and can be challenging to decipher (Myrick et al., 1983). Furthermore, in some cases, the pulp cavity may become occluded. If this occurs, dentin layers no longer accumulate; therefore, if a dolphin lived beyond the time of pulp occlusion, a complete dentin record would not be available (Myrick et al., 1983; Myrick, 1991).

Teeth were extracted from the left mandible of dead stranded bottlenose dolphins using an elevator to loosen the gum and connective tissue, and for most dolphins, an extractor was used to lift the tooth free. For most samples, tooth number eight from the proximal end of the mandible and several surrounding teeth were collected. In some cases, a section of the mandible with teeth still intact was cut from the carcass and frozen for subsequent processing and extraction. If teeth were not available from the left mandible, they were extracted from the right mandible. Teeth were either fixed in 10% neutral buffered formalin or stored at -20°C. A large-scale cleaning/preparation project was undertaken in 2017 wherein teeth were removed from formalin prior to preparation. Therefore, some teeth may have been stored in formalin for several decades before 2017; however, no records were kept for which teeth were frozen and which teeth were stored

in formalin. In 2017, formalin-fixed teeth were removed from solution and thoroughly rinsed in running tap water. Water maceration was performed on all teeth with attached soft tissue, using separate containers for each dolphin. Any soft tissue that did not detach after soaking was gently brushed away. Teeth were then rinsed and air-dried in a temperature-controlled room and stored in individually labeled Whirl-Pak bags (Nasco; Fort Atkinson, WI) at room temperature. Since a detailed storage history for the teeth was not available, it was not possible to explore the influence of preservation methods on major, minor, and trace elements. Despite disparate storage conditions, we utilized all teeth for both age estimation and SEM-EDS analysis. Formalin preservation may influence tooth elemental composition; however, to the best of our knowledge there have been no studies that investigated the effect of formalin fixation on elemental concentrations in teeth.

Teeth sectioning and age estimation

Teeth were initially sectioned down the center mid-line of the longitudinal buccal-lingual axis. One half of the tooth was used for SEM-EDS analysis, and the other half was prepared for sectioning for age determination using standard procedures (Myrick et al., 1983; Hohn et al., 1989). Teeth for age determination were fixed in 10% neutral buffered formalin for 48 hours, rinsed in water, and dried before sectioning. Slabs were cut off the longitudinal buccal-lingual axis of each tooth using a diamond wafer blade mounted on a Buehler Isomet low-speed saw (Emerson Industrial Automation, Lake Bluff, IL). The slabs were continuously rinsed in tap water for approximately 6 hours and then decalcified in RDO (rapid decalcifying agent of acids; Apex Engineering Products Corporation, Aurora, IL) for 6-12 hours based on the thickness of the resulting center slab

remaining (1-2 mm). The slabs were continuously rinsed overnight and thin-sectioned on a Leica SM2000R sledge microtome (Leica, Inc., Nussloch, Germany) attached to a Physitemp freezing stage (Physitemp, Inc., Clifton, New Jersey). Thin sections (25 μm thick) were stained in Mayer's hematoxylin, blued for 30 seconds in a weak ammonia solution, dried on a slide, and mounted in 100% glycerin. All sections were read three times by the same reader (Wayne McFee) using a Nikon SMZ1500 stereomicroscope (Nikon Instruments, Inc., Lewisville, Texas); at least one week elapsed between readings to eliminate bias. Teeth were aged based on Hohn et al. (1989); if two of the three readings were the same, this was used as the age estimate, whereas if differences between readings were >2 GLG's, a fourth reading was made. Age estimates >1 GLG were rounded to 0.50 GLG. Most teeth >5 GLG's were estimated to the last GLG.

SEM-EDS analysis

Before SEM-EDS analysis, teeth were rinsed with Milli-Q water (Millipore, Burlington, MA), placed in trace metal clean 50 ml plastic tubes, and ultrasonically cleaned in 95% ethanol for 5 minutes. Teeth were then triple rinsed with Milli-Q water, placed in trace metal clean 15 ml plastic tubes, and air-dried in a clean fume hood for 48 hours. Two analyses on each tooth were performed using an SEM (JSM-6010 PLUS/LA; JEOL USA Inc., Peabody, MA) equipped with EDS at Texas State University. The SEM produces images by scanning the sample with a focused electron beam; the incident electrons interact with the sample, resulting in the production of secondary electrons, backscattered electrons, and characteristic x-rays. Backscattered electrons reflect the composition of the sample, and when examined using an SEM in backscattered electron (BSE) imaging mode, color variation in the sample is indicative of variation in chemical

composition (Nasrazadani and Hassani, 2016). For example, in BSE imaging mode, the enamel, which is more heavily mineralized compared to dentin, appears as a bright band (Cruwys et al., 1994; Loch et al., 2014). Characteristic x-rays are generated when the high-energy electron beam ejects an electron from its shell and an electron from a higher energy state transitions to a lower energy state to fill the space (Wolfgong, 2016). This transition releases characteristic x-rays that are specific to individual elements. Energy dispersive x-ray detectors are often used in conjunction with an SEM to convert characteristic x-rays to electrical voltages to qualitatively and semi-quantitatively describe the distribution of elements in calcified tissues (Cruwys et al., 1994; Loch et al., 2014; Cáceres-Saez et al., 2016; Wang et al., 2020). Using SEM-EDS, qualitative and semi-quantitative elemental information at an individual point (point analyses) and across an area (elemental maps) can be obtained, reporting detected elements in wt % or atomic % (at %); when coupled with BSE imagery, one can begin to understand the elemental distribution across the sample.

In the first analysis, selective point analysis on three points on the enamel (point 1 = outer enamel, point 2 = mid-enamel, and point 3 = inner enamel) and two points on the pre-natal dentin [point 4 = pre-natal dentin near the enamel-pre-natal dentin junction (EDJ) and point 5 = inner pre-natal dentin] were performed, following the general methodology outlined by Loch et al. (2014) for *in situ* analysis using wavelength dispersive x-ray spectroscopy (WDXS or WDS) (Figure 6.1). The procedure was repeated for two additional transects, approximately 50 μm apart. Combining the data from the three transects, the mean and standard error (SE) wt % of each element for each point was calculated. A 20 kV accelerating voltage and a working distance of between

10-12 mm was used. In each tooth, point analysis was performed approximately halfway between the tooth neck and the top of the tooth crown. In a subset of teeth ($n = 7$), elemental maps were generated to visualize the distribution of elements across the enamel and pre-natal dentin.

In the second analysis, the potential differences in the wt % of elements across the GLG's were explored. Point analysis began halfway between the tooth neck and the bottom of the tooth root. The goal was to obtain measurements from the GLG's; however, GLG's were not visible. Therefore, the approximate location of the GLG's was identified by referencing the images from the thin-crossed sectioned teeth used for aging. Starting from the exterior of the tooth and moving toward the interior, point analyses were performed approximately every 300-350 μm until reaching the pulp cavity (Figure 6.2). When the pulp cavity was not visible, points were analyzed across half of the tooth width. On average, across all teeth, 7 points per transect were measured; the process was repeated for two more transects approximately 100 μm apart. The mean and SE wt % of the elements detected at each point were calculated. The analytical setting used a 20 kV accelerating voltage, 100 μm aperture size, and a working distance between 9-12 mm. Again, for a subset of the samples ($n = 2$), elemental maps of the area of interest were generated to qualitatively assess the distribution of elements across the GLG's.

Statistical analysis

For both analyses (enamel vs. pre-natal dentin and GLG's analysis), a repeated-measures linear mixed effects analysis of variance (ANOVA) and Tukey's post-hoc test was used to explore the potential spatial differences in elemental distribution within the teeth. The repeated-measures design was used because we measured several points on

each tooth. In all models, the response variable was the element measured, the fixed effect was the point location [enamel vs. pre-natal dentin (points 1-5) and GLG's analysis (points 1-7)], and the random effect was the individual dolphin (sample). Models with varying intercepts and varying intercepts and slopes were considered, and the model that best fit the data was selected. Residual plots were explored for violations of normality and homoscedasticity, and data were natural log-transformed when necessary. The level of significance was set at $\alpha = 0.05$, and the analysis was performed in R version 4.0.2 using the following packages: lme4 and eemans (Bates et al., 2015; Length, 2020; R Core Team, 2020). If individual elements were not detected at all points on the tooth, a value of one-half the detection limit (0.05 wt %) was applied to points where that element was not detected for descriptive and inferential statistics (Nasrazadani and Hassani, 2016; Adams and Engel, 2014).

Results

For ten dolphins, age estimates ranged between 4.5 to 18 years (Table 6.1). Hypermineralization precluded precise age estimates for two individuals; these individuals were estimated to be >11 and >16 years old, respectively (Table 6.1). Tables 6.2 and 6.3 provide a summary of the major, minor, and trace elements at each point measurement for all dolphins combined. Data pertaining to each individual dolphin, including the mean and SE calculations, for each point measurement are provided in Supplementary Tables S6.1-S6.6.

Using SEM-EDS, we first compared the distribution of elements across the enamel and pre-natal dentin. The mean \pm SE wt % for all point measurements and

dolphins combined, were as follows: O (39.6 ± 0.373), Ca (25.0 ± 0.229), P (14.6 ± 0.091), C (10.4 ± 0.287), Al (8.29 ± 0.507), Mg (1.39 ± 0.070), Na (0.639 ± 0.013), and Cl (0.130 ± 0.007). For all elements, there were significant differences in wt % values among the five points in the enamel and pre-natal dentin (Table 6.2; Figure 6.3). For all models except for Mg, the random intercept model fit the data better than the random intercept and slope model. Oxygen, Ca, and P were measured in lower wt % values in the outer enamel (point 1) compared to the other points (points 2-5). Aluminum was measured in the highest wt % in the outer enamel (point 1) and progressively decreased toward the inner pre-natal dentin (Figure 6.3 and 6.4). For C, wt % values were higher in the outer enamel and inner pre-natal dentin compared to points in the inner and mid-enamel. The wt % of Mg was lowest in the outer enamel and increased towards the inner pre-natal dentin (Figure 6.3). On average, the wt % values of Mg were 2.21 and 0.84 in the enamel (points 1, 2, and 3) and pre-natal dentin (points 4 and 5), respectively. Sodium increased from the outer enamel to the EDJ and then decreased in the inner pre-natal dentin (Figure 6.3); on average, the wt % values of Na in the enamel and pre-natal dentin were 0.593 and 0.703, respectively. Finally, Cl was present in the greatest wt % in the outer enamel (point 1); while Cl was also detected at lower wt % values in the mid-enamel and inner enamel, it was not observed in the pre-natal dentin (points 4 and 5). Elemental maps showed differences in the distribution of elements between the enamel and pre-natal dentin (Figure 6.4).

In the second analysis using SEM-EDS, we performed point analyses at seven points approximating where GLG's would occur; a summary of the major, minor, and trace elements at each point measurement for all dolphins combined is shown in

Table 6.3. The mean \pm SE wt % for all point measurements and dolphins combined, were as follows: O (41.6 ± 0.295), Ca (23.8 ± 0.260), C (16.9 ± 0.608), P (13.5 ± 0.141), Mg (2.24 ± 0.053) Al (1.43 ± 0.215), and Na (0.698 ± 0.011). For all elements, the intercepts model was a better fit than the intercepts and slope model. Except for O, there were significant differences in the wt % values of the elements across the seven points (Figure 6.5). The most common difference was between the tooth edge (point 1) and the interior points (points 2-7). At the tooth edge (point 1), Ca, P, Mg, and Na were measured in lower wt % values than the interior points (points 2-7). In contrast, C and Al were present at higher wt % values closest to the tooth edge (point 1) than in the interior points (points 2-7). Visually the only differences that could be determined in the elemental maps were between the dentin and pulp cavity (Figure 6.6).

Discussion

Using SEM-EDS, we were able to visualize the microstructure of dolphin teeth, distinguishing between the enamel and pre-natal dentin in the tooth crown, and explore the variation in major (C, Ca, O, and P) and minor elements (Cl, Mg, Na) between the enamel and pre-natal dentin. Except for Al, no trace elements were detected. Although we could not visually distinguish GLG's using the SEM, we made use of the images from tooth sections used for aging to approximate the location of GLG's and performed EDS analysis to investigate the potential variation in major, minor, and trace elements across the GLG's. Except for the point closest to the tooth edge, the wt % values of C, Ca, P, O, Mg, and Na did not vary substantially across the dentin transect. Except for Al, we did not observe any other trace elements; therefore, we could not examine how contaminants

changed over time within the lifespan of an individual or temporally across the decades among individuals. While technologies with lower detection limits (e.g., LA-ICP-MS) may be required to explore the presence and distribution of trace elements in bottlenose dolphin teeth, the information provided in the current study will be valuable to other analyses such as LA-ICP-MS that rely on Ca as an internal standard (Limbeck et al., 2015; Clark et al., 2020a,b, Clark et al., 2021). Further, measuring some elements reported in this study (e.g., O, P, C, and Cl) is either impossible or very challenging using LA-ICP-MS; therefore, SEM-EDS can serve as a complementary analysis (Perkin Elmer, 2011).

The major elements detected in the dolphin teeth were C, Ca, P, and O. Calcium and P are the primary components of hydroxyapatite; across all samples, the mean \pm SE wt % values of C and P were 24.2 ± 0.228 and 14.6 ± 0.091 , respectively. Murphy et al. [38] reported similar wt % values for Ca (24.9) and P (11.2) in bottlenose dolphin dentin, also measured by SEM-EDS. However, our values were lower than those reported by Loch et al. (2014); in analyzing the elemental distribution in the enamel and pre-natal dentin from ten dolphin species using WDX, Loch et al. (2014) reported wt % values of 46.9 and 36.2 for Ca and P, respectively for the single bottlenose dolphin tooth analyzed. Unlike Loch et al. (2014) and Brüggmann et al. (2012), which reported the element concentrations in the enamel and dentin of hippopotamid teeth, we did not determine that Ca or P were consistently present in greater wt % values in the enamel compared to the pre-natal dentin. Brüggmann et al. (2012) explain that the higher concentration of Ca and P in the enamel is a result of the reduced porosity and increased mineralization of the enamel compared to the dentin. Since the dentin has a higher percentage of organic

components than enamel, when comparing the enamel and pre-natal dentin, we expected to find a higher weight percentage of the O and C in the dentin, which are common elements found in proteins (Wang et al., 2020). Oxygen followed this general pattern, but C did not. Other major elements of proteins (e.g., collagens), such as nitrogen (N) and hydrogen (H), were not detected. Hydrogen is too light to be detected using SEM-EDS, and N generally produces too weak of a signal to be detected (Wang et al., 2020). In the GLG's analysis, an additional concern arose regarding the point closest to the tooth edge. In BSE imaging mode, the cementum was indistinguishable from the dentin; consequently, the points closest to the tooth edge may have been cementum and not dentin. It is uncertain how wide the cementum layer was in our samples; we also could not find an average cementum width in the literature for bottlenose dolphins.

Overall, except for points analyzed closest to the tooth edge, the major elements (C, Ca, O, and P) did not vary significantly across the tooth, making them good candidates for internal standards in future LA-ICP-MS analyses. In contrast to SEM-EDS methodologies, which are standardless, quantification in LA-ICP-MS involves external calibration using a standard reference material (SRM) (e.g., NIST 612 glass or NIST 1486 bone meal for teeth samples). In addition to external SRMs, signals are frequently normalized to an internal standard (e.g., Ca for teeth), and studies often assume homogeneous distributions of the internal standard (Perkin Elmer, 2011; Newbury and Ritchie, 2013; Limbeck et al., 2015) The information provided here can help provide baseline information with respect to the wt % and distribution of major elements in bottlenose dolphin teeth. The consistent distribution of major elements across teeth

supports their use as internal standards for quantification in LA-ICP-MS along with external SRMs.

The EDJ is a transition phase for major and minor elements. Cations and anions (e.g., Cl^- , Mg^{2+} , and Na^+) may also be incorporated into the hydroxyapatite structure of the enamel or dentin during the pre-eruptive period (Curzon and Featherstone, 1983). In the case of the enamel, they may also be incorporated post-eruption on the surface of the enamel (up to 150 μm depth) from the surrounding saliva [55-56]. In the present study, we observed the same trends in the variation of Cl and Mg across the enamel and pre-natal dentin as was previously reported in dolphin (Loch et al., 2014), hippopotamus (Brüggmann et al., 2012), and human teeth (Wang et al., 2020). Chlorine decreased from the enamel towards the pre-natal dentin, while Mg increased from the enamel towards the pre-natal dentin. Although the trends were not consistent across individual dolphins, on average, we found that Na followed a similar "umbrella" trend as was observed by Loch et al. (2014), in which Na initially increased from the outer enamel towards the inner enamel and then decreased moving further towards the inner pre-natal dentin. Throughout the secretory and maturation stages of enamel formation, elements enter the enamel fluid; as the bioapatite crystallizes, the enamel becomes depleted in Mg and Na and enriched in Cl. Therefore, Mg and Na are present in the greatest wt % near the EDJ, while Cl is present in the greatest wt % in the outer enamel (Brüggmann et al., 2012). The incorporation of minor elements within the tooth structure can alter the tooth function. More research is required to fully understand how changes in minor elements alter the chemical structure and functionality of dental tissues. However, a previous study focused on human, bovine, porcine, and ovine teeth suggested that the incorporation of Mg^{2+}

helps to regulate hydroxyapatite crystallization (de Dios Teruel et al., 2015). For example, Mg is present in higher concentrations in the dentin and the inhibition of crystallization may explain why crystals are smaller and less frequently observed in the dentin compared to the enamel (de Dios Teruel et al., 2015; Wang et al., 2020).

During the mineralization phase of tooth development, trace elements can be incorporated within the crystalline apatite (Reitznerová et al., 2000; Ando-Mizobata et al., 2006). Previous studies have used trace element concentration in marine mammal teeth to identify the timing of life-history events, identify the maternal transfer of contaminants, explore habitat utilization, and assess the spatial and temporal changes in environmental trace element concentrations, particularly those of anthropogenic origin (Outridge et al., 2002; Botta et al., 2015; Clark et al., 2020ab, Clark et al., 2021). Except for Al, we did not observe trace elements [e.g., Cd, Cu, Hg, Pb, Zn], which have been previously reported in marine mammal teeth (Evans et al., 1995; Ando et al., 2005; Ando-Mizobata et al., 2006; Kinghorn et al., 2008; Murphy et al., 2014; Botta et al., 2015; Nganvongpanit et al., 2017; Zheng et al., 2018; Clark et al., 2020ab; Clark et al., 2021; De María et al., 2021). Given that Al decreased in wt % moving from tooth exterior towards the tooth interior, and Al is the main component of the SEM stub, we suspect that the Al detected was related to the SEM stub and not the tooth itself. Caceres-Saez et al. (2016), measuring the major, minor, and trace elements in Commerson's dolphin (*Cephalorhynchus c. commersonii*) and Franciscana dolphin (*Pontoporia blainvillei*) bone samples using SEM-EDS also detected Al and came to a similar conclusion. Our results indicate either 1) the abovementioned trace elements were not present in our samples, or 2) they were present at concentrations below the detection

limit. Based on the findings of other studies, many trace elements that we expected to find (e.g., Cu, Cd, Hg, Zn) but did not detect are likely present in the teeth but at wt % values below the detection limit of EDS (approximately 0.1 wt %) (Nasrazadani and Hassani, 2016).

Low sensitivity due to high elemental detection limits is a significant disadvantage of using SEM-EDS technology to measure major, minor, and trace elements in dolphin teeth. Detections can be optimized if the sample is properly prepared, and the scan parameters, such as the vacuum conditions, accelerating voltage, spot size, and working distance are adjusted (Wang et al., 2020). Ideally, the surface of the sample should be smooth and flat (Newbury and Ritchie, 2013). To minimize contamination, we did not polish our samples; however, variation in the sample topography may have affected the path of the x-rays exiting the surface and negatively influenced our ability to detect elements (Newbury and Ritchie, 2013; Wang et al., 2020). Non-conductive samples are generally coated with carbon or gold-palladium (Au-Pd) to reduce surface charging. After performing preliminary scans, we determined that there were no issues with surface charging. Therefore, to avoid contamination, we did not coat the sample in carbon or Au-Pd; however, the surface coating could have potentially increased the signal strength and improved the signal-to-noise ratio (Wang et al., 2020). Because teeth are non-homogenous samples, it can be misleading to measure only one point, as some areas may have a greater wt % of elements than others. We attempted to overcome this limitation by taking measurements along several transects and averaging results. To maximize the detection of characteristic x-rays, the accelerating voltage must be 2- to 3-times higher than the energy required to eject an electron from its shell; in some cases, 20

kV may not have been great enough to optimize detections but using a higher voltage was not possible while working in low vacuum mode, which is required for any samples that have not been dehydrated. Further, the working distance, or the distance between the sample and the final piece of the lens, must be adjusted so that the angle of the outgoing characteristic x-rays intersects the detection system. Finally, overlapping peaks can complicate interpretation and as concentrations of an element decrease, the ability to correctly assign elemental peaks decreases due to reduced counts of associated characteristic x-rays (Newbury and Ritchie, 2013) Although SEM-EDS has several disadvantages, the technique provides a relatively quick method for elemental analysis; in addition, when study methodologies do not require tooth sectioning or utilize teeth that have previously been sectioned, the method is non-destructive, making it appropriate for museum specimens (Cruwys et al., 1994; Cáceres-Saez et al., 2016; Nasrazadani and Hassani, 2016; Wolfgang, 2016). To understand how trace element deposition in bottlenose dolphin teeth may be used to create a timeline of life history events and exposure to trace elements, particularly pollutants (e.g., Cd, Hg, Pb), additional research is required using technologies with lower detection limits (e.g., LA-ICP-MS).

Table 6.1. Stranding year, straight-line body length, sex, and estimated age of bottlenose dolphins used in the study.

Sample ID	Stranding year	Length (cm)	Sex	Estimated age (years)
GA 159	1987	235	Female	>11 ^a
GA 260	1989	233	Female	8
GA 277	1989	245	Male	>16 ^a
GA 279	1989	244	Male	8
GA 345	1990	225	Female	4.5
GA 710	1995	238	Male	18
GA 737	1996	222	Male	8
GA 830	1996	237	Female	16
GA 1599	2009	221	Female	11
GA 1603	2009	241	Male	11
GA 1755	2012	224	Male	9
GA 1856	2014	226	Female	10

^ahypermineralization near the pulp cavity precluded a more precise age estimate

Table 6.2 Weight percentage (wt %) of major, minor, and trace elements across the enamel and pre-natal dentin (PND) for all dolphins combined (mean \pm standard deviation; range of wt % in parenthesis) EDJ = enamel dentin junction.

Element	Outer enamel Point 1	Mid-enamel Point 2	Inner enamel Point 3	PND near EDJ Point 4	PND Point 5
<i>Major elements</i>					
C	11.6 \pm 6.40 (5.92 - 33.6)	8.69 \pm 2.28 (6.08 - 16.1)	9.30 \pm 2.84 (6.16 - 20.4)	10.2 \pm 2.21 (6.86 - 14.1)	12.0 \pm 2.48 (8.70 - 19.3)
Ca	23.7 \pm 4.91 (16.1 - 37.7)	25.7 \pm 3.19 (19.2 - 36.3)	25.5 \pm 2.03 (21.5 - 29.4)	25.0 \pm 1.73 (22.1 - 27.8)	26.0 \pm 1.74 (21.8 - 28.0)
O	34.1 \pm 5.80 (20.5 - 44.2)	38.9 \pm 5.02 (25.4 - 47.3)	41.4 \pm 3.05 (32.5 - 46.4)	41.7 \pm 2.53 (36.9 - 46.1)	41.5 \pm 2.56 (33.4 - 45.4)
P	13.44 \pm 1.83 (9.50 - 16.6)	15.0 \pm 0.939 (12.7 - 17.1)	15.1 \pm 0.803 (13.1 - 16.4)	14.8 \pm 0.737 (13.1 - 15.8)	14.8 \pm 0.504 (14.0 - 15.8)
<i>Minor elements</i>					
Cl	0.238 \pm 0.057 (0.110 - 0.390)	0.208 \pm 0.042 (0.130 - 0.340)	0.106 \pm 0.050 (0.050 - 0.170)	0.053 \pm 0.011 (0.050 - 0.100)	0.050 \pm 0.00 (0.050 - 0.050)
Na	0.477 \pm 0.153 (0.230 - 1.06)	0.598 \pm 0.110 (0.400 - 0.840)	0.705 \pm 0.108 (0.540 - 0.980)	0.742 \pm 0.162 (0.570 - 1.21)	0.668 \pm 0.174 (0.550 - 1.39)
Mg	0.298 \pm 0.394 (0.050 - 1.06)	0.734 \pm 0.623 (0.050 - 1.80)	1.42 \pm 0.414 (0.050 - 2.07)	1.86 \pm 0.362 (1.27 - 2.70)	2.57 \pm 0.384 (1.77 - 3.40)
<i>Trace elements</i>					
Al	16.2 \pm 8.45 (0.83 - 30.67)	9.80 \pm 5.65 (0.480 - 20.1)	6.50 \pm 3.80 (0.460 - 13.3)	5.79 \pm 3.35 (0.420 - 11.1)	3.52 \pm 1.67 (0.360 - 6.54)

6.3. Weight percentage (wt %) of major, minor, and trace elements at seven points across the approximate location of growth layers groups (GLG's) moving from point 1 (edge of tooth) towards the pulp cavity for all dolphins combined (mean \pm standard deviation; range of wt % in parenthesis).

Element	Point 1	Point 2	Point 3	Point 4	Point 5	Point 6	Point 7
<i>Major elements</i>							
C	34.7 \pm 17.1 (15.3 - 74.6)	17.24 \pm 1.85 (13.67 - 23.0)	14.5 \pm 1.64 (11.8 - 20.5)	13.5 \pm 1.52 (10.9 - 19.2)	14.2 \pm 3.52 (11.0 - 30.2)	13.0 \pm 1.72 (10.3 - 20.3)	12.9 \pm 2.22 (9.82 - 23.4)
Ca	16.58 \pm 6.44 (2.23 - 23.3)	23.5 \pm 1.59 (19.2 - 26.4)	24.8 \pm 2.16 (21.0 - 30.8)	25.3 \pm 1.75 (23.1 - 31.0)	24.80 \pm 2.05 (19.7 - 28.6)	26.2 \pm 2.25 (23.3 - 31.6)	25.2 \pm 1.10 (21.4 - 27.7)
O	33.7 \pm 7.00 (20.1 - 44.53)	41.5 \pm 3.01 (34.4 - 47.3)	42.6 \pm 2.66 (35.8 - 46.5)	43.2 \pm 2.19 (37.4 - 46.5)	43.34 \pm 2.42 (33.7 - 48.9)	42.3 \pm 3.07 (34.9 - 46.1)	43.8 \pm 1.73 (38.1 - 45.8)
P	9.33 \pm 3.60 (1.27 - 12.8)	13.2 \pm 0.681 (11.8 - 15.0)	14.0 \pm 0.703 (12.0 - 15.4)	14.4 \pm 0.543 (13.5 - 15.8)	14.2 \pm 1.02 (11.4 - 15.4)	14.8 \pm 0.532 (13.7 - 16.1)	14.51 \pm 0.492 (12.5 - 15.4)
<i>Minor elements</i>							
Mg	0.818 \pm 0.698 (0.050 - 2.29)	2.06 \pm 0.484 (1.32 - 2.88)	2.37 \pm 0.664 (0.005 - 3.67)	2.55 \pm 0.608 (1.85 - 4.05)	2.57 \pm 0.639 (1.73 - 4.19)	2.62 \pm 0.661 (1.00 - 3.90)	2.60 \pm 0.421 (1.96 - 3.56)
Na	0.501 \pm 0.276 (0.050 - 1.06)	0.667 \pm 0.109 (0.540 - 1.01)	0.711 \pm 0.148 (0.520 - 1.22)	0.724 \pm 0.122 (0.540 - 1.03)	0.719 \pm 0.134 (0.480 - 1.08)	0.709 \pm 0.113 (0.550 - 1.03)	0.748 \pm 0.099 (0.600 - 0.980)
<i>Trace elements</i>							
Al	4.97 \pm 7.54 (0.050 - 23.80)	1.84 \pm 2.68 (0.050 - 8.47)	1.14 \pm 1.63 (0.050 - 6.25)	0.777 \pm 1.20 (0.050 - 4.84)	0.654 \pm 1.14 (0.050 - 4.53)	0.506 \pm 1.02 (0.050 - 4.32)	0.404 \pm 0.913 (0.050 - 3.81)

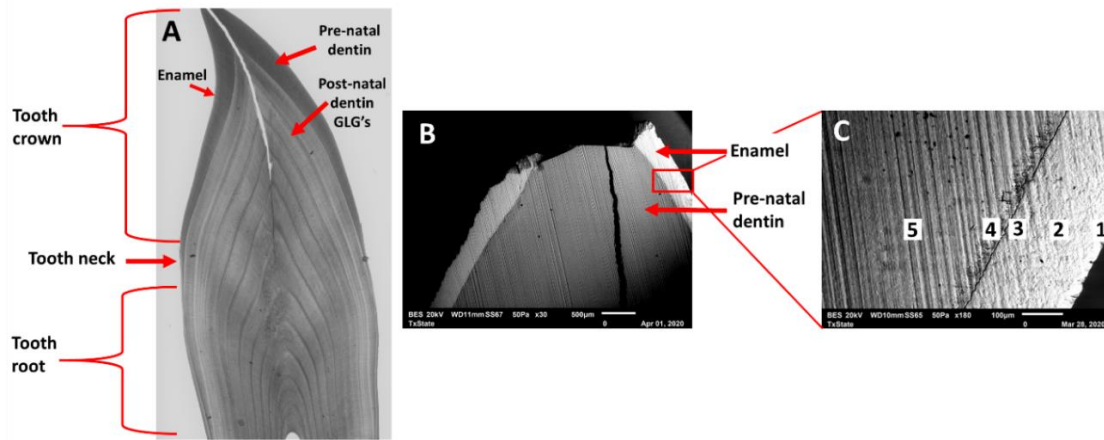


Figure 6.1. Cross-sectioned image of the top half of tooth of GA1603 (the split in the tooth was likely a result of being frozen in long-term storage) (A), backscattered electron image showing the enamel and pre-natal dentin (PND), along with a rectangle that indicates the approximate area of SEM-EDS analysis (B), and a zoomed in image of the area of the EDS analysis showing the locations for point analysis (point 1 = outer enamel, point 2 = mid-enamel, point 3 = inner enamel, point 4 = pre-natal dentin near the enamel dentin junction, and point 5 = inner pre-natal dentin) (C).

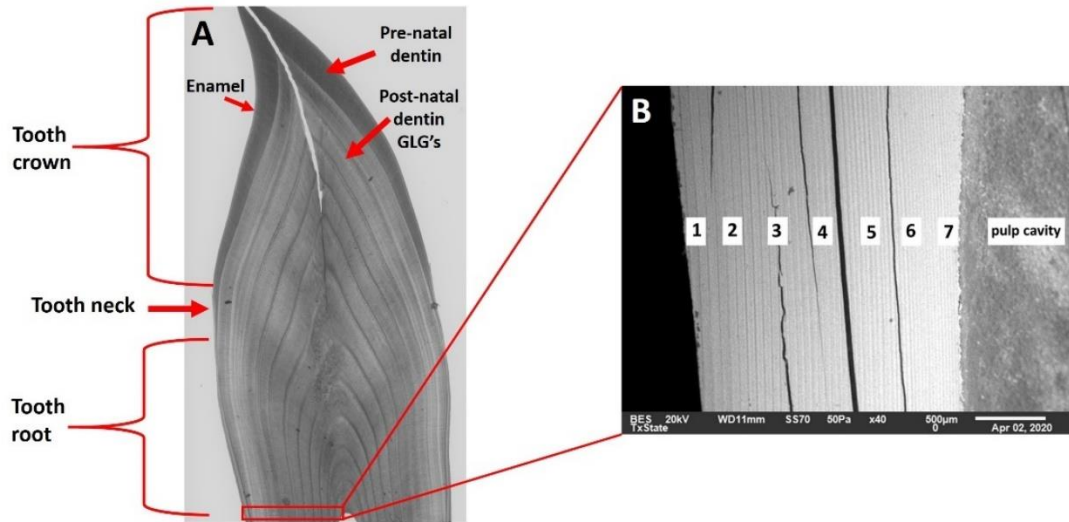


Figure 6.2. Cross-sectioned image of the top half of tooth of GA1603 (the split in the tooth was likely a result of being frozen in long-term storage) along with a the rectangle that shows general location for elemental analysis (A), and a backscattered electron image showing the general area of point analyses (points 1 - 7) used to explore the distribution of elements across the approximate location of the growth layer groups (GLG's), with newest layers deposited closest to the pulp cavity (B).

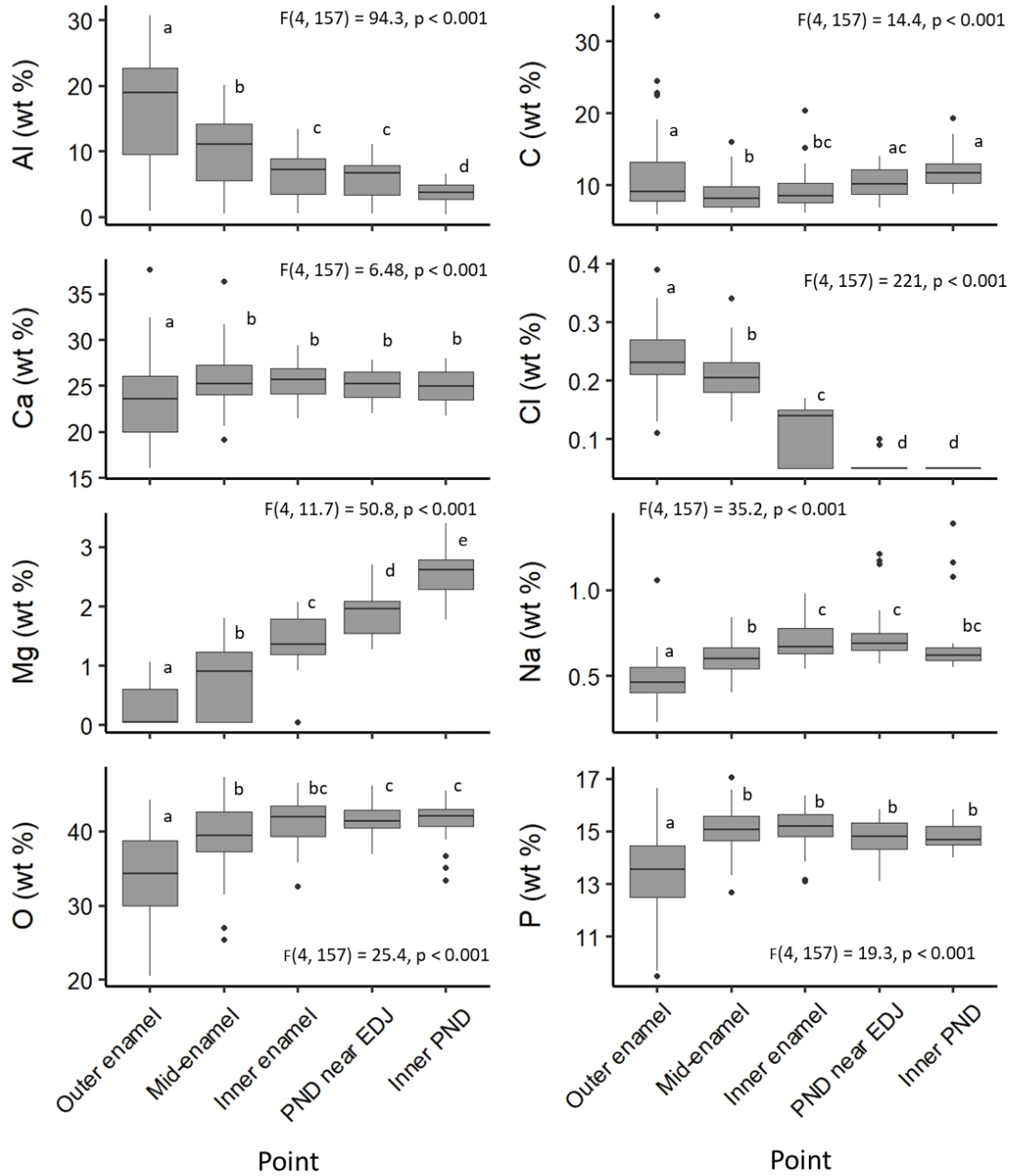


Figure 6.3. Selective point analyses for elements in the enamel and pre-natal dentin (PND) expressed as weight percentage (wt %): outer enamel (point 1), mid-enamel (point 2), inner enamel (point 3), PND near enamel dentin junction (EDJ) (point 4), inner PND (point 5). Results of the repeated-measures linear mixed effects ANOVA and Tukey's post-hoc test are shown in each panel. Lowercase letters indicate points grouped by statistically similar wt % values. Data pertaining to each individual dolphin including the mean and SE wt % at each point are provided in the Supplementary Tables S6.1-S6.3.

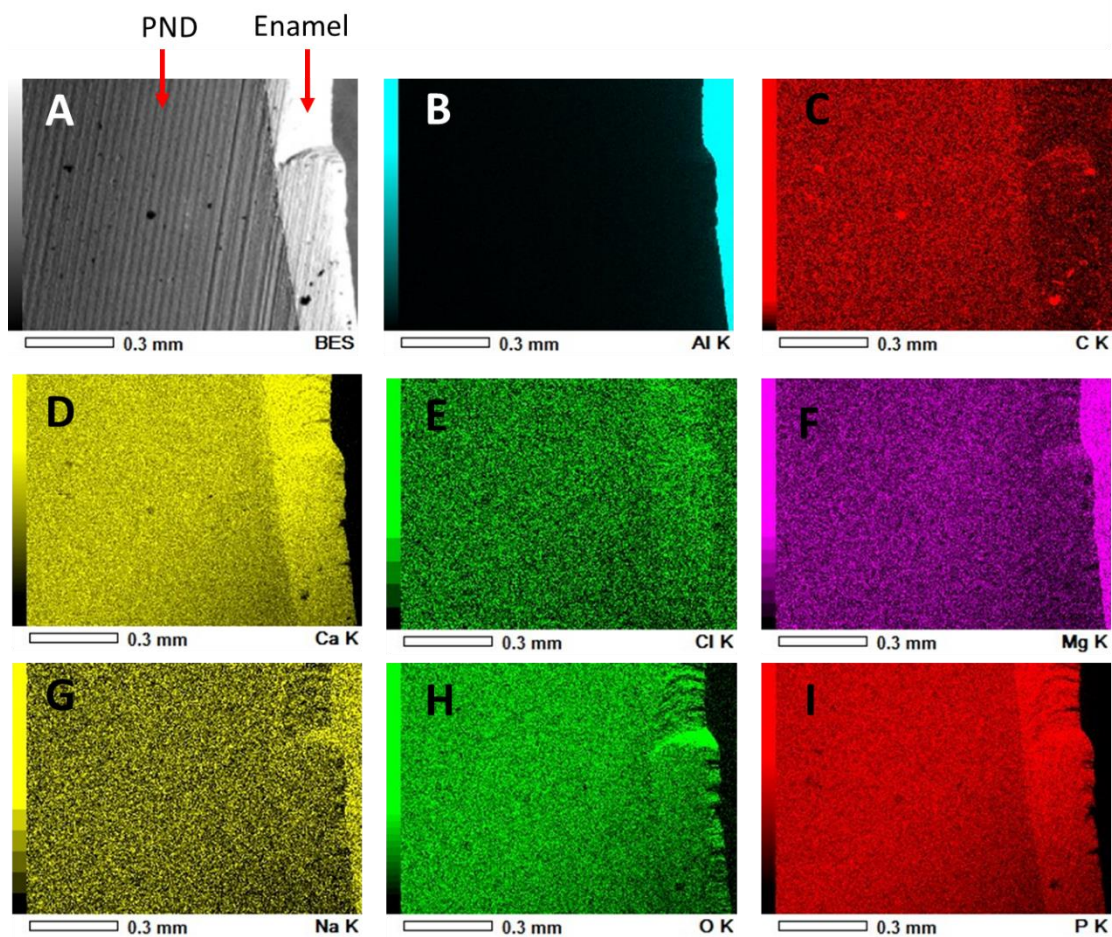


Figure 6.4. Backscattered electron image of analysis area of sample GA 260 showing the enamel and pre-natal dentin (PND) (panel A) and elemental maps for Al (panel B), C (panel C), Ca (panel D), Cl (panel E), Mg (panel F), Na (panel G), O (panel H), and P (panel I). The intensity of the color is proportional to the number of x-ray counts in which higher intensity colors correspond to higher x-ray counts or greater wt %. For references to color please refer to the online version of this article.

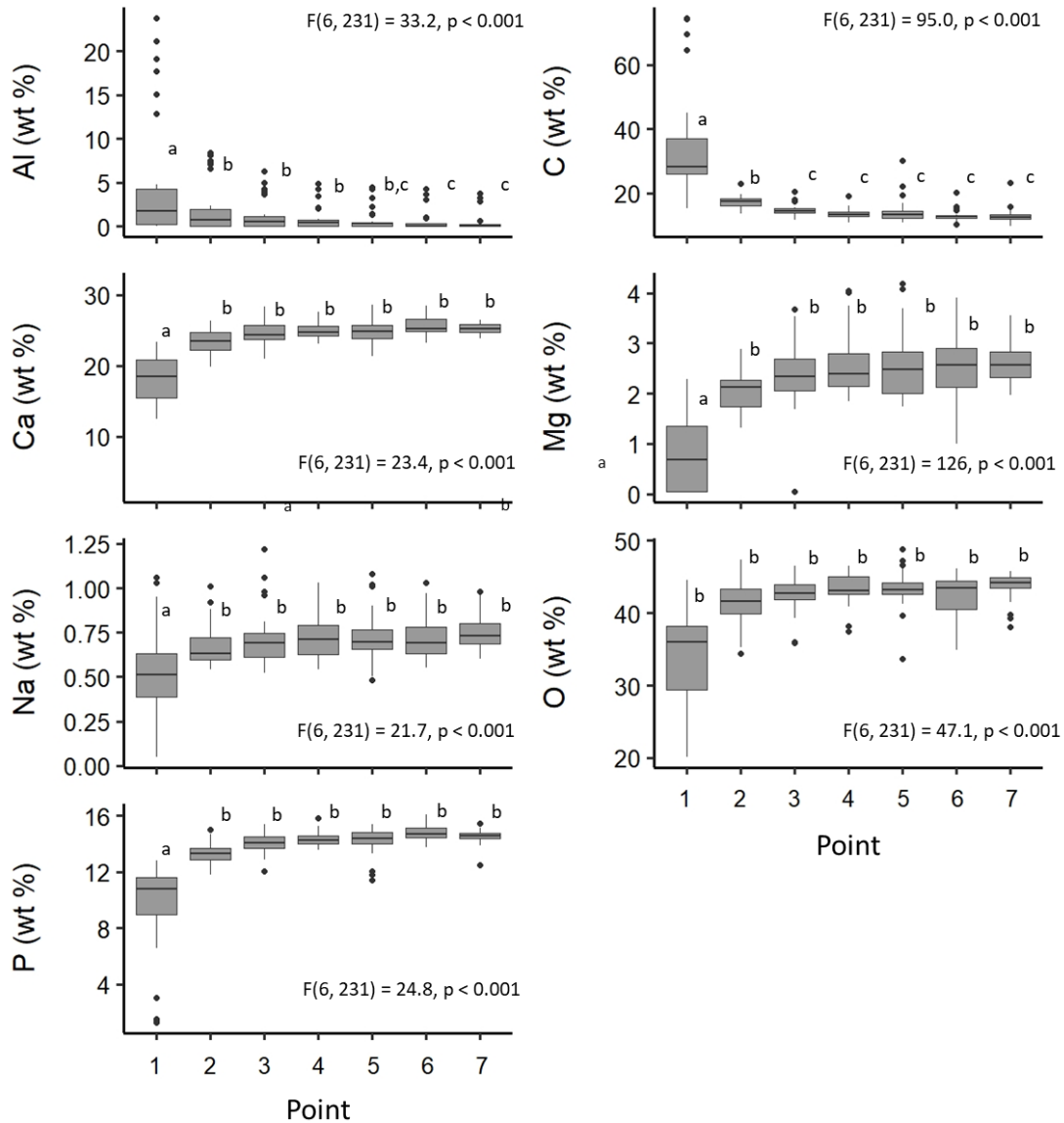


Figure 6.5. Selective point analyses for elements approximating where growth layers (GLG's) are present. Elements presented as a weight percentage (wt %), moving from the tooth edge (point 1) towards the tooth center (point 7), with points closest to the tooth edge being the oldest deposited dentin layers and points closest to the tooth center being the newest deposited dentin layers. Results of the repeated-measures linear mixed effects ANOVA and Tukey post-hoc tests are shown in each panel. Lowercase letters indicate points grouped by statistically similar wt % values. Data pertaining to each individual dolphin including the mean and SE wt % at each point are provided in the Supplementary Tables S6.4-S6.6.

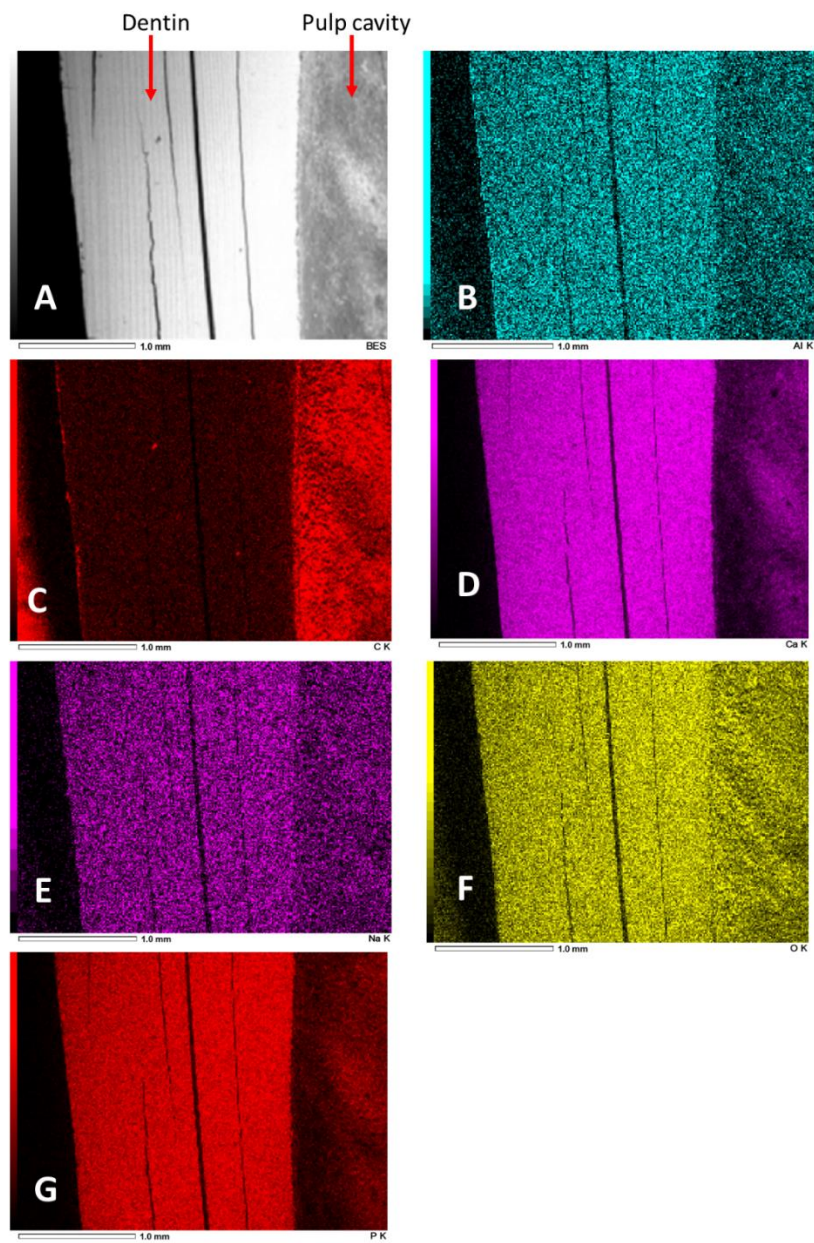


Figure 6.6. Backscattered electron image of analysis area of sample GA 1755 showing the dentin and pulp cavity (panel A) and elemental maps for Al (panel B), C (panel C), Ca (panel D), Na (panel E), O (panel F), and P (panel G). Magnesium and Cl were not detected in this particular sample. The intensity of the color is proportional to the number of x-ray counts in which higher intensity colors correspond to higher x-ray counts or greater wt %. Striations in the tooth may be a consequence of the cross-sectioning process. For references to color please refer to the online version of this article.

VII. CONCLUSIONS

Approaches to studying marine mammal toxicology are limited; obtaining tissue samples for contaminant analysis is restricted to either the non-lethal, minimally invasive sampling of free-ranging populations or the utilization of deceased stranded individuals (Peltier et al., 2014, 2014; Godard-Codding et al., 2018; Monteiro et al., 2020). In both cases, logistical and legal considerations add additional levels of complexity. However, despite the challenges, the field of marine mammal toxicology continues to progress, spurred by creativity, collaboration, and multi-disciplinary approaches. Marine mammals are charismatic megafauna capable of generating public interest in ecotoxicology. In addition, their long lifespans, position at the top of the food web, and coastal distribution make them ideal sentinel species for ecosystems and human health (Bossart, 2011; Reif et al., 2015).

Relatively small sample sizes in marine mammal toxicological studies are common; live sampling is costly and time-consuming, and collecting tissues from stranded animals is opportunistic. I had a rare opportunity to analyze tissue trace element concentrations from more than 250 individual bottlenose dolphins (*Tursiops truncatus*) for my dissertation. In addition to bottlenose dolphins, I also had the opportunity to analyze tissues from several other odontocete species that strand less frequently [Atlantic spotted dolphin (*Stenella frontalis*), Blainville's beaked whale (*Mesoplodon densirostris*), dwarf sperm whale (*Kogia sima*), melon-headed whale (*Peponocephala electra*), pantropical spotted dolphin (*Stenella attenuata*), pygmy killer whale (*Feresa attenuata*), pygmy sperm whale (*Kogia breviceps*), Risso's dolphin (*Grampus griseus*), rough-toothed dolphin (*Steno bredanensis*), and short-finned pilot whale (*Globicephala*

macrorhynchus]). Before my dissertation, except for the bottlenose dolphin (Kuehl and Haebler, 1995; Meador et al., 1999; Stein et al., 2003; Bryan et al., 2007; Woshner et al., 2008; Damseaux et al., 2017), rough-toothed dolphin (Mackey et al., 2003), and pygmy sperm whale (Bryan et al., 2012), no studies have reported trace elements in the abovementioned species from the Gulf of Mexico. Of the bottlenose dolphin studies, several studies utilized non-lethal sampling of skin, blubber, or blood. Only Kuehl and Haebler (1995), Meador et al. (1999), and Stein et al. (2003) reported the concentrations of trace elements in internal tissues (e.g., brain, kidney, liver). Further, most reported only mercury (Hg) and occasionally selenium (Se) tissue concentrations. Before my dissertation, there had been only one study that measured the concentrations of trace elements in a single bottlenose dolphin from LA (Stein et al., 2003), and no studies that focused on trace elements concentrations in inshore bottlenose dolphins from the FL panhandle. Unfortunately, the opportunity to analyze tissues from such a large number of individuals was due to the northern Gulf of Mexico (nGOM) Cetacean Unusual Mortality Event (UME) (2010-2014), which resulted in over 1,000 cetacean strandings (Litz et al., 2014). Samples utilized for my dissertation came from individuals that stranded during and in the two years following the nGOM UME. It has been suggested that combined effects of cold water temperatures, large inputs of fresh water, the impacts associated with the Deepwater Horizon Oil Spill, and the bacterial infection brucellosis may have contributed to the UME (Carmichael et al., 2012; Litz et al., 2014; Schwacke et al., 2014; Venn-Watson et al., 2015a,b, Colegrove et al., 2016).

My dissertation contributes to knowledge of trace element accumulation, especially Hg and Se, in odontocetes from the nGoM. In Chapters 2 and 4, I documented

spatial patterns in Hg accumulation for bottlenose dolphins in the nGoM consistent with those observed lower trophic level organisms from the region such as oysters [e.g., eastern oyster (*Crassostrea virginica*)] and fish [e.g., spotted seatrout (*Cynoscion nebulosus*) and golden tilefish (*Lopholatilus chamaleonticeps*)] (Ache et al., 2000; Apeti et al., 2012; Evans et al., 2015; Harris et al., 2012; Perrot et al., 2019). In addition to differences in environmental conditions and Hg sources, research from Chapter 3 suggests that differences in trophic positions among bay, sound, and estuary (BSE) bottlenose dolphins also contribute to the observed variation in Hg concentrations. Se:Hg molar ratios > 1:1 suggest that Se helps protect against Hg toxicity; however, in FL, where dolphins have greater Hg concentrations, they also have lower Se:Hg molar ratios. These differences suggest that some BSE stocks may be more susceptible to Hg toxicity than others (Chapter 4).

My dissertation also contributes to relevant methodological questions related to the effects of formalin fixation on trace element concentrations (Chapter 5) and scanning electron microscopy (SEM) coupled with energy dispersive X-ray spectroscopy (EDS) to measure trace elements in dolphin teeth (Chapter 6). My results demonstrate that formalin fixation may result in the leaching of trace elements from tissues. Contamination may also occur as trace elements, presumably from the formalin, become introduced to tissues. However, it may be possible to account for the effects of formalin fixation for some trace elements, but additional research is required. These findings are particularly relevant for museum specimens that were not originally preserved with the intent of performing trace element analyses. Using SEM-EDS, I found that while I could detect major and minor trace elements in bottlenose dolphin teeth, technologies with

lower detection limits [e.g., laser ablation inductively coupled plasma mass spectrometry (LA-ICP-MS)] would be required to measure the concentrations of trace elements within teeth. There is a growing interest in analyzing marine mammal teeth to 1) explore changes in trace element concentrations within the lifetime of an individual (Clark et al., 2020a,b) and 2) explore historical changes in trace element concentrations (De María et al., 2021). While outside the scope of this dissertation, the same teeth used in Chapter 6 for the SEM-EDS analysis were also analyzed using LA-ICP-MS. Future research will focus on interpreting the trace element concentrations reported in the bottlenose dolphin growth layer groups analyzed using LA-ICP-MS to determine changes in trace elements within individuals and differences in trace element concentrations, particularly those of anthropogenic origin, among individuals across decades.

The research presented in this dissertation highlights the complexity of interpreting tissue trace element concentrations, particularly Hg, in wildlife. Detailed studies that focus on Hg biomagnification within the specific food webs are required to more fully understand the spatial variation in Hg concentrations among bottlenose dolphins from the nGoM. For example, Hong et al. (2013) explored the bioaccumulation and biomagnification of Hg and Se within the Sarasota Bay, FL, food web to assess the risk of Hg exposure to resident bottlenose dolphins. While studies often report dolphin tissue Hg concentrations, studies rarely assess exposure risk because there is uncertainty regarding dietary sources. In Hohn et al. (2013), using $\delta^{13}\text{C}$ and $\delta^{15}\text{N}$ values and Hg and Se concentrations from organisms sampled throughout the food web, ranging from seagrasses to dolphins, the authors estimated dolphin trophic-level consumption rates of Hg and Se. In addition, traditional dietary studies based on stomach content analyses are

still valuable. For example, Bowen-Stevens (2021) recently published the first of such studies for Barataria Bay, LA, bottlenose dolphin populations. Bowen-Stevens et al. (2021) found that bottlenose dolphins from LA appear to have a greater dependence on lower trophic level prey items in LA (e.g., shrimp and anchovies) than bottlenose dolphin populations from FL, which may explain the spatial variation of Hg concentrations among bottlenose dolphins reported in my dissertation.

In addition to understanding dietary sources, recent studies have highlighted the plasticity of residency patterns observed among inshore bottlenose dolphin populations, challenging the previous assumption that BSE stocks were comprised primarily of year-round residents that displayed high levels of site fidelity (Balmer et al., 2008; Tyson et al., 2011; Shippee, 2014; Balmer et al., 2019; Toms, 2019). More photo-identification and telemetry studies are necessary to quantify the percentage of year-round residents, transients, and seasonal migrants in these stocks to better define stock boundaries and interpret contaminant concentrations.

In terms of Hg, specifically, future research should also focus on exploring differences in methylation rates as a possible explanation for spatial variation in Hg concentrations. For example, Harper et al. (2018) found that in Big Bend, FL, indicating more sulfate reduction, methylmercury (MeHg) concentrations in fauna increased. Further characterizing how the Mississippi River influences Hg concentrations in wildlife may also help explain variation in dolphin Hg concentrations. Perrot et al. (2019) suggested that reduced Hg bioaccumulation in tilefish near the Deepwater Horizon oil spill could be influenced by the Mississippi River outflow, specifically the input of nutrients and suspended particulate matter. The use of Hg stable isotope ratios may also

help explain Hg sources and potentially link Hg concentrations in wildlife to Hg sources (Demers et al., 2014).

This work suggests Se may protect against Hg toxicity in nGoM dolphins; however, this assumes that a Se:Hg molar ratio $>1:1$ is protective. More research is necessary to determine how Se protects against Hg toxicity and if a 1:1 Se:Hg molar is truly protective against Hg toxicity, or if Se is required to be in present in greater molar excess to be protective (e.g., Se:Hg molar ratio $> 5:1$) (Burger et al., 2013; Gerson et al., 2020). Further, there remain significant gaps in our understanding of mechanisms by which odontocetes can mitigate Hg and other heavy metal-induced toxicity [e.g., cadmium (Cd) and lead (Pb)] (Kershaw and Hall 2019; Hauser-Davis et al., 2020). Given that odontocetes can tolerate high concentrations of trace elements and other contaminants (e.g., PCBs) without lethal effects, future research should focus on sublethal effects and biomarkers of exposure to trace elements and other contaminants.

Specifically, research should identify biomarkers that identify the presence of contaminants and their effects (Godard-Codding and Fossi, 2018). Skin biopsies are the most common nonlethal technique used to identify the presence of trace elements and POPs in cetaceans (Goddard-Codding et al., 2011; Fossi et al., 2014). In addition to the measurement of the contaminant themselves, researchers can also look for diagnostic markers of contamination including, markers of exposure (e.g., CYP1A), markers of overall stress (e.g., cortisol), and markers of genotoxicity (e.g., lipid peroxidation) (Godard-Codding and Fossi, 2018). Although live capture of cetaceans is more invasive, Schaefer et al. (2011) analyzed the Hg concentrations in bottlenose dolphin skin and blood during live capture health assessments and associated biomarkers of Hg exposure.

The authors found positive associations between Hg concentrations in the blood and skin, and blood urea nitrogen, and gamma-glutamyl transferase suggesting adverse effects of Hg on liver and kidney function.

Finally, marine mammals face numerous threats in addition to exposure to contaminants. Marine mammal science tends to focus on a particular individual threat (e.g., climate change, contaminant exposure; fisheries interactions; noise pollution, habitat degradation), but more emphasis should be on the impacts of cumulative effects (Simmonds, 2018). Increased specialization within scientific disciplines is a consequence of scientific education and research; however, more cross-disciplinary studies will be necessary to address these cumulative stressors. Especially in marine mammal science, where access to animals is limited, new and innovative approaches are necessary. My dissertation utilized multidisciplinary methods to understand trace element concentrations in odontocetes. My work contributes to the knowledge of trace elements, especially Hg and Se, in odontocete tissues and addresses important methodological questions in marine mammal toxicology.

APPENDIX SECTION

Table S2.1. AIC_c model selection for blubber THg concentration using stranding location, bodylength, sex, and year as predictors. df = degrees of freedom, logLik = log likelihood, AIC_c = Akaike's Information Criterion for small sample sizes, delta= delta score, weight = Akaike weight. *indicates the variable was Log10 transformed

Model	df	logLik	AICc	delta	weight
Location+ Body Length* + Year	9	-88.1	195.5	0.00	0.49
Location + Body Length*	4	-93.9	196.0	0.48	0.39
Location +Body Length* + Sex + Year	11	-88.0	199.7	4.22	0.06
Location + Body Length* + Sex	6	-93.6	199.8	4.27	0.06
Body Length*	3	-107.2	220.5	25.05	1.79E-06
Body Length* + Year	8	-101.9	220.7	25.22	1.65E-06
Body Length* + Sex	5	-105.7	221.8	26.31	9.55E-07
Body Length* + Sex + Year	10	-100.2	221.8	26.35	9.36E-07
Location + Year	8	-125.0	266.9	71.45	1.51E-16
Location	3	-131.1	268.4	72.90	7.29E-17
Location + Sex + Year	10	-124.8	271.0	75.54	1.96E-17
Location + Sex	5	-131.0	272.4	76.96	9.60E-18
Year	7	-131.5	277.8	82.34	6.52E-19
Null	2	-137.4	278.8	83.33	3.97E-19
Sex + Year	9	-130.4	280.0	84.52	2.19E-19
Sex	4	-136.5	281.3	85.84	1.13E-19

Table S2.2. AIC_c model selection for blubber THg concentration using stranding location, age, sex, and year as predictors. df = degrees of freedom, logLik = log likelihood, AIC_c = Akaike's Information Criterion for small sample sizes, delta = delta score, weight = Akaike weight. *indicates the variable was Log10 transformed

Model	df	logLik	AIC _c	delta	weight
Location + Age*	4	-54.9	118.0	0.00	0.798
Location + Age* + Sex	6	-54.7	122.2	4.15	0.100
Location + Age* + Year	9	-51.4	122.4	4.35	0.090
Location + Age* + Sex + Year	11	-51.2	126.6	8.54	0.011
Age*	3	-65.3	136.7	18.69	6.98E-05
Age* + Sex	5	-64.0	138.5	20.51	2.81E-05
Age* + Year	8	-61.2	139.7	21.63	1.6E-05
Age* + Sex + Year	10	-60.1	142.1	24.11	4.65E-06
Location	3	-88.9	184.0	65.97	3.78E-15
Location + Sex	5	-87.9	186.3	68.32	1.17E-15
Location + Year	8	-85.3	187.8	69.73	5.77E-16
Location + Sex + Year	10	-83.8	189.5	71.44	2.45E-16
Sex	4	-94.5	197.3	79.26	4.91E-18
Null	2	-96.9	198.0	79.97	3.45E-18
Sex + Year	9	-90.3	200.1	82.04	1.22E-18
Year	7	-93.4	201.7	83.69	5.35E-19

Table S2.3. AICc model selection for skin THg concentration using stranding location, body length, sex, and year as predictors. df = degrees of freedom, logLik = log likelihood, AIC_c = Akaike's Information Criterion for small sample sizes, delta = delta score, weight = Akaike weight. *indicates the variable was Log10 transformed

Model	df	logLik	AIC _c	delta	weight
Location + Body Length* + Year	9	-43.2	106.0	0.00	0.61
Location + Body Length*	4	-49.7	107.7	1.67	0.27
Location + Body Length* + Sex + Year	11	-42.9	110.0	4.04	0.08
Location + Body Length* + Sex	6	-49.3	111.4	5.39	0.04
Body Length* + Sex + Year	10	-65.2	152.3	46.36	5.23E-11
Body Length* + Year	8	-68.0	153.3	47.30	3.28E-11
Body Length* + Sex	5	-76.8	164.1	58.09	1.48E-13
Body Length*	3	-79.7	165.5	59.52	7.29E-14
Location + Year	8	-77.1	171.4	65.38	3.88E-15
Location + Sex + Year	10	-76.8	175.5	69.48	5E-16
Location	3	-85.3	176.9	70.87	2.49E-16
Location + Sex	5	-85.0	180.5	74.52	4.03E-17
Year	7	-87.3	189.6	83.57	4.36E-19
Sex + Year	9	-85.6	190.8	84.82	2.34E-19
Null	2	-99.7	203.5	97.49	4.13E-22
Sex	4	-97.6	203.6	97.58	3.95E-22

Table S2.4. AIC_c model selection for skin THg concentration using stranding location, age, sex, and year as predictors df = degrees of freedom, logLik = log likelihood, AIC_c = Akaike's Information Criterion for small sample sizes, delta = delta score, weight = Akaike weight.

*indicates the variable was Log10 transformed

Model	df	logLik	AIC _c	delta	weight
Location + Age*	4	-23.5	55.4	0.00	0.76
Location + Age* + Year	9	-19.5	58.9	3.50	0.13
Location + Age* + Sex	6	-23.4	59.7	4.27	0.09
Location + Age* + Sex + Year	11	-19.4	63.6	8.23	0.01
Age* + Year	8	-44.2	105.8	50.38	8.76E-12
Age* + Sex + Year	10	-41.8	105.9	50.54	8.12E-12
Age* + Sex	5	-49.6	109.9	54.46	1.14E-12
Age*	3	-52.1	110.5	55.10	8.31E-13
Location + Year	8	-57.7	132.8	77.38	1.21E-17
Location	3	-63.5	133.2	77.82	9.68E-18
Location + Sex + Year	10	-57.5	137.2	81.84	1.3E-18
Location + Sex	5	-63.5	137.5	82.12	1.13E-18
Year	7	-68.7	152.6	97.22	5.91E-22
Sex + Year	9	-67.2	154.2	98.84	2.63E-22
Null	2	-78.1	160.2	104.85	1.3E-23
Sex	4	-76.4	161.3	105.90	7.73E-24

Table S2.5. AIC_c model selection for $\delta^{13}\text{C}$ in skin using stranding location, body length, sex, month, and year as predictors. df = degrees of freedom, logLik = log likelihood, AIC_c = Akaike's Information Criterion for small sample sizes, delta= delta score, weight = Akaike weight.

*indicates the variable was Log10 transformed

Model	df	logLik	AICc	Delta	weight
Location + Body Length* + Sex	6	-192.1	397.1	0.00	0.568
Location + Body Length* + Sex + Year	11	-187.3	399.5	2.34	0.177
Location + Body Length*	4	-195.6	399.6	2.48	0.165
Location + Body Length* + Year	9	-190.8	401.4	4.25	0.068
Location	3	-199.7	405.6	8.49	0.008
Location+ Sex	5	-197.7	406.0	8.83	0.007
Location + Year	8	-194.7	406.8	9.71	0.004
Location + Sex + Year	10	-192.8	408.0	10.82	0.003
Body Length* + Sex + Year	10	-194.7	411.8	14.61	3.81E-04
Location+ Month + Sex	17	-185.9	412.8	15.63	2.29E-04
Body length* + Year	8	-198.0	413.4	16.30	1.64E-04
Body length *+ Sex	5	-201.7	414.0	16.90	1.21E-04
Year	7	-200.4	416.0	18.89	4.5E-05
Year + Sex	9	-198.5	416.9	19.77	2.89E-05
Location + Body Length* + Month +Sex + Year	22	-180.7	417.6	20.46	2.05E-05
Location+ Body Length* + Month	15	-191.5	418.3	21.20	1.42E-05
Body Length*	3	-206.4	419.0	21.90	9.99E-06
Sex	4	-205.9	420.3	23.13	5.38E-06
Body Length* + Month + Sex	16	-191.4	420.9	23.74	3.97E-06
Body Length* + Month + Sex + Year	21	-184.1	421.2	24.07	3.38E-06
Location + Month + Sex	16	-191.7	421.5	24.38	2.88E-06
Null	2	-209.1	422.3	25.15	1.96E-06
Location + Body Length* + Month +Year	20	-186.7	423.2	26.11	1.21E-06

Location + Month	14	-195.4	423.4	26.24	1.14E-06
Location + Month + Sex + Year	21	-186.9	426.8	29.65	2.07E-07
Body Length* + Month + Year	19	-190.1	427.1	29.92	1.81E-07
Month + Sex	15	-196.1	427.5	30.34	1.46E-07
Location + Month + Year	19	-190.5	427.9	30.75	1.19E-07
Body Length* + Month	14	-197.7	428.0	30.88	1.12E-07
Month + Sex + Year	20	-189.3	428.4	31.26	9.26E-08
Month + Year	18	-193.0	429.9	32.81	4.26E-08
Month	13	-200.4	430.9	33.72	2.71E-08

Table S2.6. AIC_c model selection for $\delta^{15}\text{N}$ in skin using stranding location, body length, sex, month, and year as predictors. df = degrees of freedom, logLik = log likelihood, AIC_c = Akaike's Information Criterion for small sample sizes, delta= delta score, weight = Akaike weight.

*indicates the variable was Log10 transformed

Model	df	logLik	AICc	delta	weight
Location + Body Length*	4	-177.9	364.2	0.00	0.822
Location + Body Length* + Sex	6	-177.7	368.2	3.95	0.114
Location	3	-182.1	370.4	6.19	0.037
Location + Body Length* + Year	9	-176.1	371.8	7.56	0.019
Location + Sex	5	-182.0	374.5	10.25	4.88E-03
Location + Body Length* + Month	11	-175.9	376.2	11.95	2.09E-03
Location + Year	8	-180.7	378.7	14.46	5.96E-04
Location + Body Length* + Month	15	-172.4	379.3	15.09	4.35E-04
Location + Sex + Year	10	-180.6	383.1	18.88	6.52E-05
Location + Body Length* + Month + Sex	17	-171.8	383.5	19.24	5.46E-05
Location + Month	14	-176.2	384.2	20.01	3.71E-05
Location + Month + Sex	16	-175.7	388.7	24.44	4.06E-06
Location + Body Length* + Month + Year	20	-170.8	389.8	25.60	2.27E-06
Location + Body Length* + Month + Sex + Year	22	-170.3	394.7	30.49	1.97E-07
Location + Month + Year	19	-174.7	394.9	30.68	1.79E-07
Location + Month + Sex + Year	21	-174.3	399.9	35.65	1.49E-08
Month	13	-196.8	423.0	58.73	1.45E-13
Body Length* + Month	14	-195.6	423.2	58.92	1.32E-13
Body Length*	3	-209.9	426.1	61.86	3.03E-14
Null	2	-211.0	426.1	61.89	2.98E-14
Month + Sex	15	-196.1	426.7	62.47	2.24E-14
Sex	4	-209.3	426.9	62.68	2.02E-14
Body Length* + Sex	5	-208.2	426.9	62.68	2.02E-14
Body Length* + Month + Sex	16	-194.9	427.0	62.74	1.95E-14
Year	7	-208.5	431.9	67.66	1.67E-15
Month + Year	18	-194.6	431.9	67.69	1.64E-15
Body Length* + Year	8	-207.6	432.6	68.32	1.2E-15
Body Length* + Month + Year	19	-193.6	432.7	68.44	1.13E-15
Sex + Year	9	-207.1	433.8	69.55	6.48E-16
Body Length* + Sex + Year	10	-206.2	434.4	70.15	4.8E-16
Month + Sex + Year	20	-194.1	436.5	72.25	1.68E-16
Body Length* + Month + Sex + Year	21	-193.0	437.3	73.01	1.15E-16

Table S2.7. AIC_C model selection for $\delta^{34}\text{S}$ in skin using stranding location, body length, sex, month, and year as predictors. df = degrees of freedom, logLik = log likelihood, AIC_C = Akaike's Information Criterion for small sample sizes, delta= delta score, weight = Akaike weight.

*indicates the variable was Log10 transformed

Model	df	logLik	AIC _C	delta	Weight
Location	3	-231.8	469.8	0.00	0.585
Location + Body Length*	4	-231.8	472.0	2.16	0.199
Location + Sex	5	-231.0	472.6	2.80	0.144
Location + Body Length* + Sex	6	-231.0	474.9	5.03	0.047
Location + Year	8	-230.3	478.0	8.20	9.69E-03
Location + Month	14	-223.8	480.1	10.30	3.39E-03
Location + Body Length* + Year	9	-230.3	480.4	10.56	2.98E-03
Sex	4	-236.2	480.9	11.03	2.36E-03
Location + Sex + Year	10	-229.8	482.0	12.17	1.33E-03
Null	2	-239.0	482.1	12.30	1.25E-03
Location + Body Length* + Month	15	-223.8	482.8	13.02	8.71E-04
Month	13	-226.5	483.0	13.16	8.11E-04
Body Length* + Sex	5	-236.2	483.1	13.23	7.82E-04
Body Length*	3	-239.0	484.2	14.37	4.43E-04
Location + Body Length* + Sex+Year	11	-229.8	484.4	14.56	4.02E-04
Location + Month + Sex	16	-223.4	484.9	15.06	3.13E-04
Body Length* + Month	14	-226.5	485.6	15.79	2.17E-04
Month + Sex	15	-225.4	486.1	16.24	1.74E-04
Location +Body Length* + Month +Sex	17	-223.4	487.7	17.89	7.63E-05
Body Length* + Month + Sex	16	-225.4	488.8	19.02	4.33E-05
Year	7	-237.1	489.3	19.49	3.43E-05
Sex + Year	9	-235.3	490.4	20.62	1.95E-05
Location + Month + Year	19	-222.0	490.8	21.00	1.61E-05
Body Length* + Year	8	-237.1	491.6	21.76	1.1E-05
Body Length* + Sex + Year	10	-235.3	492.9	23.06	5.75E-06
Month + Year	18	-225.0	493.8	23.96	3.66E-06
Location + Body Length* + Month + Year	20	-222.0	493.8	23.99	3.62E-06
Location + Month + Sex + Year	21	-221.8	496.6	26.75	9.09E-07

Year					
Body Length* + Month + Year	19	-225.0	496.8	26.94	8.27E-07
Month + Sex + Year	20	-224.2	498.2	28.36	4.06E-07
Location + Body Length* + Month + Sex + Year	22	-221.7	499.6	29.82	1.96E-07
Body Length* + Month + Sex + Year	21	-224.1	501.3	31.46	8.63E-08

Table S2.8. AIC_c model selection for $\delta^{13}\text{C}$ in skin using stranding location, age, sex, month, and year as predictors. df = degrees of freedom, logLik = log likelihood, AIC_c = Akaike's Information Criterion for small sample sizes, delta = delta score, weight = Akaike weight.

*indicates the variable was Log10 transformed

Model	df	logLik	AIC _c	delta	Weight
Location + Age*	4	-153.6	315.7	0.00	0.525
Location	3	-155.2	316.7	1.00	0.318
Location + Age* + Sex	6	-153.2	319.3	3.63	0.085
Location + Sex	5	-154.8	320.1	4.46	0.056
Location + Age* + Year	9	-152.2	324.4	8.68	6.86E-03
Location + Year	8	-153.6	324.7	9.01	5.80E-03
Location + Age* + Sex + Year	11	-151.8	328.4	12.69	9.23E-04
Location + Sex + Year	10	-153.1	328.5	12.82	8.62E-04
Location + Month	14	-149.1	330.8	15.08	2.79E-04
Location + Age* + Month	15	-148.1	331.6	15.91	1.85E-04
Location + Month + Sex	16	-148.2	334.4	18.76	4.43E-05
Location + Age* + Month + Sex	17	-147.3	335.5	19.78	2.66E-05
Location + Month + Year	19	-147.9	342.5	26.86	7.71E-07
Location + Age* + Month + Year	20	-147.0	344.0	28.27	3.81E-07
Location + Month + Sex + Year	21	-146.9	346.8	31.10	9.25E-08
Location + Age* + Month + Sex + Year	22	-146.1	348.4	32.76	4.03E-08
Month	13	-170.8	371.5	55.78	4.05E-13
Age* + Month	14	-170.3	373.2	57.52	1.7E-13
Month + Sex	15	-170.2	375.8	60.09	4.69E-14
Null	2	-185.9	376.0	60.27	4.29E-14
Age*	3	-185.0	376.1	60.46	3.91E-14
Age* + Sex	5	-183.2	377.0	61.30	2.56E-14
Sex	4	-184.3	377.0	61.30	2.56E-14
Age* + Month + Sex	16	-169.7	377.5	61.84	1.96E-14
Year	7	-182.7	380.4	64.77	4.53E-15
Month + Year	18	-168.8	381.4	65.76	2.76E-15
Age* + Year	8	-182.1	381.8	66.09	2.33E-15
Sex + Year	9	-181.5	382.9	67.27	1.3E-15
Age* + Month + Year	19	-168.5	383.9	68.18	8.21E-16
Age* + Sex + Year	10	-181.0	384.2	68.55	6.82E-16
Month + Sex + Year	20	-168.5	386.9	71.20	1.81E-16
Age* + Month + Sex + Year	21	-168.2	389.4	73.72	5.15E-17

Table S2.9. AIC_c model selection for $\delta^{15}\text{N}$ in skin using stranding location, age, sex, month, and year as predictors. df = degrees of freedom, logLik = log likelihood, AIC_c = Akaike's Information Criterion for small sample sizes, delta = delta score, weight = Akaike weight.

*indicates variable was Log10 transformed

Model	df	logLik	AIC _c	delta	Weight
Location + Age*	4	-153.6	315.7	0.00	0.525
Location	3	-155.2	316.7	1.00	0.318
Location + Age* + Sex	6	-153.2	319.3	3.63	0.085
Location + Sex	5	-154.8	320.1	4.46	0.056
Location + Age* + Year	9	-152.2	324.4	8.68	6.86E-03
Location + Year	8	-153.6	324.7	9.01	5.80E-03
Location + Age* + Sex + Year	11	-151.8	328.4	12.69	9.23E-04
Location + Sex + Year	10	-153.1	328.5	12.82	8.62E-04
Location + Month	14	-149.1	330.8	15.08	2.79E-04
Location + Age* + Month	15	-148.1	331.6	15.91	1.85E-04
Location + Month + Sex	16	-148.2	334.4	18.76	4.43E-05
Location + Age* + Month + Sex	17	-147.3	335.5	19.78	2.66E-05
Location + Month + Year	19	-147.9	342.5	26.86	7.71E-07
Location + Age* + Month + Year	20	-147.0	344.0	28.27	3.81E-07
Location + Month + Year + Sex	21	-146.9	346.8	31.10	9.25E-08
Location + Age* + Month + Sex + Year	22	-146.1	348.4	32.76	4.03E-08
Month	13	-170.8	371.5	55.78	4.05E-13
Age* + Month	14	-170.3	373.2	57.52	1.7E-13
Month + Sex	15	-170.2	375.8	60.09	4.69E-14
Null	2	-185.9	376.0	60.27	4.29E-14
Age*	3	-185.0	376.1	60.46	3.91E-14
Age* + Sex	5	-183.2	377.0	61.30	2.56E-14
Sex	4	-184.3	377.0	61.30	2.56E-14
Age* + Month + Sex	16	-169.7	377.5	61.84	1.96E-14
Year	7	-182.7	380.4	64.77	4.53E-15
Month + Year	18	-168.8	381.4	65.76	2.76E-15
Age* + Year	8	-182.1	381.8	66.09	2.33E-15
Sex + Year	9	-181.5	382.9	67.27	1.3E-15
Age* + Month + Year	19	-168.5	383.9	68.18	8.21E-16
Age* + Sex + Month	10	-181.0	384.2	68.55	6.82E-16
Month + Sex + Year	20	-168.5	386.9	71.20	1.81E-16
Age* + Month + Sex + Year	21	-168.2	389.4	73.72	5.15E-17

Table S2.10. AIC_c model selection for $\delta^{34}\text{S}$ in skin using stranding location, age, sex, month, and year as predictors df = degrees of freedom, logLik = log likelihood, AIC_c = Akaike's Information Criterion for small sample sizes, delta= delta score, weight = Akaike weight. *indicates variable was Log10 transformed

Model	df	logLik	AICc	Delta	Weight
Location	3	-231.8	469.8	0.00	0.578
Location + Age*	4	-231.7	471.9	2.06	0.207
Location + Sex	5	-231.0	472.6	2.80	0.142
Location + Age* + Sex	6	-231.0	474.8	4.98	0.048
Location + Year	8	-230.3	478.0	8.20	9.57E-03
Location + Month	14	-223.8	480.1	10.30	3.35E-03
Location + Age* + Year	9	-230.3	480.4	10.57	2.93E-03
Sex	4	-236.2	480.9	11.03	2.33E-03
Location + Sex + Year	10	-229.8	482.0	12.17	1.31E-03
Null	2	-239.0	482.1	12.30	1.23E-03
Location + Age* + Month	15	-223.6	482.6	12.76	9.80E-04
Month	13	-226.5	483.0	13.16	8.01E-04
Age* + Sex	5	-236.2	483.0	13.20	7.86E-04
Age*	3	-239.0	484.2	14.35	4.43E-04
Location + Age* + Sex + Year	11	-229.8	484.5	14.65	3.81E-04
Location + Month + Sex	16	-223.4	484.9	15.06	3.10E-04
Age* + Month	14	-226.4	485.3	15.51	2.48E-04
Month + Sex	15	-225.4	486.1	16.24	1.72E-04
Location + Age* + Month + Sex	17	-223.3	487.5	17.67	8.39E-05
Age* + Month + Sex	16	-225.2	488.6	18.77	4.85E-05
Year	7	-237.1	489.3	19.49	3.39E-05
Sex + Year	9	-235.3	490.4	20.62	1.92E-05
Location + Month + Year	19	-222.0	490.8	21.00	1.59E-05
Age* + Year	8	-237.0	491.6	21.76	1.09E-05
Age* + Sex + Year	10	-235.3	492.8	23.02	5.78E-06
Month + Year	18	-225.0	493.8	23.96	3.61E-06
Location + Age* + Month + Year	20	-222.0	493.8	23.98	3.59E-06
Age* + Month + Sex + Year	21	-221.8	496.6	26.75	8.98E-07
Age* + Month + Year	19	-224.9	496.6	26.79	8.78E-07
Month + Sex + Year	20	-224.2	498.2	28.36	4.01E-07
Location+ Age* + Month + Sex + Year	22	-221.8	499.7	29.88	1.87E-07
Month+ Sex + Year	21	-224.1	501.2	31.38	8.88E-08

Table S2.11. AIC_c model selection for skin THg concentrations using $\delta^{13}\text{C}$, $\delta^{15}\text{N}$, $\delta^{34}\text{S}$, and bodylength as predictors. df = degrees of freedom, logLik = log likelihood, AIC_c = Akaike's Information Criterion for small sample sizes, delta= delta score, weight = Akaike weight.

*indicates variable was Log10 transformed

Model	df	logLik	AICc	Delta	Weight
$\delta^{13}\text{C} + \delta^{15}\text{N} + \delta^{34}\text{S} + \text{Body Length}^*$	6	-52.6	117.9	0.00	0.778
$\delta^{13}\text{C} + \delta^{15}\text{N} + \text{Body Length}^*$	5	-55.4	121.3	3.45	0.138
$\delta^{13}\text{C} + \text{Body Length}^*$	4	-57.4	123.1	5.19	0.058
$\delta^{13}\text{C} + \delta^{34}\text{S} + \text{Body Length}^*$	5	-57.1	124.7	6.80	0.026
$\delta^{15}\text{N} + \delta^{34}\text{S} + \text{Body Length}^*$	5	-67.1	144.8	26.90	1.12E-06
$\delta^{15}\text{N} + \text{Body Length}^*$	4	-68.7	145.7	27.83	7.05E-07
Body Length^*	3	-71.1	148.3	30.46	1.89E-07
$\text{Sulfur} + \text{Body Length}^*$	4	-71.1	150.5	32.58	6.55E-08
$\delta^{13}\text{C} + \delta^{15}\text{N} + \delta^{34}\text{S}$	5	-70.2	150.9	33.06	5.14E-08
$\delta^{13}\text{C} + \delta^{15}\text{N}$	4	-75.2	158.7	40.86	1.04E-09
$\delta^{13}\text{C}$	3	-77.9	162.1	44.21	1.96E-10
$\delta^{13}\text{C} + \delta^{34}\text{S}$	4	-77.2	162.8	44.87	1.4E-10
$\delta^{15}\text{N} + \delta^{34}\text{S}$	4	-86.9	182.1	64.25	8.67E-15
$\delta^{15}\text{N}$	3	-90.2	186.7	68.81	8.89E-16
Null	2	-93.7	191.5	73.61	8.05E-17
$\delta^{34}\text{S}$	3	-93.5	193.3	75.37	3.34E-17

Table S2.12. AIC_c model selection for skin THg concentrations using $\delta^{13}\text{C}$, $\delta^{15}\text{N}$, $\delta^{34}\text{S}$, and age as predictors. df = degrees of freedom, logLik = log likelihood, AIC_c = Akaike's Information Criterion for small sample sizes, delta = delta score, weight = Akaike weight *indicates variable was Log10 transformed

Model	Df	logLik	AICc	delta	Weight
$\delta^{13}\text{C} + \delta^{15}\text{N} + \delta^{34}\text{S} + \text{Age}^*$	6	-35.3	83.5	0.00	0.854
$\delta^{13}\text{C} + \delta^{15}\text{N} + \text{Age}^*$	5	-38.7	88.0	4.53	0.089
$\delta^{13}\text{C} + \text{Age}^*$	4	-40.6	89.7	6.19	0.039
$\delta^{13}\text{C} + \delta^{34}\text{S} + \text{Age}^*$	5	-40.3	91.1	7.62	0.019
$\delta^{15}\text{N} + \delta^{34}\text{S} + \text{Age}^*$	5	-46.8	104.2	20.68	2.76E-05
$\delta^{15}\text{N} + \text{Age}^*$	4	-48.5	105.3	21.84	1.54E-05
Age^*	3	-51.0	108.2	24.67	3.76E-06
$\delta^{34}\text{S} + \text{Age}^*$	4	-51.0	110.3	26.82	1.28E-06
$\delta^{13}\text{C} + \delta^{15}\text{N} + \delta^{34}\text{S}$	5	-55.3	121.2	37.65	5.69E-09
$\delta^{13}\text{C} + \delta^{15}\text{N}$	4	-60.0	128.4	44.87	1.54E-10
$\delta^{13}\text{C}$	3	-62.4	131.1	47.63	3.88E-11
$\delta^{13}\text{C} + \delta^{34}\text{S}$	4	-61.8	132.0	48.54	2.46E-11
$\delta^{15}\text{N} + \delta^{34}\text{S}$	4	-70.5	149.4	65.92	4.14E-15
$\delta^{15}\text{N}$	3	-73.1	152.5	68.97	9E-16
Null	2	-76.5	157.2	73.70	8.48E-17
$\delta^{34}\text{S} + \text{Age}^*$	3	-76.5	159.3	75.75	3.03E-17

Table S3.1. Model selection for skin Log10THg concentration using node assignment, body length, sex, condition code, and year as predictors. df = degrees of freedom, logLik = log likelihood, AICc = Akaike's Information Criterion for small sample sizes, delta= delta score, weight = Akaike weight.

Intercept	Body Length	Node	Sex	Year	Df	logLik	AICc	delta	weight
-1.54	0.0094	+	+	NA	9	-18.85	57.75	0	0.750
-1.46	0.0086	+	NA	NA	7	-22.51	60.27	2.51	0.214
-1.57	0.0089	+	+	+	14	-15.84	64.74	6.99	0.023
-1.48	0.0081	+	NA	+	12	-19.06	65.78	8.03	0.014
0.635	NA	+	NA	NA	6	-41.40	95.73	37.97	4.26E-09
0.539	NA	+	NA	+	11	-36.14	97.34	39.59	1.90E-09
0.681	NA	+	+	NA	8	-41.02	99.67	41.91	5.94E-10
0.574	NA	+	+	+	13	-35.85	102.04	44.28	1.82E-10
-1.02	0.0062	NA	+	NA	5	-53.58	117.82	60.06	6.80E-14
-0.825	0.0050	NA	+	+	10	-47.69	117.90	60.15	6.51E-14
-0.734	0.0041	NA	NA	+	8	-50.56	118.74	60.98	4.29E-14
-0.947	0.0052	NA	NA	NA	3	-58.04	122.33	64.58	7.11E-15
0.267	NA	NA	NA	+	7	-54.17	123.58	65.83	3.81E-15
0.356	NA	NA	+	+	9	-52.92	125.88	68.13	1.20E-15
0.270	NA	NA	NA	NA	2	-63.14	130.40	72.65	1.26E-16
0.391	NA	NA	+	NA	4	-61.01	130.45	72.69	1.23E-16

Table S3.2. Model selection for skin $\delta^{15}\text{N}$ using node assignment, body length, sex, condition code, and year as predictors. df = degrees of freedom, logLik = log likelihood, AICc = Akaike's Information Criterion for small sample sizes, delta= delta score, weight = Akaike weight.

Intercept	Body Length	Node	Sex	Year	df	logLik	AICc	delta	weight
16.46	NA	+	NA	+	11	-144.8	314.7	0	0.467
17.57	-0.0044	+	NA	+	12	-144.3	316.4	1.66	0.203
16.51	NA	+	NA	NA	6	-152.2	317.2	2.52	0.132
17.73	-0.0050	+	NA	NA	7	-151.6	318.4	3.73	0.072
16.32	NA	+	+	+	13	-144.2	318.7	4.05	0.062
17.73	-0.0059	+	+	+	14	-143.4	319.9	5.21	0.035
16.37	NA	+	+	NA	8	-151.8	321.3	6.55	0.018
17.83	-0.0061	+	+	NA	9	-151.0	322.1	7.37	0.012
15.28	NA	NA	+	NA	4	-173.8	356.1	41.4	4.87E-10
14.24	0.0046	NA	+	NA	5	-173.4	357.5	42.8	2.35E-10
12.98	0.0106	NA	NA	+	8	-170.0	357.6	42.9	2.30E-10
15.74	NA	NA	NA	NA	2	-176.9	358.0	43.3	1.85E-10
14.06	0.0071	NA	NA	NA	3	-176.0	358.3	43.6	1.59E-10
15.57	NA	NA	NA	+	7	-172.1	359.5	44.8	8.88E-11
13.24	0.00823	NA	+	+	10	-168.5	359.6	44.9	8.36E-11
15.19	NA	NA	+	+	9	-169.8	359.6	44.9	8.22E-11

Table S4.1. Sample size and percent moisture content [%; mean \pm standard deviation (SD)] in parentheses for each species and tissue. ND = not determined due to small sample size.

Species	Blubber	Brain	Kidney	Liver	Lung	Muscle	Placenta	Skin	Spleen	Umbilical cord	Uterus
Atlantic spotted dolphin	6 (35 \pm 12)	1 (56 \pm ND)	5 (67 \pm 22)	6 (68 \pm 5)	6 (77 \pm 7)	0	0	5 (52 \pm 13)	0	0	0
Blainville's beaked whale	1 (22 \pm ND)	1 (65 \pm ND)	1 (74 \pm ND)	1 (66 \pm ND)	1 (91 \pm ND)	0	0	1 (37 \pm ND)	0	0	0
Bottlenose dolphin	37 (37 \pm 16)	9 (72 \pm 6)	61 (77 \pm 0.18)	72 (76 \pm 7)	64 (77 \pm 3)	2 (72 \pm ND)	1 (85 \pm ND)	31 (58 \pm 9)	1 (77 \pm 1)	1 (82 \pm ND)	6 (78 \pm 5)
Dwarf sperm whale	2 (41 \pm ND)	0	0	2 (71 \pm ND)	2 (77 \pm ND)	0	0	1 (63 \pm ND)	0	0	1 (76 \pm ND)
Melon-headed whale	4 (60 \pm 6)	2 (76 \pm ND)	3 (77 \pm 0.54)	4 (69 \pm 1)	4 (77 \pm 2)	0	0	3 (64 \pm 4)	0	0	0
Pantropical spotted dolphin	2 (52 \pm ND)	0	0	1 (62 \pm ND)	1 (76 \pm ND)	0	0	2 (58 \pm ND)	0	0	0
Pygmy killer whale	1 (43 \pm ND)	0	0	1 (72 \pm ND)	1 (76 \pm ND)	0	0	0	0	0	0

Pygmy sperm whale	3	0	2	3	3	0	0	1	0	0	0
	(37 ± 2)		(78 ± ND)	(66 ± 2)	(74 ± 3)			(57 ± ND)			
Risso's dolphin	2	1	1	2	2	0	0	2	0	0	1
	(56 ± ND)	(80 ± ND)	(77 ± ND)	(62 ± ND)	(80 ± ND)			(64 ± ND)			(67 ± ND)
Rough-toothed dolphin	1	0	1	1	1	0	0	1	0	0	0
	(62 ± ND)		(76 ± ND)	(68 ± ND)	(78 ± ND)			(66 ± ND)			
Short-finned pilot whale	0		1	1	1	0	0	0	0	0	0
			(76 ± ND)	(70 ± ND)	(79 ± ND)						
<i>Stenella</i> sp.	0	1	0	1	1	0	0	1	0	1	1
		(76 ± ND)		(25 ± ND)	(74 ± ND)			(45 ± ND)		(87 ± ND)	(74 ± ND)

Table S4.2. AIC_c model selection with bottlenose dolphin (*Tursiops truncatus*) blubber THg concentration as the response variable and body length, sex, condition code, and stranding year as explanatory variables. df = degrees of freedom, logLik = log likelihood, AIC_c = Akaike's Information Criterion for small sample sizes, delta= delta score, weight = Akaike weight.

Intercept	Condition code	Length	Sex	Year	Df	logLik	AICc	delta	weight
-1.84	NA	0.01	+	NA	4	-22.45	54.19	0.00	0.31
-1.96	NA	0.01	NA	NA	3	-23.90	54.55	0.36	0.26
-2.13	0.12	0.01	+	NA	5	-21.99	55.98	1.79	0.13
-1.73	NA	0.01	NA	+	7	-19.05	56.09	1.90	0.12
-2.26	0.11	0.01	NA	NA	4	-23.48	56.26	2.07	0.11
-2.05	0.12	0.01	NA	+	8	-18.50	58.34	4.15	0.04
-1.73	NA	0.01	+	+	8	-18.89	59.11	4.92	0.03
-2.07	0.13	0.01	+	+	9	-18.28	61.49	7.30	0.01
0.00	NA	NA	NA	NA	2	-35.30	74.96	20.77	9.57E-06
0.13	NA	NA	+	NA	3	-34.77	76.29	22.10	4.94E-06
-0.11	0.05	NA	NA	NA	3	-35.26	77.28	23.09	3.01E-06
0.02	0.05	NA	+	NA	4	-34.73	78.75	24.56	1.44E-06
0.21	NA	NA	NA	+	6	-32.71	80.31	26.12	6.62E-07
0.16	0.02	NA	NA	+	7	-32.70	83.39	29.20	1.41E-07
0.21	NA	NA	+	+	7	-32.71	83.41	29.22	1.40E-07
0.16	0.02	NA	+	+	8	-32.70	86.73	32.54	2.67E-08

Table S4.3. AIC_c model selection with bottlenose dolphin (*Tursiops truncatus*) kidney THg concentration as the response variable and body length, sex, condition code, stranding location, and stranding year as explanatory variables. df = degrees of freedom, logLik = log likelihood, AIC_c = Akaike's Information Criterion for small sample sizes, delta= delta score, weight = Akaike weight.

Intercept	Condition code	Length	Location	Sex	Year	df	logLik	AICc	delta	weight
-0.79	0.19	0.01	+	NA	NA	5	-16.99	45.07	0.00	0.41
-0.30	NA	0.01	+	NA	NA	4	-18.51	45.73	0.66	0.29
-0.80	0.20	0.01	+	+	NA	6	-16.76	47.07	2.00	0.15
-0.29	NA	0.01	+	+	NA	5	-18.44	47.97	2.90	0.10
-0.82	0.23	0.01	+	NA	+	8	-15.76	50.29	5.22	0.03
-0.26	NA	0.01	+	NA	+	7	-17.85	51.81	6.74	0.01
-0.83	0.23	0.01	+	+	+	9	-15.64	52.82	7.75	0.01
-0.26	NA	0.01	+	+	+	8	-17.83	54.42	9.36	3.78E-03
-0.04	-0.30	0.01	NA	NA	NA	4	-37.20	83.11	38.04	2.23E-09
-0.04	-0.30	0.01	NA	+	NA	5	-37.20	85.48	40.41	6.81E-10
-0.98	NA	0.01	NA	NA	NA	3	-40.21	86.85	41.78	3.44E-10
-0.97	NA	0.01	NA	+	NA	4	-40.16	89.02	43.96	1.16E-10
-0.18	-0.28	0.01	NA	NA	+	7	-36.58	89.28	44.21	1.02E-10
-1.07	NA	0.01	NA	NA	+	6	-39.19	91.93	46.86	2.72E-11
-0.18	-0.28	0.01	NA	+	+	8	-36.58	91.94	46.87	2.70E-11
-1.07	NA	0.01	NA	+	+	7	-39.15	94.42	49.35	7.81E-12
1.44	NA	NA	+	NA	NA	3	-51.47	109.36	64.29	4.45E-15
1.38	NA	NA	+	+	NA	4	-51.18	111.07	66.00	1.89E-15
1.25	0.08	NA	+	NA	NA	4	-51.37	111.46	66.39	1.56E-15
1.24	0.06	NA	+	+	NA	5	-51.12	113.34	68.27	6.09E-16
1.50	NA	NA	+	NA	+	6	-51.41	116.37	71.30	1.34E-16
1.45	NA	NA	+	+	+	7	-51.05	118.22	73.15	5.31E-17
1.28	0.10	NA	+	NA	+	7	-51.28	118.68	73.61	4.22E-17

1.27	0.08	NA	+	+	+	8	-50.97	120.70	75.63	1.53E-17
2.45	-0.55	NA	NA	NA	NA	3	-63.07	132.57	87.50	4.06E-20
2.39	-0.57	NA	NA	+	NA	4	-62.48	133.67	88.60	2.34E-20
2.29	-0.55	NA	NA	NA	+	6	-62.71	138.98	93.91	1.64E-21
0.94	NA	NA	NA	NA	NA	2	-67.47	139.14	94.07	1.52E-21
2.26	-0.56	NA	NA	+	+	7	-62.18	140.47	95.40	7.80E-22
0.86	NA	NA	NA	+	NA	3	-67.21	140.84	95.77	6.48E-22
0.79	NA	NA	NA	NA	+	5	-66.92	144.92	99.85	8.43E-23
0.73	NA	NA	NA	+	+	6	-66.64	146.84	101.77	3.23E-23

Table S4.4. AIC_c model selection with bottlenose dolphin (*Tursiops truncatus*) liver THg concentration as the response variable and body length, sex, condition code, stranding location, and stranding year as explanatory variables. df = degrees of freedom, logLik = log likelihood, AIC_c = Akaike's Information Criterion for small sample sizes, delta= delta score, weight = Akaike weight.

Intercept	Condition code	Length	Location	Sex	Year	df	logLik	AICc	delta	weight
1.19	0.43	NA	+	NA	NA	4	-70.27	149.14	0.00	0.41
1.22	0.44	NA	+	+	NA	5	-70.13	151.18	2.04	0.15
1.29	0.42	-4.08E-04	+	NA	NA	5	-70.22	151.36	2.22	0.14
2.17	NA	NA	+	NA	NA	3	-72.55	151.45	2.32	0.13
2.32	NA	-7.37E-04	+	NA	NA	4	-72.41	153.42	4.28	0.05
1.31	0.43	-3.33E-04	+	+	NA	6	-70.10	153.50	4.37	0.05
2.20	NA	NA	+	+	NA	4	-72.48	153.56	4.42	0.05
2.34	NA	-6.98E-04	+	+	NA	5	-72.36	155.62	6.49	0.02
1.00	0.46	NA	+	NA	+	8	-69.44	157.17	8.03	0.01
2.02	NA	NA	+	NA	+	7	-71.82	159.39	10.26	2.44E-03
1.01	0.47	NA	+	+	+	9	-69.29	159.49	10.36	2.33E-03
1.08	0.45	-3.21E-04	+	NA	+	9	-69.41	159.73	10.60	2.06E-03
2.19	NA	-8.19E-04	+	NA	+	8	-71.65	161.58	12.45	8.18E-04
2.04	NA	NA	+	+	+	8	-71.74	161.77	12.63	7.46E-04
1.08	0.46	-2.32E-04	+	+	+	10	-69.28	162.17	13.03	6.11E-04
2.20	NA	-7.65E-04	+	+	+	9	-71.59	164.09	14.95	2.34E-04
1.78	NA	NA	NA	NA	NA	2	-81.46	167.10	17.96	5.19E-05
2.40	-0.23	NA	NA	NA	NA	3	-80.49	167.34	18.20	4.60E-05
1.60	NA	9.24E-04	NA	NA	NA	3	-81.28	168.91	19.77	2.10E-05
1.77	NA	NA	NA	+	NA	3	-81.45	169.26	20.13	1.76E-05
2.29	-0.22	4.00E-04	NA	NA	NA	4	-80.46	169.52	20.38	1.55E-05
2.39	-0.23	NA	NA	+	NA	4	-80.49	169.58	20.44	1.50E-05
1.60	NA	9.16E-04	NA	+	NA	4	-81.28	171.15	22.01	6.85E-06

1.52	NA	NA	NA	NA	+	6	-79.21	171.71	22.57	5.18E-06
2.29	-0.22	3.91E-04	NA	+	NA	5	-80.46	171.83	22.69	4.88E-06
2.04	-0.19	NA	NA	NA	+	7	-78.62	173.00	23.86	2.72E-06
1.39	NA	6.70E-04	NA	NA	+	7	-79.11	173.96	24.83	1.68E-06
1.53	NA	NA	NA	+	+	7	-79.21	174.16	25.02	1.52E-06
1.98	-0.18	2.10E-04	NA	NA	+	8	-78.61	175.52	26.38	7.71E-07
2.04	-0.19	NA	NA	+	+	8	-78.62	175.53	26.39	7.66E-07
1.40	NA	6.93E-04	NA	+	+	8	-79.10	176.48	27.35	4.76E-07
1.98	-0.18	2.29E-04	NA	+	+	9	-78.61	178.12	28.99	2.09E-07

Table S4.5. AIC_c model selection with bottlenose dolphin (*Tursiops truncatus*) lung THg concentration as the response variable and body length, sex, condition code, stranding location, and stranding year as explanatory variables. df = degrees of freedom, logLik = log likelihood, AIC_c = Akaike's Information Criterion for small sample sizes, delta= delta score, weight = Akaike weight.

267

	Condition code	Length	Location	Sex	Year	df	logLik	AICc	delta	weight
Intercept										
-0.52	NA	0.01	+	+	NA	6	-32.90	79.30	0.00	0.52
-0.69	NA	0.01	+	NA	NA	4	-36.15	81.00	1.70	0.22
-0.45	-0.03	0.01	+	+	NA	7	-32.88	81.80	2.50	0.15
-0.38	-0.12	0.01	+	NA	NA	5	-35.82	82.70	3.40	0.10
-0.53	NA	0.01	+	+	+	10	-32.49	89.21	9.91	3.68E-03
-0.65	NA	0.01	+	NA	+	8	-35.73	90.13	10.83	2.33E-03
-0.49	-0.02	0.01	+	+	+	11	-32.49	92.15	12.85	8.48E-04
-0.42	-0.09	0.01	+	NA	+	9	-35.59	92.58	13.28	6.85E-04
0.88	-0.73	0.01	NA	NA	NA	4	-51.74	112.16	32.86	3.83E-08
1.01	NA	NA	+	+	NA	5	-51.05	113.15	33.85	2.33E-08
0.80	NA	NA	+	NA	NA	3	-53.99	114.38	35.08	1.26E-08
0.82	-0.72	0.01	NA	+	NA	6	-50.58	114.66	35.36	1.10E-08
1.43	-0.26	NA	+	NA	NA	4	-53.11	114.90	35.60	9.73E-09
1.27	-0.12	NA	+	+	NA	6	-50.88	115.26	35.96	8.11E-09
0.85	-0.75	0.01	NA	NA	+	8	-50.34	119.34	40.04	1.06E-09
0.78	-0.74	0.01	NA	+	+	10	-48.79	121.80	42.51	3.08E-10
0.98	NA	NA	+	+	+	9	-50.68	122.75	43.45	1.92E-10
0.84	NA	NA	+	NA	+	7	-53.66	123.36	44.06	1.41E-10
1.62	-0.34	NA	+	NA	+	8	-52.39	123.44	44.14	1.36E-10
1.44	-0.21	NA	+	+	+	10	-50.21	124.65	45.35	7.45E-11
-1.26	NA	0.01	NA	NA	NA	3	-61.83	130.07	50.77	4.95E-12
2.59	-0.84	NA	NA	NA	NA	3	-62.68	131.77	52.47	2.11E-12

-1.20	NA	0.01	NA	+	NA	5	-60.48	132.01	52.71	1.87E-12
-1.45	NA	0.01	NA	NA	+	7	-59.73	135.49	56.19	3.29E-13
2.60	-0.82	NA	NA	+	NA	5	-62.50	136.04	56.74	2.49E-13
2.59	-0.92	NA	NA	NA	+	7	-60.23	136.50	57.20	1.98E-13
-1.39	NA	0.01	NA	+	+	9	-57.96	137.32	58.02	1.32E-13
2.58	-0.89	NA	NA	+	+	9	-59.69	140.78	61.48	2.34E-14
0.35	NA	NA	NA	NA	NA	2	-72.50	149.20	69.90	3.47E-16
0.50	NA	NA	NA	+	NA	4	-71.67	152.03	72.73	8.44E-17
0.11	NA	NA	NA	NA	+	6	-70.82	155.15	75.85	1.77E-17
0.25	NA	NA	NA	+	+	8	-69.43	157.52	78.22	5.42E-18

Table S4.6. AIC_c model selection with bottlenose dolphin (*Tursiops truncatus*) skin THg concentration as the response variable and body length, sex, condition code, and stranding year as explanatory variables. df = degrees of freedom, logLik = log likelihood, AIC_c = Akaike's Information Criterion for small sample sizes, delta= delta score, weight = Akaike weight.

Intercept	Condition code	Length	Sex	Year	df	logLik	AICc	delta	weight
-0.43	NA	5.00E-03	NA	NA	3	-4.57	16.03	0.00	0.66
-0.49	0.03	4.91E-03	NA	NA	4	-4.45	18.45	2.42	0.20
-0.48	NA	4.76E-03	NA	+	8	0.90	20.75	4.72	0.06
-0.41	NA	4.90E-03	+	NA	5	-4.36	21.13	5.10	0.05
-0.45	0.02	4.87E-03	+	NA	6	-4.32	24.15	8.12	0.01
-0.52	0.03	4.64E-03	NA	+	9	1.01	24.55	8.53	0.01
-0.52	NA	4.80E-03	+	+	10	1.30	28.41	12.38	1.36E-03
-0.62	0.05	4.63E-03	+	+	11	1.69	32.52	16.49	1.74E-04
0.62	NA	NA	NA	NA	2	-15.04	34.51	18.49	6.43E-05
0.39	0.09	NA	NA	NA	3	-14.46	35.82	19.79	3.35E-05
0.67	NA	NA	+	NA	4	-14.32	38.17	22.14	1.03E-05
0.53	NA	NA	NA	+	7	-10.28	39.42	23.40	5.52E-06
0.50	0.06	NA	+	NA	5	-14.09	40.58	24.55	3.10E-06
0.26	0.11	NA	NA	+	8	-9.16	40.86	24.83	2.70E-06
0.52	NA	NA	+	+	9	-9.39	45.35	29.33	2.84E-07
0.20	0.12	NA	+	+	10	-8.25	47.51	31.48	9.69E-08

Table S4.7. AIC_c model selection with bottlenose dolphin (*Tursiops truncatus*) blubber Se concentration as the response variable and body length, sex, condition code, and stranding year as explanatory variables. df = degrees of freedom, logLik = log likelihood, AIC_c = Akaike's Information Criterion for small sample sizes, delta= delta score, weight = Akaike weight.

Intercept	Condition code	Length	Sex	Year	df	logLik	AICc	delta	weight
-1.84	NA	0.01	+	NA	4	-22.45	54.19	0.00	0.31
-1.96	NA	0.01	NA	NA	3	-23.90	54.55	0.36	0.26
-2.13	0.12	0.01	+	NA	5	-21.99	55.98	1.79	0.13
-1.73	NA	0.01	NA	+	7	-19.05	56.09	1.90	0.12
-2.26	0.11	0.01	NA	NA	4	-23.48	56.26	2.07	0.11
-2.05	0.12	0.01	NA	+	8	-18.50	58.34	4.15	0.04
-1.73	NA	0.01	+	+	8	-18.89	59.11	4.92	0.03
-2.07	0.13	0.01	+	+	9	-18.28	61.49	7.30	0.01
0.00	NA	NA	NA	NA	2	-35.30	74.96	20.77	9.57E-06
0.13	NA	NA	+	NA	3	-34.77	76.29	22.10	4.94E-06
-0.11	0.05	NA	NA	NA	3	-35.26	77.28	23.09	3.01E-06
0.02	0.05	NA	+	NA	4	-34.73	78.75	24.56	1.44E-06
0.21	NA	NA	NA	+	6	-32.71	80.31	26.12	6.62E-07
0.16	0.02	NA	NA	+	7	-32.70	83.39	29.20	1.41E-07
0.21	NA	NA	+	+	7	-32.71	83.41	29.22	1.40E-07
0.16	0.02	NA	+	+	8	-32.70	86.73	32.54	2.67E-08

Table S4.8. AIC_c model selection with bottlenose dolphin (*Tursiops truncatus*) kidney Se concentration as the response variable and body length, sex, condition code, stranding location, and stranding year as explanatory variables. df = degrees of freedom, logLik = log likelihood, AIC_c = Akaike's Information Criterion for small sample sizes, delta= delta score, weight = Akaike weight.

Intercept	Condition code	Length	Location	Sex	Year	df	logLik	AICc	delta	weight
0.34	NA	4.31E-03	+	NA	NA	4	18.53	-28.34	0.00	0.54
0.25	0.04	4.33E-03	+	NA	NA	5	18.71	-26.33	2.01	0.20
0.34	NA	4.31E-03	+	+	NA	5	18.53	-25.96	2.38	0.17
0.25	0.04	4.34E-03	+	+	NA	6	18.71	-23.87	4.47	0.06
0.34	NA	4.33E-03	+	NA	+	7	18.88	-21.64	6.70	0.02
0.22	0.05	4.36E-03	+	NA	+	8	19.17	-19.57	8.77	0.01
0.34	NA	4.32E-03	+	+	+	8	18.89	-19.02	9.32	0.01
0.22	0.05	4.36E-03	+	+	+	9	19.17	-16.82	11.52	1.71E-03
0.54	-0.16	4.65E-03	NA	NA	NA	4	7.33	-5.95	22.39	7.47E-06
0.54	-0.16	4.62 E-03	NA	+	NA	5	7.39	-3.68	24.66	2.41E-06
0.06	NA	4.94E-03	NA	NA	NA	3	3.98	-1.54	26.80	8.23E-07
0.46	-0.15	4.65E-03	NA	NA	+	7	8.09	-0.06	28.27	3.95E-07
0.06	NA	4.95E-03	NA	+	NA	4	3.98	0.76	29.09	2.62E-07
0.46	-0.15	4.62E-03	NA	+	+	8	8.14	2.48	30.82	1.11E-07
0.01	NA	4.93E-03	NA	NA	+	6	5.15	3.25	31.59	7.51E-08
0.00	NA	4.93E-03	NA	+	+	7	5.15	5.81	34.15	2.09E-08
1.27	NA	NA	+	NA	NA	3	-13.57	33.56	61.90	1.97E-14
1.23	NA	NA	+	+	NA	4	-13.08	34.88	63.22	1.02E-14
1.32	-0.02	NA	+	NA	NA	4	-13.55	35.81	64.15	6.38E-15
1.31	-0.04	NA	+	+	NA	5	-13.02	37.12	65.46	3.32E-15
1.28	NA	NA	+	NA	+	6	-13.54	40.64	68.97	5.73E-16
1.24	NA	NA	+	+	+	7	-12.99	42.10	70.43	2.76E-16
1.32	-0.02	NA	+	NA	+	7	-13.52	43.15	71.49	1.63E-16

1.32	-0.03	NA	+	+	+	8	-12.94	44.65	72.99	7.71E-17
1.82	-0.28	NA	NA	NA	NA	3	-20.96	48.34	76.68	1.22E-17
1.78	-0.30	NA	NA	+	NA	4	-20.07	48.86	77.20	9.38E-18
1.73	-0.28	NA	NA	NA	+	6	-20.44	54.43	82.77	5.78E-19
1.04	NA	NA	NA	NA	NA	2	-25.53	55.27	83.61	3.81E-19
1.71	-0.29	NA	NA	+	+	7	-19.64	55.39	83.73	3.58E-19
1.00	NA	NA	NA	+	NA	3	-25.10	56.62	84.96	1.94E-19
0.96	NA	NA	NA	NA	+	5	-24.85	60.79	89.13	2.41E-20
0.92	NA	NA	NA	+	+	6	-24.40	62.36	90.70	1.10E-20

Table S4.9. AIC_c model selection with bottlenose dolphin (*Tursiops truncatus*) liver Se concentration as the response variable and body length, sex, condition code, stranding location, and stranding year as explanatory variables. df = degrees of freedom, logLik = log likelihood, AIC_c = Akaike's Information Criterion for small sample sizes, delta= delta score, weight = Akaike weight.

Intercept	Condition code	Length	Location	Sex	Year	df	logLik	AICc	delta	weight
0.83	0.42	NA	+	NA	NA	4	-68.08	144.76	0.00	0.42
0.86	0.43	NA	+	+	NA	5	-67.91	146.73	1.97	0.16
0.89	0.41	-2.32E-04	+	NA	NA	5	-68.07	147.04	2.28	0.13
1.78	NA	NA	+	NA	NA	3	-70.39	147.12	2.36	0.13
0.90	0.42	-1.47E-04	+	+	NA	6	-67.90	149.10	4.34	0.05
1.82	NA	NA	+	+	NA	4	-70.29	149.17	4.41	0.05
1.90	NA	-5.54E-04	+	NA	NA	4	-70.30	149.20	4.44	0.05
1.92	NA	-4.97E-04	+	+	NA	5	-70.22	151.35	6.59	0.02
0.70	0.46	NA	+	NA	+	8	-67.50	153.28	8.52	0.01
0.71	0.47	NA	+	+	+	9	-67.36	155.63	10.87	1.82E-03
1.72	NA	NA	+	NA	+	7	-70.02	155.80	11.04	1.67E-03
0.72	0.46	-8.35E-05	+	NA	+	9	-67.49	155.89	11.13	1.59E-03
1.85	NA	-5.90E-04	+	NA	+	8	-69.93	158.14	13.38	5.17E-04
1.74	NA	NA	+	+	+	8	-69.95	158.19	13.43	5.04E-04
0.71	0.47	2.94E-06	+	+	+	10	-67.36	158.33	13.57	4.71E-04
1.86	NA	-5.39E-04	+	+	+	9	-69.88	160.66	15.89	1.47E-04
1.43	NA	NA	NA	NA	NA	2	-78.32	160.81	16.05	1.36E-04
1.95	-0.20	NA	NA	NA	NA	3	-77.57	161.49	16.72	9.72E-05
1.24	NA	9.48E-04	NA	NA	NA	3	-78.11	162.57	17.80	5.67E-05
1.43	NA	NA	NA	+	NA	3	-78.32	162.99	18.23	4.58E-05
1.81	-0.18	-5.16E-04	NA	NA	NA	4	-77.51	163.61	18.85	3.36E-05
1.95	-0.20	NA	NA	+	NA	4	-77.57	163.73	18.97	3.17E-05
1.24	NA	9.57E-04	NA	+	NA	4	-78.11	164.81	20.05	1.85E-05

1.81	-0.18	5.26E-04	NA	+	NA	5	-77.51	165.92	21.16	1.06E-05
1.26	NA	NA	NA	NA	+	6	-76.92	167.13	22.37	5.78E-06
1.70	-0.16	NA	NA	NA	+	7	-76.47	168.68	23.92	2.66E-06
1.11	NA	7.96E-04	NA	NA	+	7	-76.77	169.28	24.52	1.97E-06
1.26	NA	NA	NA	+	+	7	-76.92	169.59	24.82	1.69E-06
1.57	-0.14	4.25E-04	NA	NA	+	8	-76.43	171.14	26.38	7.79E-07
1.70	-0.16	NA	NA	+	+	8	-76.47	171.22	26.46	7.50E-07
1.11	NA	8.18E-04	NA	+	+	8	-76.76	171.80	27.04	5.58E-07
1.58	-0.14	4.45E-04	NA	+	+	9	-76.42	173.75	28.99	2.11E-07

Table S4.10. AIC_c model selection with bottlenose dolphin (*Tursiops truncatus*) lung Se concentration as the response variable and body length, sex, condition code, stranding location, and stranding year as explanatory variables. df = degrees of freedom, logLik = log likelihood, AIC_c = Akaike's Information Criterion for small sample sizes, delta= delta score, weight = Akaike weight.

Intercept	Condition code	Length	Location	Sex	Year	df	logLik	AIC _c	delta	weight
0.20	NA	2.96E-03	+	+	NA	6	11.38	-9.25	0.00	0.50
0.34	-0.06	2.93E-03	+	+	NA	7	11.73	-7.43	1.83	0.20
0.08	NA	3.06E-03	+	NA	NA	4	7.70	-6.70	2.55	0.14
0.38	-0.11	2.95E-03	+	NA	NA	5	8.88	-6.70	2.55	0.14
0.67	-0.25	2.90E-03	NA	NA	NA	4	4.63	-0.57	8.68	0.01
0.20	NA	2.82E-03	+	+	+	10	12.35	-0.47	8.78	0.01
0.51	-0.15	2.72E-03	+	NA	+	9	10.58	0.24	9.50	4.31E-03
0.47	-0.11	2.69E-03	+	+	+	11	13.31	0.55	9.80	3.69E-03
0.11	NA	2.95E-03	+	NA	+	8	8.78	1.11	10.36	2.79E-03
0.67	-0.24	2.97E-03	NA	+	NA	6	5.92	1.65	10.90	2.13E-03
0.77	-0.29	2.59E-03	NA	NA	+	8	7.27	4.13	13.38	6.18E-04
0.76	-0.27	2.62E-03	NA	+	+	10	8.94	6.36	15.61	2.02E-04
-0.08	NA	3.24E-03	NA	NA	NA	3	-3.01	12.43	21.68	9.74E-06
0.00	NA	3.25E-03	NA	+	NA	5	-0.97	12.99	22.24	7.35E-06
0.83	NA	NA	+	+	NA	5	-2.52	16.09	25.35	1.56E-06
1.05	-0.10	NA	+	+	NA	6	-1.95	17.40	26.66	8.08E-07
1.14	-0.17	NA	+	NA	NA	4	-4.64	17.98	27.23	6.07E-07
0.73	NA	NA	+	NA	NA	3	-6.41	19.23	28.49	3.24E-07
-0.12	NA	0.00	NA	NA	+	7	-1.60	19.24	28.49	3.23E-07
-0.05	NA	0.00	NA	+	+	9	0.80	19.80	29.05	2.44E-07
1.28	-0.25	NA	+	NA	+	8	-0.97	20.60	29.85	1.63E-07
1.19	-0.18	NA	+	+	+	10	1.81	20.61	29.86	1.63E-07
1.40	-0.30	NA	NA	NA	NA	3	-7.16	20.72	29.97	1.54E-07

1.46	-0.36	NA	NA	NA	+	7	-2.51	21.06	30.31	1.30E-07
0.78	NA	NA	+	+	+	9	-0.02	21.43	30.68	1.08E-07
1.44	-0.33	NA	NA	+	+	9	-0.85	23.11	32.36	4.67E-08
1.40	-0.28	NA	NA	+	NA	5	-6.11	23.28	32.53	4.29E-08
0.71	NA	NA	+	NA	+	7	-4.36	24.75	34.01	2.05E-08
0.59	NA	NA	NA	NA	NA	2	-14.81	33.81	43.06	2.21E-10
0.68	NA	NA	NA	+	NA	4	-12.80	34.30	43.55	1.73E-10
0.56	NA	NA	NA	+	+	8	-9.78	38.23	47.49	2.42E-11
0.50	NA	NA	NA	NA	+	6	-12.64	38.78	48.03	1.85E-11

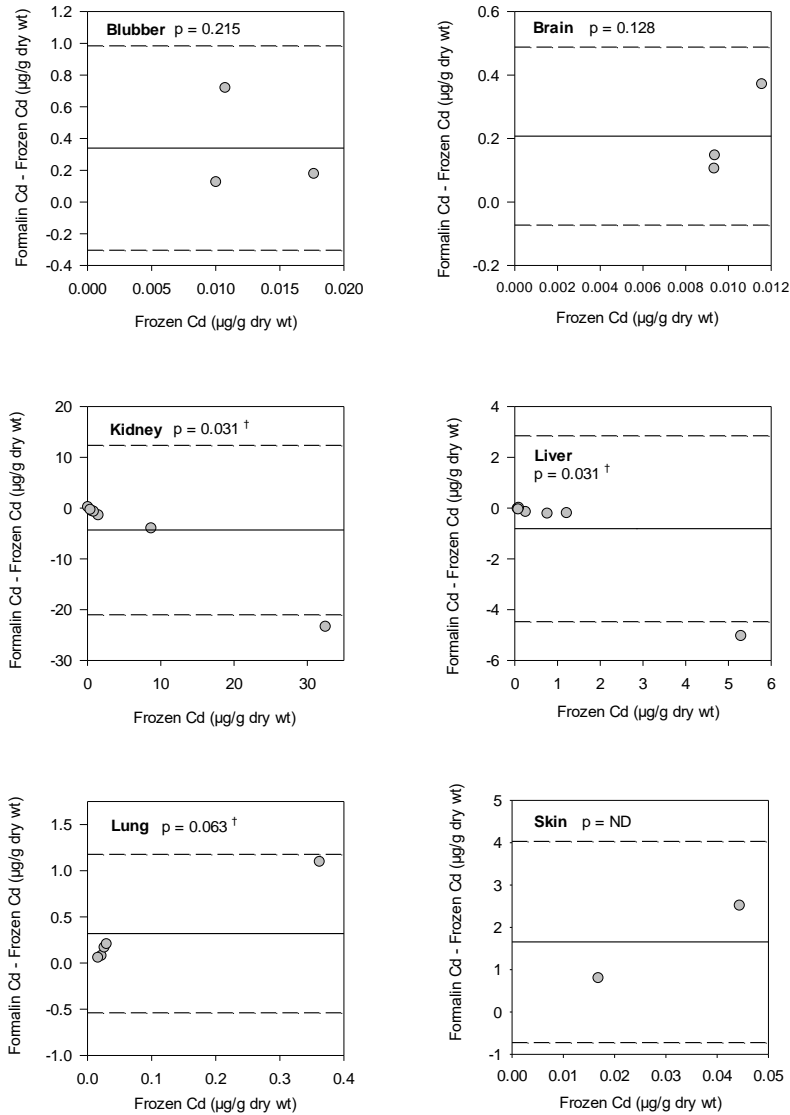
Table S4.11. AIC_c model selection with bottlenose dolphin (*Tursiops truncatus*) skin Se concentration as the response variable and body length, sex, condition code, and stranding year as explanatory variables. df = degrees of freedom, logLik = log likelihood, AIC_c = Akaike's Information Criterion for small sample sizes, delta= delta score, weight = Akaike weight.

Intercept	Condition code	Length	Sex	Year	Df	logLik	AIC _c	delta	weight
0.56	-0.11	4.30E-03	+	NA	6	6.75	2.01	0.00	0.71
0.30	NA	4.11E-03	+	NA	5	4.19	4.02	2.01	0.26
0.36	-0.10	4.47E-03	NA	NA	4	-0.09	9.72	7.71	0.02
0.16	NA	4.18E-03	NA	NA	3	-1.77	10.43	8.42	0.01
0.52	-0.10	3.92E-03	+	+	11	11.63	12.64	10.63	3.49E-03
0.32	NA	3.57E-03	+	+	10	8.80	13.41	11.40	2.37E-03
0.31	NA	3.35E-03	NA	+	8	3.67	15.20	13.20	9.65E-04
0.38	-0.05	3.60E-03	NA	+	9	4.24	18.10	16.09	2.27E-04
1.20	NA	NA	+	NA	4	-7.33	24.19	22.19	1.08E-05
1.40	-0.07	NA	+	NA	5	-6.82	26.03	24.03	4.29E-06
1.05	NA	NA	NA	NA	2	-10.97	26.37	24.36	3.63E-06
1.02	NA	NA	NA	+	7	-3.88	26.62	24.62	3.20E-06
1.17	-0.04	NA	NA	NA	3	-10.79	28.46	26.45	1.28E-06
1.09	NA	NA	+	+	9	-1.07	28.72	26.71	1.12E-06
0.99	0.01	NA	NA	+	8	-3.85	30.25	28.25	5.21E-07
1.21	-0.05	NA	+	+	10	-0.78	32.55	30.55	1.65E-07

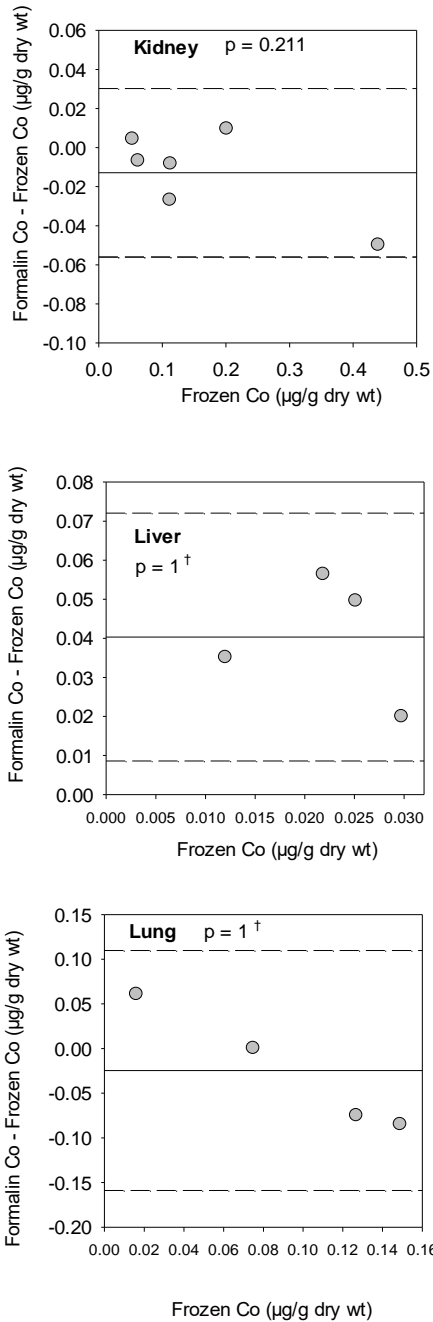
S5.1. Detection limits for trace element concentrations ($\mu\text{g/g}$ dry wt)

As = arsenic; Cd = cadmium; Co = cobalt; Cr = chromium; Cu = copper; Fe = iron; Hg = mercury; Mn = manganese; Ni = nickel; Pb = lead; Se = selenium; Sn = tin; V = vanadium; Zn = zinc; NA = not applicable

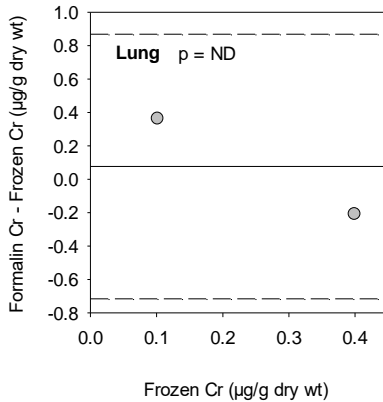
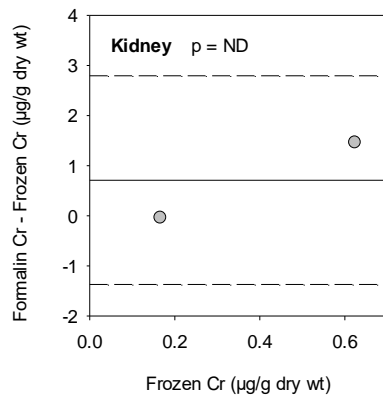
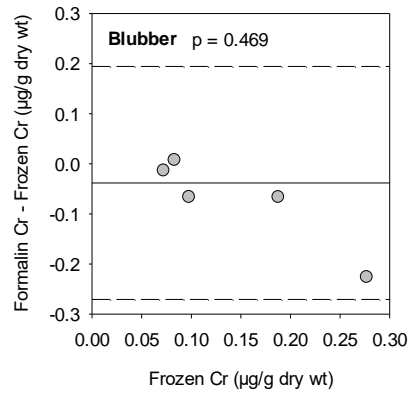
Trace Element	Long-term study			Short-term study
	Frozen blubber, brain, lung, skin	Frozen liver and kidney	All formalin tissues	All tissues
As	0.012	0.100	0.010	0.040
Cd	0.006	0.050	0.005	0.005
Co	0.006	0.010	0.005	0.005
Cr	0.060	1.00	0.050	0.050
Cu	0.120	1.00	0.100	0.100
Fe	2.40	20.0	2.00	2.00
Hg	0.024	0.250	0.050	0.025
Mn	0.060	0.500	0.050	0.020
Ni	0.120	0.100	0.050	0.100
Pb	0.012	0.050	0.010	0.005
Se	0.024	0.100	0.020	0.020
Sn	0.030	0.050	0.020	0.025
V	0.012	0.250	0.005	NA
Zn	2.40	20.0	2.00	2.00



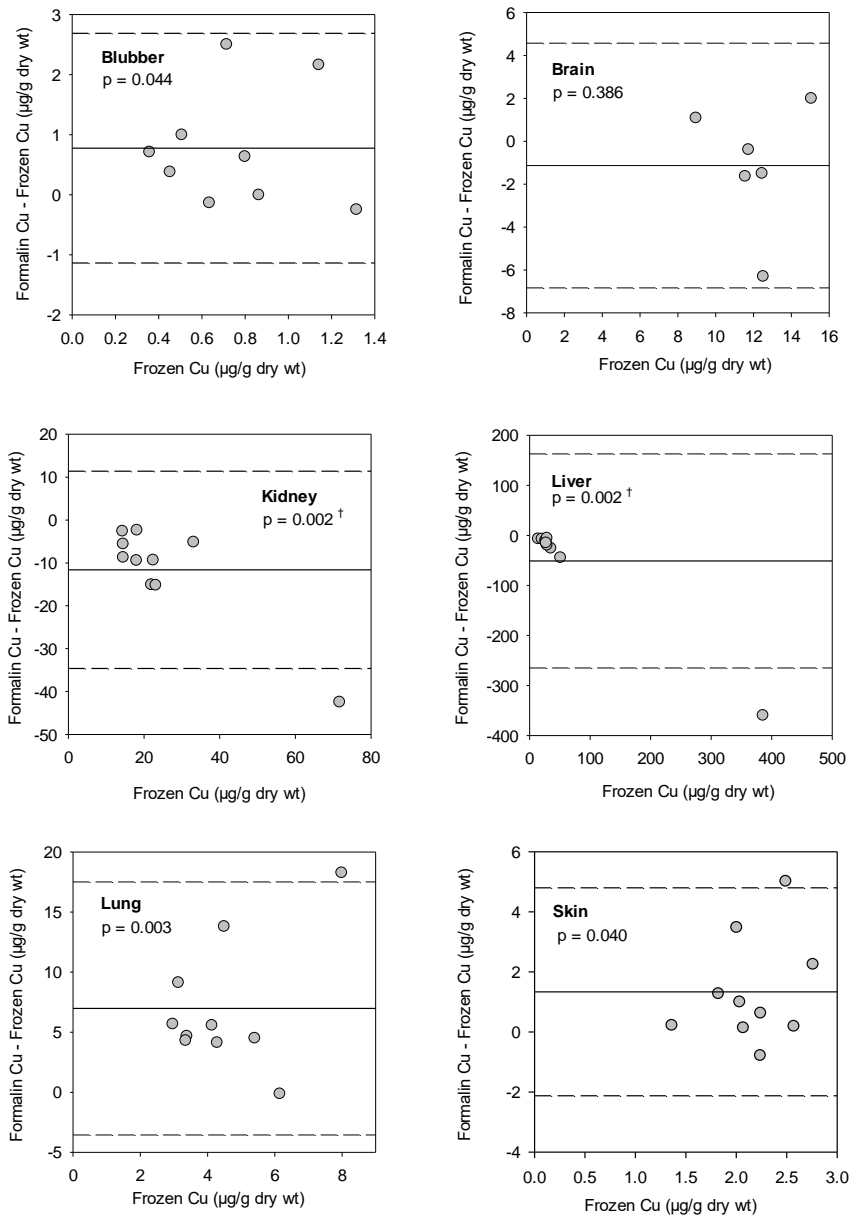
Supplementary Figure 5.1. Bland-Altman plots comparing cadmium (Cd) concentrations ($\mu\text{g/g dry wt}$) in formalin-fixed and frozen *Tursiops truncatus* tissues following long-term preservation and p values from the paired t-tests or Wilcoxon signed-rank tests (†) (ND = not determined). The solid line represents the mean within-pair difference and the dashed lines represent ± 1.96 standard deviations of the mean within-pair difference.



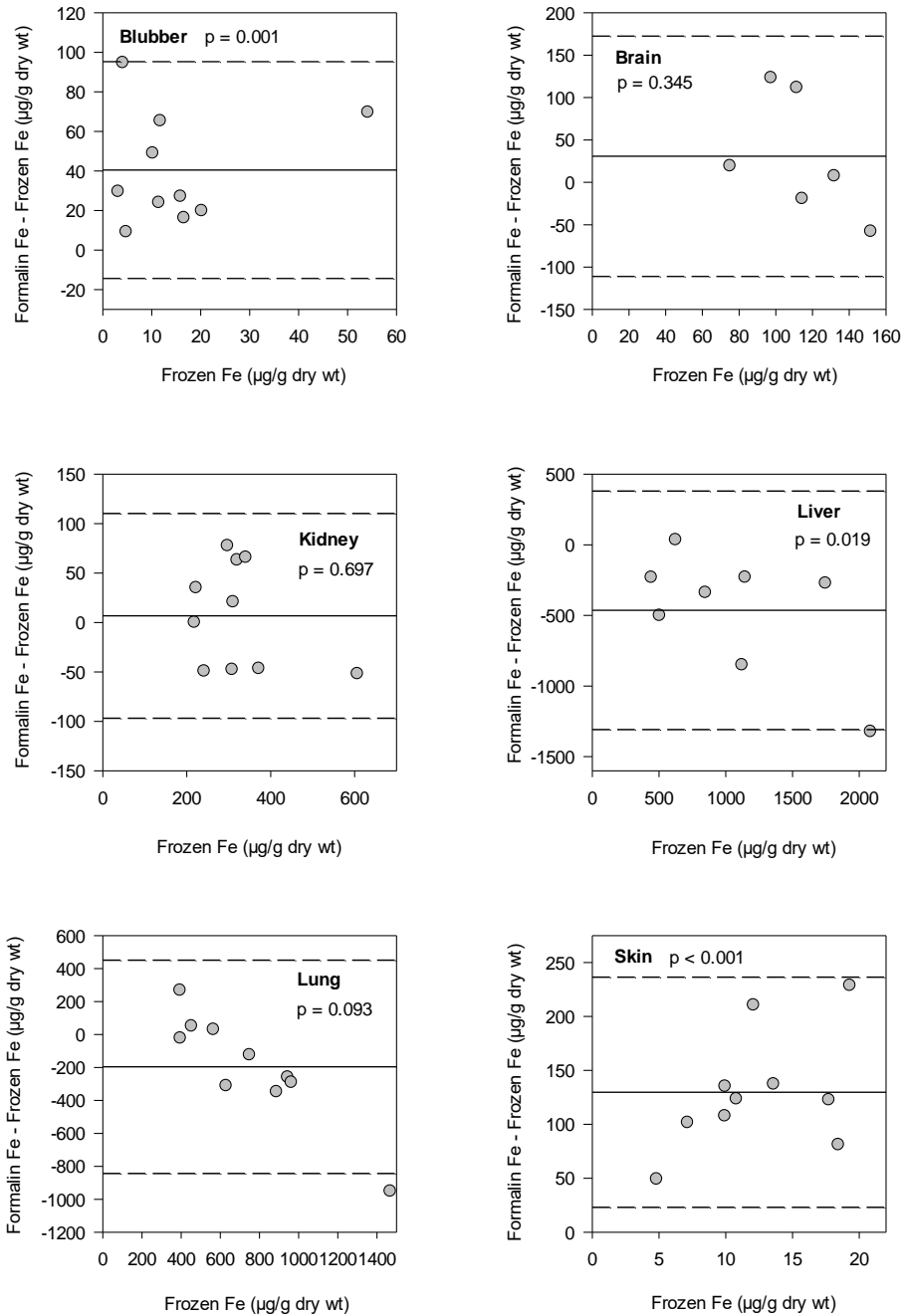
Supplementary Figure 5.2. Bland-Altman plots comparing cobalt (Co) concentrations ($\mu\text{g/g dry wt}$) in formalin-fixed and frozen *Tursiops truncatus* tissues following long-term preservation and p values from the paired t-tests or Wilcoxon signed-rank tests (†). The solid line represents the mean within-pair difference and the dashed lines represent ± 1.96 standard deviations of the mean within-pair difference.



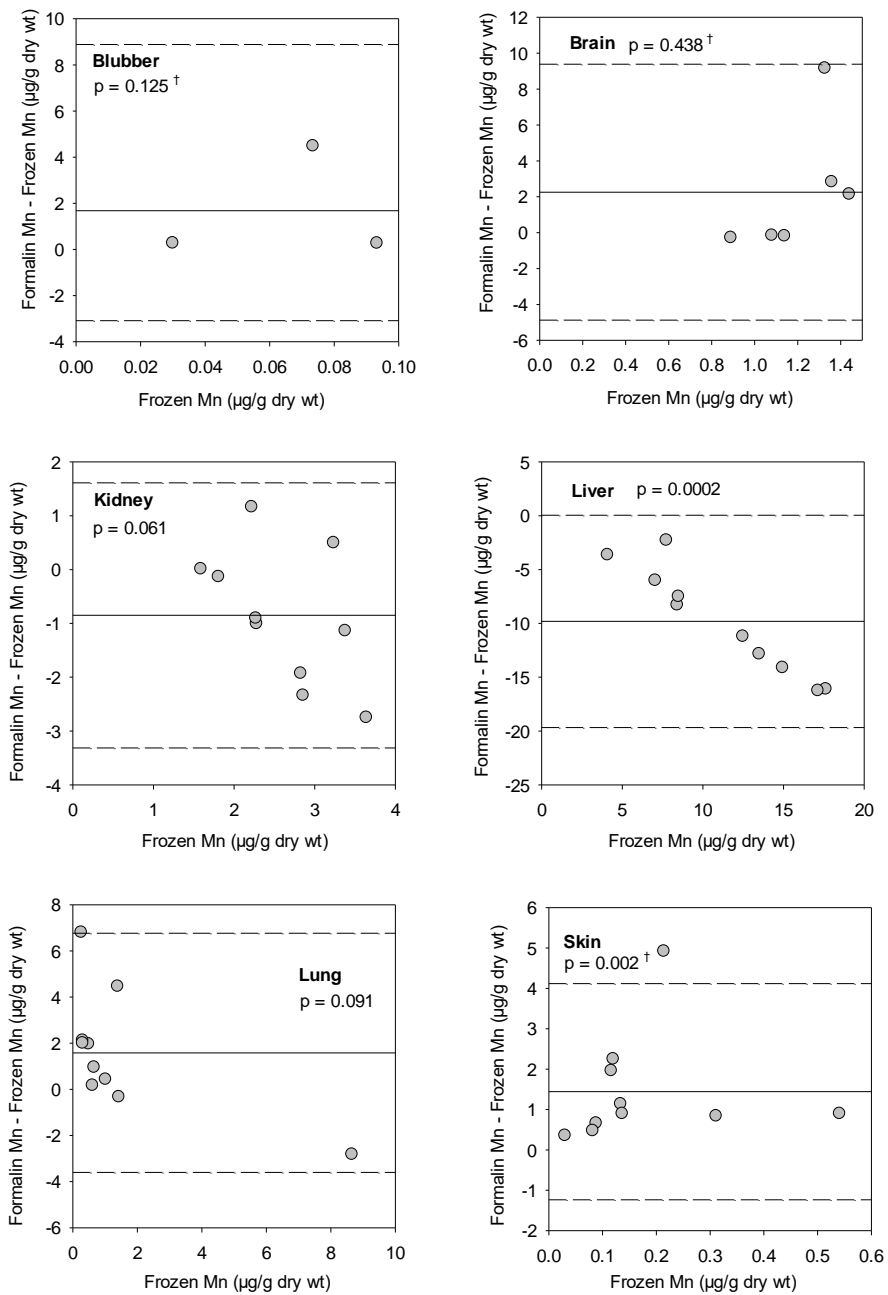
Supplementary Figure 5.3. Bland-Altman plots comparing chromium (Cr) concentrations ($\mu\text{g/g dry wt}$) in formalin-fixed and frozen *Tursiops truncatus* tissues following long-term preservation and p values from the paired t-test (ND = not determined). The solid line represents the mean within-pair difference and the dashed lines represent ± 1.96 standard deviations of the mean within-pair difference.



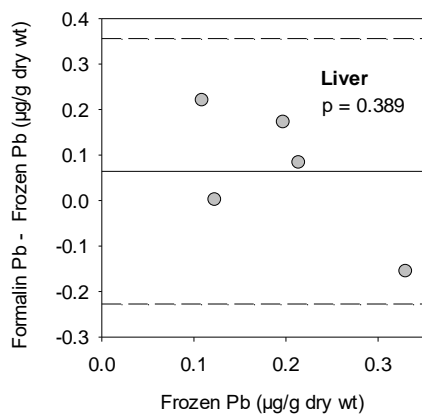
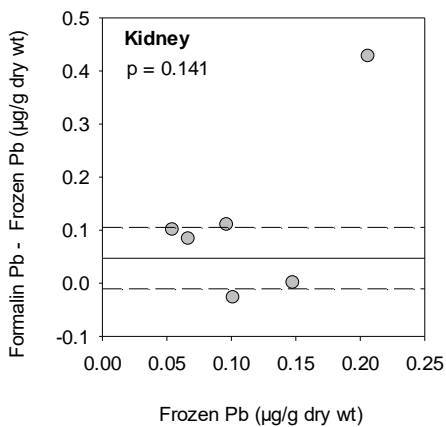
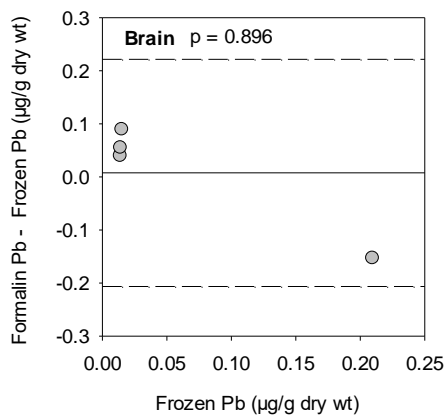
Supplementary Figure 5.4. Bland-Altman plots comparing copper (Cu) concentrations ($\mu\text{g/g}$ dry wt) in formalin-fixed and frozen *Tursiops truncatus* tissues following long-term preservation and p values from the paired t-tests or Wilcoxon signed-rank tests (†). The solid line represents the mean within-pair difference and the dashed lines represent ± 1.96 standard deviations of the mean within-pair difference.



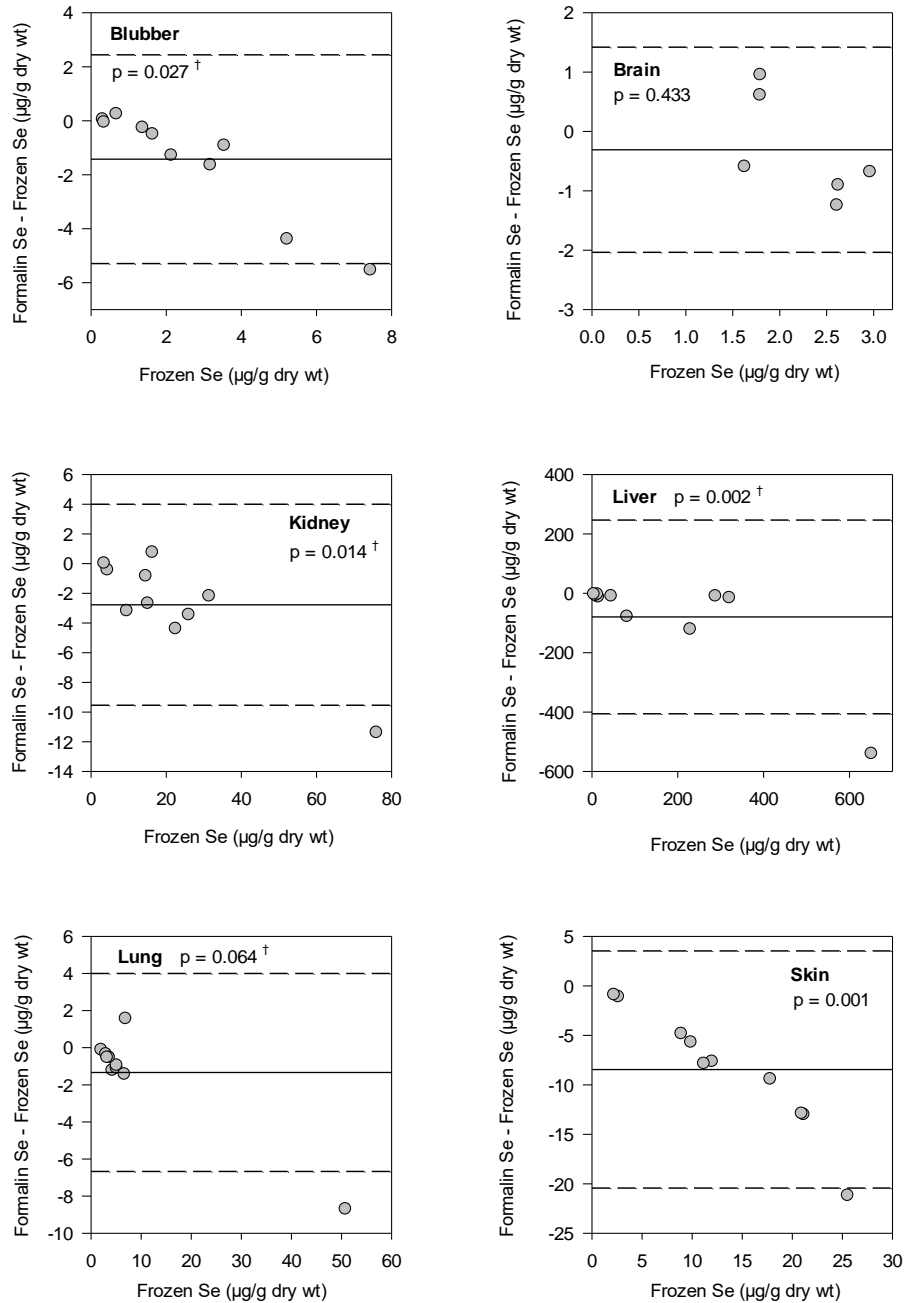
Supplementary Figure 5.5. Bland-Altman plots comparing iron (Fe) concentrations ($\mu\text{g/g}$ dry wt) in formalin-fixed and frozen *Tursiops truncatus* tissues following long-term preservation and p values from the paired t-tests. The solid line represents the mean within-pair difference and the dashed lines represent ± 1.96 standard deviations of the mean within-pair difference.



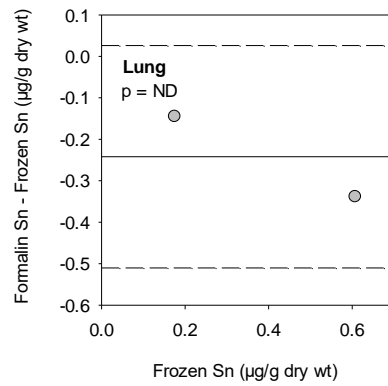
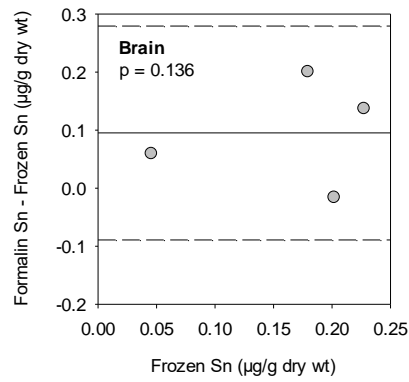
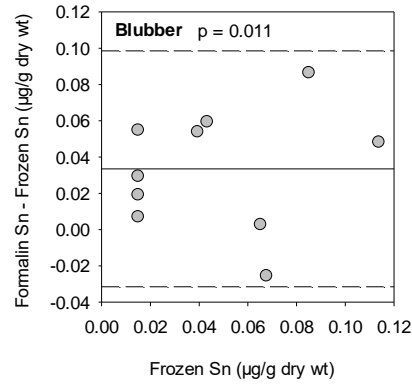
Supplementary Figure 5.6. Bland-Altman plots comparing manganese (Mn) concentrations ($\mu\text{g/g dry wt}$) in formalin-fixed and frozen *Tursiops truncatus* tissues following long-term preservation and p values from the paired t-tests or Wilcoxon signed-rank tests ([†]). The solid line represents the mean within-pair difference and the dashed lines represent ± 1.96 standard deviations of the mean within-pair difference.



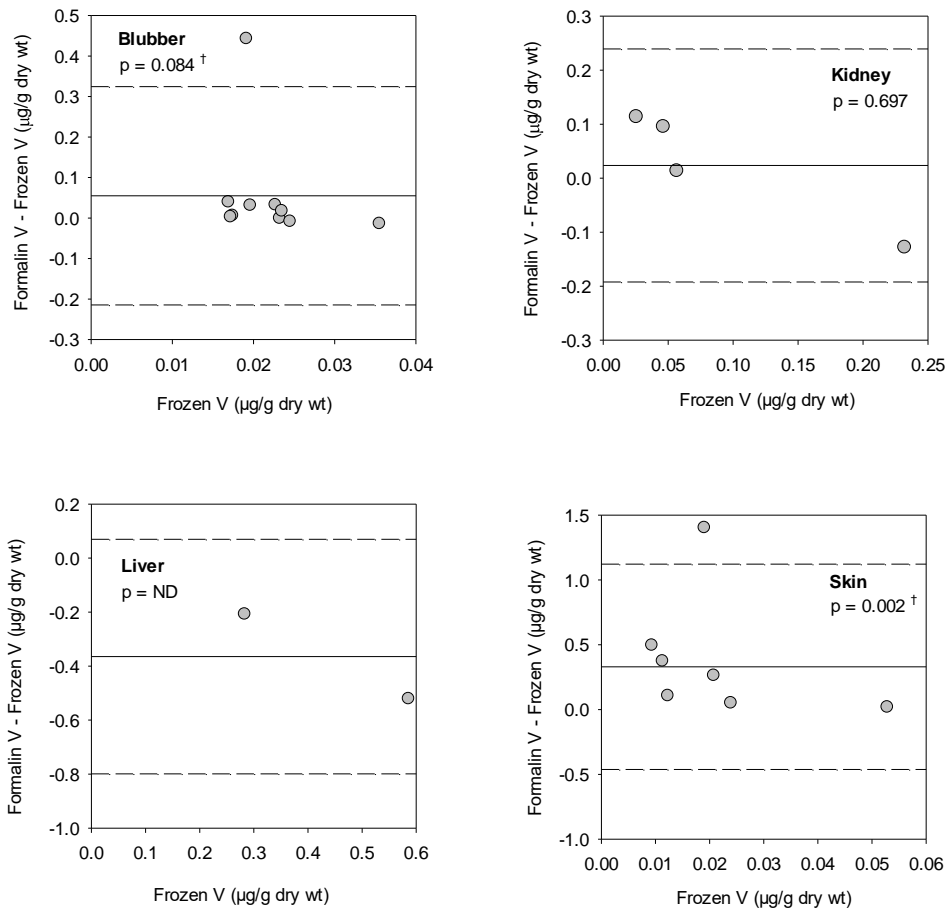
Supplementary Figure 5.7. Bland-Altman plots comparing lead (Pb) concentrations ($\mu\text{g/g}$ dry wt) in formalin-fixed and frozen *Tursiops truncatus* tissues following long-term preservation and p values from the paired t-tests. The solid line represents the mean within-pair difference and the dashed lines represent ± 1.96 standard deviations of the mean within-pair difference.



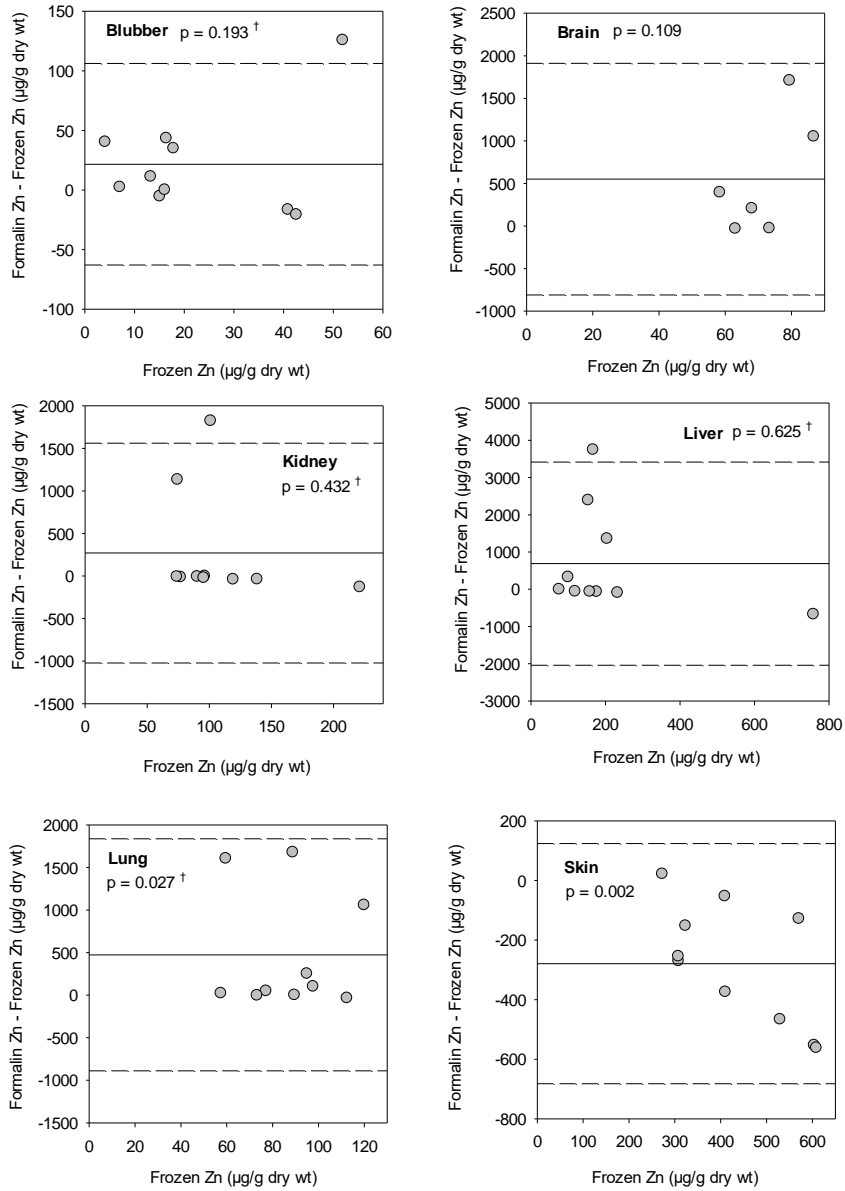
Supplementary Figure 5.8. Bland-Altman plots comparing selenium (Se) concentrations ($\mu\text{g/g}$ dry wt) in formalin-fixed and frozen *Tursiops truncatus* tissues following long-term preservation and p values from the paired t-tests or Wilcoxon signed-rank tests (†). The solid line represents the mean within-pair difference and the dashed lines represent ± 1.96 standard deviations of the mean within-pair difference.



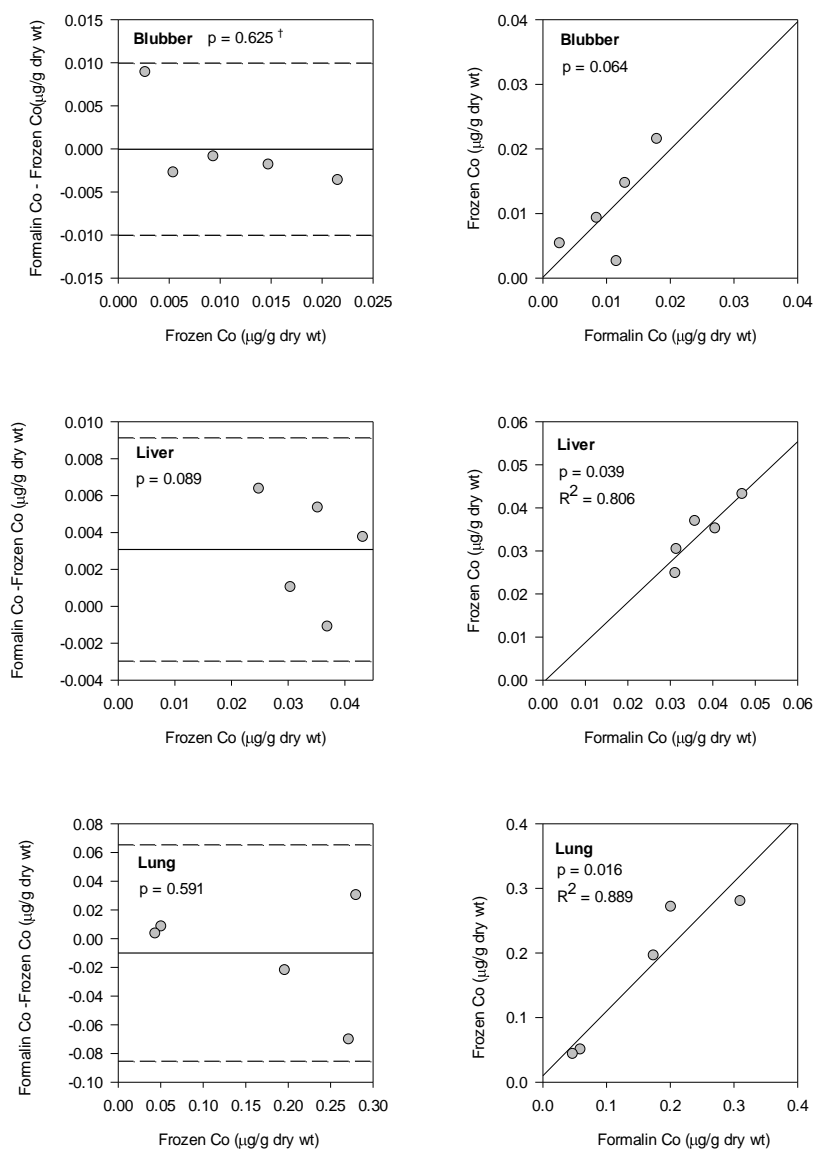
Supplementary Figure 5.9. Bland-Altman plots comparing tin (Sn) concentrations ($\mu\text{g/g}$ dry wt) in formalin-fixed and frozen *Tursiops truncatus* tissues following long-term preservation and p values from the paired t-tests (ND = not determined). The solid line represents the mean within-pair difference and the dashed lines represent ± 1.96 standard deviations of the mean within-pair difference.



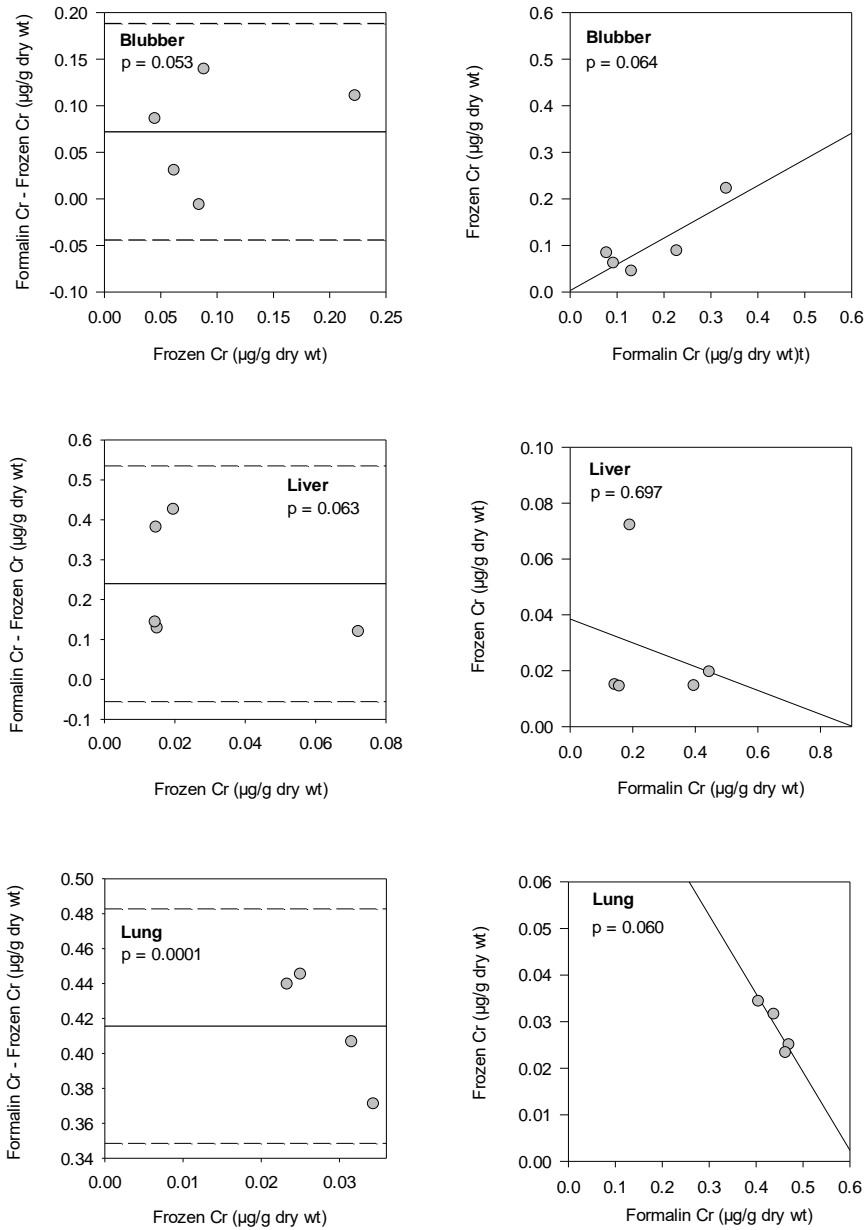
Supplementary Figure 5.10. Bland-Altman plots comparing vanadium (V) concentrations ($\mu\text{g/g dry wt}$) in formalin-fixed and frozen *Tursiops truncatus* tissues following long-term preservation and p values from the paired t-tests or Wilcoxon signed-rank tests (\dagger) (ND = not determined). The solid line represents the mean within-pair difference and the dashed lines represent ± 1.96 standard deviations of the mean within-pair difference.



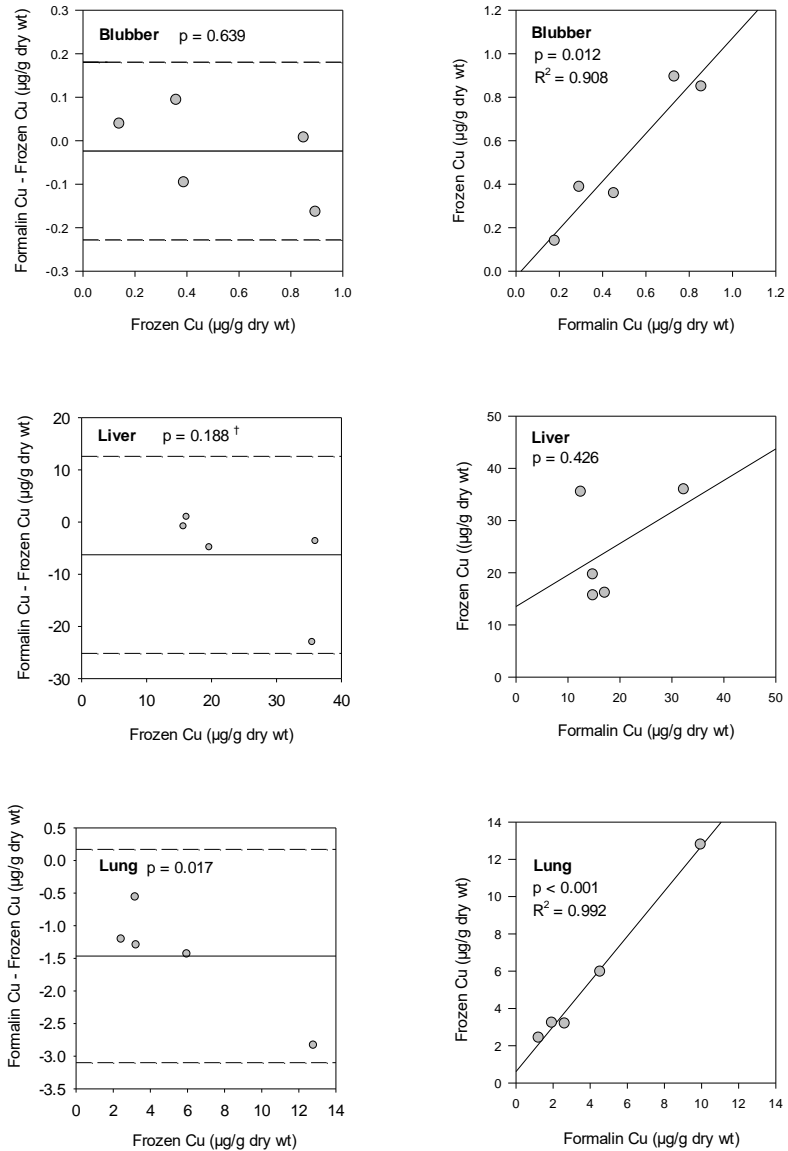
Supplementary Figure 5.11. Bland-Altman plots comparing zinc (Zn) concentrations ($\mu\text{g/g}$ dry wt) in formalin-fixed and frozen *Tursiops truncatus* tissues following long-term preservation and p values from the paired t-tests or Wilcoxon signed-rank tests (†). The solid line represents the mean within-pair difference and the dashed lines represent ± 1.96 standard deviations of the mean within-pair difference.



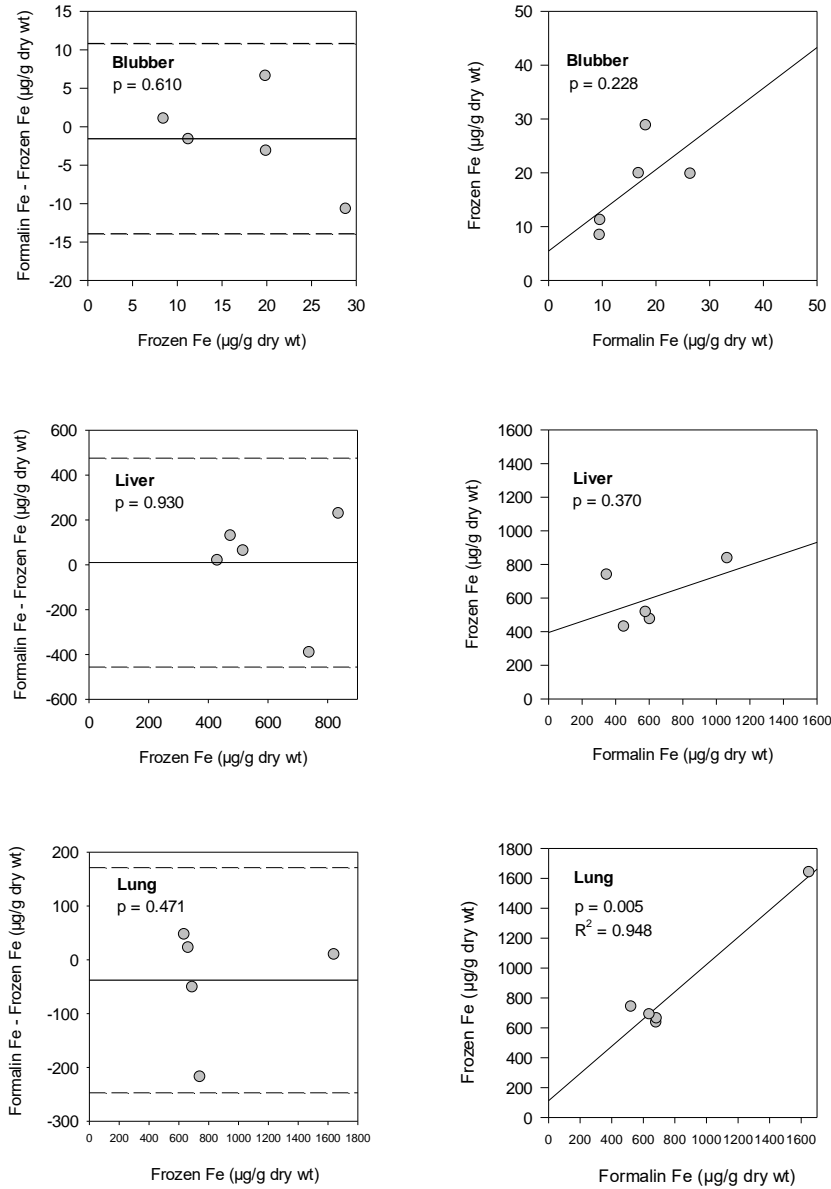
Supplementary Figure 5.12. Bland-Altman plots comparing cobalt (Co) concentrations ($\mu\text{g/g dry wt}$) in formalin-fixed and frozen *Tursiops truncatus* tissues following short-term preservation and p values from the paired t-tests or Wilcoxon signed-rank tests ([†]) (left panel) and linear regressions between Co concentrations ($\mu\text{g/g dry wt}$) in formalin-fixed and frozen *T. truncatus* tissues (right panel). In the Bland-Altman plots, the solid line represents the mean within-pair difference and the dashed lines represent ± 1.96 standard deviations of the mean within-pair difference.



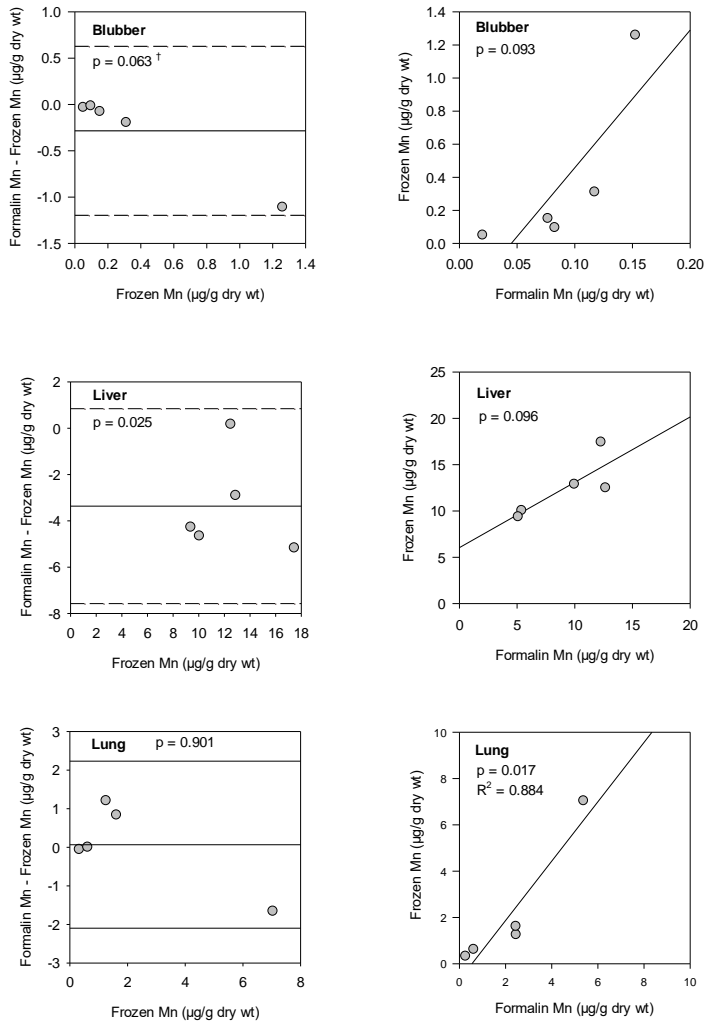
Supplementary Figure 5.13. Bland-Altman plots comparing chromium (Cr) concentrations ($\mu\text{g/g dry wt}$) in formalin-fixed and frozen *Tursiops truncatus* tissues following short-term preservation and p values from the paired t-tests (left panel) and linear regressions between Cr concentrations ($\mu\text{g/g dry wt}$) in formalin-fixed and frozen *T. truncatus* tissues (right panel). In the Bland-Altman plots, the solid line represents the mean within-pair difference and the dashed lines represent ± 1.96 standard deviations of the mean within-pair difference.



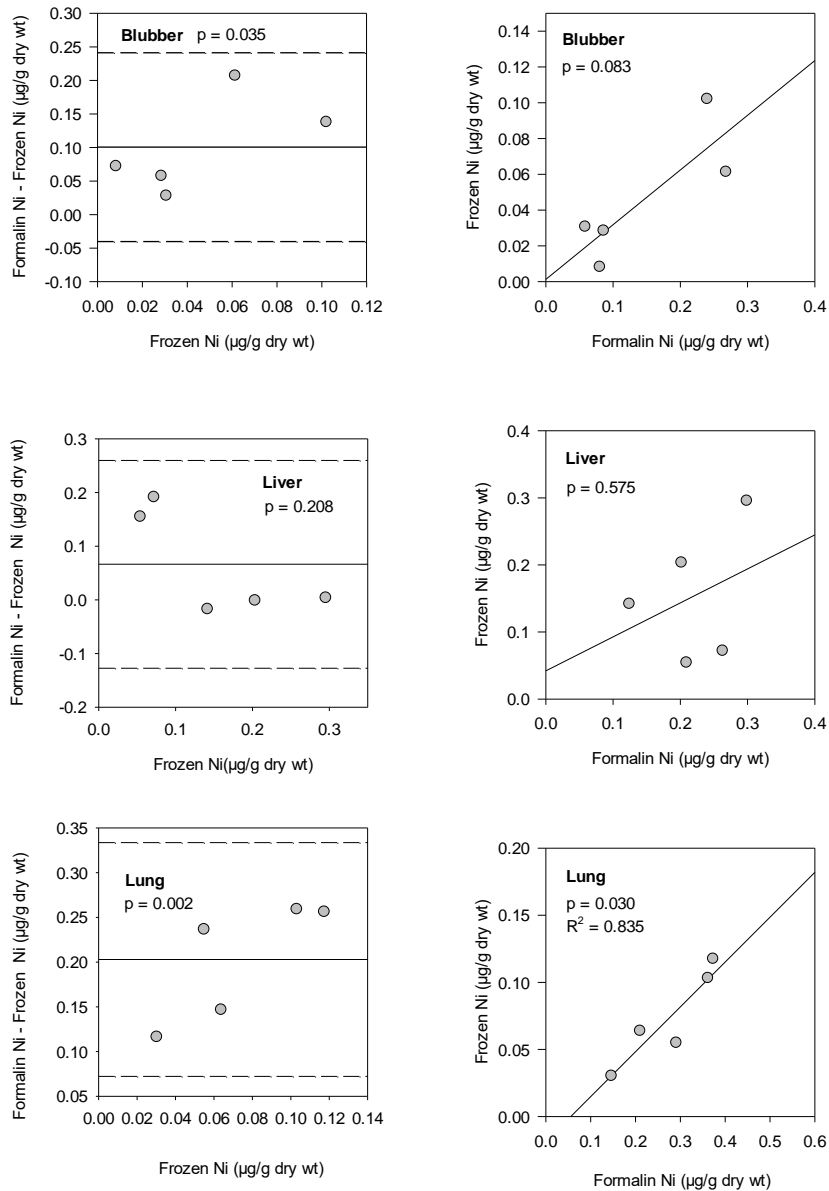
Supplementary Figure 5.14. Bland-Altman plots comparing copper (Cu) concentrations ($\mu\text{g/g}$ dry wt) in formalin-fixed and frozen *Tursiops truncatus* tissues following short-term preservation and p values from the paired t-tests or Wilcoxon signed-rank tests (†) (left panel) and linear regressions between Cu concentrations ($\mu\text{g/g}$ dry wt) in formalin-fixed and frozen *T. truncatus* tissues (right panel). In the Bland-Altman plots, the solid line represents the mean within-pair difference and the dashed lines represent ± 1.96 standard deviations of the mean within-pair difference.



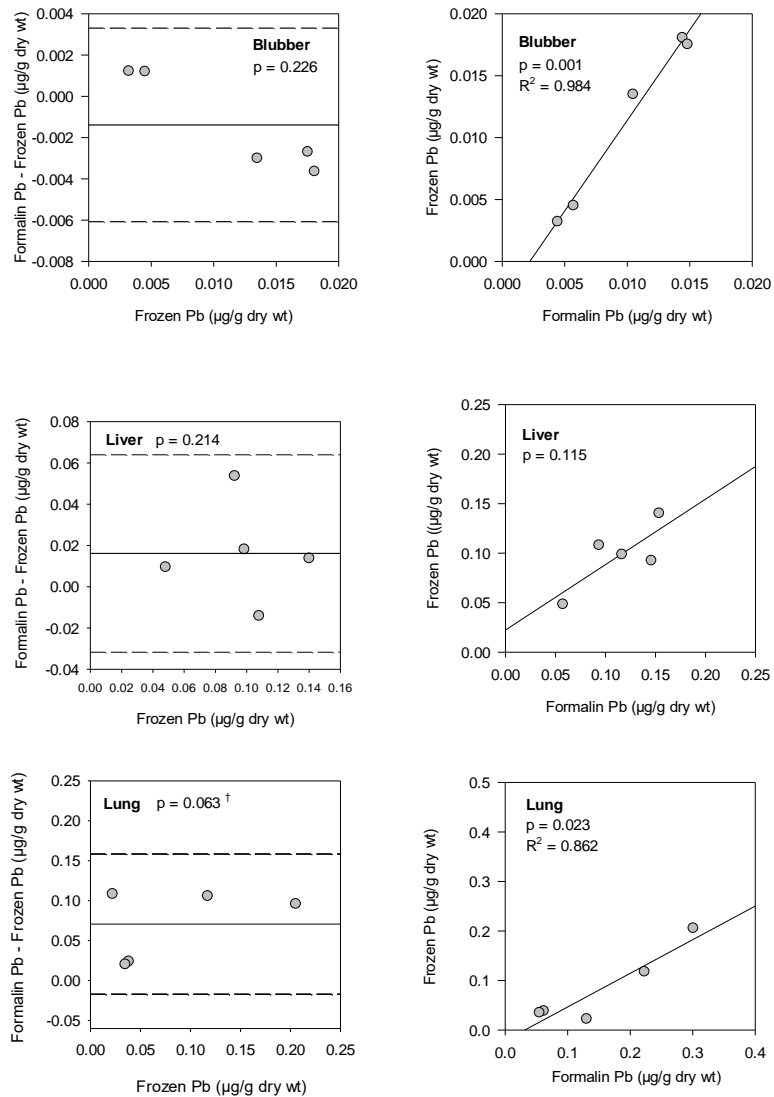
Supplementary Figure 5.15. Bland-Altman plots comparing iron (Fe) concentrations ($\mu\text{g/g dry wt}$) in formalin-fixed and frozen *Tursiops truncatus* tissues following short-term preservation and p values from the paired t-tests (left panel) and linear regressions between Fe concentrations ($\mu\text{g/g dry wt}$) in formalin-fixed and frozen *T. truncatus* tissues (right panel). In the Bland-Altman plots, the solid line represents the mean within-pair difference and the dashed lines represent ± 1.96 standard deviations of the mean within-pair difference.



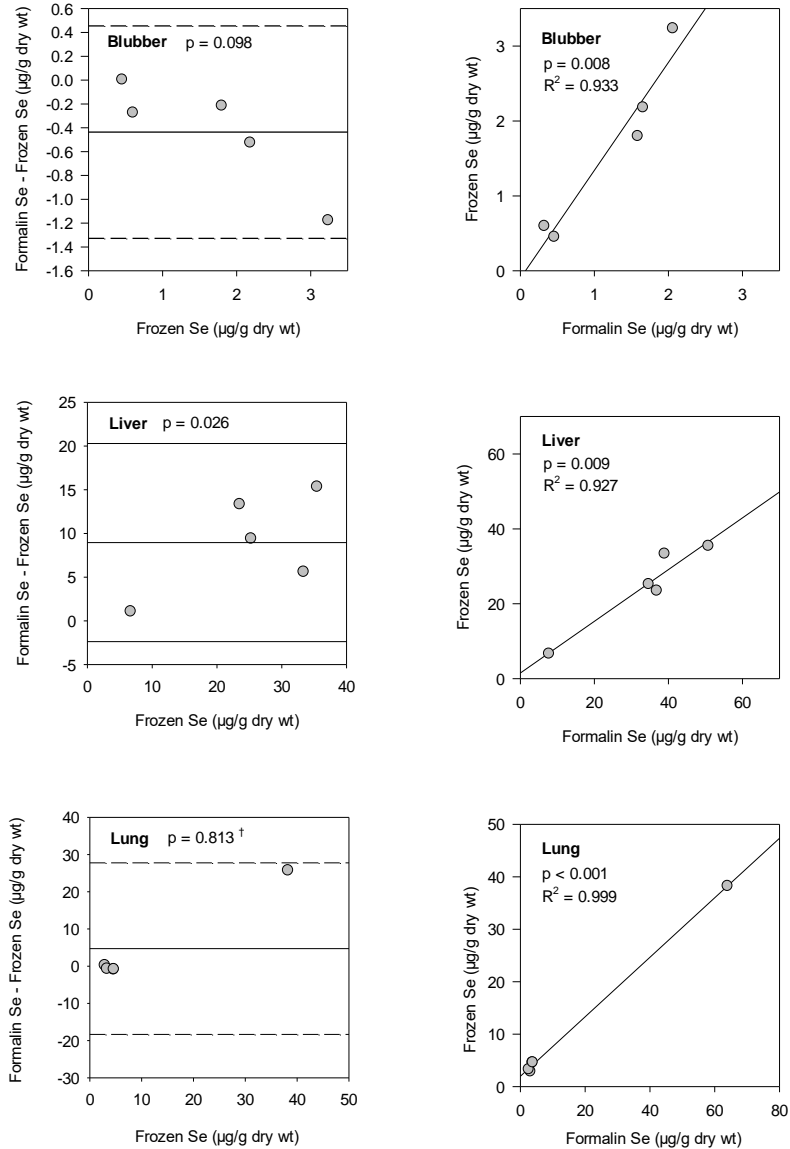
Supplementary Figure 5.16. Bland-Altman plots comparing manganese (Mn) concentrations ($\mu\text{g/g dry wt}$) in formalin-fixed and frozen *Tursiops truncatus* tissues following short-term preservation and p values from the paired t-tests or Wilcoxon signed-rank tests (†) (left panel) and linear regressions between Mn concentrations ($\mu\text{g/g dry wt}$) in formalin-fixed and frozen *T. truncatus* tissues (right panel). In the Bland-Altman plots, the solid line represents the mean within-pair difference and the dashed lines represent ± 1.96 standard deviations of the mean within-pair difference.



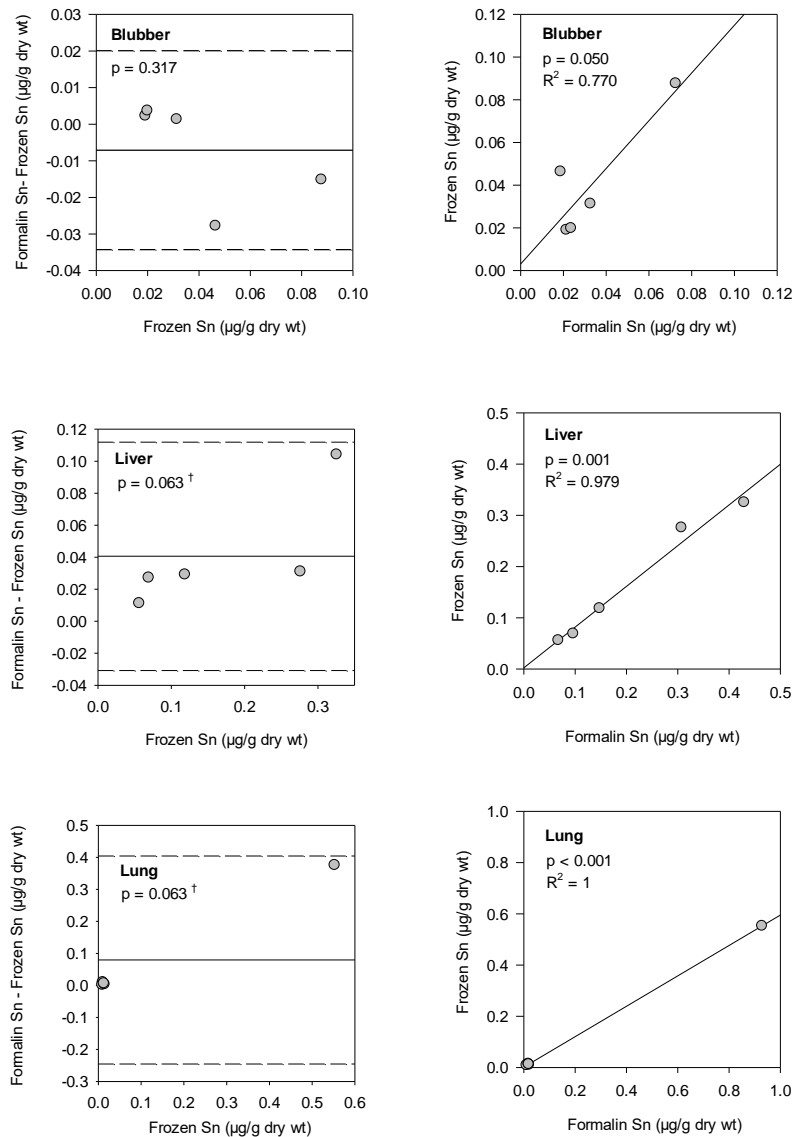
Supplementary Figure 5.17. Bland-Altman plots comparing nickel (Ni) concentrations ($\mu\text{g/g}$ dry wt) in formalin-fixed and frozen *Tursiops truncatus* tissues following short-term preservation and p values from the paired t-tests (left panel) and linear regressions between Ni concentrations ($\mu\text{g/g}$ dry wt) in formalin-fixed and frozen *T. truncatus* tissues (right panel). In the Bland-Altman plots, the solid line represents the mean within-pair difference and the dashed lines represent ± 1.96 standard deviations of the mean within-pair difference.



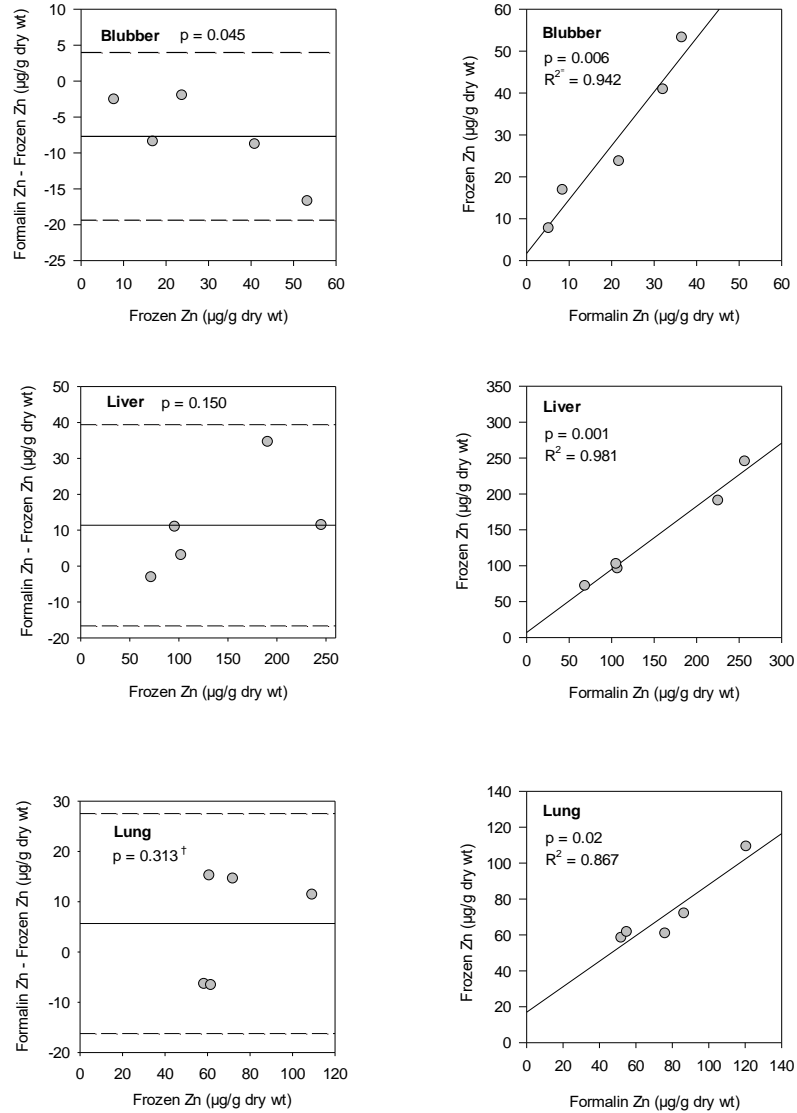
Supplementary Figure 5.18. Bland-Altman plots comparing lead (Pb) concentrations ($\mu\text{g/g dry wt}$) in formalin-fixed and frozen *Tursiops truncatus* tissues following short-term preservation and p values from the paired t-tests or Wilcoxon signed-rank tests (†) (left panel) and linear regressions between Pb concentrations ($\mu\text{g/g dry wt}$) in formalin-fixed and frozen *T. truncatus* tissues (right panel). In the Bland-Altman plots, the solid line represents the mean within-pair difference and the dashed lines represent ± 1.96 standard deviations of the mean within-pair difference.



Supplementary Figure 5.19. Bland-Altman plots comparing selenium (Se) concentrations ($\mu\text{g/g}$ dry wt) in formalin-fixed and frozen *Tursiops truncatus* tissues following short-term preservation and p values from the paired t-tests or Wilcoxon signed-rank tests (†) (left panel) and linear regressions between Se concentrations ($\mu\text{g/g}$ dry wt) in formalin-fixed and frozen *T. truncatus* tissues (right panel). In the Bland-Altman plots, the solid line represents the mean within-pair difference and the dashed lines represent ± 1.96 standard deviations of the mean within-pair difference.



Supplementary Figure 5.20. Bland-Altman plots comparing tin (Sn) concentrations ($\mu\text{g/g dry wt}$) in formalin-fixed and frozen *Tursiops truncatus* tissues following short-term preservation and p values from the paired t-tests or Wilcoxon signed-rank tests (†) (left panel) (left panel) and linear regressions between Sn concentrations ($\mu\text{g/g dry wt}$) in formalin-fixed and frozen *T. truncatus* tissues (right panel). In the Bland-Altman plots, the solid line represents the mean within-pair difference and the dashed lines represent ± 1.96 standard deviations of the mean within-pair difference.



Supplementary Figure 5.21. Bland-Altman plots comparing zinc (Zn) concentrations ($\mu\text{g/g dry wt}$) in formalin-fixed and frozen *Tursiops truncatus* tissues following short-term preservation and p values from the paired t-tests or Wilcoxon signed-rank tests (†) (left panel) and linear regressions between Zn concentrations ($\mu\text{g/g dry wt}$) in formalin-fixed and frozen *T. truncatus* tissues (right panel). In the Bland-Altman plots, the solid line represents the mean within-pair difference and the dashed lines represent ± 1.96 standard deviations of the mean within-pair difference.

Table S6.1. Summary of selected point analyses of major elements in bottlenose dolphin enamel and pre-natal dentin expressed as weight percentages (wt %) [mean \pm standard error (SE)]; PND = pre-natal dentin; EDJ = enamel dentin junction.

Sample ID	Element	Outer enamel		Mid-enamel		Inner enamel		PND near EDJ		Inner PND	
		Point 1		Point 2		Point 3		Point 4		Point 5	
		wt %	SE	wt %	SE	wt %	SE	wt %	SE	wt %	SE
GA 345	C	8.88	0.39	6.87	0.262	7.94	0.080	11.4	0.501	10.9	0.269
	Ca	29.6	4.2	31.3	2.56	27.4	0.567	25.9	0.667	27.4	0.491
	O	35.8	4.62	37.7	3.27	43.3	0.613	41.6	0.537	40.9	0.477
	P	14.8	0.601	16.2	0.422	15.8	0.140	15.0	0.318	15.5	0.188
GA 1603	C	14.2	5.29	6.95	0.093	7.47	0.125	9.72	0.476	11.3	0.593
	Ca	30.9	1.19	28.5	1.07	28.4	0.489	25.9	0.356	27.2	0.163
	O	32.8	4.37	44.9	1.36	44.9	0.769	45.9	0.120	41.9	0.047
	P	13.9	1.77	16.1	0.366	16.0	0.191	14.8	0.147	15.4	0.131
GA 279	C	15.6	6.84	8.41	0.078	10.1	0.709	13.3	0.469	17.4	1.033
	Ca	22.2	5.94	28.3	1.66	27.4	0.444	26.5	1.13	27.1	0.16
	O	33.0	6.21	41.4	1.69	41.7	0.618	39.3	1.66	35.1	0.939
	P	13.1	2.67	15.4	0.127	15.5	0.137	15.1	0.405	15.3	0.084
GA 1856	C	8.86	1.13	6.68	0.098	6.29	0.064	7.07	0.148	9.38	0.344
	Ca	20.9	1.59	24.9	0.897	26.0	0.443	25.4	0.440	25.0	0.346
	O	33.8	2.59	27.5	1.00	40.9	0.818	41.8	0.689	42.5	0.415
	P	13.7	0.765	15.4	0.347	15.7	0.123	15.3	0.294	14.9	0.127
GA 737	C	7.92	0.181	8.07	0.845	7.66	0.31	8.88	0.180	9.72	0.196
	Ca	23.3	1.86	24.5	1.65	26.2	0.195	25.6	1.00	25.4	0.45
	O	27.2	4.44	38.3	2.35	39.3	0.18	40.4	1.81	41.8	0.751
	P	13.9	0.366	14.6	0.212	15.5	0.015	14.0	0.925	15.0	0.148
GA 1599	C	18.7	2.06	11.7	0.209	10.5	0.428	11.3	0.824	15.3	0.254
	Ca	24.0	0.533	24.2	0.44	24.5	0.413	23.8	0.670	23.9	0.417
	O	30.8	3.23	39.9	0.873	42.4	0.110	43.1	1.23	39.6	0.601

GA 710	P	12.0	1.24	14.5	0.186	14.56	0.058	14.2	0.304	14.4	0.152	
	C	10.9	0.46	11.2	1.38	8.51	0.095	8.68	0.153	12.6	0.378	
	Ca	20.2	1.24	21.5	1.62	24.0	0.955	23.5	0.386	22.6	0.71	
	O	36.7	1.83	37.2	5.13	38.3	1.53	38.9	0.822	40.9	0.988	
	GA 830	P	13.1	0.335	13.2	0.284	15.0	0.247	15.0	0.209	14.4	0.132
		C	14.4	4.72	9.13	0.377	12.4	3.97	10.3	0.924	11.6	0.671
		Ca	16.8	0.715	24.0	0.317	23.6	1.09	23.0	0.606	23.7	0.537
		O	31.8	2.59	33.5	1.19	36.0	1.78	36.1	1.78	41.5	0.922
	GA 1755	P	11.4	0.776	14.9	0.119	14.5	0.680	14.0	0.355	14.6	0.098
		C	8.01	0.262	7.83	0.099	13.6	0.805	13.3	0.204	13.0	0.204
		Ca	20.5	0.294	25.5	1.93	22.2	0.590	22.3	0.081	23.2	0.171
		O	37.3	1.71	39.3	3.33	39.7	1.08	40.5	0.179	42.3	0.512
GA 260	P	13.5	0.364	14.6	0.544	13.4	0.234	13.7	0.102	14.2	0.144	
	C	6.12	0.171	6.19	0.067	6.74	0.040	6.91	0.045	9.02	0.164	
	Ca	25.7	0.593	26.2	0.419	25.1	0.864	26.6	0.178	25.6	0.809	
	O	39.2	0.415	39.5	0.909	44.0	1.32	41.9	0.451	44.1	0.738	
GA 277	P	15.8	0.193	15.8	0.202	15.1	0.33	15.7	0.117	15.0	0.265	
	C	9.07	0.072	8.76	0.456	9.20	0.682	11.4	0.630	11.9	0.721	
	Ca	23.0	2.67	25.0	0.924	24.4	0.364	23.8	0.358	23.3	0.265	
	O	34.4	3.10	33.7	4.16	41.0	1.19	40.7	1.86	42.8	0.283	
GA 159	P	12.8	0.367	15.2	0.333	15.0	0.056	14.5	0.112	14.3	0.151	
	C	21.3	6.25	12.5	1.78	10.5	0.58	10.6	0.598	11.9	0.232	
	Ca	23.0	2.72	25.9	0.94	26.7	0.402	26.0	0.568	25.7	0.106	
	O	36.4	4.19	44.2	0.312	45.0	0.792	45.1	0.11	44.7	0.322	
	P	12.4	1.40	14.7	0.508	15.1	0.165	15.0	0.312	14.9	0.016	

Table S6.2. Summary of selected point analyses of minor elements in bottlenose dolphin enamel and pre-natal dentin expressed as weight percentages (wt %) [mean \pm standard error (SE)]; PND = pre-natal dentin; EDJ = enamel dentin junction; ND = Not detected

Sample ID	Element	Outer enamel		Mid-enamel		Inner enamel		PND near EDJ		Inner PND	
		Point 1		Point 2		Point 3		Point 4		Point 5	
		wt %	SE	wt %	SE	wt %	SE	wt %	SE	wt %	SE
GA 345	Cl	0.343	0.024	0.293	0.026	0.147	0.05	0.033	0.033	ND	ND
	Mg	0.673	0.337	0.563	0.232	1.29	0.123	2.06	0.009	2.2	0.013
	Na	0.603	0.243	0.553	0.063	0.873	0.003	0.713	0.022	0.623	0.030
GA 1603	Cl	0.26	0.031	0.24	0.01	0.160	0.006	ND	ND	ND	ND
	Mg	0.547	0.301	1.28	0.099	1.19	0.040	2.06	0.128	2.77	0.11
	Na	0.437	0.079	0.643	0.049	0.750	0.026	0.657	0.003	0.583	0.018
GA 279	Cl	0.235	0.105	0.233	0.018	0.147	0.007	ND	ND	ND	ND
	Mg	0.785	0.105	1.09	0.211	1.07	0.079	1.69	0.075	1.82	0.026
	Na	0.456	0.045	0.583	0.068	0.727	0.03	0.663	0.018	0.603	0.012
GA 1856	Cl	0.247	0.019	0.207	0.003	0.043	ND	ND	ND	ND	ND
	Mg	ND	ND	0.317	ND	1.85	0.048	1.94	0.119	2.78	0.047
	Na	0.510	0.050	0.633	0.035	0.643	0.012	0.763	0.034	0.59	0.017
GA 737	Cl	0.237	0.020	0.230	0.010	0.155	0.005	ND	ND	ND	ND
	Mg	ND	ND	0.377	ND	1.32	0.055	1.39	0.035	2.27	0.032
	Na	0.377	0.091	0.570	0.085	0.630	0.040	0.655	0.075	0.676	0.026
GA 1599	Cl	0.192	0.022	0.183	0.009	0.143	0.003	ND	ND	ND	ND
	Mg	0.940	ND	1.70	0.068	1.830	0.119	1.96	0.159	2.88	0.057
	Na	0.363	0.052	0.557	0.023	0.640	0.017	0.707	0.075	0.577	0.013
GA 710	Cl	0.230	0.01	0.150	0.010	ND	ND	ND	ND	ND	ND
	Na	0.590	0.00	0.700	0.101	0.883	0.058	1.18	0.018	1.21	0.093
	Mg	ND	ND	1.16	ND	1.42	0.04	2.03	0.033	2.45	0.107
GA 830	Cl	0.225	0.015	0.227	0.003	0.150	0.006	ND	ND	ND	ND
	Na	0.425	0.015	0.437	0.032	0.557	0.009	0.687	0.039	0.65	0.017

	Mg	ND	ND	ND	ND	1.09	0.114	1.99	0.468	2.72	0.003
GA 1755	Cl	0.263	0.012	0.2	0.015	ND	ND	ND	ND	ND	ND
	Mg	ND	ND	ND	ND	1.94	0.073	2.45	0.256	2.65	0.008
	Na	0.470	0.021	0.577	0.069	0.59	0.006	0.63	0.015	0.64	0.016
GA 260	Cl	0.217	0.007	0.177	0.003	0.145	0.004	ND	ND	ND	ND
	Mg	ND	ND	1.30	0.069	1.27	0.125	1.48	0.072	2.51	0.010
	Na	0.567	0.017	0.577	0.018	0.66	0.006	0.667	0.0189	0.640	0.015
GA 277	Cl	0.217	0.012	0.177	0.003	ND	ND	0.09	ND	ND	ND
	Mg	ND	ND	1.22	0.069	1.90	0.119	2.87	0.302	3.30	0.084
	Na	0.450	0.056	0.600	0.456	0.712	0.045	0.657	0.029	0.627	0.026
GA 159	Cl	0.177	0.033	0.177	0.013	0.130	ND	ND	ND	ND	ND
	Mg	0.840	0.130	1.173	0.062	1.23	0.066	1.64	0.457	2.33	0.043
	Na	0.483	0.107	0.737	0.022	0.773	0.009	0.800	0.086	0.677	0.009

Table S6.3. Summary of selected point analyses of aluminum (Al) in bottlenose dolphin enamel and pre-natal dentin expressed as weight percentages (wt %) [mean \pm standard error (SE)]; PND = pre-natal dentin; EDJ = enamel dentin junction.

Sample ID	Outer enamel		Mid-enamel		Inner enamel		PND near EDJ		Inner PND dentine	
	Point 1		Point 2		Point 3		Point 4		Point 5	
	wt %	SE	wt %	SE	wt %	SE	wt %	SE	wt %	SE
GA 345	11.33	3.02	6.56	0.641	3.93	0.376	3.26	0.061	2.50	0.048
GA 1603	6.81	4.46	1.30	0.042	1.06	0.044	0.967	0.015	0.783	0.004
GA 279	14.6	8.03	4.55	0.470	3.41	0.064	3.47	0.162	2.78	0.042
GA 1856	22.1	1.39	14.4	0.056	8.57	0.221	7.81	0.022	4.89	0.056
GA 737	27.1	2.33	13.4	1.22	9.29	0.015	9.06	0.090	5.19	0.188
GA 1599	13.6	3.20	7.29	0.458	5.42	0.192	4.87	0.276	3.29	0.070
GA 710	19.1	0.180	15.7	2.27	12.0	0.457	10.7	0.187	6.03	0.303
GA 830	25.0	0.685	17.9	0.629	12.0	0.708	8.58	2.27	5.07	0.034
GA 1755	19.9	1.04	13.0	1.00	8.59	0.166	7.48	0.076	3.91	0.037
GA 260	12.5	0.227	10.7	0.162	6.98	0.199	6.76	0.121	3.78	0.082
GA 277	23.4	2.57	12.4	0.594	7.78	0.311	6.06	1.39	3.62	0.104
GA 159	2.10	0.657	0.513	0.017	0.47	0.006	0.423	0.040	0.389	0.018

Table S6.4. Summary of selected point analyses of major elements in bottlenose dolphin dentin across the approximate location of the growth layer groups (GLG's) expressed as weight percentages (wt %) [mean \pm standard error (SE)]; ND = not detected.

Sample ID	Element	Point 1		Point 2		Point 3		Point 4		Point 5		Point 6		Point 7	
		wt %	SE												
GA 345	C	74.5	0.095	17.1	0.370	13.8	0.125	18.3	7.29	17.7	6.26	10.7	0.299	10.8	0.611
	Ca	2.30	0.041	25.3	0.323	27.3	0.916	25.8	0.109	24.6	1.62	26.7	0.275	26.6	0.636
	O	21.8	0.038	40.8	0.285	41.2	1.40	40.7	4.28	40.7	3.48	43.4	0.653	43.6	0.498
	P	1.30	0.025	13.9	0.167	14.9	0.356	14.6	0.058	13.9	1.03	15.2	0.104	15.1	0.146
GA 1603	C	48.4	8.34	17.8	0.702	15.0	0.380	15.1	2.05	12.5	0.098	12.5	0.169	11.7	0.455
	Ca	11.8	3.38	23.4	0.504	24.2	0.130	24.8	0.065	25.1	0.105	25.1	0.141	25.8	0.225
	O	23.0	1.85	39.7	0.813	42.2	0.569	41.6	1.75	43.4	0.036	43.5	0.125	44.1	0.154
	P	5.68	1.36	13.6	0.202	13.9	0.089	14.1	0.105	14.6	0.038	14.6	0.046	14.8	0.116
GA 279	C	60.9	14.31	18.4	0.218	13.6	0.560	11.9	0.913	13.7	0.402	13.9	1.44	12.7	0.779
	Ca	17.4	4.99	24.3	0.572	25.2	0.374	25.6	0.147	25.0	0.039	25.2	0.327	25.2	0.120
	O	25.8	5.79	40.9	0.908	43.0	0.375	44.4	0.814	43.2	0.410	42.6	0.862	43.6	0.588
	P	10.4	ND	13.5	0.201	14.6	0.088	14.9	0.041	14.7	0.066	14.8	0.190	14.9	0.119
GA 1856	C	44.8	12.77	18.1	0.189	16.8	1.84	15.5	2.49	17.8	3.10	13.6	0.871	12.6	0.103
	Ca	13.0	5.10	22.2	0.300	22.6	0.799	24.9	0.195	22.1	0.811	26.0	1.22	25.5	0.325
	O	33.7	4.43	44.1	0.202	45.3	0.413	44.4	0.589	45.0	1.94	42.8	1.54	44.7	0.528
	P	7.18	2.89	12.8	0.11	13.0	0.476	14.1	0.057	12.4	0.479	14.6	0.450	14.4	0.118
GA 737	C	18.7	2.61	15.1	0.969	14.2	0.360	14.9	1.19	15.1	0.878	12.6	0.294	12.8	0.717
	Ca	11.5	4.94	22.1	1.07	23.7	0.350	24.4	0.249	23.0	1.62	25.3	0.283	25.0	0.085
	O	18.7	9.24	40.1	0.960	42.0	0.124	44.2	1.85	44.4	1.42	43.7	0.119	44.0	0.440
	P	7.77	3.17	12.9	0.550	13.6	0.157	13.9	0.096	13.2	0.879	14.6	0.101	14.6	0.119
GA 1599	C	27.6	0.957	17.5	0.223	14.7	0.139	14.3	0.522	14.0	0.473	12.7	0.179	12.4	0.348
	Ca	21.1	0.356	22.5	0.174	24.1	0.133	24.2	0.142	24.4	0.272	24.7	0.125	25.1	0.223

	O	34.8	0.865	41.7	0.274	42.4	0.139	42.7	0.317	42.8	0.142	42.37	0.180	43.4	0.639
	P	11.4	0.438	13.1	0.113	13.9	0.061	14.2	0.095	14.4	0.120	14.7	0.061	14.7	0.097
GA 710	C	30.5	1.53	16.2	0.070	14.6	0.467	13.3	0.367	13.4	0.220	12.5	0.205	12.1	0.343
	Ca	16.2	0.823	22.8	0.477	22.1	0.162	23.8	0.299	23.9	0.174	23.6	0.594	24.6	0.089
	O	36.2	0.163	42.7	0.579	45.3	0.688	42.2	0.140	44.9	0.208	44.9	0.601	45.4	0.207
	P	10.2	0.387	13.1	0.138	13.2	0.175	13.7	0.110	13.8	0.094	14.2	0.142	14.3	0.123
GA 830	C	27.2	0.688	18.2	0.695	13.9	0.914	13.3	0.842	13.0	0.946	13.8	0.504	12.8	1.15
	Ca	22.3	0.512	23.8	1.43	27.4	1.73	27.5	1.76	27.1	0.833	30.5	0.564	25.5	0.435
	O	34.5	1.03	43.1	2.46	41.3	2.62	41.0	2.20	42.3	0.503	37.5	1.33	44.3	0.465
	P	11.5	0.109	12.9	0.40	14.6	0.299	14.8	0.522	14.8	0.393	15.5	0.278	14.3	0.222
GA 1755	C	32.1	6.50	15.7	0.007	13.9	0.307	12.9	0.297	14.1	0.865	12.5	0.409	12.7	0.433
	Ca	18.0	2.76	23.7	0.230	25.6	0.235	26.8	0.687	27.3	0.715	26.2	0.215	25.6	0.213
	O	36.50	1.80	43.5	0.230	42.8	0.348	42.2	1.06	40.6	0.503	43.9	0.412	44.5	0.125
	P	10.1	1.72	13.4	0.082	14.2	0.049	14.9	0.287	15.2	0.219	14.7	0.052	14.5	0.107
GA 260	C	14.6	0.356	12.1	0.085	11.9	0.029	11.5	0.291	11.3	0.102	15.1	0.946	14.5	0.301
	Ca	22.3	0.512	23.8	1.43	27.4	1.72	27.5	1.77	27.1	0.834	30.5	0.564	25.5	0.1435
	O	44.1	0.284	45.7	0.130	45.8	0.507	46.2	0.217	46.5	0.168	45.7	0.286	46.3	0.268
	P	11.5	0.109	12.9	0.399	14.6	0.299	14.8	0.522	14.8	0.393	15.5	0.278	14.3	0.222
GA 277	C	28.3	1.05	20.3	1.39	16.9	0.810	14.9	0.769	14.7	1.18	12.7	0.304	16.9	3.25
	Ca	19.5	0.662	21.7	0.311	23.3	0.398	23.5	0.231	23.2	0.54	24.1	0.397	23.1	0.835
	O	39.2	0.519	41.7	0.842	42.4	0.208	43.0	0.649	43.6	0.266	44.4	0.309	42.8	1.80
	P	10.7	0.192	12.5	0.231	13.4	0.171	13.8	0.083	13.9	0.299	14.3	0.163	13.5	0.498
GA 159	C	16.2	0.689	14.3	0.326	12.7	0.608	12.4	0.319	12.0	0.069	15.1	2.59	16.2	0.919
	Ca	19.4	0.776	25.3	0.284	25.4	0.685	24.3	0.119	24.6	0.607	24.8	0.629	24.5	0.363
	O	32.1	0.511	35.5	0.703	39.1	1.65	41.8	0.534	41.5	0.880	38.5	1.83	0.750	0.979
	P	12.3	0.316	14.6	0.197	14.7	0.229	14.4	0.013	14.56	0.264	14.4	0.359	14.7	0.044

Table S6.5. Summary of selected point analyses of minor elements in bottlenose dolphin dentin across the approximate location of the growth layer groups (GLG's) expressed as weight percentages (wt %) [mean \pm standard error (SE)]; ND = not detected

Sample ID	Element	Point 1		Point 2		Point 3		Point 4		Point 5		Point 6		Point 7	
		wt %	SE												
GA 345	Mg	ND	ND	2.23	0.022	2.37	0.041	2.65	0.300	2.39	0.236	2.70	0.026	2.53	0.01
	Na	ND	ND	0.556	0.009	0.563	0.026	0.61	0.012	0.597	0.059	0.657	0.015	0.69	0.015
GA 1603	Mg	0.550	ND	2.37	0.047	3.04	0.006	3.20	0.094	3.26	0.036	3.22	0.022	2.83	0.024
	Na	0.213	0.052	0.600	0.021	0.703	0.012	0.723	0.029	0.743	0.009	0.750	0.006	0.74	0.006
GA 279	Mg	1.53	ND	2.18	0.040	2.55	0.041	2.53	0.009	2.58	0.071	2.61	0.092	2.85	0.032
	Na	0.540	0.036	0.65	0.025	0.740	0.013	0.837	0.014	0.877	0.015	0.823	0.024	0.827	0.013
GA 1856	Mg	0.883	0.356	2.07	0.017	2.20	0.070	2.25	0.025	2.04	0.093	2.30	0.023	2.25	0.042
	Na	0.635	0.012	0.753	0.019	0.933	0.144	0.683	0.033	0.65	0.026	0.647	0.026	0.64	0.012
GA 737	Mg	ND	ND	1.60	0.081	1.90	0.012	1.87	0.019	1.89	0.084	2.10	0.03	2.06	0.072
	Na	0.545	0.045	0.767	0.020	0.777	0.020	0.810	0.012	0.79	0.006	0.008	0.015	0.853	0.023
GA 1599	Mg	2.14	0.077	2.87	0.009	3.02	0.060	3.29	0.055	3.28	0.049	3.61	0.047	3.50	0.043
	Na	0.687	0.074	0.630	0.015	0.633	0.007	0.64	0.006	0.68	0.017	0.683	0.003	0.70	0.006
GA 710	Mg	1.48	0.072	2.14	0.049	2.31	0.006	2.37	0.021	2.47	0.009	2.64	0.084	2.65	0.047
	Na	1.01	0.033	0.934	0.038	1.00	0.031	0.997	0.028	1.04	0.022	0.943	0.059	0.964	0.012
GA 830	Mg	0.683	0.007	1.33	0.006	2.09	0.207	2.11	0.048	2.16	0.086	2.05	0.049	2.35	0.009
	Na	0.433	0.022	0.627	0.044	0.657	0.044	0.713	0.057	0.663	0.032	0.597	0.02	0.753	0.022
GA 1755	Mg	0.857	0.155	1.76	0.012	1.69	0.009	1.90	0.038	1.93	0.017	1.64	0.324	2.02	0.003
	Na	0.470	0.029	0.58	0.006	0.597	0.009	0.567	0.022	0.537	0.019	0.564	0.013	0.607	0.003
GA 260	Mg	0.683	0.007	1.33	0.006	2.09	0.207	2.11	0.048	2.16	0.086	2.04	0.049	2.35	0.009
	Na	0.433	0.022	0.627	0.044	0.657	0.044	0.713	0.057	0.663	0.032	0.597	0.02	0.753	0.021
GA 277	Mg	1.33	0.019	2.78	0.060	3.55	0.067	3.93	0.097	3.99	0.153	3.84	0.049	2.99	0.104
	Na	0.553	0.030	0.633	0.020	0.603	0.018	0.62	0.006	0.673	0.003	0.713	0.009	0.693	0.033
GA 159	Mg	ND	ND	2.13	0.029	2.41	0.051	2.47	0.046	2.65	0.03	2.62	0.122	2.80	0.097

Na	0.650	0.025	0.633	0.015	0.674	0.027	0.77	0.012	0.717	0.012	0.737	0.038	7.50	0.036
----	-------	-------	-------	-------	-------	-------	------	-------	-------	-------	-------	-------	------	-------

Table S6.6. Summary of selected point analyses of aluminum (Al) in bottlenose dolphin dentin across the approximate location of the growth layer groups (GLG's) expressed as weight percentages (wt %).

Sample ID	Point 1		Point 2		Point 3		Point 4		Point 5		Point 6		Point 7	
	wt %	SE												
GA 345	0.17	0.006	ND	ND										
GA 1603	10.6	3.41	1.65	0.081	0.943	0.037	0.607	0.042	0.417	0.019	0.323	0.012	0.260	ND
GA 279	0.21	ND	ND	ND	ND	ND	ND	ND	ND	ND	0.260	ND	ND	ND
GA 1856	ND	ND	ND	ND	ND	ND	ND	ND	0.32	ND	ND	ND	ND	ND
GA 737	41.5	19.1	7.51	0.289	3.84	0.082	2.09	0.037	1.71	0.299	0.973	0.032	0.663	0.012
GA 1599	2.36	0.283	1.69	0.143	1.18	0.079	0.773	0.041	0.523	0.022	0.347	0.013	0.293	0.007
GA 710	4.26	0.292	2.24	0.081	1.15	0.05	0.68	0.114	0.42	0.01	0.315	0.004	0.25	ND
GA 830	0.22	ND	ND	ND										
GA 1755	1.97	0.185	1.31	0.107	0.903	0.055	0.563	0.009	0.37	0.02	ND	ND	ND	ND
GA 260	0.22	ND	ND	ND										
GA 277	0.40	0.006	0.35	0.00	0.297	0.009	0.230	ND	ND	ND	ND	ND	ND	ND
GA 159	19.3	0.988	7.54	0.568	5.17	0.568	4.20	0.394	4.02	0.374	3.69	0.358	3.31	0.269

REFERENCES

- Ache, B.W., Boyle, J.D., Morse, C.E., 2000. A survey of the occurrence of mercury in the fishery resources of the Gulf of Mexico. US EPA Gulf of Mexico Program. Stennis Space center, Mississippi.
- Adams, D.H., Engel, M.E. 2014. Mercury, lead, and cadmium in blue crabs, *Callinectes sapidus*, from the Atlantic coast of Florida, USA: a multipredator approach. *Ecotox Environ Safe* 102:196-201.
- Adams, D.H., McMichael, R.H., 2007. Mercury in king mackerel, *Scomberomorus cavalla*, and Spanish mackerel, *S. maculatus*, from waters of south-eastern USA: regional and historical trends. *Mar. Freshwater Res.* 58, 187-193.
<https://doi.org/10.1071/MF06096>.
- Adams, D.H., Onorato, G.V., 2005. Mercury concentrations in red drum, *Sciaenops ocellatus*, from estuarine and offshore waters of Florida. *Mar. Pollut. Bull.* 50, 291-300. <https://doi.org/10.1016/j.marpolbul.2004.10.049>.
- Adams, D.H., Sonne, C., 2013. Mercury and histopathology of the vulnerable goliath grouper, *Epinephelus itajara*, in US waters: A multi-tissue approach. *Environ. Res.* 126, 254-263. <https://doi.org/10.1016/j.envres.2013.05.010>.
- Adriano, D.C. 2001. Trace Elements in Terrestrial Environments. Springer-Verlag, New York, NY.
- Akaike, H., 1973 Information theory as an extension of the maximum likelihood principle, in: Petrov B.N., Csaki, F. (Eds.), Second international symposium on information theory. Budapest, Akademiai Kiado, pp. 267–281.

- Alava, J.J., Calle, P., Tirapé, A., Biedenbach, G., Cadena, O. A., Maruya, K., Lao, Wenjian, Aguiire, W., Jimenez, P., Dominguez, G.A., Bossart, G.D., Fair, P.A. 2020. Persistent Organic Pollutants and Mercury in Genetically Identified Inner Estuary Bottlenose Dolphin (*Tursiops truncatus*) Residents of the Guayaquil Gulf, Ecuador: Ecotoxicological Science in Support of Pollutant Management and Cetacean Conservation. *Front. Mar. Sci.* 7:22. <https://doi.org/10.3389/fmars.2020.0012>.
- Ali, H., Khan, E. 2018. Trophic transfer, bioaccumulation, and biomagnification of non-essential hazardous heavy metals and metalloids in food chains/webs—Concepts and implications for wildlife and human health. *Hum. Ecol. Risk Assess.* 25(6), 1353-1376. <https://doi.org/10.1080/10807039.2018.1469398>.
- Ali, H., Khan, E., Ilahi, I. 2019. Environmental chemistry and ecotoxicology of hazardous heavy metals: environmental persistence, toxicity, and bioaccumulation. *J. Chem.* 2019, 6730305. <https://doi.org/10.1155/2019/6730305>.
- Alves-Stanley, C.D., Worthy, G.A., 2009. Carbon and nitrogen stable isotope turnover rates and diet–tissue discrimination in Florida manatees (*Trichechus manatus latirostris*). *J. Exp. Biol.* 212(15), 2349-2355. <https://doi.org/10.1242/jeb.027565>.
- Ando, N., Isono, T., Sakurai, Y. 2005 Trace elements in the teeth of Steller sea lions (*Eumetopias jubatus*) from the North Pacific. *Ecol Res.* <https://doi.org/10.1007/s11284-005-0037-x>
- Ando-Mizobata, N., Sakai M., Sakurai, Y. 2006. Trace-element analysis of Steller sea lion (*Eumetopias jubatus*) teeth using a scanning X-ray analytical microscope. *Mamm Study.* [https://doi.org/10.3106/13486160\(2006\)31\[65:TAOSSL\]2.0.CO;2](https://doi.org/10.3106/13486160(2006)31[65:TAOSSL]2.0.CO;2)

- Andre, J., Boudou, A., Ribeyre, F., Berhard, M., 1991. Comparative study of mercury accumulation in dolphins (*Stenella coeruleoalba*) from French Atlantic and Mediterranean coasts. *Sci. Total. Environ.* 104, 191-209.
[https://doi.org/10.1016/0048-9697\(91\)90072-M](https://doi.org/10.1016/0048-9697(91)90072-M).
- Apeti, D.A., Lauenstein, G.G., Evans, D.W., 2012. Recent status of total mercury and methyl mercury in the coastal waters of northern Gulf of Mexico using oysters and sediments from NOAA's mussel watch program. *Mar. Pollut. Bull.* 64, 2399-2408. <https://doi.org/10.1016/j.marpolbul.2012.08.006>.
- Armfield, B.A., Zheng, Z., Bajpai, S., Vinyard, C.J., Thewissen, J.G.M. 2013. Development and evolution of the unique cetacean dentition. *PeerJ*.
<https://doi.org/10.7717/peerj.24>.
- Arnold, T.W., 2010. Uninformative parameters and model selection using Akaike's Information Criterion. *J. Wildlife Manage.* 74, 1175-1178.
<https://doi.org/10.1111/j.1937-2817.2010.tb01236.x>.
- Aubail, A., Dietz, R., Rigét, F., Simon-Bouhet, B., Caurant, F. 2010. An evaluation of teeth of ringed seals (*Phoca hispida*) from Greenland as a matrix to monitor spatial and temporal trends of mercury and stable isotopes. *Sci. Total Environ.* 408(21), 5137-5146.
- Aubail, A., Méndez-Fernandez, P., Bustamante, P., Churlaud, C., Ferreira, M., Vingada, J.V., Caurant, F., 2013. Use of skin and blubber tissues of small cetaceans to assess the trace element content of internal organs. *Mar. Pollut. Bull.* 76, 158-169.
<https://doi.org/10.1016/j.marpolbul.2013.09.008>.

- Augier, H., Park, W.K., Ronneau, C. 1993. Mercury contamination of the striped dolphin *Stenella coeruleoalba* Meyen from the French Mediterranean coasts. Mar. Pollut. Bull. 26(6), 306-311. [https://doi.org/10.1016/0025-326X\(93\)90572-2](https://doi.org/10.1016/0025-326X(93)90572-2).
- Azad, A.M., Frantzen, S., Bank, M.S., Nilsen, B M., Duinker, A., Madsen, L., Maage, A. 2019. Effects of geography and species variation on selenium and mercury molar ratios in Northeast Atlantic marine fish communities. Sci. Tot. Environ. 652, 1482-1496. <https://doi.org/10.1016/j.scitotenv.2018.10.405>.
- Bacci, E., 1989. Mercury in the Mediterranean. Mar. Pollut. Bull. 20, 59-63. [https://doi.org/10.1016/0025-326X\(89\)90227-0](https://doi.org/10.1016/0025-326X(89)90227-0).
- Ballarin C, Papini L, Bortolotto A, Butti C, Peruffo A, Sassu R, Mazzariol S, Cozzi B. 2005. An on-line tissue bank for marine mammals of the Mediterranean Sea and adjacent waters. *Hystrix It J Mamm* 16:127-133.
- Balmer, B., Watwood, S., Quigley, B., Speakman, T., Barry, K., Mullin, K., Rosel, P, Sinclair, C., Zolman, E., Schwacke, L. 2019. Common bottlenose dolphin (*Tursiops truncatus*) abundance and distribution patterns in St Andrew Bay, Florida, USA. Aquat. Conserv. 29(3), 486-498. <https://doi.org/10.1002/aqc.3001>.
- Balmer, B., Ylitalo, G., Watwood, S., Quigley, B., Bolton, J., Mullin, K., Rosel, P., Rowles, T., Speakman, T., Wilcox, L., Zolman, E., Schwacke, L. 2019. Comparison of persistent organic pollutants (POPs) between small cetaceans in coastal and estuarine waters of the northern Gulf of Mexico. Mar. Pollut. Bull. 145, 239-247. <https://doi.org/10.1016/j.marpolbul.2019.05.017>.

- Balmer, B.C., Wells, R.S., Nowacek, S.M., Nowacek, D.P., Schwacke, L.H., McLellan, W.A., Sharf, F.S., 2008. Seasonal abundance and distribution patterns of common bottlenose dolphins (*Tursiops truncatus*) near St. Joseph Bay, Florida, USA. *J. Cetacean Res. Manage.* 10, 157-167.
- Baptista, G., Kehrig, H. A., Di Benedetto, A. P. M., Hauser-Davis, R. A., Almeida, M. G., Rezende, C. E., Siciliano, S., de Moura, J.F., Moreira, I. 2016. Mercury, selenium and stable isotopes in four small cetaceans from the Southeastern Brazilian coast: influence of feeding strategy. *Environ. Pollut.* 218, 1298-1307.
<https://doi.org/10.1016/j.envpol.2016.08.088>.
- Barragán-Barrera, D.C., Luna-Acosta, A., May-Collado, L.J., Polo-Silva, C.J., Riet-Sapriza, F.G., Bustamante, P., Hernandex-Avila, M., Velez N., Farias-Curtidor, N. Caballero, S. 2019. Foraging habits and levels of mercury in a resident population of bottlenose dolphins (*Tursiops truncatus*) in Bocas del Toro Archipelago, Caribbean Sea, Panama. *Mar. Pollut. Bull.* 145, 343-356.
<https://doi.org/10.1016/j.marpolbul.2019.04.076>.
- Barratclough, A., Wells, R.S., Schwacke, L.H., Rowles, T.K., Gomez, F.M., Fauquier, D. A., Sweeney, J.C., Townsend, F.I., Hansen, L.J., Zolman E.S., Balmer, B.C., Smith, C.R. 2019. Health assessments of common bottlenose dolphins (*Tursiops truncatus*): past, present, and potential conservation applications. *Front. Vet. Sci.* 6, 444. <https://doi.org/10.3389/fvets.2019.00444>.
- Barros, N.B. 1993. Feeding ecology and foraging strategies of bottlenose dolphins on the central east coast of Florida/ Doctoral dissertation, University of Miami.

- Barros, N.B., Odell, D.K. 1990. Food habitats of Bottlenose dolphins in the southeastern united states. In : Leatherwood, S, Reeves, R.R. (Eds.) The bottlenose dolphin. Academic press, San Diego Ca. pp .309-328
- Barros, N.B., Ostrom, P.H., Stricker, C.A., Wells, R.S., 2010. Stable isotopes differentiate bottlenose dolphins off west-central Florida. Mar. Mam. Sci. 26, 324-336. <https://doi.org/10.1111/j.1748-7692.2009.00315.x>.
- Bassos-Hull, K., Perrtree, R.M., Shepard, C.C. Schiling, S., Barleycorn, A.A., Allen, J.B., Balmer, B.C., Pine, W.E., Wells, R.S., 2013. Long-term site fidelity and seasonal abundance estimates of common bottlenose dolphins (*Tursiops truncatus*) along the southwest coast of Florida and responses to natural perturbations. J. Cetacean Res. Manage. 13, 19-30.
- Bates, D., Maechler, M., Bolker, B., Walker, S. 2015. Fitting Linear Mixed-Effects Models Using lme4. J Stat Softw. <https://doi.org/10.18637/jss.v067.i01>.
- Becker, P.R., Wilkinson, D.M., Lillestolen, T.I. 1994. Marine Mammal Health and Stranding Response Program: Program Development Plan. NOAA Technical Memorandum NMFS-OPR-94-2.
- Bellante, A., D'Agostino, F., Traina, A., Piazzese, D., Milazzo, M.F., Sprovieri, M., 2017. Hg and Se exposure in brain tissues of striped dolphin (*Stenella coeruleoalba*) and bottlenose dolphin (*Tursiops truncatus*) from the Tyrrhenian and Adriatic Seas. Ecotoxicology. 26(2), 250-260. <https://doi.org/10.1007/s10646-017-1759-6>.

- Benoit, J.M., Gilmour, C.C., Mason, R.P., Heyes, A., 1999. Sulfide controls on mercury speciation and bioavailability to methylating bacteria in sediment pore waters. *Environ. Sci. Technol.* 33, 951-957. <https://doi.org/10.1021/es9808200>.
- Berens McCabe, E.J., Gannon, D.P., Barros, N.B., Wells, R.S., 2010. Prey selection by resident common bottlenose dolphins (*tursiops truncatus*) in Sarasota Bay, Florida. *Mar. Biol.* 157, 931-941. <https://doi.org/10.1007/s00227-009-1371-2>.
- Bergamaschi, B.A., Krabbenhof, D.P., Aiken, G.R., Patino, E., Rumbold, D.G., Orem, W.H., 2012. Tidally driven export of dissolved organic carbon, total mercury, and methylmercury from mangrove-dominated estuary. *Environ. Sci. Technol.* 46, 1371-1378. <https://doi.org/10.1021/es2029137>.
- Berry, M.J., Ralston, N.V.C., 2008. Mercury toxicity and mitigating role of selenium. *EcoHealth.* 5, 456-459. <https://doi.org/10.1007/s10393-008-0204-y>.
- Berta A., Sumich J.L., Kovacs K.M. 2006. Diet, foraging, structures and strategies. In: Berta A, Sumich JL, Kovacs KM (eds) *Marine mammals: evolutionary biology*, 2nd edition. Academic Press, Burlington, pp 312–355
- Bilandžić, N., Sedak, M., Đokić, M., Gomerčić, M.Đ., Gomerčić, T., Zadavec, M., Benić, M., Crnić, A.P., 2012. Toxic element concentrations in the bottlenose (*Tursiops truncatus*), striped (*Stenella coeruleoalba*) and Risso's (*Grampus griseus*) dolphins stranded in Eastern Adriatic Sea. *Bull. Environ. Contam. Toxicol.* 89, 467-473. <https://doi.org/10.1007/s00128-012-0716-6>.
- Bischoff, K., Lamm, C., Erb, H.N., Hillebrandt, J.R. 2008. The effects of formalin fixation and tissue embedding of bovine liver on copper, iron, and zinc analysis. *J Vet. Diagn. Invest.* 20:220-224.

- Blanco, C., Salomón, O., Raga, J.A., 2001. Diet of bottlenose dolphin (*Tursiops truncatus*) in western Mediterranean Sea. J. Mar. Biol. Assoc. U.K. 81, 1053-1058. <https://doi.org/10.1017/S0025315401005057>.
- Bland, M.J., Altman, D.G. 1986. Statistical methods for assessing agreement between two methods of clinical measurement. Lancet 327: 307-301.
- Bloom, N.S. 1992. On the chemical form of mercury in edible fish and marine invertebrate tissue.
- Bolea-Fernandez, E., Rua-Ibarz, A., Krupp, E. M., Feldmann, J., Vanhaecke, F. 2019. High-precision isotopic analysis sheds new light on mercury metabolism in long-finned pilot whales (*Globicephala melas*). Sci. Rep. 9(1), 1-10. <https://doi.org/10.1038/s41598-019-43825-z>.
- Borrell, A., Aguilar, A., Tornero, V., Drago, M. 2014. Concentrations of mercury in tissues of striped dolphins suggest decline of pollution in Mediterranean open waters. Chemosphere, 107, 319-323. <https://doi.org/10.1016/j.chemosphere.2013.12.076>
- Borrell, A., Clusa, M., Aguilar, A., Drago, M., 2015. Use of epidermis for monitoring of tissular trace elements in Mediterranean striped dolphin (*Stenella coeruleoabla*). Chemosphere. 122, 228-294. <http://doi.org/10.1016/j.chemosphere.2014.10.080>.
- Bossart, G.D. 2011. Marine mammals as sentinel species for oceans and human health. Vet. Pathol. 48:676-690.

- Botta, S., Albuquerque, C., Hohn, A.A., da Silva, V.M.F., Santos, M.C.D.O., Meirelles C, Barbosa, L, Di Benedetto, A.P.M., Ramos, R.M.A., Bertozzi, C., Cremer, M.J., Franco-Trecu, V., Miekeley, N., Secchi, E.R. 2015. Ba/Ca ratios in teeth reveal habitat use patterns of dolphins. *Mar Ecol Prog Ser*.
<https://doi.org/10.3354/meps11158>.
- Bowen, W.D., Northridge, S. 2010. Morphometrics, age estimation, and growth. In: Boyd IL, Bowen, W.D., Iverson, S.J. (eds) *Marine mammal ecology and conservation: A handbook of techniques*. Oxford University Press Inc., New York, pp 98-117
- Bowen, S.R. 2011 Diet of Bottlenose dolphins (*Tursiops truncatus*) from the northwestern Florida panhandle and foraging behavior near Savannah, Georgia. Msc. Thesis. Savannah State university Savannah, GA.
- Bowen-Stevens, S.R., Gannon, D. P., Hazelkorn, R. A., Lovewell, G., Volker, K. M., Smith, S., Tumlin, M.C, Litz, J. 2021. Diet of Common Bottlenose Dolphins, *Tursiops truncatus*, that Stranded in and Near Barataria Bay, Louisiana, 2010–2012. *Southeast. Nat.* 20(1), 117-134. <https://doi.org/10.1656/058.020.0113>.
- Bradley, M.A., Barst, B.D., Basu, N. 2017. A review of mercury bioavailability in humans and fish. *Int. J. Env. Res. Pub. He.* 14(2), 169. <https://doi.org/10.3390/ijerph14020169>
- Branco, V., Vale, C., Canário, J., dos Santos, M.N. 2007. Mercury and selenium in blue shark (*Prionace glauca*, L. 1758) and swordfish (*Xiphias gladius*, L. 1758) from two areas of the Atlantic Ocean. *Environ. Pollut.* 150(3), 373-380.
<https://doi.org/10.1016/j.envpol.2007.01.040>.

- Bricker, S.B, Longstaff, B., Dennison, W., Jones, A., Boicourt, K., Wicks, C., Woerner, J. 2007. Effects of nutrient enrichment in the nation's estuaries: A decade of change. NOAA coastal ocean program decision analysis series 26. National Centers for Coastal Ocean Science, Silver Spring, MD, USA. 328 p.
- Browning, H.M., Acevedo-Whitehouse, K., Gulland, F.M., Hall, A.J., Finlayson, J., Dagleish, M.P., Billington, K.J., Colegrove, K., Hammond, J.A. 2014. Evidence for a genetic basis of urogenital carcinoma in the wild California sea lion. Proc. R. Soc. B. 281(1796): 20140240. <https://doi.org/10.1098/rspb.2014.0240>.
- Browning, N.E., Dold, C., Jack, I.F., Worthy, G.A., 2014. Isotope turnover rates and diet–tissue discrimination in skin of ex situ bottlenose dolphins (*Tursiops truncatus*). J. of Exp. Biol. 217(2), 214-221. <https://doi.org/10.1242/jeb.093963>.
- Browning, N.E., Dold, C., Jack, I.F., Worthy, G.A.J., 2014. Isotope turnover rates and diet–tissue discrimination in skin of ex situ bottlenose dolphins (*Tursiops truncatus*). J. Exp. Biol. 217, 214-221. <https://doi.org/10.1242/jeb.093963>.
- Brügmann, G., Krause, J., Brachert, T.C., Kullmer, O., Schrenk, F., Ssemmanda, I., Mertz, D.F. 2012. Chemical composition of modern and fossil Hippopotamid teeth and implications for paleoenvironmental reconstructions and enamel formation-Part 1: Major and minor element variation. Biogeosciences. <https://doi.org/10.5194/bg-9-119-2012>.
- Bryan, C.E., Christopher, S.J., Balmer, B.C., Wells, R.S., 2007. Establishing baseline levels of trace elements in blood and skin of bottlenose dolphins in Sarasota Bay, Florida: implications for non-invasive monitoring. Sci. Total. Environ. 388, 325-342. <https://doi.org/10.1016/j.scitotenv.2007.07.046>.

- Bryan, C.E., Davis, W.C., McFee, W.E., Neumann, C.A., Schulte, J., Bossart, G. D., Christopher, S.J., 2012. Influence of mercury and selenium chemistries on the progression of cardiomyopathy in pygmy sperm whales, *Kogia breviceps*. *Chemosphere*. 89, 556-562. <https://doi.org/10.1016/j.chemosphere.2012.05.051>.
- Buckles, E.L., Lowenstine, L. J., Funke, C., Vittore, R. K., Wong, H.-N., St Leger, J. A., Greig, D.J., Duerr, R.S., Gulland, F.M.D., Stott, J.L. 2006. Otarine herpesvirus-1, not papillomavirus, is associated with endemic tumours in California sea lions (*Zalophus californianus*). *J. Comp. Pathol.* 135, 183–189. <https://doi.org/10.1016/j.jcpa.2006.06.007>.
- Buesa, R.J. 2008. Histology without formalin?. *Ann Diagn Pathol* 12:387-396.
- Burger, J., Jeitner, C., Donio, M., Pittfield, T., Gochfeld, M. 2013. Mercury and selenium levels, and selenium: mercury molar ratios of brain, muscle and other tissues in bluefish (*Pomatomus saltatrix*) from New Jersey, USA. *Sci. Tot. Environ.* 443, 278-286. <https://doi.org/10.1016/j.scitotenv.2012.10.040>.
- Burnham, K.P., Anderson, D.R., 2002. *Model Selection and Multimodel Inference*. Springer-Verlag, New York.
- Burreau, S., Zebühr, Y., Broman, D., Ishaq, R. 2006. Biomagnification of PBDEs and PCBs in food webs from the Baltic Sea and the northern Atlantic Ocean. *Sci. Tot. Environ.* 366(2-3), 659-672. <https://doi.org/10.1016/j.scitotenv.2006.02.005>.
- Burrows, D.G., Reichert, W.L., Hanson, M.B. 2014. Effects of decomposition and storage conditions on $\delta^{13}\text{C}$ and $\delta^{15}\text{N}$ isotope values of killer whale (*Orcinus orca*) skin and blubber tissues. *Mar. Mam. Sci.* 30, 747-762. <https://doi.org/10.1111/mms.12076>.

- Bush, V.J., Moyer, T.P., Batts, K.P., Parisi, J.E. 1995. Essential and toxic element concentrations in fresh and formalin-fixed human autopsy tissues. *Clin. Chem.* 41:284-294.
- Cáceres-Saez, I., Panebianco, M.V., Perez-Catán, S., Dellabianca, N.A., Negri, M.F., Ayala, C.N., Goodall, R.N.P., Cappozzo, H.L. 2016. Mineral and essential element measurements in dolphin bones using two analytical approaches. *Chem Ecol.* <https://doi.org/10.1080/02757540.2016.1177517>
- Cáceres-Saez, I., Dellabianca, N.A., Goodall, R.N.P., Cappozzo, H.L., Guevara, S.R., 2013. Mercury and selenium in subantarctic Commerson's Dolphins (*Cephalorhynchus c. commersonii*). *Biol. Trace Elem. Res.* 151(2), 195-208. <https://doi.org/10.1007/s12011-012-9555-x>.
- Cáceres-Saez, I., Goodall, R.N.P., Dellabianca, N.A., Cappozzo, H.L., Guevara, S.R., 2015. The skin of Commerson's dolphins (*Cephalorhynchus commersonii*) as a biomonitor of mercury and selenium in Subantarctic waters. *Chemosphere*, 138, 735-743. <https://doi.org/10.1016/j.chemosphere.2015.07.026>.
- Cáceres-Saez, I., Haro, D., Blank, O., Aguayo-Lobo, A., Dougnac, C., Arredondo, C., Guevara, S.R. 2021. Trace elements in subantarctic false killer whale (*Pseudorca crassidens*) tissues, including the skin as an offshore bioindicator. *Environ. Sci. Pollut. Res.* 1-12.

- Cáceres-Saez, I., Haro, D., Blank, O., Aguayo-Lobo, A.A., Dougnac, C., Arredondo, C., Cuppozzo H.L., Guevara, S.R., 2018. High status of mercury and selenium in false killer whales (*Pseudorca crassidens*, Owen 1846) stranded on Southern South America: A possible toxicological concern? *Chemosphere*, 199, 637-646. <https://doi.org/10.1016/j.chemosphere.2018.02.046>
- Cai, Y., Rooker, J.R., Gill, G.A., Turner, J.P. 2007. Bioaccumulation of mercury in pelagic fishes from the northern Gulf of Mexico. *Can. J. Fish. Aquat. Sci.* 64(3), 458-469. <https://doi.org/10.1139/f07-017>
- Campbell, L.M., Drevnick, P.E. 2015. Use of catalogued long-term biological collections and samples for determining changes in contaminant exposure to organisms. In Blais, J.M., Rosen, M.R., Smol, J.P., eds, *Environmental Contaminants: Using natural archives to track sources of long-term trends in pollution*, Springer Dordrecht, Berlin, Germany, pp 431–459.
- Capelli, R., Das, K., De Pellegrini, R., Drava, G., Lepoint, G., Miglio, C., Minganti., V., Poggi, R., 2008. Distribution of trace elements in organs of six species of cetaceans from the Ligurian Sea (Mediterranean), and the relationship with stable carbon and nitrogen ratios. *Sci. Total Environ.* 390, 569-578. <https://doi.org/10.1016/j.scitotenv.2007.10.036>.
- Cardellicchio, N., Decataldo, A., Di Leo, A., Misino, A., 2002. Accumulation and tissue distribution of mercury and selenium in striped dolphins (*Stenella coeruleoalba*) from the Mediterranean Sea (southern Italy). *Environ. Pollut.* 116, 265-271. [https://doi.org/10.1016/S0269-7491\(01\)00127-0](https://doi.org/10.1016/S0269-7491(01)00127-0).

- Cardellicchio, N., Giandomenico, S., Ragone, P., Di Leo, A. 2000. Tissue distribution of metals in striped dolphins (*Stenella coeruleoalba*) from the Apulian coasts, Southern Italy. *Mar. Environ. Res.* 49(1), 55-66. [https://doi.org/10.1016/S0141-1136\(99\)00048-3](https://doi.org/10.1016/S0141-1136(99)00048-3).
- Carmichael, R. H., Graham, W. M., Aven, A., Worthy, G., Howden, S., 2012. Were multiple stressors a 'perfect storm' for northern Gulf of Mexico bottlenose dolphins (*Tursiops truncatus*) in 2011?. *PLoS one*, 7(7), e41155. <https://doi.org/10.1371/journal.pone.0041155>.
- Carvalho, M.L., Pereira, R.A., Brito, P.J., 2002. Heavy metals in soft tissues of *Tursiops truncatus* and *Delphinus delphis* from west Atlantic Ocean by X-ray spectrometry. *Sci. Total. Environ.* 292, 247-254. [https://doi.org/10.1016/S0048-9697\(01\)01131-7](https://doi.org/10.1016/S0048-9697(01)01131-7).
- Caurant, F., Navarro, M., Amiard, J.C., 1996. Mercury in pilot whales: possible limits to the detoxification process. *Sci. Total Environ.* 186(1-2), 95-104. [https://doi.org/10.1016/0048-9697\(96\)05087-5](https://doi.org/10.1016/0048-9697(96)05087-5).
- Caut, S., Angulo, E., Courchamp, F., 2009. Variation in discrimination factors ($\Delta^{15}\text{N}$ and $\Delta^{13}\text{C}$): the effect of diet isotopic values and applications for diet reconstruction. *J. Appl. Ecol.* 46(2), 443-453. <https://doi.org/10.1111/j.1365-2664.2009.01620.x>.
- Caut, S., Laran, S., Garcia-Hartmann, E., Das, K., 2011. Stable isotopes of captive cetaceans (killer whales and bottlenose dolphins). *J. Exp. Biol.* 214(4), 538-545. <https://doi.org/10.1242/jeb.045104>.

- Chanton, J.P., Lewis, F.G., 1991. Plankton and dissolved inorganic carbon isotopic composition in a river-dominated estuary: Apalachicola Bay, Florida. *Estuaries*. 22, 575-583. <https://doi.org/10.2307/1353045>.
- Chanton, J.P., Martens, C.S., Goldhaber, M.B., 1987. Biogeochemical cycling in an organic-rich coastal marine basin. 8. A sulfur isotopic budget balanced by differential diffusion across the sediment-water interface. *Geochimica et Cosmochimica Acta*. 51, 1201-1208. [https://doi.org/10.1016/0016-7037\(87\)90212-2](https://doi.org/10.1016/0016-7037(87)90212-2).
- Chasar, L.C., Chanton, J.P., Koeing, C.C., Coleman, F.C., 2005. Evaluating the effect of environmental disturbance on trophic structure of Florida Bay, USA: multiple stable isotope analyses of contemporary and historical specimens. *Limnol. Oceanogr.* 50, 1059-1072. <https://doi-org.libproxy.txstate.edu/10.4319/lo.2005.50.4.1059>.
- Cheal, A. J., Gales, N. J. 1991. Body mass and food intake in captive, breeding bottlenose dolphins, *Tursiops truncatus*. *Zoo Biol*, 10(6), 451-456. <https://doi.org/10.1002/zoo.1430100603>.
- Chen, C.Y., Dionne, M., Mayes, B.M., Ward, D.M., Sturup, S., Jackson, B.P., 2009. Mercury bioavailability and bioaccumulation in estuarine food webs in the Gulf of Maine. *Environ. Sci. Technol.* 43(6), 1804-1810. <https://doi.org/10.1021/es8017122>.
- Chen, C.Y., Folt, C. L., 2005. High plankton densities reduce mercury biomagnification. *Environ. Sci. Technol.* 39(1), 115-121. <https://doi.org/10.1021/es0403007>.

- Chen, M.H., Zhuang, M.F., Chou, L.S., Liu, J.Y., Shih, C.C., Chen, C.Y. 2017. Tissue concentrations of four Taiwanese toothed cetaceans indicating the silver and cadmium pollution in the western Pacific Ocean. *Mar. Pollut. Bull.* 124, 993-1000.
- Chételat, J., Ackerman, J.T., Eagles-Smith, C.A., Hebert, C.E., 2020. Methylmercury exposure in wildlife: A review of the ecological and physiological processes affecting contaminant concentrations and their interpretation. *Sci. Total Environ.* 711:135117. <https://doi.org/10.1016/j.scitotenv.2019.135117>.
- Choy, C.A., Popp, B.N., Kaneko, J.J., Drazen, J.C., 2009. The influence of depth on mercury levels in pelagic fishes and their prey. *PNAS.* 106(33), 13865-13869. <https://doi.org/10.1073/pnas.0900711106>.
- Clark, C.T., Horstmann, L., Misarti, N. 2020a. Evaluating tooth strontium and barium as indicators of weaning age in Pacific walruses. *Methods Ecol Evol.* <https://doi.org/10.1111/2041-210X.13482>
- Clark, C.T., Horstmann, L., Misarti, N. 2020b. Evaluating tooth strontium and barium as indicators of weaning age in Pacific walruses. *Methods Ecol Evol* 11(12):1626-1638. <https://doi.org/10.1111/2041-210X.13482>
- Clark, C.T., Horstmann, L., Misarti, N. 2021. Walrus teeth as biomonitors of trace elements in Arctic marine ecosystems. *Sci Total Environ.* <https://doi.org/10.1016/j.scitotenv.2021.145500>
- Clarkson, T.W. 1993. Molecular and ionic mimicry of toxic metals. *Annu. Rev. Pharmacol. Toxicol.* 32,547-571. <https://doi.org/10.1146/annurev.pa.33.040193.002553>.

Clarkson, T.W. 1997. The toxicology of mercury. *Crit. Rev. Cl. Lab. Sci.* 34(4), 369-403.
<https://doi.org/10.3109/10408369708998098>.

Colegrove, K.M., Venn-Watson, S., Litz, J., Kinsel, M.J., Terio, K.A., Fougères, E., Ewing, R., Pabst, D.A., McLellan, W.A., Raverty, S., Saliki, J., Fire, S., Rappucci, G., Bowen-Stevens, S., Noble, L., Costidis, A., Barbieri, M., Field, C., Smith, S., Carmichael, R.H., Chevis, C., Hatchett, W., Shannon, D., Tumlin, M., Lovewell, G., McFee, W., Rowles, T.K. 2016. Fetal distress and in utero pneumonia in perinatal dolphins during the Northern Gulf of Mexico unusual mortality event. *Dis. Aquat. Organ.* 119(1), 1-16.
<https://doi.org/10.3354/dao02969>.

Colegrove, K.M., Venn-Watson, S., Litz, J., Kinsel, M.J., Terio, K. A., Fougères, E., Ewinf, R., Pabst, D.A., McLellan, W.A., Raverty, S., Saliki, J., Fire, S, Rappucci, G., Bowen-Stevens, S., Noble, L., Costidis, A., Barbieri, M., Field, C., Smith, S., Carmichael, R.H., Chevis, C., Hatchett, W., Shannon, D., Tumlin, M., Lovewell, G., McFree, W, Rowles, T.K. 2016. Fetal distress and in utero pneumonia in perinatal dolphins during the Northern Gulf of Mexico unusual mortality event. *Dis. Aquat. Org.* 119, 1-16. <https://doi.org/10.3354/dao02969>.

Compeau, G.C., Bartha, R. 1985. Sulfate-reducing bacteria: principal methylators of mercury in anoxic estuarine sediment. *Appl. Environ. Microbiol.*, 50(2), 498-502.

Connell, D.W., Lam, P., Richardson, B., Wu, R. 2009. *Introduction to ecotoxicology*. Blackwell Science. Malden, MA.

- Cozzi, B., Huggenberger, S., Oelschläger, H., 2017. General appearance and hydrodynamics (including skin anatomy). In: Cozzi, B., Huggenberger, S., Oelschläger, H. (Eds.), *Anatomy of Dolphins*. Academic Press, London, pp. 21-31. <https://doi.org/10.1016/B978-0-12-407229-9.00002-6>.
- Cruwys, E., Robinson, K., Davis, N.R. 1994. Microprobe analysis of trace metals in seal teeth from Svalbard, Greenland, and South Georgia. *Polar Rec.* <https://doi.org/10.1017/S0032247400021057>.
- Curzon, M.E.J., Featherstone, J.D.B. 1983. Chemical composition in enamel. In: Lazari EP, Levy BM (eds) *CRC handbook of experimental aspects of oral biochemistry*. CRC Press, Boca Raton, FL, pp 123-135.
- Cuy, J.L., Mann, A.B., Livi, K.J., Teaford, M.F., Weihs, T.P. 2002. Nanoindentation mapping of mechanical properties of human molar tooth enamel. *Arch Oral Biol.* [https://doi.org/10.1016/S0003-9969\(02\)00006-7](https://doi.org/10.1016/S0003-9969(02)00006-7).
- D'Surney, J., Smithh, M.D. 2005. Chemicals of Environmental Concern. In *Encyclopedia of Toxicology*. Wexler, P. (Ed.) Elsevier pp 526-530.
- Damseaux, F., Kiszka, J.J., Heithaus, M.R., Scholl, G., Eppe, G., Thomé, J.P., Lewis J., Hao, W., Fontaine, M.C., Das, K., 2017. Spatial variation in the accumulation of POPs and mercury in bottlenose dolphins of the Lower Florida Keys and the coastal Everglades (South Florida). *Environ. Pollut.* 220, 577-587. <https://doi.org/10.1016/j.envpol.2016.10.005>.
- Damseaux, F., Siebert, U., Pomeroy, P., Lepoint, G., Das, K. 2021. Habitat and resource segregation of two sympatric seals in the North Sea. *Sci. Total Environ.* 764, 142842. <https://doi.org/10.1016/j.scitotenv.2020.142842>

- Das, K., Debacker, V., Pillet, S., Bouquegneau, J. M. 2003. Heavy metals in marine mammals. In Vos, J.G., Bossart, G., Fournier, M. & O'Shea, T. (Eds)., Toxicology of Marine Mammals London, UK: Taylor and Francis.
- de Dios Teruel J., Alcolea A., Hernández A., Ruiz, A.J.O. 2015. Comparison of chemical composition of enamel and dentine in human, bovine, porcine and ovine teeth. Arch Oral Biol. <https://doi.org/10.1016/j.archoralbio.2015.01.014>.
- De Guise, S. 1998. Effects of in vitro exposure of beluga whale leukocytes to selected organochlorines. Journal of Toxicology and Environmental Health Part A, 55(7), 479-493. <https://doi.org/10.1080/009841098158287>
- De María, M., Szteren, D., García-Alonso, J., de Rezende, C.E., Gonçalves, R.A., Godoy, J.M., Barboza, F.R. 2021. Historic variation of trace elements in pinnipeds with spatially segregated trophic habits reveals differences in exposure to pollution. Sci. Total Environ. 750, 141296. <https://doi.org/10.1016/j.scitotenv.2020.141296>
- Deegan, L.A., Peterson, B.J., Portier, R., 1990. Stable isotopes and cellulase activity as evidence for detritus as a food source for juvenile Gulf menhaden. Estuaries, 13(1), 14-19. <https://doi.org/10.2307/1351427>
- Dehn, L. A., Follmann, E. H., Rosa, C., Duffy, L. K., Thomas, D. L., Bratton, G. R., Taylor, R.J., O'Hara, T.M., 2006. Stable isotope and trace element status of subsistence-hunted bowhead and beluga whales in Alaska and gray whales in Chukotka. Mar. Pollut. Bull. 52(3), 301-319. <https://doi.org/10.1016/j.marpolbul.2005.09.001>.

- Demers, J.D., Sherman, L.S., Blum, J.D., Marsik, F. J., Dvonch, J.T. 2015. Coupling atmospheric mercury isotope ratios and meteorology to identify sources of mercury impacting a coastal urban-industrial region near Pensacola, Florida, USA. *Global Biogeochemical Cycles*, 29(10), 1689-1705.
- Deming, A.C., Colegrove, K.M., Duignan, P.J., Hall, A.J., Wellehan, J.F., Gulland, F. M. 2018. Prevalence of urogenital carcinoma in stranded California sea lions (*Zalophus californianus*) from 2005–15. *J. Wildl. Dis.* 54(3), 581-586.
<https://doi.org/10.7589/2017-08-208>
- Desforges, J. P., Levin, M., Jasperse, L., De Guise, S., Eulaers, I., Letcher, R. J., Dietz, R. 2017. Effects of polar bear and killer whale derived contaminant cocktails on marine mammal immunity. *Environ. Sci. Technol.* 51(19), 11431-11439.
<https://doi.org/10.1021/acs.est.7b03532>
- Di Guilo, R.T., Newman, M.C. 2008. Chapter 29. Ecotoxicology. In Klaassen, C.D. (Ed) Casarett and Doull's Toxicology: The Basic Science of Poisons. McGraw-Hill. New York, NY. pp 1157-1188.
- Dietz, R., Sonne, C., Basu, N., Braune, B., O'Hara, T., Letcher, R.J., Scheuhammer, T., Anderson, M., Andreasen, C., Andriashek, D., Asmund, G., Aubail, A., Baagøe, H., Born, E.W., Chan, H.M., Derocher, A.E., Grandjean, P., Knott, K., Kirkegaard, M., Krey, A, Lunn, N., Messier, F., Obbard, M., Olsen, M.T., Ostertag, S., Peacock, E., Renzoni, A., Rigét, F.F., Skarre, J.U., Stern, G., Stirling, I., Taylor, M., Wiig, Ø., Wilson, S, Aars, J., 2013. What are the toxicological effects of mercury in Arctic biota?. *Sci. Tot. Environ.* 443, 775-790.
<https://doi.org/10.1016/j.scitotenv.2012.11.046>.

- Dirtu, A. C., Malarvannan, G., Das, K., Dulau-Drouot, V., Kiszka, J.J., Lepoint, G., Mongin, P., Covaci, A. 2016. Contrasted accumulation patterns of persistent organic pollutants and mercury in sympatric tropical dolphins from the southwestern Indian Ocean. *Environ. Res.* 146, 263-273.
<https://doi.org/10.1016/j.envres.2016.01.006>.
- Dorozhkin S.V., Epple M. 2002. Biological and medical significance of calcium phosphates. *Angew Chem Int Ed.* [https://doi.org/10.1002/1521-3773\(20020902\)41:17<3130::AID-ANIE3130>3.0.CO;2-1](https://doi.org/10.1002/1521-3773(20020902)41:17<3130::AID-ANIE3130>3.0.CO;2-1)
- Duckworth, R.M. 2006. *The teeth and their environment: Physical, chemical and biochemical influences.* Karger Publishers, Basel, Switzerland.
- Durante, C.A., Reis, B.M.M., Azevedo, A., Crespo, E.A., Lailson-Brito, J. 2020. Trace elements in trophic webs from South Atlantic: The use of cetaceans as sentinels. *Mar. Pollut. Bull.* 150, 110674.
- Durden, W.N., Stolen, M. K., Adams, D.H., Stolen, E.D. 2007. Mercury and selenium concentrations in stranded bottlenose dolphins from the Indian River Lagoon system, Florida. *Bull. Mar. Sci.* 81(1), 37-54.
- DWH MMIQT (Deepwater Horizon Marine Mammal Injury Quantification Team), 2015. Models and analysis for the quantification of injury to Gulf of Mexico cetaceans from the Deepwater Horizon oil spill. DWH Marine Mammal NRDA Technical Working Group report.
<https://www.doi.gov/deepwaterhorizon/adminrecord> (accessed 23 Oct 2019)

- Eaton, D.L., Gilbert, S.G. 2008. Chapter 2. Principles of Toxicology. In Klaassen, C.D. (Ed). Casarett and Doull's Toxicology: The Basic Science of Poisons. McGraw-Hill. New York, NY. pp 11-45.
- Ebisuda, K., Kunita, T., Kubota, R., Tanabe, S. 2002. Arsenic concentrations and speciation in the tissues of ringed seals (*Phoca hispida*) from Pangnirtung, Canada. Appl. Organometal Chem. 16:415-457.
- Ellingham, S.T., Thompson, T.J., Islam, M. 2018. Scanning electron microscopy–energy-dispersive X-ray (SEM/EDX): a rapid diagnostic tool to aid the identification of burnt bone and contested cremains. J Forensic Sci. <https://doi.org/10.1111/1556-4029.13541>
- Elliott, K.H., Braune, B.M., Elliott, J.E. 2021. Beyond bulk $\delta^{15}\text{N}$: Combining a suite of stable isotopic measures improves the resolution of the food webs mediating contaminant signals across space, time and communities. Environ. Int. 148, 106370. <https://doi.org/10.1016/j.envint.2020.106370>.
- El-Shahawi, M.S., Hamza, A., Bashammakh, A.S., Al-Saggaf, W.T. 2010. An overview on the accumulation, distribution, transformations, toxicity and analytical methods for the monitoring of persistent organic pollutants. Talanta, 80(5). 1587-1597. <https://doi.org/10.1016/j.talanta.2009.09.055>.
- Endo, T., Kimura, O., Hisamichi, Y., Minoshima, Y., Haraguchi, K., Kakumoto, C., Kobayashi, M. 2006. Distribution of total mercury, methyl mercury, and selenium in pod of killer whales (*Orcinus Orca*) stranded in the northern area of Japan: comparison of mature females with calves. Environ. Pollut. 144:145-150.

- Endo, T., Haraguchi, K., Hotta, Y., Hisamichi, Y., Lavery, S., Dalebout, M.L., Baker, C.S., 2005. Total mercury, methyl mercury, and selenium levels in the red meat of small cetaceans sold for human consumption in Japan. *Environ. Sci. Technol.* 39(15), 5703-5708. <https://doi.org/10.1021/es050215e>.
- Endo, T., Hisamichi, Y., Kimura, O., Haraguchi, K., Lavery, S., Dalebout, M.L., Funahashi, N., Baker, C.S. 2010. Stable isotope ratios of carbon and nitrogen and mercury concentrations in 13 toothed whale species taken from the western Pacific Ocean off Japan. *Environ. Sci. Technol.* 44(7), 2675-2681. <https://doi.org/10.1021/es903534r>.
- Esposito, M., Capozzo, D., Sansone, D., Lucifora, G., La Nucara, R., Picazio, G., Gallo, P. 2020. Mercury and cadmium in striped dolphins (*Stenella coeruleoalba*) stranded along the Southern Tyrrhenian and Western Ionian coasts. *Mediterranean Marine Science*, 21(3), 519-526.
- Evans D, Cohen M, Hammerschmidt C.R., Landing W., Rumbold D., Simons J., Wolfe S. 2013. White paper on Gulf of Mexico mercury fate and transport: Applying scientific research to reduce the risk from mercury in Gulf of Mexico seafood. Gulf of Mexico Alliance, Ocean Springs, MS, USA.
- Evans R.D., Richner P., Outridge P.M. 1995. Micro-spatial variations of heavy metals in the teeth of walrus as determined by laser ablation ICP-MS: the potential for reconstructing a history of metal exposure. *Arch Environ Contam Toxicol.* <https://doi.org/10.1007/BF00213969>.

- Evans, D.W., Cohen, M., Hammerschmidt, C., Landing, W., Rumbold, D., Simons, J., Wolfe, S. H., 2015. White paper on Gulf of Mexico mercury fate and transport: Applying scientific research to reduce the risk from mercury in Gulf of Mexico seafood.
- Ewald, J. D., Kirk, J. L., Li, M., Sunderland, E.M. 2019. Organ-specific differences in mercury speciation and accumulation across ringed seal (*Phoca hispida*) life stages. *Sci. Total Environ.* 650, 2013-2020.
<https://doi.org/10.1016/j.scitotenv.2018.09.299>
- Fish, M.P., Mowbray, W.H. 1970 *Sounds of Western North Atlantic fishes: a reference file of biological underwater sounds.* Johns Hopkins Press, Baltimore
- Fitzgerald, W.F., Lamborg, C.H., Hammerschmidt, C.R., 2007. Marine biogeochemical cycling of mercury. *Chem. Rev.* 107, 641-662.
<https://doi.org/10.1021/cr050353m>.
- Fitzgerald, W.F., Lamborg, C.H., Hammerschmidt, C.R., 2007. Marine biogeochemical cycling of mercury. *Chem. Rev.* 107, 641-662.
<https://doi.org/10.1021/cr050353m>.
- Fossi, M.C., Casini, S., Maltese, S., Panti, C., Spinsanti, G., Marsili, L., 2014. An “ex vivo” model to evaluate toxicological responses to mixtures of contaminants in cetaceans: integumentum biopsy slices. *Environmental Toxicology* 29 (10), 1107–1121.
- Fox, J., Hong, J. 2009. Effect displays in R for multinomial and proportional-odds logit models: Extensions to the effects package. *J. Stat. Softw.*32(1), 1-24.

- Frodello, J.P., Romeo, M., Viale, D. 2000. Distribution of mercury in the organs and tissues of five toothed-whale species of the Mediterranean. *Environmental Pollution*, 108(3), 447-452.
- Frodello, J.P., Viale, D., Marchand, B., 2002. Metal concentrations in the milk and tissues of a nursing *Tursiops truncatus* female. *Mar. Pollut. Bull.* 44, 551-554.
[https://doi.org/10.1016/S0025-326X\(02\)00067-X](https://doi.org/10.1016/S0025-326X(02)00067-X).
- Fry, B., Chumchal, M.M., 2012. Mercury bioaccumulation in estuarine food webs. *Ecol. Appl.* 22(2), 606-623. <https://doi.org/10.1890/11-0921.1>.
- Gajdosechova, Z., Lawan, M. M., Urgast, D.S., Raab, A., Scheckel, K.G., Lombi, E., Kopittke, P.M., Loeshner, K., Larsen, E.H., Woods, G., Brownlow, A., Read, F.L., Feldmann, J., Krupp, E.M., 2016. In vivo formation of natural HgSe nanoparticles in the liver and brain of pilot whales. *Sci. Rep.* 6(1), 1-11.
<https://doi.org/10.1038/srep34361>.
- Galligan, T.M., Balmer, B.C., Schwacke, L. H., Bolton, J.L., Quigley, B. M., Rosel, P.E., Ylitalo, G.M., Boggs, A.S. 2019. Examining the relationships between blubber steroid hormones and persistent organic pollutants in common bottlenose dolphins. *Environ. Pollut.* 249, 982-991.
<https://doi.org/10.1016/j.envpol.2019.03.083>.
- García-Alvarez N, Fernández A, Boada LD, Zumbado M, Zaccaroni A, Arbelo M, Sierra E, Almunia J, Luzardo OP. 2015. Mercury and selenium status of bottlenose dolphins (*Tursiops truncatus*): a study in stranded animals on the Canary Islands. *Sci Total Environ* 536:489-498.

- García-Barrera, T., Gómez-Ariza, J. L., González-Fernández, M., Moreno, F., García-Sevillano, M. A., Gómez-Jacinto, V. 2012. Biological responses related to agonistic, antagonistic and synergistic interactions of chemical species. *Analytical and bioanalytical chemistry*, 403(8), 2237-2253. <https://doi.org/10.1007/s00216-012-5776-2>.
- Gellein, K., Flaten, T.P., Erikson, K.M., Aschner, M., Syversen, T. 2008. Leaching of trace elements from biological tissue by formalin fixation. *Biol. Trace Elem. Res.* 121:221-225.
- Geraci, J.R., Lounsbury, V.J. 2005. *Marine mammals ashore: a field guide for strandings*, 2nd ed, National Aquarium in Baltimore Inc., Baltimore, MD, USA. pp 202-213.
- Gerofke, A., Kömp, P., McLachlan, M.S. 2005. Bioconcentration of persistent organic pollutants in four species of marine phytoplankton. *Environ. Toxicol. Chem.* 24(11), 2908-2917. <https://doi.org/10.1897/04-566R.1>.
- Gerson, J.R., Walters, D.M., Eagles-Smith, C.A., Bernhardt, E.S., Brandt, JE. 2020). Do two wrongs make a right? Persistent uncertainties regarding environmental Selenium–Mercury interactions. *Environ. Sci. Technol.* 54(15), 9228-9234.
- Gibbs, R.H. Jr, Jarosewich, E., Windom, H.L. 1974. Heavy metal concentrations in museum fish specimens: effects of preservatives and time. *Science* 184:475-477.
- Giménez, J., Ramírez, F., Almunia, J., Forero, M.G., de Stephanis, R., 2016. From the pool to the sea: Applicable isotope turnover rates and diet to skin discrimination factors for bottlenose dolphins (*Tursiops truncatus*). *J. Exp. Mar. Biol.* 475, 54-61. <https://doi.org/10.1016/j.jembe.2015.11.001>.

- Godard-Codding, C.A., Collier, T.K. 2018. Field sampling techniques and ecotoxicological biomarkers in cetaceans. In: Marine Mammal Ecotoxicology. Fossi, M.C., Panti, C. (Eds.). Academic Press, London, U.K., pp. 237-259.
- Godard-Codding, C.A., Collier, T.K. 2018. The effects of oil exposure on cetaceans. In: Fossi, M.C., Panti, C. (Eds.), Marine Mammal Ecotoxicology. Academic Press, London, U.K., pp. 75-93.
- Godard-Codding, C.A., Clark, R., Fossi, M.C., Marsili, L., Maltese, S., West, A.G., Valenzuela, L., Rowntree, V., Polyak, I., Cannon, J.C., Pinkerton, K., 2011. Pacific Ocean-wide profile of CYP1A1 expression, stable carbon and nitrogen isotope ratios, and organic contaminant burden in sperm whale skin biopsies. Environmental Health Perspectives 119 (3), 337–343.
- Goldberg, M., Kulkarni, A.B., Young, M., Boskey, A. 2011 Dentin: structure, composition and mineralization: The role of dentin ECM in dentin formation and mineralization. Front Biosci (Elite Ed). <https://doi.org/10.2741/e281>
- Gray, J.S. 2002. Biomagnification in marine systems: the perspective of an ecologist. Mar. Pollut. Bull. 45(1-12), 46-52. [https://doi.org/10.1016/S0025-326X\(01\)00323-X](https://doi.org/10.1016/S0025-326X(01)00323-X).
- Gregus, Z. 2008. Chapter 3. Mechanisms of Toxicity. In Klaassen, C.D. (Ed). Casarett and Doull's Toxicology: The Basic Science of Poisons. McGraw-Hill. New York, NY. pp 45-106.
- Gruber, J.A., 1981. Ecology of the Atlantic bottlenose dolphin (*Tursiops truncatus*) in the Pass Cavallo area of Matagorda Bay, Texas. M. Sc. thesis. Texas A&M University, College Station.

- Gui, D., Yu, R.Q., Karczmarski, L., Ding, Y., Zhang, H., Sun, Y., Zhang, M., Wu, Y. 2017. Spatiotemporal trends of heavy metals in Indo-Pacific humpback dolphins (*Sousa chinensis*) from the western Pearl River Estuary, China. *Environ. Sci. Technol.* 51(3), 1848-1858. <https://doi.org/10.1021/acs.est.6b05566>.
- Gulland, F., Hall, A.J., Ylitalo, G.M., Colegrove, K. M., Norris, T., Duignan, P. J., Halaska, B., Acevedo Whitehouse, K., Lowenstine, L.J., Deming, A.C., Rowles, T. K. 2020. Persistent Contaminants and Herpesvirus OtHV1 Are Positively Associated With Cancer in Wild California Sea Lions (*Zalophus californianus*). *Front. Mar. Sci.* 7, 1093. <https://doi.org/10.3389/fmars.2020.602565>.
- Gulland, F.M., Trupkiewicz, J.G., Spraker, T.R., Lowenstine, L.J. 1996. Metastatic carcinoma of probable transitional cell origin in 66 free-living California sea lions (*Zalophus californianus*), 1979 to 1994. *J. Wildl. Dis.* 32, 250–258. <https://doi.org/10.7589/0090-3558-32.2.250>.
- Halbach, S., 1985. The octanal/water distribution of mercury compounds. *Arch. Toxicol.* 57, 139-141. <https://doi.org/10.1007/BF00343125>.
- Hall, A.J., McConnell, B.J., Rowles, T.K., Aguilar, A., Borrell, A., Schwacke, L., Wells, R.S. 2006. Individual-based model framework to assess population consequences of polychlorinated biphenyl exposure in bottlenose dolphins. *Environmental Health Perspectives*, 114(Suppl 1), 60-64. <https://doi.org/10.1289/ehp.8053>.
- Hall, B.D., Aiken, G.R., Krabbenhoft, D.P., Marvin-DiPasquale, M., Swarzenski, C.M. 2008. Wetlands as principal zones of methylmercury production in southern Louisiana and the Gulf of Mexico region. *Environ. Pollut.* 154(1), 124-134. <https://doi.org/10.1016/j.envpol.2007.12.017>.

- Hall, L.A., Woo, I., Marvin-DiPasquale, M., Tsao, D.C., Krabbenhoft, D.P., Takekawa, J.Y., De La Cruz, S.E. 2020. Disentangling the effects of habitat biogeochemistry, food web structure, and diet composition on mercury bioaccumulation in a wetland bird. *Environ. Pollut.* 256, 113280.
<https://doi.org/10.1016/j.envpol.2019.113280>.
- Hall, R.A., Zook, E.G., Meaburn, G.M., 1978. National Marine Fisheries Service Survey of Trace Elements in the Fishery Resource. NOAA Technical Report NMFS SSRF-721 Washington, D.C., pp. 313.
- Hameed M., Dijoo Z.K., Bhat R.A., Qayoom I., 2020. Concerns and Threats of Heavy Metals' Contamination on Aquatic Ecosystem. In: Bhat R.A., Hakeem K.R. (eds) *Bioremediation and Biotechnology*, Vol 4. Springer, Cham.
https://doi.org/10.1007/978-3-030-48690-7_1.
- Hammerschmidt, C.R., Fitzgerald, W.F., 2006. Bioaccumulation and trophic transfer of methylmercury in Long Island Sound. *Arch. Environ. Con. Tox.* 51, 416-424.
<https://doi.org/10.1007/s00244-005-0265-7>.
- Hammerschmidt, C.R., Fitzgerald, W.F., 2006. Bioaccumulation and trophic transfer of methylmercury in Long Island Sound. *Arch. Environ. Con. Tox.* 51, 416-424.
<https://doi.org/10.1007/s00244-005-0265-7>.
- Harper, A., Landing, W., Chanton, J.P., 2018. Controls on the variation of methylmercury concentration in seagrass bed consumer organisms of the Big Bend, Florida, USA. *Estuaries Coasts*, 41(5), 1486-1495.
<https://doi.org/10.1007/s12237-017-0355-6>.

- Harris, R., Pollman, C., Hutchinson, D., Landing, W., Axelrad, D., Morey, S.L., Dukhovskoy, D., Vijayaraghavan, K., 2012b. A screening model analysis of mercury sources, fate and bioaccumulation in the Gulf of Mexico. *Environ. Res.* 119, 53-63. <https://doi.org/10.1016/j.envres.2012.08.013>
- Harris, R., Pollman, C., Landing, W., Evans, E., Axelrad, D., Hutchinson, D., Morey, S.L., Rumbold, D., Dukhovskoy, D., Adams, D.H., Vijayaraghavan, K., Holmes, C., Atkinson, R.D., Myers, T., Sunderland, E., 2012. Mercury in the Gulf of Mexico: sources to receptors. *Environ. Res.* 119, 42-52. <https://doi.org/10.1016/j.envres.2012.08.001>.
- Hauser-Davis, R. A., Figueiredo, L., Lemos, L., de Moura, J. F., Rocha, R. C., Saint’Pierre, T., Siciliano, S. 2020. Subcellular Cadmium, Lead and Mercury Compartmentalization in Guiana Dolphins (*Sotalia guianensis*) From Southeastern Brazil. *Frontiers in Marine Science*, 7, 1072.
- Hayes, S.A., Josephson, E., Maze-Foley, K., Rosel, P. 2019. US Atlantic and Gulf of Mexico Marine mammal Stock Assessments-2018. National Oceanic and Atmospheric Administration, NOAA Technical Memorandum NMFS NE Woods Hole, Massachusetts. p 164.
- Helminen, M., Karppanen, E., Koivisto, J. 1968. Mercury in Finnish Freshwater seals (*Phocahispida Saimensis Nordq.*) in 1967. *Finsk. Veterninartidskr*, 74, 87-89.
- Henriksson, K., Karppanen, E., Helminen, M. 1969. Mercury content in seals from lakes and sea. *Nordisk hygienisk tidskrift*, 50(2), 54-59.
- Hershko, C. 2007. Mechanism of iron toxicity. *Food and nutrition bulletin*, 28. S501-S509.

- Hertz, E., Trudel, M., Cox, M.K., Mazumder, A., 2015. Effects of fasting and nutritional restriction on the isotopic ratios of nitrogen and carbon: a meta-analysis. *Ecol. Evol.* 5(21), 4829-4839. <https://doi.org/10.1002/ece3.1738>.
- Hickie, B.E., Cadieux, M.A., Riehl, K.N., Bossart, G.D., Alava, J.J., Fair, P.A. 2013. Modeling PCB-bioaccumulation in the bottlenose dolphin (*Tursiops truncatus*): estimating a dietary threshold concentration. *Environ. Sci. Technol.* 47(21), 12314-12324. <https://doi.org/10.1021/es403166b>.
- Hickie, B.E., Mackay, D., de Koning, J. 1999. Lifetime pharmacokinetic model for hydrophobic contaminants in marine mammals. *Environmental Toxicology and Chemistry: An International Journal*, 18(11), 2622-2633. <https://doi.org/10.1002/etc.5620181132>.
- Hickie, B.E., Ross, P.S., Macdonald, R.W., Ford, J. K. 2007. Killer whales (*Orcinus orca*) face protracted health risks associated with lifetime exposure to PCBs. *Environmental Science & Technology*, 41(18), 6613-6619. <https://doi.org/10.1021/es0702519>.
- Hill, J.J., Chumchal, M.M., Drenner, R.W., Pinder, J.E. III, Drenner, S.M. 2010. Use of preserved museum fish to evaluate historical and current mercury contamination in fish from two rivers in Oklahoma, USA. *Environ Monit Assess* 161:509-516.
- Hobson, K.A., Schell, D.M., Renouf, D., Noseworthy, E., 1996. Stable carbon and nitrogen isotopic fractionation between diet and tissues of captive seals: implications for dietary reconstructions involving marine mammals. *Can. J. Fish. Aquat. Sci.* 53(3), 528-533. <https://doi.org/10.1139/f95-209>.

- Hohn A.A., Scott M.D., Wells R.S., Sweeny J.C., Irvine A.B. 1989. Growth layers in teeth from free-ranging, known-age bottlenose dolphins. *Mar Mamm Sci* 5:315-342. <https://doi.org/10.1111/j.1748-7692.1989.tb00346.x>.
- Hohn, A.A. 2009. Age estimations. In: Perrin WF, Wursig B, Thewissen JGM (eds) *Encyclopedia of marine mammals*, 2nd edn. Academic Press, London, pp 11-17.
- Hohn, A.A., Thomas, L., Carmichael, R.H., Litz, J., Clemons-Chevis, C., Shippee, S.F., Sinclair, S., Smith, S., Speakman, T.R., Tumlin, M.C., Zolman, E.S., 2017. Assigning stranded bottlenose dolphins to source stocks using stable isotope ratios following the *Deepwater Horizon* oil spill. *Endanger. Species. Res.* 33, 235-252. <https://doi.org/10.3354/esr00783>.
- Hong, Y.S., Hull, P., Rifkin, E., & Bouwer, E. J. 2013. Bioaccumulation and biomagnification of mercury and selenium in the Sarasota Bay ecosystem. *Environ. Toxicol. Chem.* 32(5), 1143-1152. <https://doi.org/10.1002/etc.2169>.
- Hong, Y.S., Hunter, S., Clayton, L.A., Rifkin, E., Bouwer, E.J., 2012. Assessment of mercury and selenium concentrations in captive bottlenose dolphin's (*Tursiops truncatus*) diet fish, blood, and tissue. *Sci. Total. Environ.* 414, 220-226. <https://doi.org/10.1016/j.scitotenv.2011.11.021>.
- Houde, M., Bujas, T.A., Small, J., Wells, R.S., Fair, P.A., Bossart, G.D., Solomon, K.R., Muir, D.C. 2006. Biomagnification of perfluoroalkyl compounds in the bottlenose dolphin (*Tursiops truncatus*) food web. *Environ. Sci. Technol.* 40(13), 4138-4144. <https://doi.org/10.1021/es060233b>.

- Huang, Y., Rajput, I. R., Sanganyado, E., Yajing, S., Yu, F., Liang, B., Liu, W. 2020. Immune stimulation effect of PBDEs via prostaglandin pathway in pantropical spotted dolphin: An in vitro study. *Chemosphere*, 254, 126717. <https://doi.org/10.1016/j.chemosphere.2020.126717>
- Hubard, C.W., Maze-Foley, K., Mullin, K.D., Schroder, W.W., 2004. Seasonal abundance and site fidelity of bottlenose dolphins (*Tursiops truncatus*) in the Mississippi Sound. *Aquat. Mamm.* 30, 299-310. <https://doi.org/10.1578/AM.30.2.2004.299>.
- Hussey, N.E., MacNeil, M.A., McMeans, B.C., Olin, J.A., Dudley, S.F., Cliff, G., Winter, S.P., Fennessy, S.T., Fisk, A.T., 2014. Rescaling the trophic structure of marine food webs. *Ecol. Lett.* 17(2), 239-250. <https://doi.org/10.1111/ele.12226>
- Irvine, A.B., Scott, M.D., Wells R.S., Kaufmann J.H., 1981. Movements and activities of the Atlantic bottlenose dolphin, *Tursiops truncatus*, near Sarasota, Florida. *Fish. Bull.* 79, 671-688.
- Irwin, L.J., Würsig, B., 2004. A small resident community of bottlenose dolphins, *Tursiops truncatus*, in Texas: Monitoring recommendations. *Gulf Mex. Sci.* 22, 13-21. <https://doi.org/10.18785/goms.2201.02>.
- Isobe, T., Ochi, Y., Ramu, K., Yamamoto, T., Tajima, Y., Yamada, T.K., Amano, M., Miyazaki, N., Takahashi, S., Tanabe, S. 2009. Organohalogen contaminants in striped dolphins (*Stenella coeruleoalba*) from Japan: present contamination status, body distribution and temporal trends (1978–2003). *Mar. Pollut. Bull.* 58(3), 396-401. <https://doi.org/10.1016/j.marpolbul.2008.10.008>.

- Itano, K., Kawai, S. 1986. Changes in mercury content and biological half-life of mercury in striped dolphins. In: Fujiyama T (ed) Studies on the levels of organochlorine compounds and heavy metals in marine organisms. University of Ryukus,. P 49-73
- Itano, K., Kawai, S., 1981. Changes of mercury and selenium contents and biological half-life of mercury in the striped dolphin, in: Fujiyama, F. (Ed.), Studies of the Levels of Organochlorine Compounds and Heavy Metals in the Marine Organisms. University of Ryukyus, Japan, pp. 49–72.
- Itano, K., Kawai, S.I., Miyazaki, N., Tatsukawa, R., Fujiyama, T. 1984. Mercury and selenium levels at the fetal and suckling stages of striped dolphin, *Stenella coeruleoalba*. Agric. Biol. Chem. 48(7), 1691-1698.
<https://doi.org/10.1271/bbb1961.48.1691>.
- Kaneko, J.J., Ralston, N.V.C., 2007. Selenium and mercury in pelagic fish in the central north Pacific near Hawaii. Biol. Trace Elem. Res. 119, 242-254.
<https://doi.org/10.1007/s12011-007-8004-8>.
- Kang, D., Amarasiriwardena, D., Goodman, A.H. 2004 Application of laser ablation–inductively coupled plasma-mass spectrometry (LA–ICP–MS) to investigate trace metal spatial distributions in human tooth enamel and dentine growth layers and pulp. Anal Bioanal Chem. <https://doi.org/10.1007/s00216-004-2504-6>.

- Karouna-Renier, N.K., Snyder, R.A., Lange, T., Gibson, S., Allison, J.G., Wagner, M.E., Rao, K.R. 2011. Largemouth bass (*Micropterus salmoides*) and striped mullet (*Mugil cephalus*) as vectors of contaminants to human consumers in northwest Florida. *Mar. Environ. Res.* 72(3), 96-104.
<https://doi.org/10.1016/j.marenvres.2011.06.003>.
- Kastelein, R.A., Staal, C., Wiepkema, P.R. 2003. Food consumption, food passage time, and body measurements of captive Atlantic bottlenose dolphins (*Tursiops truncatus*). *Aquat. Mamm.* 29(1), 53-66.
<http://doi.org/10.1578/016754203101024077>.
- Kastelein, R.A., Vaughan, N., Walton, S., Wiepkema, P.R. 2002. Food intake and body measurements of Atlantic bottlenose dolphins (*Tursiops truncates*) in captivity. *Mar. Environ. Res.* 53(2), 199-218. [https://doi.org/10.1016/S0141-1136\(01\)00123-4](https://doi.org/10.1016/S0141-1136(01)00123-4).
- Kehrig, H.A., Seixas, T.G., Palermo, E.A., Di Benedetto, A.P.M., Souza, C.M.M., Malm, O. 2008. Different species of mercury in the livers of tropical dolphins. *Anal Lett* 41:1691-1699.
- Kehrig, H.A., Hauser-Davis, R.A., Seixas, T. G., Pinheiro, A.B., Di Benedetto, A.P.M. 2016. Mercury species, selenium, metallothioneins and glutathione in two dolphins from the southeastern Brazilian coast: mercury detoxification and physiological differences in diving capacity. *Environ. Pollut.* 213, 785-792.
<https://doi.org/10.1016/j.envpol.2016.03.041>.

- Kehrig, H. D. A., Seixas, T. G., Palermo, E. A., Baêta, A. P., Castelo-Branco, C. W., Malm, O., Moreira, I., 2009. The relationships between mercury and selenium in plankton and fish from a tropical food web. *Environ. Sci. Pollut. Res.* 16(1), 10-24. <https://doi.org/10.1007/s11356-008-0038-8>.
- Kehrig, H.A., Seixas, T.G., Malm, O., Di Benedetto, A.P.M., Rezende, C.E., 2013. Mercury and selenium biomagnification in a Brazilian coastal food web using nitrogen stable isotope analysis: a case study in an area under the influence of the Paraíba do Sul River plume. *Mar. Pollut. Bull.* 75(1-2), 283-290. <https://doi.org/10.1016/j.marpolbul.2013.06.046>.
- Kennicutt, M.C. 2017. Chapter 2. Water quality of the Gulf of Mexico. In Ward, H.E. (Ed). *Habitats and Biota of the Gulf of Mexico: Before the Deepwater Horizon Oil Spill. Volume 1: Water Quality, Sediments, Sediment Contaminants, Oil and Gas Seeps, Coastal Habitats, Offshore Plankton and Benthos, and Shellfish.* Springer. New York, NY. pp 217-274.
- Kennicutt, M.C. 2017a. Chapter 4. Sediment contaminants of the Gulf of Mexico. In Ward, H.E. (Ed). *Habitats and Biota of the Gulf of Mexico: Before the Deepwater Horizon Oil Spill. Volume 1: Water Quality, Sediments, Sediment Contaminants, Oil and Gas Seeps, Coastal Habitats, Offshore Plankton and Benthos, and Shellfish.* Springer. New York, NY. pp 217-274.
- Kerr, R., Kintisch, E., Stokstad, E. 2010. Will Deepwater Horizon set a new standard for catastrophe?. *Science.* 328(5979), 674-675. <https://doi.org/10.1126/science.328.5979.674>.

- Kershaw, J.L., Hall, A.J., 2019. Mercury in cetaceans: Exposure, bioaccumulation and toxicity. *Sci. Total Environ.* 694:133683.
<https://doi.org/10.1016/j.scitotenv.2019.133683>.
- Khan, M.A., Wang, F., 2009. Mercury-selenium compounds and their toxicological significance: Toward a molecular understanding of the mercury-selenium antagonism. *Environ. Toxicol. Chem.* 28(8), 1567-1577.
<https://doi.org/10.1897/08-375.1>.
- Kiernan J.A. 2000. Formaldehyde, formalin, paraformaldehyde and glutaraldehyde: what they are and what they do. *Micros today* 8:8-13.
- King, D.P., Hure, M.C., Goldstein, T., Aldridge, B.M., Gulland, F.M D., Saliki, J.T., Buckles, E.L., Lowenstine, L.J., Scott, J.L. 2002. Otarine herpesvirus-1: a novel gammaherpesvirus associated with urogenital carcinoma in California sea lions (*Zalophus californianus*). *Vet. Microbiol.* 86, 131–137.
[https://doi.org/10.1016/s0378-1135\(01\)00497-7](https://doi.org/10.1016/s0378-1135(01)00497-7).
- Kinghorn, A., Humphries, M.M., Outridge, P., Chan, H.M. 2008. Teeth as biomonitors of selenium concentrations in tissues of beluga whales (*Delphinapterus leucas*). *Sci Total Environ.* <https://doi.org/10.1016/j.scitotenv.2008.04.031>.
- Knoff, A., Hohn, A., Macko, S., 2008. Ontogenetic diet changes in bottlenose dolphins (*Tursiops truncatus*) reflected through stable isotopes. *Mar. Mam. Sci.* 24, 128-137. <https://doi.org/10.1111/j.1748-7692.2007.00174.x>.
- Koizumi, N., Hatayama, F., Sumino, K. 1994. Problems in the analysis of cadmium in autopsied tissues. *Environ Res* 64:192-198.

- Krey, A., Ostertag, S.K., Chan, H.M., 2015. Assessment of neurotoxic effects of mercury in beluga whales (*Delphinapterus leucas*), ringed seals (*Pusa hispida*), and polar bears (*Ursus maritimus*) from the Canadian Arctic. *Sci. Total Environ.* 509, 237-247. <https://doi.org/10.1016/j.scitotenv.2014.05.134>.
- Krouwer, J.S. 2008. Why Bland–Altman plots should use X, not $(Y + X)/2$ when X is a reference method. *Statist Med* 27:778-780.
- Kuehl, D.W., Haebler, R., 1995. Organochlorine, organobromine, metal, and selenium residues in bottlenose dolphin (*Tursiops truncatus*) collected during an unusual mortality event in the Gulf of Mexico, 1990. *Arch. Environ. Con. Tox.* 228, 494-499. <https://doi.org/10.1007/BF00211632>.
- Kujawinski, E.B., Kido Soule, M.C., Valentine, D.L., Boysen, A.K., Longnecker, K., Redmond, M.C. 2011. Fate of dispersants associated with the Deepwater Horizon oil spill. *Environ Sci. Technol.* 45(4), 1298-1306. <https://doi.org/10.1021/es103838p>.
- Kunito T, Kubota R, Fujihara J, Agusa T, Tanabe S. 2008. Arsenic in Marine Mammals, Seabirds, and Sea Turtles. In Whitacre DM, eds, *Reviews of Environmental Contamination and Toxicology*, Vol 195. Springer, New York, NY, USA, pp 31-69.
- Lahaye, V., Bustamante, P., Dabin, W., Churlaud, C., Caurant, F. 2007. Trace element levels in foetus–mother pairs of short-beaked common dolphins (*Delphinus delphis*) stranded along the French coasts. *Environ. Int.* 33(8), 1021-1028. <https://doi.org/10.1016/j.envint.2007.05.008>.

- Lailson-Brito, J., Cruz, R., Dorneles, P.R., Andrade, L., de Freitas Azevedo, A., Fragoso, A.B., Vidal, L.G., Costa, M.D., Lemos, T.B., Almedia, R., Carvalho, D.P., Bastos, W.R., Malm, O., 2012. Mercury-selenium relationships in liver of Guiana dolphin: the possible role of Kupffer cells in the detoxification process by tiemannite formation. *PLoS One*, 7: e42162.
<https://doi.org/10.1371/journal.pone.0042162>.
- Lamborg, C.H., Hammerschmidt, C. R., Bowman, K. L., Swarr, G. J., Munson, K. M Ohnemus, D.C., Lam, P.J., Heimburger, Lars-Eric, Rijkenberg, A., Saito, M.A. 2014. A global ocean inventory of anthropogenic mercury based on water column measurements. *Nature*, 512(7512), 65-68. <https://doi.org/10.1038/nature13563>.
- Lamborg, C.H., Von Damm, K.L., Fitzgerald, W.F., Hammerschmidt, C.R., Zierenberg, R. 2006. Mercury and monomethylmercury in fluids from Sea Cliff submarine hydrothermal field, Gorda Ridge. *Geophy. Res. Lett.* 33(17).
<https://doi.org/10.1029/2006GL026321>
- Lane, D.W., Peach, D.F. 1997. Some observations on the trace element concentrations in human dental enamel. *Biol Elem Res.* <https://doi.org/10.1007/BF02783305>
- Lane, S.M., Smith, C.R., Mitchell, J., Balmer, B.C., Barry, K P., McDonald, T., Mori, C.S., Rosel, P.E., Rowles, T.K., Speakman, T.R., Townsend, F.I., Tumlin, M.C, Wells, R.S., Zolman, E.S., Schwacke, L.H. 2015. Reproductive outcome and survival of common bottlenose dolphins sampled in Barataria Bay, Louisiana, USA, following the Deepwater Horizon oil spill. *Proc. Royal Soc. B.* 282: 20151944. <https://doi.org/10.1098/rspb.2015.1944>

- Lavoie, R.A., Hebert, C.E., Rail, J.F., Braune, B.M., Yumvihoze, E., Hill, L.G., Lean, D.R., 2010. Trophic structure and mercury distribution in a Gulf of St. Lawrence (Canada) food web using stable isotope analysis. *Sci. Total Environ.* 408(22), 5529-5539. <https://doi.org/10.1016/j.scitotenv.2010.07.053>.
- Lavoie, R.A., Jardine, T.D., Chumchal, M.M., Kidd, K.A., Campbell, L.M., 2013. Biomagnification of mercury in aquatic food webs: a worldwide meta-analysis. *Environ. Sci. Technol.* 47(23), 13385-13394. <https://doi.org/10.1021/es403103t>
- Lavoie, R.A., Kyser, T.K., Friesen, V.L., Campbell, L.M. 2015., Tracking overwintering areas of fish-eating birds to identify mercury exposure. *Environ. Sci. Technol.* 49(2), 863-872. <https://doi.org/10.1021/es502813t>.
- Law, R.J., 1996. Metals in marine mammals. In: Beyer, W.N., Heinz, G.H., Redmon-Norwood, A.W. (Eds.), *Environmental contaminants in wildlife: Interpreting tissue concentrations*. CRC Press, Boca Raton, pp. 357–376.
- Leaner, J.J., Mason, R.P. 2002. Methylmercury accumulation and fluxes across the intestine of channel catfish, *Ictalurus punctatus*. *Comp. Biochem. Phys. C.*, 132(2), 247-259. [https://doi.org/10.1016/S1532-0456\(02\)00072-8](https://doi.org/10.1016/S1532-0456(02)00072-8).
- Lee, C.S., Fisher, N.S., 2016. Methylmercury uptake by diverse marine phytoplankton. *Limnol. Oceanogr.*, 61(5), 1626-1639. <https://doi.org/10.1002/lno.10318>.
- Lehman-McKeen, L.D. 2008. Chapter 5. Absorption, distribution, and excretion of toxicants. In Casarett and Doull's *Toxicology: The Basic Science of Poisons*. Klaassen, C.D. (Ed). McGraw-Hill. New York, NY. pp 131-160.

- Lemes, M., Wang, F., Stern, G.A., Ostertag, S.K., Chan, H.M. 2011. Methylmercury and selenium speciation in different tissues of beluga whales (*Delphinapterus leucas*) from the western Canadian Arctic. *Environ. Toxicol. Chem.* 30(12), 2732-2738. <https://doi.org/10.1002/etc.684>.
- Lemos, L.S., de Moura, J.F., Hauser-Davis, R.A., de Campos, R.C., Siciliano, S. 2013. Small cetaceans found stranded or accidentally captured in southeastern Brazil: Bioindicators of essential and non-essential trace elements in the environment. *Ecotoxicology and environmental safety*, 97, 166-175. <https://doi.org/10.1016/j.ecoenv.2013.07.025>
- Length, R. 2020. emmeans: Estimated Marginal Means, aka Least-Squares Means. R package version 1.5.0. <https://CRAN.R-project.org/package=emmeans>
- Leonzio, C., Focardi, S., Fossi, C. 1992. Heavy metals and selenium in stranded dolphins of the Northern Tyrrhenian (NW Mediterranean). *Sci. Total Environ.* 119, 77-84. [https://doi.org/10.1016/0048-9697\(92\)90257-S](https://doi.org/10.1016/0048-9697(92)90257-S).
- Levin, M., Jasperse, L., Desforges, J.P., O'Hara, T., Rea, L., Castellini, J.M., Maniscalco, J.M., Fadely, B., Keogh, M. 2020. Methyl mercury (MeHg) in vitro exposure alters mitogen-induced lymphocyte proliferation and cytokine expression in Steller sea lion (*Eumetopias jubatus*) pups. *Sci. Total Environ.* 725, 138308. <https://doi.org/10.1016/j.scitotenv.2020.138308>.
- Limbeck, A., Galler, P., Bonta, M., Bauer, G., Nischkauer, W., Vanhaecke, F. 2015. Recent advances in quantitative LA-ICP-MS analysis: challenges and solutions in the life sciences and environmental chemistry. *Anal. Bioanal. Chem.* <https://doi.org/10.1007/s00216-015-8858-0>.

- Lischka, A., Betty, E.L., Braid, H.E., Pook, C.J., Gaw, S., Bolstad, K.S.R. 2021. Trace element concentrations, including Cd and Hg, in long-finned pilot whales (*Globicephala melas edwardii*) mass stranded on the New Zealand coast. Mar. Pollut. Bull. 165, 112084.
- Litz, J. A., Baran, M. A., Bowen-Stevens, S. R., Carmichael, R. H., Colegrove, K. M., Garrison, L. P., Fire, S.E., Fourgeres, E.M., Hardy, R., Holmes, S., Jones, W., Mase-Guthrie, B.E., Odell, D.K., Rosel, P.E., Saliki, J.T., Shannon, D.K., Shippe, S.F., Smith, S.M., Stratton, E.M., Tumlin, M.C., Whitehead, H.R., Worthy, G.A.J., Rowles, T.K., 2014. Review of historical unusual mortality events (UMEs) in the Gulf of Mexico (1990-2009): providing context for the multi-year northern Gulf of Mexico cetacean UME declared in 2010. Dis. Aquat. Organ. 112, 161-175. <https://doi.org/10.3354/dao02807>.
- Liu, G., Cai, Y., Mao, Y., Scheidt, D., Kalla, P., Richards, J., Scinto, L.J., Tachiev, G., Roelant, D., Appleby, C., 2009. Spatial variability in mercury cycling and relevant biogeochemical controls in the Florida Everglades. Environ. Sci. Technol. 43(12), 4361-4366. <https://doi.org/10.1021/es803665c>.
- Liu, J. Goyer, R.A., Waalkes, M.P. Chapter 21. Toxic Effects of Metals. In Casarett and Doull's Toxicology: the basic science of poisons. Klaassen, C.D (Ed). pp. 931-980.
- Liu, J.Y., Chou, L.S., Chen, M.H. 2015. Investigation of trophic level and niche partitioning of 7 cetacean species by stable isotopes, and cadmium and arsenic tissue concentrations in the western Pacific Ocean. Mar. Pollut. Bull. 93(1-2), 270-277. <https://doi.org/10.1016/j.marpolbul.2015.01.012>.

- Loch, C., Swain, M.V., Fraser, S.J., Gordon, K.C., Kieser, J.A., Fordyce, R.E. 2014
Elemental and chemical characterization of dolphin enamel and dentine using X-
ray and Raman microanalyzes (Cetacea: Delphinoidea and Inioidea). *J Struct
Biol.* <https://doi.org/10.1016/j.jsb.2013.11.006>.
- Loch, C., Swain, M.V., van Vuuren, L.J., Kieser, J.A., Fordyce, R.E. 2013 Mechanical
properties of dental tissues in dolphins (Cetacea: Delphinoidea and Inioidea).
Arch Oral Biol. <https://doi.org/10.1016/j.archoralbio.2012.12.003>
- Loizaga De Castro, R., Saporiti, F., Vales, D.G., García, N. A., Cardona, L., Crespo, E.A.
2016. Feeding ecology of dusky dolphins *Lagenorhynchus obscurus*: evidence
from stable isotopes. *J. Mammal.* 97(1), 310-320.
<https://doi.org/10.1093/jmammal/gyv180>.
- López-Berenguer, G., Peñalver, J., Martínez-López, E. 2020. A critical review about
neurotoxic effects in marine mammals of mercury and other trace elements.
Chemosphere, 246, 125688. <https://doi.org/10.1016/j.chemosphere.2019.125688>
- Loseto, L.L., Stern, G.A., Ferguson, S. H., 2008. Size and biomagnification: how habitat
selection explains beluga mercury levels. *Environ. Sci. Technol.* 42, 3982-3988.
<https://doi.org/10.1021/es7024388>.
- Love, M., Baldera, A., Yeung, C., Robbins, C., 2013. The Gulf of Mexico ecosystem: a
coastal and marine atlas. New Orleans, LA: Ocean Conservancy, Gulf Restoration
Center, pp. 25.

- Lynch, K.M., Fair, P.A., Houde, M., Muir, D.C., Kannan, K., Bossart, G.D., Bartell, S.M., Gribble, M.O. 2019. Temporal Trends in Per-and Polyfluoroalkyl Substances in Bottlenose Dolphins (*Tursiops truncatus*) of Indian River Lagoon, Florida and Charleston, South Carolina. *Environ. Sci. Technol.* 53(24), 14194-14203. <https://doi.org/10.1021/acs.est.9b04585>.
- Mackey, E. A., Oflaz, R. D., Epstein, M. S., Buehler, B., Porter, B. J., Rowles, T., Wise, S.A., Becker, P. R. 2003. Elemental composition of liver and kidney tissues of rough-toothed dolphins (*Steno bredanensis*). *Arch. Environ. Contam. Toxicol.* 44, 0523-0532. <https://doi.org/10.1007/s00244-002-2039-9>.
- Mackey, E.A., Becker, P.R., Demiralp, R., Greenberg, R.R., Koster, B.J., Wise, S.A. 1996. Bioaccumulation of vanadium and other trace metals in livers of Alaskan cetaceans and pinnipeds. *Arch. Environ. Contam. Toxicol.* 30(4), 503-512. <https://doi.org/10.1007/BF00213402>.
- Macko, S. A. 2018. A perspective on marine pollution. In *The Marine Environment and United Nations Sustainable Development Goal 14* (pp. 291-308). https://doi.org/10.1163/9789004366619_020
- Major, M. A., Rosenblatt, D. H., Bostian, K. A., 1991 The octanol/water partition coefficient of methylmercuric chloride and methylmercuric hydroxide in pure water and salt solutions. *Environ. Toxicol. Chem.* 10, 5-8. <https://doi.org/10.1002/etc.5620100102>.

- Mangal, V., Stenzler, B.R., Poulain, A.J., Guéguen, C., 2018. Aerobic and anaerobic bacterial mercury uptake is driven by algal organic matter composition and molecular weight. *Environ. Sci. Technol.* 53(1), 157-165.
<https://doi.org/10.1021/acs.est.8b04909>
- Mann, J., Connor, R.C., Barre, L.M., Heithaus, M.R., 2000. Female reproductive success in bottlenose dolphins (*Tursiops* sp.): life history, habitat, provisioning, and group-size effects. *Behav. Ecol.* 11, 210-219.
<https://doi.org/10.1093/beheco/11.2.210>
- Marcogliese, D.J., Pietroock, M. 2011. Combined effects of parasites and contaminants on animal health: parasites do matter. *Trends in parasitology*, 27(3), 123-130.
<https://doi.org/10.1016/j.pt.2010.11.002>
- Markert, B., Friese, K. (Eds.). (2000). *Trace elements: their distribution and effects in the environment*. Elsevier. Oxford.
- Martin A.R., Reeves, R.R. 2009. Chapter 1. Diversity and Zoogeography. In *Marine Mammal Biology: An Evolutionary Approach*. Hoelzel, A.R. (Ed.) Blackwell Publishing Malden, MA. pp. 1-37.
- Martínez-López, E., Peñalver, J., Escriña, A., Lara, L., Gens, M.J., Dolores, E.M., Alcaraz, A., García-Fernández, A.J. 2019. Trace metals in striped dolphins (*Stenella coeruleoalba*) stranded along the Murcia coastline, Mediterranean Sea, during the period 2009–2015. *Chemosphere*, 229, 580-588.
<https://doi.org/10.1016/j.chemosphere.2019.04.214>

- Martínez-López, E., Peñalver, J., Lara, L., García-Fernández, A. J., 2019b. Hg and Se in Organs of Three Cetacean Species from the Murcia Coastline (Mediterranean Sea). *Bull. Environ. Contam. Toxicol.* 103, 521-527.
<https://doi.org/10.1007/s00128-019-02697-9>.
- Martoja, R., Viale, D., 1977. Storage of mercuric selenide concretions in the liver of cetacean mammals: a possible process for detoxification of methylmercury by selenium. 285. *Comptes Rendus Hebdomadaires des Seances de l'Academie des Sciences, Paris*, pp. 109-112.
- Mason, R.P., Choi, A.L., Fitzgerald, W.F., Hammerschmidt, C.R., Lamborg, C.H., Soerensen, A. L., Sunderland, E.M. 2012. Mercury biogeochemical cycling in the ocean and policy implications. *Environ. Res.* 119, 101-117.
<https://doi.org/10.1016/j.envres.2012.03.013>.
- Mason, R.P., Reinfelder, J.R., Morel, F.M. 1996. Uptake, toxicity, and trophic transfer of mercury in a coastal diatom. *Environ. Sci. Technol.* 30(6), 1835-1845.
<https://doi.org/10.1021/es950373d>.
- Masset, T., Frossard, V., Perga, M. E., Cottin, N., Piot, C., Cachera, S., Naffrechoux, E. 2019. Trophic position and individual feeding habits as drivers of differential PCB bioaccumulation in fish populations. *Sci. Total. Environ.* 674, 472-481.
<https://doi.org/10.1016/j.scitotenv.2019.04.196>.
- McCormack M.A., Battaglia, F, McFee W, Dutton J., 2020a. Mercury concentrations in blubber and skin from stranded dolphins (*Tursiops truncatus*) along the Florida and Louisiana coasts (Gulf of Mexico, USA) in relation to biological variables. *Environ. Res.* 180:108886. <https://doi.org/10.1016/j.envres.2019.108886>

- McCormack, M.A., Fielding, R., Kiszka, J.J., Paz, V., Jackson, B P., Bergfelt, D.R., Dutton, J., 2020b. Mercury and selenium concentrations, and selenium: mercury molar ratios in small cetaceans taken off St. Vincent, West Indies. *Environ. Res.* 181:108908. <https://doi.org/10.1016/j.envres.2019.108908>.
- McCutchan Jr, J.H., Lewis Jr, W.M., Kendall, C., McGrath, C.C., 2003. Variation in trophic shift for stable isotope ratios of carbon, nitrogen, and sulfur. *Oikos*, 102(2), 378-390. <https://doi.org/10.1034/j.1600-0706.2003.12098.x>.
- McFee, W.E., Adams, J.D., Fair, P.A., Bossart, G.D., 2012. Age distribution and growth of two bottlenose dolphin (*Tursiops truncatus*) populations from capture-release studies in the Southeastern United States. *Aquat. Mamm.* 38, 17-30. <http://doi.org/10.1578/AM.38.1.2012.17>.
- McKenzie, R.C., 2000. Selenium, ultraviolet radiation and the skin. *Clin. Exp. Dermatol.* 25(8), 631-636. <https://doi.org/10.1046/j.1365-2230.2000.00725.x>.
- McKinney, M.A., Atwood, T.C., Pedro, S., Peacock, E. 2017. Ecological change drives a decline in mercury concentrations in southern Beaufort Sea polar bears. *Environ. Sci. Technol.* 51(14), 7814-7822. <https://doi.org/10.1021/acs.est.7b00812>
- Meador, J. P., Ernest, D., Hohn, A. A., Tilbury, K., Gorzelany, J., Worthy, G., Stein, J. E. 1999. Comparison of elements in bottlenose dolphins stranded on the beaches of Texas and Florida in the Gulf of Mexico over a one-year period. *Archives of Environ. Contam. Toxicol.* 36(1), 87-98.
- Meldrum, R.D. 2001. Erroneous aluminum and cobalt tissue concentrations from using formalin. *J. Biomed. Mater. Res.* 57:59-62.

- Méndez-Fernandez, P., Polesi, P.G., Taniguchi, S., Marcos, C.D.O., Montone, R.C. 2016. Validating the use of biopsy sampling in contamination assessment studies of small cetaceans. *Mar. Pollut. Bull.* 107(1), 364-369.
<https://doi.org/10.1016/j.marpolbul.2016.04.021>
- Metcalf, T.L., Metcalf, C.D., 1997. The trophodynamics of PCBs, including mon-and non-*ortho* congeners, in the food web of North-Central Lake Ontario. *Sci. Total Environ.* 201, 245-272. [https://doi.org/10.1016/S0048-9697\(97\)84061-2](https://doi.org/10.1016/S0048-9697(97)84061-2).
- Miller, D.L., Woshner, V., Styer, E.L., Ferguson, S., Knott, K.K., Gray, M.J., Wells, R.S., O'Hara, T.M., 2011. Histologic findings in free-ranging Sarasota Bay bottlenose dolphin (*Tursiops truncatus*) skin: mercury, selenium, and seasonal factors. *J. Wildl. Dis.* 47, 1012-1018. 1012-1018. <https://doi.org/10.7589/0090-3558-47.4.1012>.
- Monteiro, S.S., Bozzetti, M., Torres, J., Tavares, A.S., Ferreira, M., Pereira, A.T., Sá, S., Araújo, H., Bastos-Santos, J., Oliveira, I., Vingada, J.V., Eira, C. 2020. Striped dolphins as trace element biomonitoring tools in oceanic waters: accounting for health-related variables. *Sci. Total Environ.* 699:134410.
- Monteiro, S.S., Torres, J., Ferreira, M., Marcalo, A., Nicolau, L., Vingada, J.V., Eira, C., 2016. Ecological variables influencing trace element concentrations in bottlenose dolphins (*Tursiops truncatus*, Montagu 1821) stranded in continental Portugal. *Sci. Total Environ.* 544, 837-844.
<https://doi.org/10.1016/j.scitotenv.2015.12.037>.

- Murphy S, Perrott M, McVee J, Read FL, Stockin KA (2014) Deposition of growth layer groups in dentine tissue of captive common dolphins (*Delphinus delphis*). NAMMCO Sci. Publ. <https://doi.org/10.7557/3.3017>
- Myick A.C., Hohn A.A., Sloan, P.A., Kimura M., Stanley D.D. 1983. Estimating age of spotted and spinner dolphins (*Stenella attenuata* and *Stenella longirostris*) from teeth. NOAA Technical Memorandum. Southwest Fisheries Science Center, National Marine Fisheries Service. Report number NOAA-TM-NMFS-SWFC-30. La Jolla, California, pp 17.
- Myrick Jr, A.C. 1991. Some new and potential uses of dental layers in studying delphinid populations. In: Pryor K, Norris, KS (eds) Dolphin societies: discoveries and puzzles. University of California Press, Los Angeles, pp 251-279.
- Nakata, H., Sakakibara, A., Kanoh, M., Kudo, S., Watanabe, H., Nagai, N., Tanabe, S. 2002. Evaluation of mitogen-induced responses in marine mammal and human lymphocytes by in-vitro exposure of butyltins and non-ortho coplanar PCBs. Environ. Pollut. 120(2), 245-253. [https://doi.org/10.1016/S0269-7491\(02\)001550](https://doi.org/10.1016/S0269-7491(02)001550).
- Nakazawa, E., Ikemoto, T., Hokura, A., Terada, Y., Kunito, T., Tanabe, S., Nakai, I., 2011. The presence of mercury selenide in various tissues of the striped dolphin: evidence from μ -XRF-XRD and XAFS analyses. Metallomics. 3, 719-725. <https://doi.org/10.1039/C0MT00106F>.
- Nasrazadani, S., Hassani, S. 2016. Modern analytical techniques in failure analysis of aerospace, chemical, and oil and gas industries. In: Makhlof ASH, Aliofkhazraei M (eds) Handbook of materials failure analysis with case studies from the oil and gas industry. Elsevier, Oxford, UK, pp 39–54.

- National Atmospheric Deposition Program, 2007. Mercury deposition network (MDN):
A NADP network. NADP Program Office, Illinois State Water Survey,
Champaign, IL. <http://nadp.slh.wisc.edu/maplib/pdf/mdn/hg_dep_2013.pdf>,
accessed 5 June 2019.
- National Research Council. 2003. Bioavailability of contaminants in soils and sediments:
Processes, tools and applications. Washington DC: NationalAcademies Press. 432
- Ndu, U., Lamb, J., Janssen, S., Rossi, R., Satgé, Y., Jodice, P. 2020. Mercury, cadmium,
copper, arsenic, and selenium measurements in the feathers of adult eastern brown
pelicans (*Pelecanus occidentalis carolinensis*) and chicks in multiple breeding
grounds in the northern Gulf of Mexico. Environ. Monit. Assess. 192(5), 1-9.
<https://doi.org/10.1007/s10661-020-8237-y>.
- Neff, J.M. 2002. Fates and effects of mercury from oil and gas exploration and
production operations in the marine environment. American Petroleum Institute,
Washington, D.C., USA.
- Newbury, D.E., Ritchie, N.W.M. 2013 Is scanning electron microscopy/energy dispersive
X-ray spectrometry (SEM/EDS) quantitative?. Scanning. 141-168.
<https://doi.org/10.1002/sca.21041>
- Newsome, S.D., Clementz, M.T., Koch, P.L., 2010. Using stable isotope biogeochemistry
to study marine mammal ecology. Mar. Mam. Sci. 26, 509-572.
<https://doi.org/10.1111/j.1748-7692.2009.00354.x>.

- Nganvongpanit, K., Buddhachat, K., Piboon, P., Euppayo, T., Kaewmong, P., Cherdasukjai, P., Kittiwatanawong, K., Thitaram, C. 2017. Elemental classification of the tusks of dugong (*Dugong dugong*) by HH-XRF analysis and comparison with other species. *Sci Rep.* <https://doi.org/10.1038/srep4616>.
- Nigro, M., Campana, A., Lanzillotta, E., Ferrara, R., 2002. Mercury exposure and elimination rates in captive bottlenose dolphins. *Mar. Pollut. Bull.* 44, 1071-1075. [https://doi.org/10.1016/S0025-326X\(02\)00159-5](https://doi.org/10.1016/S0025-326X(02)00159-5).
- NMFS-OPR (National Marine Fisheries Service – Office of Protected Resources). 2019a. Active and closed unusual mortality events. <https://www.fisheries.noaa.gov/national/marine-life-distress/active-and-closed-unusual-mortality-events> (accessed 6 February 2020).
- NMFS-OPR. (National Marine Fisheries Service – Office of Protected Resources). 2019b. 2010–2014 Cetacean Unusual Mortality Event in Northern Gulf of Mexico (Closed). <https://www.fisheries.noaa.gov/national/marine-life-distress/2010-2014-cetacean-unusual-mortality-event-northern-gulf-mexico> (accessed 6 February 2020).
- Noren, D.P. Mocklin, J.A. 2012. Review of cetacean biopsy techniques: Factors contributing to successful sample collection and physiological and behavioral impacts. *Mar. Mamm. Sci.* 28(1), 154-199. <https://doi.org/10.1111/j.1748-7692.2011.00469.x>
- O' Shea, T.J., Tanabe, S. 2003. Persistent ocean contaminants and marine mammals: a retrospective overview. In Vos, J. G., Bossart, G., Fournier, M., O'Shea, T. (Eds.) *Toxicology of marine mammals*. Taylor & Francis, New York, NY.

- Oliveira Ribeiro, C.A., Rouleau, C., Pelletier, E., Audet, C., Tjälve, H., 1999. Distribution kinetics of dietary methylmercury in the arctic charr (*Salvelinus alpinus*). Environ. Sci. Technol. 33(6), 902-907. <https://doi.org/10.1021/es980242n>.
- Olsson, U. 1985. Impaired ketone body metabolism in the selenium deficient rat. Possible implications. Metabolism, 34(11), 993-998. [https://doi.org/10.1016/0026-0495\(85\)90069-1](https://doi.org/10.1016/0026-0495(85)90069-1).
- Ouédraogo, O., Chételat, J., Amyot, M. 2015. Bioaccumulation and trophic transfer of mercury and selenium in African sub-tropical fluvial reservoirs food webs (Burkina Faso). PloS one, 10(4), e0123048. <https://doi.org/10.1371/journal.pone.0123048>.
- Outridge, P.M., Veinott, G., Evans, R.D. 1995 Laser ablation ICP-MS analysis of incremental biological structures: archives of trace-element accumulation. Env Rev. <https://doi.org/10.1139/a95-007>.
- Outridge, P.M., Hobson, K.A., McNeely, R., Dyke, A. 2002. A comparison of modern and preindustrial levels of mercury in the teeth of beluga in the Mackenzie Delta, Northwest Territories, and walrus at Igloodik, Nunavut, Canada. Arctic. 55, 123-132.
- Ozersky, T., Pastukhov, M.V., Poste, A.E., Deng, X.Y., Moore, M.V. 2017. Long-term and ontogenetic patterns of heavy metal contamination in Lake Baikal seals (*Pusa sibirica*). Environ. Sci. Technol. 51(18), 10316-10325. <https://doi.org/10.1021/acs.est.7b00995>

- Pacyna, J. M., Pacyna, E.G. 2001. An assessment of global and regional emissions of trace metals to the atmosphere from anthropogenic sources worldwide. *Environmental Reviews*. 9(4), 269-298.
- Page-Karjian, A., Lo, C.F., Ritchie, B., Harms, C.A., Rotstein, D.S., Han, S., Perrault, J. R. 2020. Anthropogenic Contaminants and Histopathological Findings in Stranded Cetaceans in the Southeastern United States, 2012–2018. *Frontiers in Marine Science*, 7, 630. <https://doi.org/10.3389/fmars.2020.00630>
- Palmisano, F., Cardellicchio, N., Zambonin, P.G., 1995. Speciation of mercury in dolphin liver: a two-stage mechanism for the demethylation accumulation process and role of selenium. *Mar. Environ. Res.* 40(2), 109-121. [https://doi.org/10.1016/0141-1136\(94\)00142-C](https://doi.org/10.1016/0141-1136(94)00142-C).
- Pancaldi, F., Páez-Osuna, F., Marmolejo-Rodríguez, A. J., Whitehead, D. A., González-Armas, R., Soto-Jiménez, M. F., Galván-Magaña, F. 2021. Variation of essential and non-essential trace elements in whale shark epidermis associated to two different feeding areas of the Gulf of California. *Environmental Science and Pollution Research*, 1-14.
- Parsons, E.C.M. 2004. The potential impacts of pollution on humpback dolphins, with a case study on the Hong Kong population. *Aquat. Mamm.* 30:18-37.
- Payo-Payo, A., Ruiz, B., Cardona, L., Borrell, A., 2013. Effect of tissue decomposition on stable isotopes signatures of striped dolphins *Stenella coeruleoabla* and loggerhead sea turtles *Caretta caretta*. *Aquat. Biol.* 18, 141-147. <https://doi.org/10.3354/ab00497>.

- Pedro, S., Boba, C., Dietz, R., Sonne, C., Rosing-Asvid, A., Hansen, M., Provatas, A., McKinney, M.A. 2017. Blubber-depth distribution and bioaccumulation of PCBs and organochlorine pesticides in Arctic-invading killer whales. *Sci. Tot. Environ.* 601, 237-246. <https://doi.org/10.1016/j.scitotenv.2017.05.193>.
- Peltier, H., Dabin, W., Daniel, P., Van Canneyt, O., Dorémus, G., Huon, M., Ridoux, V., 2012. The significance of stranding data as indicators of cetacean populations at sea: modelling the drift of cetacean carcasses. *Ecol. Indic.* 18, 278-290. <https://doi.org/10.1016/j.ecolind.2011.11.014>.
- Peltier, H., Jepson, P. D., Dabin, W., Deaville, R., Daniel, P., Van Canneyt, O., Ridoux, V. 2014. The contribution of stranding data to monitoring and conservation strategies for cetaceans: Developing spatially explicit mortality indicators for common dolphins (*Delphinus delphis*) in the eastern North-Atlantic. *Ecol. Indic.*, 39, 203-214. <https://doi.org/10.1016/j.ecolind.2013.12.019>.
- Perkin Elmer 2011. The 30-minute guide to ICP-MS. http://www.perkinelmer.com/CMSResources/Images/4474849tch_icpmsthirtyminuteguide.pdf
- Perrot, V., Landing, W.M., Grubbs, R.D., Salters, V.J. 2019. Mercury bioaccumulation in tilefish from the northeastern Gulf of Mexico 2 years after the Deepwater Horizon oil spill: Insights from Hg, C, N and S stable isotopes. *Sci. Total Env.* 666, 828-838. <https://doi.org/10.1016/j.scitotenv.2019.02.295>.

- Peterson, B.D., McDaniel, E.A., Schmidt, A.G., Lepak, R.F., Tran, P.Q., Marick, R.A., Ogorek, J.M., DeWild, J.F., Krabbenhoft, D.P., McMahon, K. D., 2020. Mercury methylation trait dispersed across diverse anaerobic microbial guilds in a eutrophic sulfate-enriched lake. *bioRxiv*.
<https://doi.org/10.1101/2020.04.01.018762>.
- Peterson, B.J., Fry, B., 1987. Stable isotopes in ecosystem studies. *Ann. Rev. Ecol. Syst.* 18, 293-320. <https://doi.org/10.1146/annurev.es.18.110187.001453>.
- Peterson, B.J., Howarth, R.W., Garritt, R.H., 1985. Multiple stable isotopes used to trace the flow of organic matter in estuarine food webs. *Science*. 227, 1361-1363.
<http://doi.org/10.1126/science.227.4692.1361>.
- Peterson, S.A., Ralston, N.V.C., Whanger, P.D., Oldfield, J.E., Mosher, W.D., 2009. Selenium and mercury interactions with emphasis on fish tissue. *Environ. Bioindic.* 4, 318-334. <https://doi.org/10.1080/15555270903358428>.
- Peterson, S.H., Ackerman, J.T., Crocker, D.E., Costa, D.P., 2018. Foraging and fasting can influence contaminant concentrations in animals: an example with mercury contamination in a free-ranging marine mammal. *Proc. R. Soc. B.* 285:20172782.
<https://doi.org/10.1098/rspb.2017.2782>.
- Pirrone, N., Cinnirella, S., Feng, X., Finkelman, R.B., Friedli, H. R., Leaner, J., Mason, R., Mukerjee, A.B., Stracher, G.A., Streets, D.G., Telmer, K. 2010. Global mercury emissions to the atmosphere from anthropogenic and natural sources. *Atmos. Chem. Phy.* 10, 5951-5964. <http://doi.org/10.5194/acp-10-5951-2010>.

- Pompe-Gotal, J., Srebocan, E., Gomecic, H., Crnic, A.P., 2009. Mercury concentrations in the tissues of bottlenose dolphins (*Tursiops truncatus*) and striped dolphins (*Stenella coeruleoabla*) stranded on the Croatian Adriatic coast. *Vet. Med-Czech.* 54, 598-604. <http://doi.org/10.17221/3060-VETMED>.
- Post, D.M., 2002. Using stable isotopes to estimate trophic position: models, methods, and assumptions. *Ecology*, 83(3), 703-718. [https://doi.org/10.1890/0012-9658\(2002\)083\[0703:USITET\]2.0.CO;2](https://doi.org/10.1890/0012-9658(2002)083[0703:USITET]2.0.CO;2).
- Post, D.M., Layman, C.A., Arrington, D.A., Takimoto, G., Quattrochi, J., Montana, C.G., 2007. Getting to the fat of the matter: models, methods and assumptions for dealing with lipids in stable isotope analyses. *Oecologia*. 152, 179-198. <https://doi.org/10.1007/s00442-006-0630-x>.
- Poste, A.E., Pastukhov, M.V., Braaten, H.F.V., Ozersky, T., Moore, M. 2018. Past and present mercury accumulation in the Lake Baikal seal: Temporal trends, effects of life history, and toxicological implications. *Enviorn. Tox. Chem.*, 37(5), 1476-1486. <https://doi.org/10.1002/etc.4095>.
- Poulopoulos, J. 2013. Long-term changes to food web structures and mercury biomagnification in three large, inland North American lakes. PhD thesis. Queen's University, Kingston, Ontario, Canada.
- Presley, B.J., Wade, T.L., Santchi, P., Baskaran, M., 1998. Historical Contamination of Mississippi River Delta, Tampa Bay and Galveston Bay Sediments, National Status and Trends program for Marine Environmental Quality. NOAA Technical Memorandum NOA ORCA 127. Silver Spring, MD.

- Quan, M., Mülders, M.S., Meltzer, D.G.A. 2002. The effect of storage conditions on samples for the evaluation of copper status in blesbok (*Damaliscus pygargus phillipsi*). J. S. Afr. Vet. Ass. 73:111-114.
- Quezada-Romegialli, C., Jackson, A.L., Hayden, B., Kahilainen, K.K., Lopes, C., Harrod, C., 2018. tRophicPosition: Bayesian Trophic Position Calculation with Stable Isotopes. R package version 0.7.5. <https://cran.r-project.org/package=tRophicPosition>
- R Core Team. 2020. R: A language and environment for statistical computing. R Foundation for Statistical Computing, Vienna, Austria. <https://www.R-project.org/>
- R Core Team. 2018. R: A language and environment for statistical computing. R Foundation for Statistical Computing, Vienna, Austria. <https://www.R-project.org/>.
- Rabalais, N.N., Turner, R.E., Wiseman, W.J., 2001. Hypoxia in the Gulf of Mexico. J. Environ. Qual. 30, 320-329. <http://doi.org/10.2134/jeq2001.302320x>.
- Ralston, N.V.C., 2008. Selenium health benefit values as seafood safety criteria. EcoHealth. 5, 442-455. <https://doi.org/10.1007/s10393-008-0202-0>.
- Ralston, N.V.C., Raymond, L.J., 2010. Dietary selenium's protective effects against methylmercury toxicity. Toxicol. 278, 112-123. <https://doi.org/10.1016/j.tox.2010.06.004>.
- Ramprashad, F., Ronald, K. 1977 A surface preparation study on the effect of methyl mercury on the sensory hair cell population in the cochlea of the harp seal (*Pagophilus groenlandicus* Erxleben, 1977). Can. J. Zool. 55, 223–230

- Rautray, T.R., Das, S., Rautray, A.C. 2010. In situ analysis of human teeth by external PIXE. Nucl Instrum Methods Phys Res B.
<https://doi.org/10.1016/j.nimb.2010.01.004>
- Rawson, A.J., Bradley, J.P., Teetsov, A., Rice, S.B., Haller, E.M., Patton, G.W. 1995. A role for airborne particulates in high mercury levels of some cetaceans. Ecotoxicol. Environ. Safe. 30(3), 309-314.
<https://doi.org/10.1006/eesa.1995.1035>.
- Rawson, A.J., Patton, G.W., Hofmann, S., Pietra, G.G., Johns, L., 1993. Liver abnormalities associated with chronic mercury accumulation in stranded Atlantic bottlenose dolphins. Ecotoxicol. Environ. Safe. 25(1), 41-47.
<https://doi.org/10.1006/eesa.1993.1005>.
- Read, A.J., Wells, R.S., Hohn, A.A., Scott, M.D., 1993. Patterns of growth in wild bottlenose dolphins, *Tursiops truncatus*. J. Zool. 231, 107-123.
<https://doi.org/10.1111/j.1469-7998.1993.tb05356.x>.
- Reddy, M.L., Reif, J.S., Bachand, A., Ridgway, S.H. 2001. Opportunities for using Navy marine mammals to explore associations between organochlorine contaminants and unfavorable effects on reproduction. Sci. Total Environ. 274(1-3), 171-182.
[https://doi.org/10.1016/S0048-9697\(01\)00741-0](https://doi.org/10.1016/S0048-9697(01)00741-0).
- Reif, J.S., Schaefer, A.M., Bossart, G.D. 2015. Atlantic bottlenose dolphins (*Tursiops truncatus*) as a sentinel for exposure to mercury in humans: closing the loop. Vet. Sci. 2(4), 407-422. <https://doi.org/10.3390/vetsci2040407>.
- Reijnders, P.J.H. 1986. Reproductive failure in common seals feeding on fish from polluted coastal waters. Nature 324, 456–457

- Reitznerová, E., Amarasiriwardena, D., Kopčáková, M., Barnes, R.M. 2000. Determination of some trace elements in human tooth enamel. *Fresenius. J. Anal. Chem.* <https://doi.org/10.1007/s002160000461>
- Remili, A., Letcher, R.J., Samarra, F. I., Dietz, R., Sonne, C., Desforges, J.P., Vikingsson, G., Blair, D., McKinney, M.A. 2021. Individual Prey Specialization Drives PCBs in Icelandic Killer Whales. *Environ. Sci. Technol.* <https://doi.org/10.1021/acs.est.0c08563>.
- Renaud, C.B., Nriagu, J.O., Wong, H.K.T. 1995. Trace metals in fluid-preserved museum fish specimens. *Sci. Total Environ.* 159:1-7.
- Rice, G.E., Senn, D.B., Shine, J.P., 2009. Relative importance of atmospheric and riverine mercury sources to the northern Gulf of Mexico. *Environ. Sci. Technol.* 43(2), 415-422.
- Richir, J., Gobert, S. 2016. Trace elements in marine environments: occurrence, threats and monitoring with special focus on the Coastal Mediterranean. *Journal of environmental and analytical toxicology*, 6(1).
- Robbins, C.T., Felicetti, L.A., Florin, S.T. 2010. The impact of protein quality on stable nitrogen isotope ratio discrimination and assimilated diet estimation. *Oecologia*, 162(3), 571-579. <https://doi.org/10.1007/s00442-009-1485-8>.
- Robbins, C.T., Felicetti, L.A., Sponheimer, M. 2005. The effect of dietary protein quality on nitrogen isotope discrimination in mammals and birds. *Oecologia*, 144(4), 534-540. <https://doi.org/10.1007/s00442-005-0021-8>.

- Roditi-Elasar, M., Kerem, D., Hornung, H., Kress, N., Shoham-Frider, E., Goffman, O., Spanier, E., 2003. Heavy metal levels in bottlenose and striped dolphins off the Mediterranean coast of Israel. *Mar. Pollut. Bull.* 46, 503-512.
[https://doi.org/10.1016/S0025-326X\(03\)00003-1](https://doi.org/10.1016/S0025-326X(03)00003-1).
- Rojo-Nieto, E., Fernández-Maldonado, C. 2017. Assessing trace elements in striped dolphins from the Strait of Gibraltar: Clues to link the bioaccumulation in the westernmost Mediterranean Sea area and nearest Atlantic Ocean. *Chemosphere*, 170, 41-50. <https://doi.org/10.1016/j.chemosphere.2016.12.009>.
- Romero, M.B., Polizzi, P., Chiodi, L., Robles, A., Das, K., Gerpe, M. 2017. Metals as chemical tracers to discriminate ecological populations of threatened Franciscana dolphins (*Pontoporia blainvillei*) from Argentina. *Environ. Sci. Pollut. Res.* 24:3940-3950.
- Romero, M.B., Polizzi, P., Chiodi, L., Medici, S., Blando, M., Gerpe, M. 2018. Preliminary Assessment of Legacy and Current-Use Pesticides in Franciscana Dolphins from Argentina. *Bull. Environ. Contam. Toxicol.* 101(1), 14-19.
<https://doi.org/10.1007/s00128-018-2352-2>.
- Rosel, P.E., Wilcox, L.A., Sinclair, C., Speakman, T.R., Tumlin, M.C., Litz, J.A., Zolman, E.S., 2017. Genetic assignment to stock of stranded common bottlenose dolphins in southeastern Louisiana after the Deepwater Horizon oil spill. *Endanger. Species Res.* 33, 221-234. <https://doi.org/10.3354/esr00780>.
- Rossmann, S., Ostrom, P.H., Fordon, F., Zipkin, E.F., 2016. Beyond carbon and nitrogen: guidelines for estimating three-dimensional isotopic niche space. *Ecol. Evol.* 6, 2405-2413. <https://doi.org/10.1002/ece3.2013>.

- Rossmann, S., Ostrom, P.H., Stolen, M., Barros, N.B., Ganhi, H., Stricker, C.A., Wells, R.S., 2015. Individual specialization in the foraging habitats of female bottlenose dolphins living in a trophically diverse and habitat rich estuary. *Oecologia*. 178, 415-425. <https://doi.org/10.1007/s00442-015-3241-6>.
- Ruelas-Inzunza, J., Pérez-Osuna, F. 2005. Mercury in fish and shark tissues from two coastal lagoons in the Gulf of California, Mexico. *B. Environ. Contam. Tox.* 74(2), 294-300. <https://doi.org/10.1007/s00128-004-0583-x>.
- Sanganyado, E., Bi, R., Teta, C., Buruaem Moreira, L., Yu, X., Yajing, S., Dalu, R., Rashid Rajput, I, Liu, W. 2020. Toward an integrated framework for assessing micropollutants in marine mammals: Challenges, progress, and opportunities. *Crit. Rev. Environ. Sci. Technol.* 1-48. <https://doi.org/10.1080/10643389.2020.1806663>
- Santschi, P.H., Presley, B.J., Wade, T.L., Garcia-Romero, B., Baskaran, M. 2001. Historical contamination of PAHs, PCBs, DDTs, and heavy metals in Mississippi river Delta, Galveston bay and Tampa bay sediment cores. *Mar. Environ. Res.* 52(1), 51-79. [https://doi.org/10.1016/S0141-1136\(00\)00260-9](https://doi.org/10.1016/S0141-1136(00)00260-9).
- Sañudo-Wilhelmy, S.A., Gill, G.A. 1999. Impact of the Clean Water Act on the levels of toxic metals in urban estuaries: The Hudson River estuary revisited.
- Sato I., Sera K., Suzuki T., Kobayashi H., Tsuda S. 2006. Effects of formalin-preservation on element concentrations in animal tissues. *J Toxicol Sci* 31:191-195.
- Sauvé, S., Desrosiers, M. 2014. A review of what is an emerging contaminant. *Chemistry Central Journal*, 8(1), 1-7. <https://doi.org/10.1186/1752-153X-8-15>

- Savery, L.C., Evers, D. C., Wise, S.S., Falank, C., Wise, J., Gianios Jr, C., Kerr, I., Payne, R., Thompson, W.D., Perkins, C., Zheng, T., 2013. Global mercury and selenium concentrations in skin from free-ranging sperm whales (*Physeter macrocephalus*). *Sci Tot. Environ.* 450, 59-71.
<https://doi.org/10.1016/j.scitotenv.2013.01.070>.
- Schaefer, A.M., Jensen, E.L., Bossart, G.D., Reif, J.S. 2014. Hair mercury concentrations and fish consumption patterns in Florida residents. *Int. J. Env. Res. Pub. He.* 1(7), 6709-6726. <https://doi.org/10.3390/ijerph110706709>
- Schaefer, A.M., Stavros, H.C.W., Bossart, G.D., Fair, P.A., Goldstein, J.D., Reif, J.S., 2011. Associations between mercury and hepatic, renal, endocrine, and hematological parameters in Atlantic bottlenose dolphins (*Tursiops truncatus*) along the eastern coast of Florida and South Carolina. *Arch. Environ. Cont. Tox.* 61, 688-695. <https://doi.org/10.1007/s00244-011-9651-5>.
- Scheuhammer, A.M., Meyer, M.W., Sandheinrich, M.B., Murray, M.W., 2007. Effects of environmental methylmercury on the health of wild birds, mammals, and fish. *Ambio.* 361, 12-20. [https://doi.org/10.1579/0044-7447\(2007\)36\[12:eoemot\]2.0.co;2](https://doi.org/10.1579/0044-7447(2007)36[12:eoemot]2.0.co;2).
- Scholz, N. L., Fleishman, E., Brown, L., Werner, I., Johnson, M. L., Brooks, M. L., Schlenk, D. 2012. A perspective on modern pesticides, pelagic fish declines, and unknown ecological resilience in highly managed ecosystems. *BioScience*, 62(4), 428-434.

- Schomburg, L., Schweizer, U., Köhrle, J., 2004. Selenium and selenoproteins in mammals: extraordinary, essential, enigmatic. *Cell. Mol. Life Sci.* 61, 1988–1995. <https://doi.org/10.1007/s00018-004-4114-z>.
- Schwake, L.H., Smith, C. R., Townsend, F.I., Wells, R.S., Hart, L.B., Balmer, B.C., Collier, T.K., De Guise, S., Fry, M.M., Guilette, L.J., Lamb, S.V., Lane, S.M., McFee, W.E., Place, N.J., Tumlin, M.C., Ylitalo, G.M., Zolman, E.S., Rowles, T.K. 2014. Health of common bottlenose dolphins (*Tursiops truncatus*) in Barataria Bay, Louisiana, following the *Deepwater Horizon* oil spill. *Environ. Sci. Technol.* 48, 93-103. <https://pubs.acs.org/doi/10.1021/es403610f>.
- Seixas, T.G., Kehrig, H.D.A., Fillmann, G., Di Benedetto, A.P.M., Souza, C.M., Secchi, E.R., Moreira, I., Malm, O., 2007. Ecological and biological determinants of trace elements accumulation in liver and kidney of *Pontoporia blainvillei*. *Sci. Total Environ.* 385(1-3), 208-220. <https://doi.org/10.1016/j.scitotenv.2007.06.045>.
- Selin N.E., Jacob, D.J., 2008. Seasonal and spatial patterns of mercury wet deposition in the United States: constraints on the contribution from North American atmospheric sources. *Atmos. Environ.* 42, 5193-5204. <https://doi.org/10.1016/j.atmosenv.2008.02.069>.
- Selin, N.E., 2009. Global biogeochemical cycling of mercury: a review. *Annu. Rev. Env. Resour.* 34, 43-63. <https://doi.org/10.1146/annurev.enviro.051308.084314>.
- Senn, D.B., Chesney, E.J., Blum, J.D., Bank, M.S., Maage, A., Shine, J.P., 2010. Stable isotope (N, C, Hg) study of methylmercury sources and trophic transfer in the northern Gulf of Mexico. *Environ. Sci. Technol.* 44(5), 1630-1637. <https://doi.org/10.1021/es902361j>.

- Sforna M.C., Lugli F. 2017. MapIT!: a simple and user-friendly MATLAB script to elaborate elemental distribution images from LA-ICP-MS data. *J Anal At Spectrom.* <https://doi.org/10.1039/C7JA00023E>
- Shane, S.H., 1977. The population biology of the Atlantic bottlenose dolphin, *Tursiops truncatus*, in the Aransas Pass area of Texas. M. Sc. thesis. Texas A&M University, College Station.
- Sherman, L.S., Blum, J.D., Keeler, G.J., Demers, J.D., Dvonch, J.T. 2012. Investigation of local mercury deposition from a coal-fired power plant using mercury isotopes. *Env. Sci. Technol.* 46(1), 382-390. <https://doi.org/10.1021/es202793c>.
- Shippee, S. 2014. Movements, fishery interactions, and unusual mortalities of bottlenose dolphins. Dissertation University of Central Florida. Orlando, FL.
- Shoham-Frider, E., Amiel, S., Roditi-Elasar, M., Kress, N., 2002. Risso's dolphin (*Grampus griseus*) stranding on the coast of Israel (eastern Mediterranean). Autopsy results and trace metal concentrations. *Sci. Total Environ.* 295, 157-166. [https://doi.org/10.1016/S0048-9697\(02\)00089-X](https://doi.org/10.1016/S0048-9697(02)00089-X).
- Silva, M.A., 1999. Diet of common dolphins, *Delphinus delphis*, off the Portuguese continental coast. *J. Mar. Biol. Assoc. U.K.* 79, 531-540. <https://doi.org/10.1017/S0025315498000654>.
- Simmer J.P., Fincham A.G. 1995. Molecular mechanisms of dental enamel formation. *Crit Rev Oral Biol Med.* <https://doi.org/10.1177/10454411950060020701>

- Simmonds, M.P. 2018. Chapter 17. Marine mammals multiple stressors: implications for and conservation and policy. In Fossi, M. C., & Panti, C. (Eds.) Marine mammal ecotoxicology: impacts of multiple stressors on population health. Academic Press.
- Sluis, M.Z., Boswell, K.M., Chumchal, M.M., Wells, R.J.D., Soulen, B., Cowan Jr., J., H., 2013. Regional variation in mercury and stable isotopes of red snapper (*Lutjanus campechanus*) in the northern Gulf of Mexico, USA. Environ. Toxicol. Chem. 32, 434-441. <http://doi.org/10.1002/etc.2077>.
- Smith, N.P., 1993. Tidal and nontidal flushing of Florida's Indian River Lagoon. Estuaries. 16, 739-746. <https://doi.org/10.2307/1352432>.
- Sorensen, K. C., Venn-Watson, S., Ridgway, S. H. 2008. Trace and non-trace elements in blood cells of bottlenose dolphins (*Tursiops truncatus*): Variations with values from liver function indicators. J. Wildl. Dis. 44(2), 304-317. <https://doi.org/10.7589/0090-3558-44.2.304>.
- Soto-Jiménez, F.M. 2011. Trace element trophic transfer in aquatic food webs. Hydrobiológica 21:239–248 http://www.scielo.org.mx/scielo.php?pid=S0188-88972011000300003&script=sci_arttext&tlng=en.
- Stavros, H.C.W., Bossart, G.D., Hulsey, T.C., Fair, P.A., 2007. Trace element concentrations in skin of free-ranging bottlenose dolphins (*Tursiops truncatus*) from the southeast Atlantic coast. Sci. Total. Environ. 388, 300-315. <https://doi.org/10.1016/j.scitotenv.2007.07.030>.

- Stavros, H.C.W., Stolen, M., Durden, W.M., McFee, W., Bossart, G.D., Fair, P.A., 2011. Correlation and toxicological inference of trace elements in tissues from stranded and free-ranging bottlenose dolphins (*Tursiops truncatus*). *Chemosphere*. 82, 1649-1661. <https://doi.org/10.1016/j.chemosphere.2010.11.019>.
- Steffy, D.A., Nichols, A.C., Morgan, L.J., Gibbs, R. 2013. Evidence that the Deepwater Horizon oil spill caused a change in the nickel, chromium, and lead average seasonal concentrations occurring in sea bottom sediment collected from the eastern Gulf of Mexico continental shelf between the years 2009 and 2011. *Water Air Soil Pollut.* 224(11), 1756. <https://doi.org/10.1007/s11270-013-1756-1>
- Stein, J.E., Tilbury, K.L., Meador, J.P., Gorzelany, J., Worthy, G.A., Krahn, M.M. 2003. Ecotoxicological investigations of bottlenose dolphin (*Tursiops truncatus*) strandings: accumulation of persistent organic chemicals and metals. In: Vos, J.G., Bossart, G., Fournier, M., O'Shea, T. (Eds.), *Toxicology of Marine Mammals*. Taylor & Francis Inc., New York, pp. 458-488.
- Stock, S.R., Finney, L.A., Telser, A., Maxey, E., Vogt, S., Okasinski, J.S. 2017. Cementum structure in Beluga whale teeth. *Acta Biomater.* <https://doi.org/10.1016/j.actbio.2016.11.015>.
- Stoeppler, M. 1991. Cadmium. In: Merian E, Clarkson TW (eds) *Metal and their compounds in the environment*. VCH, New York, p 803–851.
- Stolen, M.K., Odell, D.K., Barros, N.B., 2002. Growth of bottlenose dolphins (*Tursiops truncatus*) from the Indian River Lagoon system, Florida, USA. *Mar. Mam. Sci.* 18, 348-357. <https://doi.org/10.1111/j.1748-7692.2002.tb01042.x>.

- Storelli, M.M., Marcotrigiano, G.O. 2000. Environmental contamination in bottlenose dolphin (*Tursiops truncatus*): relationship between levels of metals, methylmercury, and organochlorine compounds in an adult female, her neonate, and a calf. *Bull Environ Contam Toxicol* 64:333-340.
- Storelli, M.M., Zizzo, N., Marcotrigiano, G.O., 1999. Heavy metals and methylmercury in tissues of Risso's dolphin (*Grampus griseus*) and Cuvier's beaked whale (*Ziphius cavirostris*) stranded in Italy (South Adriatic Sea). *Bull. Environ. Contam. Toxicol.* 63, 703-710. <https://doi.org/10.1007/s001289901037>.
- Sullivan, J.M., Pando, K.M., Everson, R.J., Robinson, F.R. 1993. The effect of formalin fixation on the concentration of selenium in porcine liver. *J. Vet. Diagn. Invest.* 5:131-133.
- Sun, X., Zhan, F., Yu, R. Q., Chen, L., Wu, Y. 2020. Bio-accumulation of organic contaminants in Indo-Pacific humpback dolphins: Preliminary unique features of the brain and testes. *Environ. Pollut.* 267, 115511. <https://doi.org/10.1016/j.envpol.2020.115511>
- Swaine, D.J. 2000. Why trace elements are important. *Fuel Processing Technology*, 65, 21-33. [https://doi.org/10.1016/S0378-3820\(99\)00073-9](https://doi.org/10.1016/S0378-3820(99)00073-9)
- Sydeman, W.J., Jarman, W.M. 1998. Trace metals in seabirds, Steller sea lion, and forage fish and zooplankton from central California. *Mar. Pollut Bull.* 36, 828-832.
- Symonds, M.R., Moussalli, A., 2011. A brief guide to model selection, multimodel inference and model averaging in behavioural ecology using Akaike's information criterion. *Behav. Ecol. Sociobiol.* 65, 13-21. <https://doi.org/10.1007/s00265-010-1037-6>.

- Takeuchi, N.Y., Walsh, M.T., Bonde, R.K., Powell, J.A., Bass, D.A., Gaspard III, J. C., Barber, D.S. 2016. Baseline reference range for trace metal concentrations in whole blood of wild and managed west Indian manatees (*Trichechus manatus*) in Florida and Belize. *Aquatic Mammals*, 42(4), 440.
<http://doi.org/10.1578/AM.42.4.2016.44>.
- Taylor, S., Terkildsen, M., Stevenson, G., de Araujo, J., Yu, C., Yates, A., McIntosh, R.R., Gray, R. 2021. Per and polyfluoroalkyl substances (PFAS) at high concentrations in neonatal Australian pinnipeds. *Sci. Tot. Environ.* 147446.
<https://doi.org/10.1016/j.scitotenv.2021.147446>.
- Teo, S.L., Boustany, A., Dewar, H., Stokesbury, M.J., Weng, K.C., Beemer, S., Seitz, A.C., Farwell, C.J., Prince, E.D., Block, B.A., 2007. Annual migrations, diving behavior, and thermal biology of Atlantic bluefin tuna, *Thunnus thynnus*, on their Gulf of Mexico breeding grounds. *Mar. Bio.* 151(1), 1-18.
<https://doi.org/10.1007/s00227-006-0447-5>.
- Theron, P.F, Rimmer, R., Nicholls, H.A. 1974. Causes of variation of copper, iron, manganese, zinc and magnesium levels in bovine livers. *Jl S Afr Vet Ass* 45:73-76.
- Tillander, M., Miettinen J.K., Koivisto, I. 1972 Excretion rate of methyl mercury in the seal (*Pusa hispida*). In: Ruivo M (ed) *Marine pollution and sea life*. FAO Fishing News, London, pp 303–306.

- Titcomb, E.M., Reif, J.S., Fair, P.A., Stavros, H.C.W., Mazzoil, M., Bossart, G.D., Schaefer, A.M. 2017. Blood mercury concentrations in common bottlenose dolphins from the Indian River Lagoon, Florida: Patterns of social distribution. *Mar. Mamm.Sci.* 33(3), 771-784. <https://doi.org/10.1111/mms.12390>
- Tollit, D.J., Pierce, G.J., Hobson, K.A., Bowen, W.D., Iverson, S.J., 2010. Diet, in Boyd, I.L., Bowen, W.D., Iverson, S.J. (Eds.), *Marine Mammal Ecology and Conservation: a Handbook of Techniques*. Oxford University Press Inc., New York, pp. 191-221.
- Toms, C. 2019. Filling the Gaps: Common Bottlenose Dolphin (*Tursiops truncatus*) Population Dynamics, Structure, and Connectivity Within Florida Panhandle Bays, Sounds, and Estuaries. Dissertation University of Central Florida. Orlando, FL.
- Tornero, V., Hanke, G. 2016. Chemical contaminants entering the marine environment from sea-based sources: A review with a focus on European seas. *Mar. Pollut. Bull.* 112(1-2), 17-38. <https://doi.org/10.1016/j.marpolbul.2016.06.091>
- Trukhin, A.M., Boyarova, M.D. 2020. Organochlorine pesticides (HCH and DDT) in blubber of spotted seals (*Phoca largha*) from the western Sea of Japan. *Mar. Pollut. Bull.* 150, 110738. <https://doi.org/10.1016/j.marpolbul.2019.110738>.
- Tsygankov, V.Y., Lukyanova, O.N., Boyarova, M.D. 2018. Organochlorine pesticide accumulation in seabirds and marine mammals from the Northwest Pacific. *Mar. Pollut. Bull.* 128, 208-213. <https://doi.org/10.1016/j.marpolbul.2018.01.027>.

- Tunnell, J.W. 2009 The Gulf of Mexico. In: Earle SA, Glover LK (eds) Ocean: An illustrated atlas. National Geographic Society, Washington, DC, USA, pp 136–137
- Tyson, R.B., Nowacek, S.M, Nowacek, D.P. 2011. Community structure and abundance of bottlenose dolphins *Tursiops truncatus* in coastal waters of the northeast Gulf of Mexico. Mar. Ecol. Prog. Ser. 438, 253-265.
<https://doi.org/10.3354/meps09292>
- U.S. Environmental Protection Agency (USEPA) (2011b), National Emission Inventory (NEI) Data. [Available at <https://www.epa.gov/air-emissions-inventories/2011-national-emissions-inventory-nei-data>, Accessed May 28 2021]
- U.S. EPA, 1998. Method 6020A: Inductively Coupled Plasma-Mass Spectrometry. US Environmental Protection Agency, Washington, DC.
- U.S. EPA, 2007. Method 7473: mercury in solids and solutions by thermal decomposition, amalgamation, and atomic absorption spectrophotometry. US Environmental Protection Agency, Washington, DC. .
- Ungar, P. 2010. Mammal teeth: origin, evolution and diversity. The John Hopkins University Press, Baltimore
- United States Environmental Protection Agency (U.S. EPA) (2011), National Emission Inventory (NEI) Data. [Available at <https://www.epa.gov/air-emissions-inventories/2011-national-emissions-inventory-nei-data>, Accessed May 28 2021]
- Vahter, M., Marafante, E., Dencker, L. 1983. Metabolism of arsebobetaine in mice, rats, and rabbits. Sci. Total Environ. 30:197-211.

- Valiela, I., Collins, G., Kremer, J., Laitha, K., Geist, M., Seely, B., Brawley, J., Sham, C.H., 1997. Nitrogen loading from coastal watersheds to receiving estuaries: new method and application. *Ecol. Appl.* 7, 358-380. [https://doi.org/10.1890/1051-0761\(1997\)007\[0358:NLFCWT\]2.0.CO;2](https://doi.org/10.1890/1051-0761(1997)007[0358:NLFCWT]2.0.CO;2)
- Vallet-Regí, M., Navarrete, D.A. 2016. Biological apatites in bone and teeth. In: Vallet-Regí, M., Navarrete, D.A. (eds) *Clinical use: from materials to applications*. The Royal Society of Chemistry, Cambridge, pp 1-29
- Vanderklift, M.A., Ponsard, S., 2003. Sources of variation in consumer-diet $\delta^{15}\text{N}$ enrichment: a meta-analysis. *Oecologia*, 136(2), 169-182. <https://doi.org/10.1007/s00442-003-1270-z>.
- Venn-Watson, S., Colegrove, K.M., Litz, J., Kinsel, M., Terio, K., Saliki, J., Fire, S., Carmichael, R., Chevis, C., Hatchett, W., Pitchford, J., Tumlin, M., Field, C., Smith, S., Ewing, R., Fauquier, D., Lovewell, G., Whitehead, H., Rotstein, D., McFee, W., Fourgeres, E., Rowles, T. 2015a. Adrenal gland and lung lesions in Gulf of Mexico common bottlenose dolphins (*Tursiops truncatus*) found dead following the Deepwater Horizon oil spill. *PLoS one*, 10(5), e0126538. <https://doi.org/10.1371/journal.pone.0126538>
- Venn-Watson, S., Garrison, L., Litz, J., Fougères, E., Mase, B., Rappucci, G., Stratton, E., Carmichael, R., Odell, D., Shannon, D., Shippee, S., Smith, S., Staggs, L., Tumlin, M., Whitehead, H., Rowles, T. 2015b. Demographic clusters identified within the northern Gulf of Mexico common bottlenose dolphin (*Tursiops truncatus*) unusual mortality event: January 2010-June 2013. *PLoS one*, 10(2), e0117248. <https://doi.org/10.1371/journal.pone.0117248>.

- Villanger, G.D., Kovacs, K.M., Lydersen, C., Haug, L.S., Sabaredzovic, A., Jenssen, B.M., Routti, H. (2020). Perfluoroalkyl substances (PFASs) in white whales (*Delphinapterus leucas*) from Svalbard—A comparison of concentrations in plasma sampled 15 years apart. *Environ. Pollut.* 263, 114497. <https://doi.org/10.1016/j.envpol.2020.114497>.
- Vollmer, N.L., Rosel, P.E., 2013. A review of common bottlenose dolphins (*Tursiops truncatus*) in the northern Gulf of Mexico: population biology, potential threats, and management. *Southeast Nat.* 12, 1-43. <https://doi.org/10.1656/058.012.m601>.
- Voutsas, E., 2007. Estimation of volatilization of organic chemicals from soil. In *Thermodynamic, solubility and environmental issues*. In: Letcher, T. (Ed.), Elsevier, pp. 205-227. <https://doi.org/10.1016/B978-044452707-3/50013-6>.
- Wagemann, R., Kozłowska, H. 2005. Mercury distribution in the skin of beluga (*Delphinapterus leucas*) and narwhal (*Monodon monoceros*) from the Canadian Arctic and mercury burdens and excretion by moulting. *Sci. Tot. Environ.* 351, 333-343. <https://doi.org/10.1016/j.scitotenv.2004.06.028>.
- Wagemann, R., Trebacz, E., Boila, G., Lockhart, W.L. 1998. Methylmercury and total mercury in tissues of arctic marine mammals. *Sci. Total Environ.* 218, 19-31. [https://doi.org/10.1016/S0048-9697\(98\)00192-2](https://doi.org/10.1016/S0048-9697(98)00192-2).
- Wang, F., Li, G., Wu, Z., Fan, Z., Yang, M., Wu, T., Wang, J., Zhang, C., Wang, S. 2019. Tracking diphodont development in miniature pigs in vitro and in vivo. *Biol Open.* <https://doi.org/10.1242/bio.037036>.

- Wang, R., Zhao, D., Wang, Y. 2020. Characterization of elemental distribution across human dentin-enamel junction by scanning electron microscopy with energy-dispersive X-ray spectroscopy. *Microsc Res Tech.*
<https://doi.org/10.1002/jemt.23648>,
- Ward, C.H., Tunnell, J.W. Jr. 2017. Chapter 1. Habitats and biota of the Gulf of Mexico an overview. In Ward, H.E. (Ed). *Habitats and Biota of the Gulf of Mexico: Before the Deepwater Horizon Oil Spill. Volume 1: Water Quality, Sediments, Sediment Contaminants, Oil and Gas Seeps, Coastal Habitats, Offshore Plankton and Benthos, and Shellfish.* Springer. New York, NY. pp 1-54.
- Waring, G.T., Josephson, E., Maze-Foley, K., Rosel, P., 2015. US Atlantic and Gulf of Mexico marine mammal stock assessments-2014. NOAA Tech. Memo. NMFS-NE-231. US Department of Commerce, Woods Hole, MA.
- Weber, J.H. 1993. Review of possible paths for abiotic methylation of mercury (II) in the aquatic environment. *Chemosphere.* 26(11), 2063-2077.
[https://doi.org/10.1016/0045-6535\(93\)90032-Z](https://doi.org/10.1016/0045-6535(93)90032-Z).
- Weijs, L., Hickie, B.E., Blust, R., Covaci, A. 2014. Overview of the current state-of-the-art for bioaccumulation models in marine mammals. *Toxics.* 2(2), 226-246.
<https://doi.org/10.3390/toxics2020226>
- Weijs, L., Zaccaroni, A. 2016. Toxicology of marine mammals: new developments and opportunities. *Arch. Environ. Contam. Toxicol.* 70(1), 1-8.
<https://doi.org/10.1007/s00244-015-0233->

- Wells, R.S., Rhinehart, H.L., Cunningham, P., Whaley, J., Baran, M., Koberna, C., Costa, D.P., 1999. Long distance offshore movements of bottlenose dolphins. *Marine Mammal Science*. 15(4): 1098-1114. <https://doi.org/10.1111/j.1748-7692.1999.tb00879.x>
- Wells, R.S., Schwacke, L.H., Rowles, T.K., Balmer, B.C., Zolman, E., Speakman, T., Townsend, F.I., Tumlin, M.C., Barleycorn, A., Wilkinson, K.A., 2017. Ranging patterns of common bottlenose dolphins *Tursiops truncatus* in Barataria Bay, Louisiana, following the *Deepwater Horizon* oil spill. *Endanger. Species. Res.* 33, 159-180. <https://doi.org/10.3354/esr00732>.
- Wells, R.S., Scott, M.D., 1990. Estimating bottlenose dolphin population parameters from individual identification and capture-release techniques. *Rep. Int. Whaling Comm. Special Issue 12*, 407-415.
- Wells, R.S., Scott, M.D., Irvine, A.B., 1987. The social structure of free-ranging bottlenose dolphins, in: Genoways H.H. (Ed.), *Current Mammalogy*. Springer, Boston, MA, pp. 247-305.
- Wenthrup-Bryne, E., Armstrong, C.A., Armstrong, R.S., Collins, B.M. 1997. Fourier transform Raman microscopic mapping of molecular components in human tooth. *L. Raman Spectrosc.* [https://doi.org/10.1002/\(SICI\)1097-4555\(199702\)28:2/3<151::AID-JRS71>3.0.CO;2-5](https://doi.org/10.1002/(SICI)1097-4555(199702)28:2/3<151::AID-JRS71>3.0.CO;2-5).
- Werth, A.J. 2000. Feeding in marine mammals. In: Schwenk K (ed) *Feeding: form, function and evolution in tetrapod vertebrates*. Academic Press, San Diego, pp 487-526

- Wild, L. A., Mueter, F., Witteveen, B., Straley, J. M., 2020. Exploring variability in the diet of depredating sperm whales in the Gulf of Alaska through stable isotope analysis. *R. Soc. Open Sci.* 7(3), 191110. <https://doi.org/10.1098/rsos.191110>
- Wilhelm, S.M., Liang, L., Cussen, D., Kirchgessner, D.A. 2007. Mercury in crude oil processed in the United States (2004). *Environ. Sci. Technol.* 41(13), 4509-4514. <https://doi.org/10.1021/es062742j>.
- Wilson, R.M., Chanton, J., Lewis, G., Nowacek, D., 2009. Combining organic matter source and relative trophic position determinations to explore trophic structure. *Estuar. Coast.* 32, 990-1010. <https://doi.org/10.1007/s12237-009-9183-7>.
- Wilson, R.M., Kucklick, J.R., Balmer, B.C., Wells, R.S., Chanton, J.P., Nowacek, D.P., 2012. Spatial distribution of bottlenose dolphins (*Tursiops truncatus*) inferred from stable isotopes and priority organic pollutants. *Sci. Total. Environ.* 425, 223-230. <https://doi.org/10.1016/j.scitotenv.2012.02.030>.
- Wilson, R.M., Nelson, J.A., Balmer, B.C., Nowacek, D.P., Chanton, J.P., 2013. Stable isotope variation in the northern Gulf of Mexico constrains bottlenose dolphin (*Tursiops truncatus*) foraging ranges. *Mar. Biol.* 160, 2967-2980. <https://doi.org/10.1007/s00227-013-2287-4>.

- Wise Jr, J.P., Wise, J.T., Wise, C.F., Wise, S.S., Gianios Jr, C., Xie, H., Thompson, W.D., Perkins, C, Falank, C., & Wise Sr, J.P. 2014) Concentrations of the genotoxic metals, chromium and nickel, in whales, tar balls, oil slicks, and released oil from the gulf of Mexico in the immediate aftermath of the deepwater horizon oil crisis: is genotoxic metal exposure part of the deepwater horizon legacy? *Environ. Sci. Technol.*48, 2997-3006.
<https://doi.org/10.1021/es405079b>.
- Wolfgong W.J. 2016. Chapter 14 - Chemical analysis techniques for failure analysis: Part 1, common instrumental methods. In: Makhlof ASH, Aliofkhazraei M (eds), *Handbook of material failure analysis with case studies from the aerospace and automotive industries*. Elsevier, pp. 279-307
- Worthy, G.A.J., 2001. Nutrition and energetics. In: Dierauf L.A., Gulland F.M.D. (Eds.), *Handbook of marine mammal medicine*. CRC Press, Boca Raton, pp. 791–828.
- Worthy, G., Wells, R., Martin, S., Shippee, S., 2013. Impacts of the 2010 Deepwater Horizon Oil Spill on estuarine bottlenose dolphin populations in the west Florida panhandle (No. 10-1101). Final Tech Report, Florida Institute of Technology, Contract.
- Woshner, V., Knott, K., Wells, R., Willetto, C., Swor, R., O’Hara, T., 2008. Mercury and selenium in blood and epidermis of bottlenose dolphins (*Tursiops truncatus*) from Sarasota Bay, FL: interaction and relevance to life history and hematologic parameters. *EcoHealth*. 5, 360-370. <https://doi.org/10.1007/s10393-008-0164-2>.

- Würsig, B. 2017. Chapter 13. Marine mammals of the Gulf of Mexico. In Ward, C. H. (Ed.). Habitats and Biota of the Gulf of Mexico: Before the Deepwater Horizon Oil Spill: Volume 2: Fish Resources, Fisheries, Sea Turtles, Avian Resources, Marine Mammals, Diseases and Mortalities Springer Nature. New York, NY. pp 1489-1587.
- Yang J., Kuniyo, T., Tanabe, S., Amano, M., Muyazki, N., 2002. Trace elements in skin of Dall's porpoises (*Phocoenoides dalli*) from the northern waters of Japan: an evaluation for utilization as non-lethal tracers. Mar. Pollut. Bull. 45, 230-236. [https://doi.org/10.1016/S0025-326X\(01\)00328-9](https://doi.org/10.1016/S0025-326X(01)00328-9).
- Yasukawa, A., Yokoyama, T., Kandori, K., Ishikawa, T. 2007. Reaction of calcium hydroxyapatite with Cd²⁺ and Pb²⁺ ions. Colloid. Surf. A-Physiochem. Eng. Asp. <https://doi.org/10.1016/j.colsurfa.2006.11.042>
- Ylitalo, G.M., Stein, J.E., Hom, T.E., Johnson, L.J., Tilbury, K.L., Hall, A.J., Rowles, T., Greig, D., Lowenstine, L.J., Gulland, F.M.D. 2005. The role of organochlorines in cancer-associated mortality in California sea lions (*Zalophus californianus*). Mar. Pollut. Bull. 50, 30–39. <https://doi.org/10.1016/j.marpolbul.2004.08.005>.
- Zheng, Y., Zhang, Y., Tang, W., Guo, H., Zhu, Y., Dong, Z., Jiang, H. 2018. Preliminary in situ teeth study of the narrow-ridged finless porpoises remains using microsynchrotron radiation X-ray fluorescence and laser ablation inductively coupled plasma mass spectrometry. XRay Spectrom. <https://doi.org/10.1002/xrs.2955>.

Zurr, A.F., Ieno, E.N., Elphick, C.S., 2010. A protocol for data exploration to avoid common statistical problems. *Methods Ecol. Evol.* 1, 3-14.

<https://doi.org/10.1111/j.2041-210X.2009.00001.x>.